

Strategies for enhancing chromatographic efficiencies in chiral and achiral supercritical and
liquid chromatography

By

Daipayan Roy

Presented to the Faculty of the Graduate School of
The University of Texas at Arlington in Partial Fulfillment
of the Requirements for the Degree of

DOCTOR OF PHILOSOPHY

THE UNIVERSITY OF TEXAS AT ARLINGTON

August 2020

I dedicate this thesis to all teachers across the globe who are the unsung warriors of this pandemic. Despite the challenges of the current situation they have ensured that students keep getting their education through novel routes and thereby keeping the future of humankind secure.

Acknowledgement

When I began the journey for my degree in 2015, I had not even seen a high-performance liquid chromatograph (HPLC). Now five years later, the focus of my work revolves around HPLC. First and foremost, I would like to thank my doctoral advisor Dr. Daniel W. Armstrong. His contribution to what I am today is unmatched. He has taught me the idiosyncrasies of conducting research, writing scientific papers, and thinking like a scientist. I see him strive for excellence every single day and that is something I hope to remember and apply towards my career as well. I would also like to take this opportunity to acknowledge my thesis committee members Dr. Purnendu Dasgupta, Dr. Saiful Chowdhury, Dr. Frederick MacDonnell, and Dr. Alejandro Bugarin for their feedback and taking their valuable time and being a part of my graduate committee.

I would also like to thank Dr. M. Farooq Wahab for being a friend, philosopher, and guide. He was not only there to solve day to day problems that I encountered but also open to discuss every intellectual problem and challenges. He has always provided constructive criticism to every scientific idea that I presented and thereby refined the idea and helped me produce concrete publishable research.

I would like to thank members of AZYP LLC. especially Dr. J.T. Lee for providing high efficiency columns and sharing his immense experience in chiral chromatography. I am also grateful to Dr. Terry Berger for his support to my research. I would also like to extend my appreciation to AbbVie Inc. and Dr. Russell Hertzler for providing me the opportunity to apply the skills I gained during my PhD to an industrial setting.

I would like to thank my labmates Garrett, Mohsen, Sam, Nimisha, Elizabeth, Abiud, Siqi, Yadi, Rahul for making the journey towards a PhD enjoyable and for their valuable comments during group meetings. I would also like Anne Ellis, Angel Escalante, and Barbara Smith for their support.

My appreciation goes out to my friends especially Sinjinee, Abhishek, Aditya, Sarbajit, Rongon, Soumyava, Kabir, and Suman.

Finally, and most importantly, I would like to thank my mother Sumita Roy and my father Dipak Roy for their unconditional love and support. They have been on my side through good times and bad and have always put my priorities above theirs. Words cannot do justice to how indebted I feel for all that they have done.

July 29th, 2020

Daipayan Roy

Abstract

Strategies for enhancing chromatographic efficiencies in chiral and achiral supercritical and liquid chromatography

Daipayan Roy

The University of Texas, Arlington, 2020

Supervising Professor: Daniel W. Armstrong

The fundamental aim of chromatography has been to achieve baseline separation between the components of a mixture in the shortest possible time. Recently there has been a shift in the chromatographic focus of enantiomeric separations, with an emphasis on increasing the efficiency of columns. Superficially porous particles (SPP) introduced about a decade ago lead to a surge in efficiency as compared to the traditionally used fully porous particles (FPP). Recently chiral selectors bonded to superficially porous particles have been commercialized.

This work reports new methods for enantioseparation using chiral selectors like macrocyclic glycopeptides, modified cyclodextrins and cyclofructans bonded to SPPs. Novel methodologies have been developed for 150 pharmaceutically relevant small molecules using both HPLC and SFC. Also, a newly developed macrocyclic glycopeptide stationary phase was used to separate enantiomers of nicotine related compounds. This work also focuses on the advantages of switching from FPPs to SPPs in SFC, by comparing van Deemter plots.

This work investigates the effect of water as an additive in supercritical fluid chromatography. Investigation reveals distinct behaviors of different stationary phase chemistries with the addition of water. Polar stationary phases showed up to a nine-fold gain in efficiency.

This phenomenon was exploited to make SFC more environmentally sustainable. The modifier methanol, which is toxic to humans, was replaced by azeotropic ethanol which is nontoxic and is derived from a renewable source. The inherent water in this azeotrope produced increased efficiencies and decreased retention times and therefore resulted in lower consumption of organic modifier consumption, thereby making SFC 'greener'.

List of Illustrations

Figure 1.1 Structures of different chiral selectors 2

Figure 1.2 A typical van Deemter plot (dashed line). The individual components are shown with solid lines. 4

Figure 2.1 Representative chromatograms on different stationary phases (A) VancoShell (10cmX0.46cm) Analyte: Fluoxetine M.P.- 75/25 CO₂/MeOH- 3% water- 0.1% TEA- 0.1% TFA, 4 ml/min, T= 30°C (B) NicoShell (10cmX0.46cm) Analyte: Nicotine M.P.- 60/40 CO₂/MeOH- 0.1% TEA , 4 ml/min, T= 30°C (C) NicoShell (10cmX0.46cm) Analyte: Tramadol M.P.- 60/40 CO₂/MeOH- 0.2% TEA- 0.3% TFA , 4 ml/min, T= 30°C (D) LarihcShell (10cmX0.46cm) Analyte: Norephedrine M.P.- 80/20 CO₂/MeOH- 0.2% TEA- 0.3% TFA , 4 ml/min, T= 25°C (E) LarihcShell (10cmX0.46cm) Analyte: 1-(1-Naphthyl)ethylamine M.P.- 80/20 CO₂/MeOH- 0.2% TEA- 0.3% TFA , 4 ml/min, T= 25°C (F) TeicoShell (10cmX0.46cm) Analyte: Dichloroprop M.P.- 60/40 CO₂/MeOH- 0.1% ammonium formate, 4 ml/min, T= 30°C UV detection at 254 nm 22

Figure 2.2 Effect of additives on the separation of the enantiomers of 1-(1-Naphthyl)ethylamine , Chromatographic conditions: LarihcShell-P, (10×0.46 cm), 4 ml/min, 10 MPa backpressure, 25 °C, UV detection at 254 nm. Mobile phase: (A) 80/20 CO₂/MeOH- 0.1% TEA (B) 80/20 CO₂/MeOH- 0.1% TFA (C) 80/20 CO₂/MeOH- 0.1% TEA- 0.1% TFA (D) 80/20 CO₂/MeOH- 0.2% TEA- 0.3% TFA 23

Figure 2.3 The van Deemter plot showing plate height (H) in mm versus flow rate in SFC on TeicoShell (2.7 μm) and Chirobiotic T (5 μm) chiral columns. SFC van Deemter with analyte 3-phenylphthalide. Chromatographic conditions: 75/25 CO₂/MeOH; Backpressure regulator maintained at 8 MPa and temperature at 30°C. UV detection at 254 nm. 34

Figure 2.4 The van Deemter plot showing plate height (H) in mm versus flow rate in SFC on LarihcShell-P (2.7 μm) and Larihc-CF6-P (5 μm) chiral columns. SFC van Deemter with analyte 1-(1-naphthyl)ethylamine. Chromatographic conditions: 80/20 CO₂/MeOH-0.2% TEA-0.3% TFA; Backpressure regulator maintained at 8 MPa and temperature at 25°C. UV detection at 254 nm. 35

Figure 2.5 Ultrafast chiral separations on SFC. (A) 1-(1-naphthyl)ethylamine, M.P. 80/20 CO₂/Methanol-0.2% TEA-0.3% TFA, 14 mL/min (B) 1,2,2- triphenylethylamine, M.P. 80/20 CO₂/Methanol-0.2% TEA-0.3% TFA, 14 mL/min (C) 3-phenylphthalide M.P. 95/5 CO₂/Methanol, 10 mL/min (D) 5,5-diphenyl-4-methyl-2-oxazolidinone M.P. 60/40 CO₂/Methanol, 10 mL/min. All separations were performed at a backpressure of 10 Mpa and under ambient temperature. 36

Figure 2.S1 Natural logarithm of experimental retention factor versus backpressure measured in MPa for chiral columns TeicoShell, NicoShell, VancoShell and LarihcShell-P. Chromatographic conditions for different columns: TeicoShell (10 X 0.46 cm), 5-Methyl-5-phenyl hydantoin 60/40 CO₂/Methanol-0.1% ammonium formate; NicoShell (10 X 0.46 cm), Mepivacaine, 75/25 CO₂/Methanol-0.1% TEA-0.1% TFA; VancoShell (10 X 0.46 cm), Methylphenidate, 80/20 CO₂/Methanol-0.1% TEA-0.1% TFA; LarihcShell (10 X 0.46 cm), 4-chlorophenyl alaninol, 80/20 CO₂/Methanol-0.2% TEA-0.3% TFA. Flow rate 4 mL/min 41

Figure 3.1 A) Plot of electrostatic character (y-axis) and the hydrophilic character (x-axis) for the chiral stationary phases used in SFC. B) Projection of selectivity on the cytosine/uracil axis. Experimental conditions: 80/20 (v/v) ACN/ 25 mM ammonium acetate pH 6.8, flow rate: 1 mL/min and UV detection at 254 nm. The dead time was measured with water or acetone 50

Figure 3.2 3D plot for efficiency gains with water addition under different modifier concentrations (A) Gain in efficiency for Chiralpak IA-3 column with neutral analyte: hydrobenzoin. (B) Gain in efficiency for TeicoShell column with neutral analyte: (±) cis-4,5-diphenyl-2-oxazolidinone. Experimental condition: 60-95/40-5 CO₂/ MeOH with 0-15% H₂O, flow rate: 4 mL/min, temp.: 25°C, outlet pressure: 8 MPa. UV detection at 220 nm 53

Figure 3.3 Superficial linear velocity vs. reduced plate height curves for (±) cis-4,5-diphenyl-2-oxazolidinone enantiomers with and without water in the mobile phase. Experimental conditions: TecioShell 10x0.46 cm (A) 82/18 CO₂/ MeOH and (B) 82/18 CO₂/ MeOH+6% H₂O, temp.: 40°C, outlet pressure: 12 MPa. UV detection at 254 nm 59

Figure 3.4 Reduction in analysis times with the introduction of increasing amount of water under different modifier compositions. Experimental condition: TecioShell 10 x 0.46 cm (A) 60/40 CO₂/ MeOH and (B) 90/10 CO₂/ MeOH, flow rate: 4 mL/min, temp.: 25°C and outlet pressure: 8 MPa. Amounts of water recorded are the amount present in the entire mobile phase. Analyte: (±) cis-4,5-diphenyl-2-oxazolidinone and UV detection at 220 nm. 61

Figure 3.5 Modulating peak shapes by varying adsorption isotherm with water under SFC conditions. Experimental condition: TecioShell 10 x 0.46 cm (A) 90/10 CO₂/ MeOH-0.1% (w/v) ammonium formate and (B) 90/10 CO₂/ MeOH-0.1% (w/v) ammonium formate+ 6% H₂O, flow rate: 4 mL/min, temp.:25°C and outlet pressure: 8 MPa. Analyte: 2-(4-chlorophenoxy)propionic acid and UV detection at 220 nm. 64

Figure 3.S1 Plot of energy of transition of Nile red dye vs. methanol percentage in the mobile phase. Transition energy calculated by $E_{NR} = 28591.44/\text{wavelength}(\text{nm})$ 67

Figure 3.S2 3D plot representing % water in the modifier, % modifier in the mobile phase and number of theoretical plates for 2-(4-chlorophenoxy)propionic acid on TeicoShell (10 x 0.46 cm). Experimental condition: 60-95/40-5 CO₂/ MeOH-0.1% (w/v) ammonium formate+ 0-15% H₂O. Flow rate: 4 mL/min, temperature: ambient and outlet pressure: 8 MPa. UV detection at 220 nm 69

Figure 3.S3 3D plot representing % water in the modifier, % modifier in the mobile phase and number of theoretical plates for metoprolol on TeicoShell (10 x 0.46 cm). Experimental condition: 75-95/25-5 CO₂/ MeOH-0.1% (v/v) triethylamine-trifluoroacetic acid+ 0-6% H₂O. Flow rate: 4 mL/min, temperature: ambient and outlet pressure: 8 MPa 70

Figure 3.S4 3D plot representing % water in the modifier, % modifier in the mobile phase and number of theoretical plates for tryptophan on LarihcShell-P (10 x 0.46 cm). Experimental condition: 75-95/25-5 CO₂/ MeOH-0.2% (v/v) triethylamine-0.3% (v/v) trifluoroacetic acid+ 0-6% H₂O. Flow rate: 4 mL/min, temperature: ambient and outlet pressure: 8 MPa. UV detection at 220 nm 71

Figure 3.S5 3D plot representing % water in the modifier, % modifier in the mobile phase and number of theoretical plates for 1-(1-naphthyl)ethylamine on LarihcShell-P (10 x 0.46 cm). Experimental condition: 70-95/30-5 CO₂/ MeOH-0.2% (v/v) triethylamine-0.3% (v/v) trifluoroacetic acid+ 0-6% H₂O. Flow rate: 4 mL/min, temperature: ambient and outlet pressure: 8 MPa. UV detection at 220 nm 72

Figure 3.S6 3D plot representing % water in the modifier, % modifier in the mobile phase and number of theoretical plates for tryptophanamide on LarihcShell-P (10 x 0.46 cm). Experimental condition: 70-95/30-5 CO₂/ MeOH-0.2% (v/v) triethylamine-0.3% (v/v) trifluoroacetic acid+ 0-6% H₂O. Flow rate: 4 mL/min, temperature: ambient and outlet pressure: 8 MPa. UV detection at 220 nm 73

Figure 3.S7 Effect of water on enantiomeric separations with NicoShell (10 x 0.46 cm).
Experimental conditions: A. Analyte: Bupivacaine; Mobile phase: 80/20 CO₂/ MeOH- 0.1% (v/v) triethylamine-0.1% (v/v) trifluoroacetic acid. B. Analyte: Proglumide; Mobile phase: 80/20 CO₂/ MeOH- 0.1% (w/v) ammonium formate. Temperature: ambient, Flow rate: 4 mL/min, Outlet pressure: 8 MPa, UV detection at 220 nm. 74

Figure 3.S8 Effect of water on enantiomeric separations with VancoShell (10 x 0.46 cm).
Experimental conditions: A. Analyte: Fluoxetine; Mobile phase: 85/15 CO₂/ MeOH- 0.1% (v/v) triethylamine-0.1% (v/v) trifluoroacetic acid. B. Analyte: Nicardipine; Mobile phase: 80/20 CO₂/ MeOH- 0.1% (w/v) ammonium formate. Temperature: ambient, Flow rate: 4 mL/min, Outlet pressure: 8 MPa, UV detection at 220 nm. 75

Figure 3.S9 Effect of water on enantiomeric separations with LarihcShell-P (10 x 0.46 cm).
Experimental conditions: A. Analyte: Tryptophan; Mobile phase: 85/15 CO₂/ MeOH- 0.2% (v/v) triethylamine-0.3% (v/v) trifluoroacetic acid. B. Analyte: Tryptophanamide; Mobile phase: 80/20 CO₂/ MeOH- 0.2% (v/v) triethylamine-0.3% (v/v) trifluoroacetic acid. Temperature: ambient, Flow rate: 4 mL/min, Outlet pressure: 8 MPa, UV detection at 220 nm. 76

Figure 3.S10 Effect of water on enantiomeric separations with Qshell (10 x 0.46 cm).
Experimental conditions: A. Analyte: N-benzoyl-d,l-valine; Mobile phase: 80/20 CO₂/ MeOH- 0.1% (w/v) ammonium formate-0.3% (v/v) formic acid. B. Analyte: Dansyl-d,l-serine; Mobile phase: 80/20 CO₂/ MeOH- 0.1% (w/v) ammonium formate-0.3% (v/v) formic acid. Temperature: ambient, Flow rate: 4 mL/min, Outlet pressure: 8 MPa, UV detection at 220 nm. 76

Figure 3.S11 Chromatogram under non-linear condition. Experimental conditions: Column TeicoShell 10 x 0.46 cm. Analyte: 2-(4-chlorophenoxy)propionic acid; Mobile phase: 90/10 CO₂/ MeOH-1% water. Temperature: ambient, Flow rate: 4 mL/min, Outlet pressure: 8 MPa, UV detection at 220 nm. 77

Figure 4.1 Effect of methanol (a,d), absolute ethanol (b,e), and '190 proof' ethanol (c,f) on the separation of cis-4,5-diphenyl-2-oxazolidinone (left) and bupivacaine (right) with TeicoShell and NicoShell stationary phase respectively. Mobile Phase: (a,b,c) 80/20 CO₂/modifier, (d,e,f) 90/10 CO₂/modifier-0.1% TEA-TFA (v/v). All separations were performed using Flow rate: 4 mL/min, Temperature: Ambient, Backpressure: 8 MPa 87

Figure 4.2 Representative chromatograms: Analyte: Amphetamine Conditions: Stationary phase: VancoShell Mobile Phase: (a) 75/25 CO₂/MeOH-0.1% TEA-TFA (v/v) and (b) 75/25 CO₂/190

proof EtOH-0.1% TEA-TFA (v/v). Analyte: Prilocaine Conditions: Stationary Phase: NicoShell Mobile Phase: (c) 80/20 CO₂/MeOH-0.05% ammonium formate (w/v) and (d) 80/20 CO₂/'190 proof' EtOH-0.05% ammonium formate (w/v). Analyte: Tryptophan Conditions: Stationary Phase: LarihcShell-P Mobile Phase: (a) 75/25 CO₂/MeOH-0.2% TEA-0.3% TFA (v/v) and (b) 75/25 CO₂/'190 proof' EtOH-0.2% TEA-0.3% TFA (v/v). All separations were performed using Flow rate: 4 mL/min, Temperature: Ambient, Backpressure: 8 MPa 94

Figure 4.3 Effect of variation of modifier concentration on retention factor of the second eluted enantiomer and the efficiency on **a.** cis-4,5-diphenyl-2-oxazolidinone and **b.** bupivacaine 96

Figure 4.4 Enantiomeric separation of carprofen on ChiralPak IA column (15 x 0.46 cm) with different modifiers **a.** methanol **b.** absolute ethanol **c.** '190 proof' ethanol. Mobile Phase: 70/30 CO₂/modifier. All separations were performed using Flow rate: 4 mL/min, Temperature: ambient, Backpressure: 8 MPa. 98

Figure 4.5 Separation of 4 β blockers namely alprenolol, metoprolol, propranolol and pindolol with methanol, absolute ethanol and '190 proof' ethanol. Conditions: Stationary Phase: NicoShell, Mobile Phase: 80/20 CO₂/modifier-0.1% (v/v) TEA-0.1% (v/v) TFA. All separations were performed using Flow rate: 4 mL/min. 99

Figure 4.6 Increasing column loadability with '190 proof' ethanol in chiral SFC. Conditions: Stationary Phase: VancoShell, Mobile Phase: a. 80/20 CO₂/MeOH-0.1% (v/v) TEA-0.1% (v/v) TFA b. 80/20 CO₂/'190 proof' ethanol-0.1% (v/v) TEA-0.1% (v/v) TFA. Separations were performed using Flow rate: 4 mL/min, Temperature: ambient. Backpressure: 8 MPa 101

Figure 4.S1 Structures of chiral selectors 105

Figure 4.S2 Effect of methanol (a), absolute ethanol (b), and "190 proof" ethanol (c) on the separation of hydrobenzoin with ChiralPak IA stationary phase respectively. Mobile Phase: 75/25 CO₂/modifier. All separations were performed using Flow rate: 4 mL/min, Temperature: Ambient, Backpressure: 8 MPa 106

Figure 4.S3 Representative chromatograms: Analyte: Fenoprofen Conditions: Stationary phase: Whelk O1 Mobile Phase: (a) 80/20 CO₂/MeOH-0.1% TEA-TFA (v/v) and (b) 80/20 CO₂/Ethanol -0.1% TEA-TFA (v/v) 107

Figure 5.1 Influence of water on the separation of neutral compounds on FructoShell-N column (2.7 μm particles, 10 x 0.46 cm). Conditions: 80/20 CO_2/MeOH + 0.1% (v/v) TEA + 0.1% (v/v) TFA (empty squares and triangles); 80/20 CO_2/MeOH + 0.1% (v/v) TEA + 0.1% (v/v) TFA + 6% (v/v) H_2O (full squares and triangles); flow rate 4 ml/min, back pressure 8 MPa; detection: UV, 220nm. Compounds numbers are same as that in Table 5.1. X-axis denotes compound numbers; the left y-axis denotes retention factor and the right y-axis denotes efficiency. 117

Figure 5.2 Influence of water on the separation of basic compounds on FructoShell-N column (2.7 μm particles, 10 x 0.46 cm). Conditions: 80/20 CO_2/MeOH + 0.1% (v/v) TEA + 0.1% (v/v) TFA (empty squares and triangles); 80/20 CO_2/MeOH + 0.1% (v/v) TEA + 0.1% (v/v) TFA + 6% (v/v) H_2O (full squares and triangles); flow rate 4 ml/min, back pressure 8 MPa; detection: UV, 220nm. Compounds numbers are same as that in Table 5.1. X-axis denotes compound numbers; the left y-axis denotes retention factor and the right y-axis denotes efficiency. 118

Figure 5.3 SFC chromatograms of nicotinic acid (A) and 1-methyl-3-phenylpropylamine (B) and 3,5-dinitrobenzoic acid (C) on FructoShell-N column with 90/10 CO_2/MeOH + 0.1% (v/v) TEA + 0.1% (v/v) TFA mobile phase without and with addition of 6% (v/v) H_2O to modifier. 120

Figure 5.4 Influence of water on the separation of basic compounds on SilicaShell column. Conditions: 80/20 CO_2/MeOH + 0.1% (v/v) TEA + 0.1% (v/v) TFA (empty squares and triangles); 80/20 CO_2/MeOH + 0.1% (v/v) TEA + 0.1% (v/v) TFA + 6% (v/v) H_2O (full squares and triangles); flow rate 4 ml/min, back pressure 8 MPa; detection: UV, 220nm. Compounds numbers are same as that in Table 5.1. X-axis denotes compound numbers; the left y-axis denotes retention factor and the right y-axis denotes efficiency. 123

Figure 5.5 SFC chromatogram of phenylsuccinic acid on SilicaShell column with 90/10 CO_2/MeOH + 0.1% (v/v) TEA + 0.1% (v/v) TFA mobile phase without (bottom) and with (top) addition of 6% (v/v) H_2O to modifier. 124

Figure 5.6 Influence of water on the separation of analytes on C18 column. Conditions: 90/10 CO_2/MeOH + 0.1% (v/v) TEA + 0.1% (v/v) TFA (empty squares and triangles); 90/10 CO_2/MeOH + 0.1% (v/v) TEA + 0.1% (v/v) TFA + 6% (v/v) H_2O (full squares and triangles); flow rate 4 ml/min, back pressure 8 MPa, detection: UV, 220nm. Compounds numbers are same as that in Table 5.1. X-axis denotes compound numbers; the left y-axis denotes retention factor and the right y-axis denotes efficiency. 127

Figure 5.7 Influence of water on the separation of basic compounds on Xselect C18 SB column. Conditions: 80/20 CO₂/MeOH + 0.1% (v/v) TEA + 0.1% (v/v) TFA (empty squares and triangles); 90/10 CO₂/MeOH + 0.1% (v/v) TEA + 0.1% (v/v) TFA + 6% (v/v) H₂O (full squares and triangles); flow rate 4 ml/min, back pressure 8 MPa; detection: UV, 220nm. Compounds numbers are same as that in Table 5.1. X-axis denotes compound numbers; the left y-axis denotes retention factor and the right y-axis denotes efficiency. 128

Figure 5.8 Discriminant analysis for FructoShell-N column with use of 80/20 CO₂/MeOH + 0.1% (v/v) TEA + 0.1% (v/v) TFA without and with addition of 6% (v/v) H₂O (A); SilicaShell column with use of 80/20 CO₂/MeOH + 0.1% (v/v) TEA + 0.1% (v/v) TFA without and with addition of 6% (v/v) H₂O (B); and C18 column with use of 90/10 CO₂/MeOH + 0.1% (v/v) TEA + 0.1% (v/v) TFA without and with addition of 6% (v/v) H₂O (C). Compounds numbers are same as that in Table 5.1. 133

Figure 5.S1 Water disturbance peak for FructoShell-N column. Retention time of water was determined by the procedure in Experimental Section (Section 2.5). The representative disturbance peak was measured at 210 nm wavelength using 10x0.46 cm FructoShell-N column with 80/20 CO₂/MeOH mobile phase and flow rate of 4 mL/min and 8 MPa backpressure. Similar water disturbance peaks were obtained with SilicaShell at 1.87 mins using 10x0.46 cm column with 80/20 CO₂/MeOH mobile phase and flow rate of 4 mL/min and 8 MPa backpressure. Using 10x0.46 cm FructoShell-N, SilicaShell and C18 column with 90/10 CO₂/MeOH mobile phase and flow rate of 4 mL/min and 8 MPa backpressures the retention times were 2.27, 4.99 and 0.31 min. respectively. 160

Figure 5.S2 Plot of electrostatic character vs. hydrophilicity character: CF₆ – Cylofructan-6 stationary phase (FructoShell-N); Silica- silica stationary phase (SilicaShell); Reversed phase stationary phases (C18) and Xselect C18 SB. 161

Figure 5.S3 Influence of water on the separation of neutral compounds on FructoShell-N column. Conditions: 90/10 CO₂/MeOH + 0.1% (v/v) TEA + 0.1% (v/v) TFA (empty squares and triangles); 90/10 CO₂/MeOH + 0.1% (v/v) TEA + 0.1% (v/v) TFA + 5.7% (v/v) H₂O (full squares and triangles); flow rate 4 ml/min, back pressure 8 MPa; detection: UV, 220nm. Compound number as in Table 5.1. 162

Figure 5.S4 Influence of water on the separation of basic compounds on FructoShell-N column. Conditions: 90/10 CO₂/MeOH + 0.1% (v/v) TEA + 0.1% (v/v) TFA (empty squares and triangles); 90/10 CO₂/MeOH + 0.1% (v/v) TEA + 0.1% (v/v) TFA + 5.7% (v/v) H₂O (full

squares and triangles); flow rate 4 ml/min, back pressure 8 MPa; detection: UV, 220nm. Compound number as in Table 5.1. 163

Figure 5.S5 Influence of water on the separation of acidic compounds on FructoShell-N column (2.7 μm particles, 10 x 0.46 cm). Conditions: 90/10 CO_2/MeOH + 0.1% (v/v) TEA + 0.1% (v/v) TFA (empty squares and triangles); 90/10 CO_2/MeOH + 0.1% (v/v) TEA + 0.1% (v/v) TFA + 5.7% (v/v) H_2O (full squares and triangles); flow rate 4 ml/min, back pressure 8 MPa, detection: UV 220nm. Compound number as in Table 5.1. 164

Figure 5.S6 Influence of water on the separation of acidic compounds on FructoShell-N column (2.7 μm particles, 10 x 0.46 cm). Conditions: 80/20 CO_2/MeOH + 0.1% (v/v) TEA + 0.1% (v/v) TFA (empty squares and triangles); 80/20 CO_2/MeOH + 0.1% (v/v) TEA + 0.1% (v/v) TFA + 5.7% (v/v) H_2O (full squares and triangles); flow rate 4 ml/min, back pressure 8 MPa; detection: UV, 220nm. Compound number as in Table 5.1 165

Figure 5.S7 Formation of silyl ethers on silica surface (A) and types of silanols present on silica surface (B) 166

Figure 5.S8 Influence of water on the separation of basic compounds on SilicaShell column. Conditions: 90/10 CO_2/MeOH + 0.1% (v/v) TEA + 0.1% (v/v) TFA (empty squares and triangles); 90/10 CO_2/MeOH + 0.1% (v/v) TEA + 0.1% (v/v) TFA + 5.7% (v/v) H_2O (full squares and triangles); flow rate 4 ml/min, back pressure 8 MPa; detection: UV, 220nm. Compound number as in Table 5.1. 166

Figure 5.S9 Influence of water on the separation of acidic compounds on SilicaShell column. Conditions: 90/10 CO_2/MeOH + 0.1% (v/v) TEA + 0.1% (v/v) TFA (empty squares and triangles); 90/10 CO_2/MeOH + 0.1% (v/v) TEA + 0.1% (v/v) TFA + 5.7% (v/v) H_2O (full squares and triangles); flow rate 4 ml/min, back pressure 8 MPa, detection: UV, 220nm. Compound number as in Table 5.1. 167

Figure 5.S10 Influence of water on the separation of acidic compounds on SilicaShell column. Conditions: 80/20 CO_2/MeOH + 0.1% (v/v) TEA + 0.1% (v/v) TFA (empty squares and triangles); 80/20 CO_2/MeOH + 0.1% (v/v) TEA + 0.1% (v/v) TFA + 5.7% (v/v) H_2O (full squares and triangles); flow rate 4 ml/min, back pressure 8 MPa, detection: UV, 220nm. Compound number as in Table 5.1. 168

Figure 5.S11 Influence of water on the separation of neutral compounds on SilicaShell column. Conditions: 90/10 CO₂/MeOH + 0.1% (v/v) TEA + 0.1% (v/v) TFA (empty squares and triangles); 90/10 CO₂/MeOH + 0.1% (v/v) TEA + 0.1% (v/v) TFA + 5.7% (v/v) H₂O (full squares and triangles); flow rate 4 ml/min, back pressure 8 MPa; detection: UV, 220nm. Compound number as in Table 5.1 169

Figure 5.S12 Influence of water on the separation of neutral compounds on SilicaShell column. Conditions: 80/20 CO₂/MeOH + 0.1% (v/v) TEA + 0.1% (v/v) TFA (empty squares and triangles); 80/20 CO₂/MeOH + 0.1% (v/v) TEA + 0.1% (v/v) TFA + 5.7% (v/v) H₂O (full squares and triangles); flow rate 4 ml/min, back pressure 8 MPa; detection: UV, 220nm. Compound number as in Table 5.1. 170

Figure 5.S13 Influence of water on the separation of acidic compounds on Xselect C18 SB column. Conditions: 80/20 CO₂/MeOH + 0.1% (v/v) TEA + 0.1% (v/v) TFA (empty squares and triangles); 80/20 CO₂/MeOH + 0.1% (v/v) TEA + 0.1% (v/v) TFA + 5.7% (v/v) H₂O (full squares and triangles); flow rate 4 ml/min, back pressure 8 MPa; detection: UV, 220nm. Compound number as in Table 5.1 171

Figure 5.S14 Influence of water on the separation of basic compounds on Xselect C18 SB column. Conditions: 80/20 CO₂/MeOH + 0.1% (v/v) TEA + 0.1% (v/v) TFA (empty squares and triangles); 80/20 CO₂/MeOH + 0.1% (v/v) TEA + 0.1% (v/v) TFA + 5.7% (v/v) H₂O (full squares and triangles); flow rate 4 ml/min, back pressure 8 MPa; detection: UV, 220nm. Compound number as in Table 5.1 172

Figure 5.S15 Influence of water on the separation of neutral compounds on Xselect C18 SB column. Conditions: 80/20 CO₂/MeOH + 0.1% (v/v) TEA + 0.1% (v/v) TFA (empty squares and triangles); 80/20 CO₂/MeOH + 0.1% (v/v) TEA + 0.1% (v/v) TFA + 5.7% (v/v) H₂O (full squares and triangles); flow rate 4 ml/min, back pressure 8 MPa; detection: UV, 220nm. Compound number as in Table 5.1 173

Figure 5.S16 Influence of water on the separation of acidic compounds on Xselect C18 SB column. Conditions: 90/10 CO₂/MeOH + 0.1% (v/v) TEA + 0.1% (v/v) TFA (empty squares and triangles); 90/10 CO₂/MeOH + 0.1% (v/v) TEA + 0.1% (v/v) TFA + 5.7% (v/v) H₂O (full squares and triangles); flow rate 4 ml/min, back pressure 8 MPa; detection: UV, 220nm. Compound number as in Table 5.1. 174

Figure 5.S17 Influence of water on the separation of neutral compounds on Xselect C18 SB column. Conditions: 90/10 CO₂/MeOH + 0.1% (v/v) TEA + 0.1% (v/v) TFA (empty squares and triangles); 90/10 CO₂/MeOH + 0.1% (v/v) TEA + 0.1% (v/v) TFA + 5.7% (v/v) H₂O (full squares and triangles); flow rate 4 ml/min, back pressure 8 MPa; detection: UV, 220nm. Compound number as in Table 5.1 175

Figure 5.S18 Discriminant analysis for FructoShell-N column with use of 90/10 CO₂/MeOH + 0.1% (v/v) TEA + 0.1% (v/v) TFA without and with addition of 5.7% (v/v) H₂O (A); SilicaShell column with use of 90/10 CO₂/MeOH + 0.1% (v/v) TEA + 0.1% (v/v) TFA without and with addition of 5.7% (v/v) H₂O (B); Xselect C18 SB column with use of 90/10 CO₂/MeOH + 0.1% (v/v) TEA + 0.1% (v/v) TFA without and with addition of 5.7% (v/v) H₂O (C) 176

Figure 6.1 Method development of chiral amines. Method development of chiral amines using SPP CSPs: CDShell-RSP (RSP), LarihcShell-P (LS-P), NicoShell (NS), and VancoShell (VS) in (A) reversed phase (RP) and (B) polar organic mode (POM). See Supplemental data for polar ionic mode (PIM) and normal phase (NP) method development and chromatographic parameter abbreviations (Rs, tR2), and section 2.1 for all solvent abbreviations (ACN, MeOH, AA, TEA, NH₄HCO₂). Other abbreviations include temperature (temp.) and Δ, which represents “switch to.” See Figure 6.S1 and section 6.S1 in Supplemental data for more information. 208

Figure 6.2 Baseline separations results of 150 chiral 1°, 2°, and 3° amines with four superficially porous particle (SPP) chiral stationary phases (CSPs). (A) Number of baseline separations by each CSP compared to the total amines tested. (B) Number of amines baseline separation by each or more than one CSP. See Results and Discussion for further explanation. 209

Figure 6.3 The principle of complementary separations. (A, B). The principle of complementary separations: the difference between (A) complementary and (B) unique complementary separations using (A) alprenolol and (B) tramadol. See Tables 1–3 for all chromatographic results. 210

Figure 6.4 Chromatographic enantioseparation of 18 racemic controlled substance stimulant amines using liquid chromatography electrospray-mass spectrometry (LC-ESI-MS). Total ion chromatogram (TIC) and extracted ion chromatograms (EIC) are shown. Conditions: CDShell-RSP, 150 x 4.6 mm (i.d.), ACN-NH₄HCO₂ (pH 3.6, 16 mM) (10:90), 0.4 mL/min, 25 °C. 1. rac-cathinone, 2. rac-3FMC, 3. rac-pentedrone, 4. rac-amphetamine, 5. rac-aminorex, 6. rac-methamphetamine, 7. rac-PMA, 8. rac-mephedrone, 9. rac-methylone, 10. rac-α-PVP, 11. rac-ethylone, 12. rac-4-MEC, 13. rac-MDA, 14. rac-pentylone, 15. rac-MDMA, 16. rac-3,4-DMMC,

17. rac-MDEA, 18. rac-4-EMC. See sections Experimental and Tables 6.1-3 for other acronyms and information. 212

Figure 6.S1 (A,B,C,D). Method development of chiral amines using SPP CSPs: CDShell-RSP (RSP), LarihcShell-P (LS-P), NicoShell 226

Figure 6.S2 Effect of temperature. All separations of methylone were performed with V, 100 x 4.6 mm (i.d.), at 1.0 mL/min using UV at 220 nm. Mobile phase conditions: MeOH-NH₄HCO₂ (100:0.1, v/w) [1] 30 °C, [2] 25 °C, [3] 15 °C, [4] 10 °C. 228

Figure 6.S3 (A,B,C,D): Effect of additives in reversed phase All separations were of methorphan with 100 x 4.6 mm (i.d.) columns: (A,B,D) RSP, (C) VS at 1.0 mL/min (except [5,6] at 0.5 mL/min) and 25 °C using UV at 230 nm. Mobile phase conditions: [1,3,5,7] ACN-NH₄HCO₂ (16 mM, pH 3.6) (30:70, v/v), [2] ACN-NH₄HCO₂ (16 mM, pH 3.6) (20:80, v/v), [4,6] MeOH-NH₄HCO₂ (16 mM, pH 3.6) (30:70, v/v), [7] ACN-NH₄HCO₂ (16 mM, pH [5.0]) (30:70, v/v), [8] ACN-NH₄HCO₂ (16 mM, pH [6.2]) (30:70, v/v). 228

Figure 6.S4 (A,B,C): Effect of additives in the polar organic mode. All separations were of 1-(1-naphthylethylamine) with 100 x 4.6 mm (i.d.) columns, (A) VS and (B,C) LS-P, at 1 mL/min and 25 °C using UV at 220 nm. [1,3,5] ACN-MeOH-AA-TEA (60:40:0.3:0.2, v/v/v/v), [2,4] ACN-MeOH-AA-TEA (80:20:0.3:0.2, v/v/v/v), [6] ACN-MeOH-TFA-TEA (90:10:0.3:0.2, v/v/v/v). See section 6.S1 for all abbreviations. 229

Figure 6.S5 (A,B): Effect of additives in the polar ionic mode: (A) salt additives and concentration effect (B) acid and base additive ratios. All separations of amphetamine were performed with V, 100 x 4.6 mm (i.d.), at 1.0 mL/min, and 25 °C using UV at 220 nm. Mobile phase conditions: [1] MeOH-NH₄TFA (100:0.1, v/w), [2] MeOH-NH₄HCO₂ (100:0.5, v/w), [3] MeOH-NH₄HCO₂ (100:0.1, v/w), [4] MeOH-NH₄HCO₂ (100:0.05, v/w), [5] MeOH-AA-TEA (100:0.1:0.1, v/v/v), [6] MeOH-AA-TEA (100:0.1:0.05, v/v/v), [7] MeOH-AA-TEA (100:0.1:0.02, v/v/v), [8] MeOH-AA-NH₄OH (100:0.1:0.02, v/v/v). See section 6.S1 for all abbreviations. 230

Figure 6.S6 (A,B): Effect of additives in normal phase. All separations were of cathinone with LS-P, 100 x 4.6 mm (i.d.), at 1 mL/min, and 25 °C using UV at 254 nm. [1] Hex-EtOH (70:30, v/v), [2] Hep-EtOH (70:30, v/v), [3] Hex-EtOH-TEA (70:30:0.1, v/v/v), [4] HexEtOH-TFA (70:30:0.1, v/v/v), [5] Hex-EtOH-TFA-TEA (70:30:0.3:0.2, v/v/v/v). See section 6.S1 for all abbreviations. 231

Figure 7.1 Ultra-fast LC enantioseparation of nicotine (NIC) using NicoShell, 50 x 4.6 mm (i.d.), PIM4 at 4 mL/min. S: S-NIC; R: R-NIC; t₀: impurities at dead time. See Materials and methods for other acronyms and calculations ($k_1 = 0.7$, $\alpha = 1.64$, $R_s = 2.6$). 248

Figure 7.2 Separation of ring-closed and ring-open equilibrating tobacco alkaloids. (A) OPBN (peak 1) to 5HCOT (peaks 2,3) (TIC scan from 110 to 220 m/z and product ion scan from 50 – 200 m/z) (B) NAN (peak 4) to MMYS (peak 5) (TIC scan from 150 – 220 m/z and product ion scan from 50 - 200 m/z) Conditions: CDSshell-RSP, 100 x 4.6 mm (i.d.), RP5, 1.0 mL/min, 25 °C. R.I.: Relative intensity, TIC: total ion chromatogram, SIM: selective ion monitoring. See Materials and methods for other acronyms and information. 253

Figure 7.3 Chromatographic separation and detection of 10 tobacco alkaloids (A) and 7 nicotine metabolites (B). Total ion chromatograms (TIC) and extracted ion chromatograms (EIC) are shown. (A) Conditions: NicoShell, 100 x 4.6 mm (i.d.), PIM4, 1 mL/min. Tobacco alkaloids: 1. β -NNT, 2. MYS, 3. BPY, 4. β -NT, 5. (S,R)-NIC, 6. MANB, 7. (S,R)-ANT, 8. (S,R)-ANB, 9. MET, 10. (R,S)-NNIC. (B) Conditions: TeicoShell, 150 x 4.6 mm (i.d.), POM3, 0.5 mL/min. Nicotine metabolites: 11. OPBA, 12. LAC, 13. rac-5THF, 14. (S,R)-COT, 15. T3HC, 16. rac-NCOT, 17. (S)-CNO. 255

Figure 7.4 The direct separation of tobacco-specific nitrosamines. R = R-NNN, S = S-NNN, E = E isomer, Z = Z isomer based on previous reports (see Discussion), see Materials and methods and *Table 7.1* for other acronyms used. (A) rac-NNAL, TeicoShell, 100 x 4.6 mm (i.d.), RP3, 0.3 mL/min, 25 °C. (B) NNK, CDSshell-RSP, 100 x 4.6 mm (i.d.), RP4, 1.0 mL/min, 25 °C. (C) rac-NNN, Q-Shell, 250 x 4.6 mm (i.d.), RP3, 0.3 mL/min, 25 °C. (D) R-NNN, Q-Shell, 250 x 4.6 mm (i.d.), RP3, 0.3 mL/min, 25 °C. 256

List of Tables

<i>Table 2.1</i> Chiral SFC screening protocol	18
<i>Table 2.2</i> Optimized chiral separations at backpressure 10 MPa	26
<i>Table 3.1</i> Effect of water on enantioseparation under super/subcritical conditions	54
<i>Table 3.S1</i> Solvatochromism effects in SFC with Nile Red Dye.	67
<i>Table 4.1</i> Comparison between methanol, ethanol and '190 proof' ethanol	84
<i>Table 4.2</i> Representative separations with methanol and azeotropic ethanol as modifiers	89
<i>Table 5.1</i> Analytes and their characteristics used in study	112
<i>Table 5.S1</i> Characteristics and measured data for compounds used for study on FructoShell-N stationary phase with use 90/10 CO ₂ /MeOH + 0.1% (v/v) TEA + 0.1% (v/v) TFA and 90/10 CO ₂ /MeOH + 0.1% (v/v) TEA + 0.1% (v/v) TFA +5.7% (v/v) H ₂ O mobile phases	137
<i>Table 5.S2</i> Characteristics and measured data for compounds used for study on FructoShell-N stationary phase with use 80/20 CO ₂ /MeOH + 0.1% (v/v) TEA + 0.1% (v/v) TFA and 80/20 CO ₂ /MeOH + 0.1% (v/v) TEA + 0.1% (v/v) TFA +5.7% (v/v) H ₂ O mobile phases	142
<i>Table 5.S3</i> Characteristics and measured data for compounds used for study on SilicaShell stationary phase with use 90/10 CO ₂ /MeOH + 0.1% (v/v) TEA + 0.1% (v/v) TFA and 90/10 CO ₂ /MeOH + 0.1% (v/v) TEA + 0.1% (v/v) TFA +5.7% (v/v) H ₂ O mobile phases	144
<i>Table 5.S4</i> Characteristics and measured data for compounds used for study on SilicaShell stationary phase with use 80/20 CO ₂ /MeOH + 0.1% (v/v) TEA + 0.1% (v/v) TFA and 80/20 CO ₂ /MeOH + 0.1% (v/v) TEA + 0.1% (v/v) TFA +5.7% (v/v) H ₂ O mobile phases	147

<i>Table 5.S5</i> Characteristics and measured data for compounds used for study on Poroshell 120 EC-C18 stationary phase with use 90/10 CO ₂ /MeOH + 0.1% (v/v) TEA + 0.1% (v/v) TFA and 90/10 CO ₂ /MeOH + 0.1% (v/v) TEA + 0.1% (v/v) TFA +5.7% (v/v) H ₂ O mobile phases	151
<i>Table 5.S6</i> Characteristics and measured data for compounds used for study on Xselect C18 SB stationary phase with use 80/20 CO ₂ /MeOH + 0.1% (v/v) TEA + 0.1% (v/v) TFA and 80/20 CO ₂ /MeOH + 0.1% (v/v) TEA + 0.1% (v/v) TFA +5.7% (v/v) H ₂ O mobile phases	154
<i>Table 5.S7</i> Characteristics and measured data for compounds used for study on Xselect C18 SB stationary phase with use 90/10 CO ₂ /MeOH + 0.1% (v/v) TEA + 0.1% (v/v) TFA and 90/10 CO ₂ /MeOH + 0.1% (v/v) TEA + 0.1% (v/v) TFA +5.7% (v/v) H ₂ O mobile phases	157
<i>Table 6.1</i> Optimized chiral separations of primary (1°) amines.	182
<i>Table 6.2</i> Optimized chiral separations of secondary (2°) amines.	192
<i>Table 6.3</i> Optimized chiral separations of tertiary (3°) amines.	202
<i>Table 6.S1</i> Chromatographic data referring to Supplemental figures S2, S3(A,B,C,D), S4(A,B,C), S5(A,B), S6(A,B).	232
<i>Table 7.1</i> Structures of nicotine-related compounds (all chiral compounds denoted by *).	242
<i>Table 7.2</i> Optimized enantiomeric separations of nicotine-related compounds using macrocyclic glycopeptides.	248

Contents

1. Acknowledgements	iii
2. Abstract	v
3. List of Illustrations	vii
4. List of Tables	xix
5. Chapter 1: Introduction	1
1.1 Parameters affecting chromatographic resolution	1
1.2 Superficially porous particles	5
1.3 Supercritical fluid chromatography	5
1.4 Fundamentals of green chemistry	8
1.5 Organization of the dissertation	10
1.6 References	10
6. Chapter 2: Fast Super/subcritical Fluid Chromatographic Enantioseparations on Superficially Porous Particles Bonded with Broad Selectivity Chiral Selectors Relative to Fully Porous Particles	13
2.1 Abstract	13
2.2 Introduction	14
2.3 Experimental	16
2.4 Results and Discussion	19
2.5 Conclusions	36
2.6 Acknowledgements	37
2.7 References	37
2.8 Supporting Information	41
7. Chapter 3: Ramifications and Insights on the Role of Water in Chiral Sub/Supercritical Fluid Chromatography	42

3.1 Abstract	42
3.2 Introduction	43
3.3 Experimental	45
3.4 Results and Discussion	47
3.5 Conclusions	64
3.6 Acknowledgements	65
3.7 References	65
3.8 Supporting Information	66
8. Chapter 4: Greener Super/subcritical Fluid Chromatography: Replacing Methanol as the Co-solvent for Chiral Separations	78
4.1 Abstract	78
4.2 Introduction	79
4.3 Experimental	81
4.4 Results and Discussion	85
4.5 Conclusion	101
4.6 Acknowledgements	102
4.7 References	102
4.8 Supporting Information	105
9. Chapter 5: Enhancing Supercritical Fluid Chromatographic Efficiency: Predicting Effects of Small Aqueous Additives	108
5.1 Abstract	108
5.2 Introduction	108
5.3 Experimental	110
5.4 Results and Discussions	115
5.5 Conclusion	134
5.6 Acknowledgement	134
5.7 References	135
5.8 Supplementary Information	138

10. Chapter 6: Effective methodologies for enantiomeric separations of 150 pharmacology and toxicology related 1°, 2°, and 3° amines with core-shell chiral stationary phases	177
6.1 Abstract	177
6.2 Introduction	177
6.3 Experimental	180
6.4 Results and Discussions	207
6.5 Conclusions	217
6.6 References	217
6.7 Supporting Information	220
11. Chapter 7: A comprehensive methodology for the chiral separation of 40 tobacco alkaloids and their carcinogenic E/Z-(R,S)-tobacco-specific nitrosamine metabolites	235
7.1 Abstract	235
7.2 Introduction	235
7.3 Materials and Methods	241
7.4 Results	247
7.5 Discussion	257
7.6 References	261
12. Chapter 8: Summary and Future Outlook	265
Appendix A: List of co-authors	266

CHAPTER 1

Introduction

1.1 Parameters affecting chromatographic resolution

The fundamental aim of chromatography is to completely resolve analyte peaks within the shortest possible time window.

The resolution *Equation (1.1)* highlights the terms that directly affect chromatographic separations¹

$$R_s = \left(\frac{\sqrt{N}}{4}\right) \left(\frac{\alpha - 1}{\alpha}\right) \left(\frac{k_2}{1 + k_2}\right) \quad \text{Equation (1.1)}$$

Where R_s represents the resolution between two peaks, 'N' represents the efficiency or the plate count, ' α ' represents the selectivity and ' k ' is the retention factor.¹ Optimization of selectivity or separation factor (α) has the greatest impact on chromatographic resolution. For this reason, chromatographers have historically engaged in research to develop new stationary phases to cope with the ever-increasing need for novel separations. Octadecyl or 'C18' is the most widely used stationary phase for achiral separations as it provides selectivity for a wide range of analytes.² However, chiral separations are much more complex and hence a wide range of chiral selectors including but not limited to polysaccharides, macrocyclic glycopeptides, and pi-complex compounds, have been developed to provide novel selectivity.³⁻⁶ Figure 1.1 shows the structures of some commonly used chiral selectors.

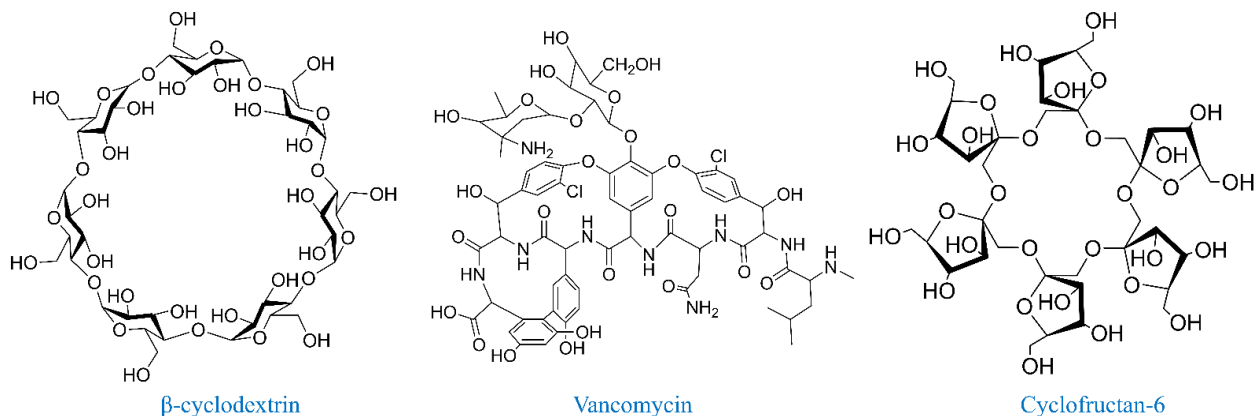


Figure 1.1 Structures of different chiral selectors

As is evident from Equation (1), the retention factor (k) also plays an important role in the resolution of peaks and for successful separation of components they must be retained to some degree. However, for values of $k > 5$, the influence of k on resolution (R_s) is relatively low.¹

The third factor influencing R_s is the number of theoretical plates (N). Equation (1.1) shows that there is a square root dependence of the number of theoretical plates on resolution. With an increasing number of novel compounds being produced every day, both in industry and academia, the need for high throughput separations are of utmost interest. Since retention factors are small for faster separations and most are limited to stationary phases that are commercially available, increasing efficiency to increase peak capacity is an obvious strategy.

This thesis focuses on the development of strategies to enhance ‘ N ’. If chromatographic peaks are Gaussian, efficiency is mathematically expressed as

$$N = 5.54 \left(\frac{t_R}{W_h} \right)^2 \quad \text{Equation (2.2)}$$

where t_R is the retention time of the analyte and W_h is the width of the peak at half height. Thus, for a given retention time, narrower peaks have higher efficiency. Since ‘ N ’ can be increased by

increasing the length of the column, plate height or ‘H’ has been commonly used in literature and in this thesis since it incorporates both efficiency and column length (L) and is mathematically expressed as:

$$H = L/N \qquad \text{Equation (3.3)}$$

Factors affecting efficiency at a given flow rate are (i) stationary phase packing, (ii) particle size of the stationary phase support and (iii) analyte diffusion coefficient.⁷

1.1 (i) Stationary phase packing

For a long time, stationary phase packing was considered as an art, but recent findings have changed the notion. Column packing can be considered as an ultrahigh pressure filtration process. Concentrated non-agglomerated slurries have been shown to yield high efficiencies for packed analytical and narrow bore columns.⁷

1.1 (ii) Particle size of stationary phase support

The van Deemter equation in chromatography expresses peak variance (width) as a summation of three factors as a function of linear velocity (u).⁸ Figure 1.2 is a representative van Deemter plot with plate heights plotted on the y-axis and linear velocity plotted on the x-axis. Mathematically it is expressed by

$$H = A + \frac{B}{u} + Cu \qquad \text{Equation (4.4)}$$

Where the ‘A’ is the term is the eddy diffusion parameter, the ‘B’ term represents longitudinal diffusion and the ‘C’ term is a summation of all factors contributing to resistance to mass transfer.

The ‘A’ term is related to particle diameter (d_p) by,

$$A = 2\lambda d_p \quad \text{Equation (5.5)}$$

Where ‘ λ ’ is the packing factor which is dependent on particle morphology and uniformity of the packing. The ‘B’ term is independent of particle diameter. The ‘C’ term has a square dependence on particle diameter and can be mathematically expressed as

$$C \propto \frac{d_p^2}{D_M} \quad \text{Equation (6.6)}$$

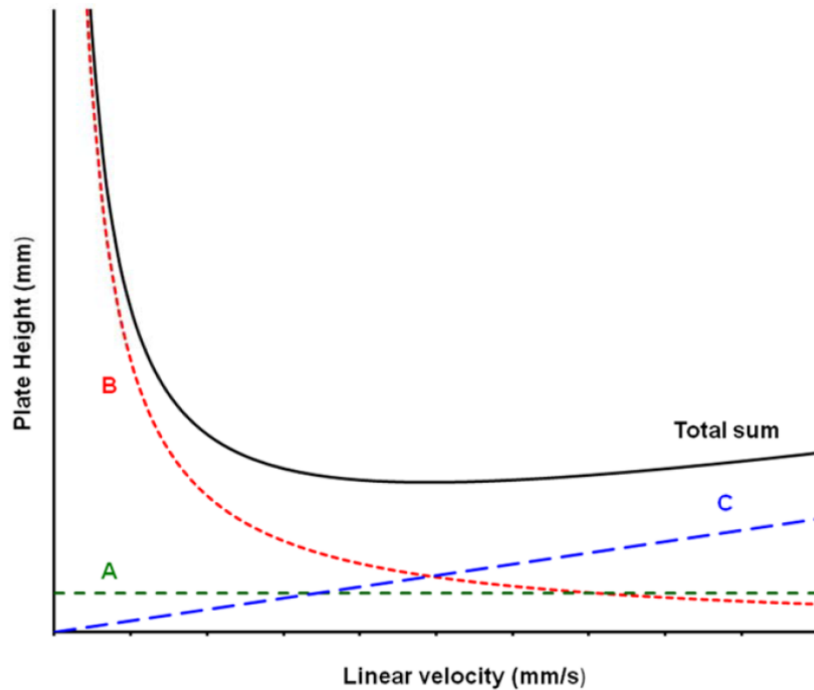


Figure 1.2. A typical van Deemter plot (solid line). The individual components are shown with dashed lines.⁹

Thus, smaller particle size stationary phase supports produce smaller plate heights or higher efficiencies. This has led column developers to use smaller particles. Before the 21st century, columns packed with 10 μm particles were commonplace, however currently particles as small as 1.9 μm are commercially available and widely used.¹⁰ A caveat in using smaller particles is the increased backpressure. This has led to a researcher to shift focus to other particle morphologies,

including superficially porous or core-shell particles, from the conventional fully porous particles.¹¹⁻¹² The details about fully porous particles will be given in a subsequent section.

1.1 (iii) Analyte diffusion and mass transfer kinetics

Mass transfer kinetics of analytes between the stationary phase and mobile phase has been deemed one the most important factors contributing to a column's performance. Many enantiomeric separations are known to have slow on-off kinetics and hence have historically resulted in lower efficiencies compared to achiral separations.

1.2 Superficially porous particles

Superficially porous particles (SPP) or core-shell particles were first proposed by Csaba Horvath about 50 years ago.¹³ These particles have a solid impenetrable core surrounded by a porous layer. Gritti and Guichon reported that all the terms i.e. 'A' term or eddy dispersion term, 'B' term or longitudinal diffusion term, and 'C' term or resistance to mass transfer kinetics term are lower for the SPPs compared to the fully porous counterpart, thus leading to higher efficiencies.¹⁴⁻¹⁵ However, the stated work also noted that at linear velocities above the optimal linear velocity, decreases in the 'B' and 'C' terms are negligible and the decrease of the 'A' term predominates. Commercially introduced in 2007, 2.7 μm SPPs showed efficiencies comparable to sub 2 μm FPPs while providing much lower backpressures.

However, a vast majority of the methods for enantiomeric separations currently in use have not incorporated the advantages offered by these superficially porous particles. This is mostly due to the lack of commercialization of these stationary phases. But with recent commercialization, the need for new chiral separation methods incorporating the advantages of SPPs is essential for high throughput experimentation.

1.3 Supercritical fluid chromatography

Supercritical fluid chromatography (SFC) was first introduced by Ernst Klesper in the early 1960s and was initially named as high pressure gas chromatography.¹⁶ During the early years of development of SFC, pure supercritical fluid was used as the mobile phase. The most commonly used supercritical fluid is carbon dioxide since it has an easily accessible supercritical point. The critical temperature and pressures for carbon dioxide are 31°C (304.13 K) and 73.8 bar (7.38 MPa). Other gas with accessible supercritical points such as N₂O (critical temperature: 36.4°C and critical pressure: 72.45 bar) and NH₃ (critical temperature: 132.4°C and critical pressure: 112.8 bar) proved to be hazardous because of the risk of explosion.

Carbon dioxide can interact with a variety of analytes using acid-base interactions and induced dipole interactions. However, carbon dioxide has limited solubility for most analytes commonly encountered in industry and academia along with a very low polarity comparable to n-pentane as measured with solvatochromic dyes like Nile Red and Reichardt's dye.¹⁷ To overcome this limitation of SFC, an organic modifier is routinely employed in addition to supercritical CO₂. Such mobile phase mixtures produce peaks with good peak shapes and acceptable retention times. A small amount of organic acid or base or even sometimes water additives are included and have proved to positively influence selectivity, decrease retention times and increase efficiency.

Supercritical fluid chromatography has been rapidly gaining prominence both in academia and industry. With the advent of better instrumentation in the mid-1980s, according to Web of Science the number of publications increased from 2 a year in 1980 to about 330 publications in 2019. The rapid rise in research and development involving SFC is a result of a variety of factors. Most notably, since SFC uses non-toxic supercritical CO₂ as the major component of the mobile phase, far less environmentally hazardous organic solvents are consumed. Along with this, the lower

viscosity and the higher diffusivity leads to faster and more efficient separations.¹⁸ It is also important to note that liquid chromatographic separations often use mass spectrometry detection for identification of compounds. SFC which was originally conceived as an alternative to normal phase liquid chromatography (NPLC) is mass spectrometry compatible unlike NPLC. As mentioned earlier, an inherent characteristic for most enantiomeric separations is the low mass transfer kinetics, hence SFC is rapidly becoming the technique of choice for chiral separations.

1.3.1 Superficially porous particles for SFC

As discussed, SPPs result in reduction of all three terms contributing to band broadening. On the other hand, in SFC the contributions from 'B' and 'C' term are significantly lower than HPLC due to the enhanced diffusivity and reduced viscosity of the supercritical CO₂ mobile phase. This may lead us to believe that the SPPs may not result in superior performance compared to FPPs. However, SPPs also offer lower contributions from the 'A' term which dominates the contribution to band broadening at high flow rates. Since SFC is mostly operated under flow rates much higher than the van Deemter optima, the use of SPPs can result in better performance. Chapter 2 of this thesis discusses in detail the effect of using SPPs as compared to FPPs in SFC.

1.3.2 Water as an additive in SFC

Organic acids and bases like acetic acid, trifluoroacetic acid, triethyl amine, and diethyl amine are commonly used in SFC as additives in order to influence selectivity, retention and efficiency by competing with the analyte for the active sites on the stationary phase.¹⁹⁻²¹ The use of water as an additive is a recent development. Though the first reported use can be traced back to a patent in the 1970s, a resurgence in the research with water additive is quite recent.²²⁻²³ In the 1990s researchers tried to use water as a modifier in SFC mobile phase by trying to saturate carbon

dioxide with the water. Though this approach yielded novel selectivity, it failed to generate widespread enthusiasm due to the low solubility of water in carbon dioxide and the poor reproducibility of the technique.

The addition of methanol to carbon dioxide significantly increases the solubility of water in this mobile phase. It has been reported that higher alcohols like isopropanol result in higher water solubility.²⁴ Water has been reported to be beneficially as an additive often by providing hydrogen bonds in addition to the organic modifier and also results in the formation of carbonic acid. The most common reason for the addition of water to SFC mobile phase is to aid in the solubility of polar analytes. The use of water for achiral separations was shown to enhance efficiency and decrease retention times in some cases and in other cases exhibited no significant advantages.²⁵⁻²⁶

Chapters 3 and 5 of this dissertation focuses on the effect of addition of small amounts of water to the mobile phase for enantiomeric separations and achiral separations under SFC conditions, respectively.

1.4 Fundamentals of green chemistry

With the growing concern over the increasing impact of humans in polluting the environment, researchers aimed at mitigating such effects by designing products and processes to reduce the use hazardous substances. The basic principles of green chemistry as defined by the U.S. Environment Protection Agency (EPA) are: (i) prevent pollution at a molecular level, (ii) a philosophy that applies to all areas of chemistry, not a single discipline of chemistry, (iii) applies innovative scientific solutions to real-world environmental problems, (iv) results in source reduction because it prevents the generation of pollution, (v) reduces the negative impacts of chemical products and processes on human health and the environment, (vi) lessens and sometimes eliminates hazards

from existing products and processes, and (vii) designs chemical products and processes to reduce their intrinsic hazards.

The principles of green chemistry fundamentally differ from the field of cleaning up pollution. The focus is minimizing or eliminating hazardous chemicals at the source rather than devising strategies to clean up, post pollution. A greener analytical technique must satisfy the three 'R' criteria which entails (i) 'R'eduction of solvent consumed and waste generated, (ii) 'R'eplacement of commonly used solvents with a greener alternative, and (iii) 'R'ecycling of materials used.

1.4.1 Green chemistry implication of SFC

As discussed earlier, due to the lower environmental impact of carbon dioxide and its use as the majority mobile phase for SFC, SFC is being hailed as a greener technique as compared to HPLC. However, since pure carbon dioxide is unable to elute most commonly encountered analytes the addition of a polar alcohol becomes necessary. Methanol has been the most widely used alcohol for eluting compounds. It is the most polar alcohol and leads to a higher polarity of the bulk mobile phase. With the recent focus on high throughput separations, the amount of methanol being used in the SFC mobile phase has significantly increased. Methanol significantly reduces the 'greenness' of the technique since methanol is produced from natural gas which is a non-renewable source. In addition, methanol is highly toxic when ingested and can cause blindness and even death in severe cases. Also, according to the widely followed Prat *et al.*'s solvent selection guide for 51 solvents, methanol is not listed as a recommended solvent.²⁷

On the contrary, ethanol is mostly produced by fermentation of corn and is nontoxic to humans. However, previous studies with ethanol as the modifier showed decreased chromatographic efficiencies and increased retention times especially with macrocyclic glycopeptide stationary

phases. To solve this problem this thesis proposes the use of minimum boiling azeotropic ethanol as an alternative. Azeotropic ethanol contains 95.63% ethanol and 4.37% water by weight. The word azeotrope is derived from Greek and means constant boiling. A minimum boiling azeotrope such as ethanol-water boils at 78.2°C which is lower than the boiling point of both ethanol (78.4°C) and water (100°C). It is greener as compared to methanol and costs a fraction of the amount. It is also readily available and can be purified using simple distillation.

1.5 Organization of the dissertation

The primary goal of this thesis is to outline strategies that result in increased chromatographic efficiency allowing high throughput experimentation. Chapter 2 discusses advantages of using superficially porous particles in SFC. It also demonstrates new methods for enantiomeric separation of one hundred pharmaceutically relevant small molecules using macrocyclic chiral selectors bound to superficially porous particles. Chapter 3 discusses the fundamentals of the effect of water on the efficiency and retention time of enantioseparations and highlights the differences in effects produced with different stationary phase chemistries. In Chapter 4 a simple method to make SFC more environmentally friendly by substituting toxic methanol with azeotropic ethanol. Chapter 5 discusses the effect of water on achiral separations with four different stationary phases with widely different polarities in SFC. Chapter 6 discusses novel methodologies for enantioseparation using superficially porous particles. Chapter 7 discusses a novel stationary phase used to separate a wide range of nicotine related compounds. Chapter 8 concludes the thesis with a summary and future outlook.

1.6 References

1. Sandra, P., Resolution–definition and nomenclature. *J. High Resolut. Chromatogr.* **1989**, *12* (2), 82-86.

2. Molnar, I.; Horváth, C., Reverse-phase chromatography of polar biological substances: separation of catechol compounds by high-performance liquid chromatography. *Clin. Chem.* **1976**, 22 (9), 1497-1502.
3. Welch, C. J., Evolution of chiral stationary phase design in the Pirkle laboratories. *J. Chromatogr. A* **1994**, 666 (1-2), 3-26.
4. Okamoto, Y.; Aburatani, R.; Miura, S.-I.; Hatada, K., Chiral Stationary Phases for HPLC: Cellulose Tris (3, 5-dimethylphenylcarbamate) and Tris (3, 5-dichlorophenylcarbamate) Chemically Bonded to Silica Gel*. *J. Liq. Chromatogr.* **1987**, 10 (8-9), 1613-1628.
5. Okamoto, Y., Separate optical isomers by chiral HPLC. *Chemtech* **1987**, 17 (3), 176-181.
6. Armstrong, D. W.; Tang, Y.; Chen, S.; Zhou, Y.; Bagwill, C.; Chen, J.-R., Macrocyclic antibiotics as a new class of chiral selectors for liquid chromatography. *Anal. Chem.* **1994**, 66 (9), 1473-1484.
7. Wahab, M. F.; Patel, D. C.; Wimalasinghe, R. M.; Armstrong, D. W., Fundamental and practical insights on the packing of modern high-efficiency analytical and capillary columns. *Anal. Chem.* **2017**, 89 (16), 8177-8191.
8. Van Deemter, J.; Zuiderweg, F.; Klinkenberg, A. v., Longitudinal diffusion and resistance to mass transfer as causes of nonideality in chromatography. *Chem. Eng. Sci.* **1956**, 5 (6), 271-289.
9. Wahab, M. F., Development of High Efficiency and New Selectivity Liquid Chromatographic Phases for the Separation of Ionic and Hydrophilic Analytes. **2013**.
10. Barhate, C. L.; Wahab, M. F.; Breitbach, Z. S.; Bell, D. S.; Armstrong, D. W., High efficiency, narrow particle size distribution, sub-2 μm based macrocyclic glycopeptide chiral stationary phases in HPLC and SFC. *Anal. Chim. Acta* **2015**, 898, 128-137.
11. Spudeit, D. A.; Dolzan, M. D.; Breitbach, Z. S.; Barber, W. E.; Micke, G. A.; Armstrong, D. W., Superficially porous particles vs. fully porous particles for bonded high performance liquid chromatographic chiral stationary phases: isopropyl cyclofructan 6. *J. Chromatogr. A* **2014**, 1363, 89-95.
12. Patel, D. C.; Breitbach, Z. S.; Wahab, M. F.; Barhate, C. L.; Armstrong, D. W., Gone in seconds: praxis, performance, and peculiarities of ultrafast chiral liquid chromatography with superficially porous particles. *Anal. Chem.* **2015**, 87 (18), 9137-9148.
13. Horvath, C. G.; Preiss, B.; Lipsky, S. R., Fast liquid chromatography. Investigation of operating parameters and the separation of nucleotides on pellicular ion exchangers. *Anal. Chem.* **1967**, 39 (12), 1422-1428.
14. Gritti, F.; Guiochon, G., Possible resolution gain in enantioseparations afforded by core-shell particle technology. *J. Chromatogr. A* **2014**, 1348, 87-96.
15. Gritti, F., Quantification of individual mass transfer phenomena in liquid chromatography for further improvement of column efficiency. *LC-GC North America* **2014**, 32, 928-940.
16. Klesper, K., High pressure gas chromatography above critical temperatures. *J. Org. Chem.* **1962**, 27, 700-701.
17. Deye, J. F.; Berger, T. A.; Anderson, A. G., Nile Red as a solvatochromic dye for measuring solvent strength in normal liquids and mixtures of normal liquids with supercritical and near critical fluids. *Anal. Chem.* **1990**, 62 (6), 615-622.
18. Gere, D. R., Supercritical fluid chromatography. *Science* **1983**, 222 (4621), 253-259.
19. Berger, T. A.; Deye, J. F., Role of additives in packed column supercritical fluid chromatography: suppression of solute ionization. *J. Chromatogr. A* **1991**, 547, 377-392.

20. Berger, T. A., Separation of polar solutes by packed column supercritical fluid chromatography. *J. Chromatogr. A* **1997**, 785 (1-2), 3-33.
21. Lesellier, E.; Gurdale, K.; Tchaplal, A., Phase ratio and eluotropic strength changes on retention variations in subcritical fluid chromatography (SubFC) using packed octadecyl columns. *Chromatographia* **2002**, 55 (9-10), 555-563.
22. Roselius, R.; Vitzthum, O.; Hubert, P., Selective extraction of nicotine from tobacco. *German patent* **1973**, 2, 15.
23. Pyo, D., Separation of vitamins by supercritical fluid chromatography with water-modified carbon dioxide as the mobile phase. *J. Biochem. Biophys. Meth.* **2000**, 43 (1-3), 113-123.
24. Li, J.; Thurber, K. B., A comparison of methanol and isopropanol in alcohol/water/CO₂ mobile phases for packed column supercritical fluid chromatography. *Can. J. Anal. Sci. Spectrosc.* **2008**, 53 (2), 59-65.
25. Liu, J.; Regalado, E. L.; Mergelsberg, I.; Welch, C. J., Extending the range of supercritical fluid chromatography by use of water-rich modifiers. *Org. Biomol. Chem.* **2013**, 11 (30), 4925-4929.
26. Liu, J.; Makarov, A. A.; Bennett, R.; Haidar Ahmad, I. A.; DaSilva, J.; Reibarkh, M.; Mangion, I.; Mann, B. F.; Regalado, E. L., Chaotropic Effects in Sub/Supercritical Fluid Chromatography via Ammonium Hydroxide in Water-Rich Modifiers: Enabling Separation of Peptides and Highly Polar Pharmaceuticals at the Preparative Scale. *Anal. Chem.* **2019**, 91 (21), 13907-13915.
27. Prat, D.; Hayler, J.; Wells, A., A survey of solvent selection guides. *Green Chem.* **2014**, 16 (10), 4546-4551.

Chapter 2

Fast Super/subcritical Fluid Chromatographic Enantioseparations on Superficially Porous Particles Bonded with Broad Selectivity Chiral Selectors Relative to Fully Porous Particles

2.1 Abstract

Superficially porous particles (SPPs) have shown advantages in enantiomeric separations in HPLC by conserving selectivity while providing higher efficiency separations with significantly reduced analysis times. The question arises as to whether the same advantages can be found to the same extent in super/subcritical fluid chromatography. In this work, the low viscosity advantage of carbon dioxide/MeOH mixtures is coupled with high-efficiency 2.7 μm superficially porous particles for enantiomeric separations. Given the fact that the viscosity of the mobile phase is typically ten times lower than liquid mobile phases it is possible to use flow rates as high as 14 mL/min on 5 cm packed columns. Superficially porous particles (SPPs) were grafted with teicoplanin (TeicoShell), a chemically modified macrocyclic glycopeptide (NicoShell), vancomycin (VancoShell), and isopropyl derivatized cyclofructan-6 (LarihcShell-P). One hundred chiral analytes were separated in a very short time frame, as little as 0.2 minutes (13 seconds). Even shorter separations can be obtained with advances in SFC instrumentation. The LarihcShell-P is the only chiral crown ether-based selector which showed high selectivity for primary amines. The Teicoshell column offered unique separations for acidic and neutral analytes. The NicoShell and the VancoShell were useful in separating amine (secondary and tertiary) containing pharmaceutical drugs and controlled substances. By chemically modifying a macrocyclic glycopeptide (NicoShell) we report the first enantiomeric separation of nicotine under SFC conditions within 3 minutes with a resolution of >3 . Additionally, van Deemter plots are constructed comparing the fully porous particles and superficially porous particles bonded with

the same chiral selectors. In toto the SPP advantages also were found for SFC. However instrumental shortcomings involving extra column effects and high pressure limitations need to be addressed by instrument manufacturers to realize the full advantages of SPPs and other smaller particle supports.

2.2. Introduction

Traditionally the focus of enantiomeric separations was to develop broad selectivity chiral stationary phases for various classes of compounds [1-5]. In the last few years, the goals have shifted to reducing analysis times and increasing the efficiency of these chromatographic processes[6-9]. A significant step forward in that direction has been the introduction of superficially porous particles (SPPs) or core-shell particles. Core shell particles albeit of a higher size were first used by Hovarth and Kirkland about 50 years ago[10, 11]. Recent theoretical studies by Gritti and Guichon attributed the higher efficiency of the SPPs due to the reduction of all three terms in the van Deemter equation namely, eddy dispersion (A term), longitudinal diffusion (B term), and solid-liquid mass transfer resistance (C term) that contribute to band broadening [12]. According to their studies, column efficiency is more sensitive to the adsorption-desorption process only when the adsorption rate constant is small (10000 s^{-1}), which implies slow adsorption-desorption kinetics. This is indeed the case with many enantiomeric separations. Hence switching from fully porous particles (FPPs) to SPP chromatographic supports offered a gain in resolution resulting from B and C terms. Contributions from B term is smaller for core shell particles due to the impenetrable solid core occupying 25% of the column volume and disallowing sample diffusion across this volume, and C term is also smaller in core shell particles as average diffusion length across the core shell particle is smaller. However it was noted that at speeds above optimal velocities the gain from this term is negligible[13]. Another important parameter, the A term is

much smaller for core shell particles than for the fully porous particles. Reduction in long-range eddy dispersion led to gains in efficiencies in columns packed with core-shell particles[13]. At higher reduced velocities, the eddy dispersion contribution to band broadening is significantly lower for SPPs [13]. Experimental evidence involving SPP supports for enantiomeric separations under HPLC conditions point to their superiority, providing higher efficiency and reduced analysis times[14].

SFC has emerged as an alternative to normal phase enantiomeric separations by HPLC primarily due its “green” nature by using very small amounts of organic solvents [15]. Unlike normal phase liquid chromatography, the CO₂/MeOH is compatible with electrospray ionization and mass spectrometry detection. An additional advantage of its lower viscosity is that it is possible to use higher flow rates on analytical columns (e.g., 14 mL/min on 5 x 4.6 mm id, 2.7 μm SPP) [16]. With the success of SPP supports in HPLC a natural question arises as to whether the aforementioned SPP advantages in HPLC enantiomeric separations also occur with supercritical fluid chromatography (SFC). As predicted by theory the contributions from ‘B’ and ‘C’ terms are relatively low at high linear velocities and with fast mass transfer kinetics. Hence under SFC conditions, it would seem that efficiency gains from these terms would be minimal for SPPs as compared to their fully porous particle counterparts. However, a gain in efficiency from the smaller eddy diffusion term is expected for the SPPs even under SFC conditions. A few reports have investigated the use of SPPs under SFC conditions for achiral chromatography and found them to be superior compared to the FPPs[17-21]. Reports comparing 2.6 μm SPPs with 1.8 μm FPPs observed both higher efficiency and lower pressure drops for the core shell particles[20, 21]. However similar extensive studies are lacking in chiral chromatography due to the limited commercialization of chiral stationary phases bonded to SPPs. Previous reports using SPPs for

enantiomeric separations have shown separations of a selected number of compounds in SFC, but they did not discuss whether it provides the broad benefits characteristic of HPLC[7, 22, 23].

The aim of this work is to study the relative merits of 2.7 μm SPPs for enantiomeric separations under super/subcritical conditions. Though studies comparing SPPs and FPPs under SFC condition exist for achiral chromatography, such studies are few in regard to enantiomeric separations. This study encompasses four different chiral stationary phases comprised of native macrocyclic glycopeptides namely VancoShell and TeicoShell, a modified macrocyclic glycopeptide namely NicoShell, and a derivatized cyclofructan namely LarihcShell-P. These SPP stationary phases have been previously tested in liquid chromatography and have separated enantiomers of chiral compounds with high selectivities, high efficiencies and much shorter retention times. In this study, we report the rapid SFC separation of one hundred chiral compounds that contain a wide array of functionalities. This work is the first instance of a NicoShell chiral stationary phase being used in supercritical fluid chromatography. The 2.7 μm SPPs used in this study and the commercially available 5 μm fully porous particles have been compared using van Deemter curves in order to document the differences offered by the change in morphology of the chromatographic supports.

2.3 Experimental

2.3.1 SFC Instrumentation

A Jasco 2000 series SFC (SFC-2000-7) equipped with a carbon dioxide pump (PU-2086), a modifier pump (PU-2086), a back-pressure regulator (BP-2080) with a heat controller (HC-2068-01), an autosampler (AS-2059-SFC) which was modified by installing a 2 μL injection loop to reduce extra column band broadening, a column oven (CO-2060) and a variable-wavelength high

pressure compatible UV detector (UV-2075) was used for all SFC analyses. The carbon dioxide pump was chilled to -10 °C using a Julabo chiller. The back-pressure regulator was maintained at 10 MPa, and the heat controller was maintained at 60°C. Data analysis was conducted using ChromNAV (1.17.01 Build 8) connected via an LC-NET II/ADC. Time accumulation (moving average) filter[24] was used in UV detector setting along with a 100 Hz data collection rate with a 0.0005 min response time to minimize instrumental artifacts and avoid peak distortion. All tubing used had an internal diameter of 254 µm. The plumbing was maintained throughout the system to get maximum efficiency according to previous findings [23].

2.3.2 Chiral Stationary Phases and Analytes

TeicoShell (10cm x 0.46cm), LarihcShell-P (10 x 0.46cm), VancoShell (10 x 0.46cm, 15 x 0.46cm) and NicoShell (10 x 0.46cm, 15 x 0.46cm) columns were obtained from AZYP LLC. (Arlington, USA). The different column chemistries were bonded to 2.7 µm superficially porous particles. Chirobiotic T column (10 x 0.46cm) with 5µm fully porous particles was obtained from Supelco Inc (Bellefonte, PA, USA). Analytes used in the study were obtained from different manufacturers namely Cerilliant Corporation (Round Rock, TX, USA), Sigma-Aldrich (St. Louis, MO, USA) and LKT laboratories (Minneapolis, MN, USA). Analytes were dissolved in methanol (concentration between 1 and 5 mg/mL)

2.3.3 Other Chemicals

SFC-grade carbon dioxide was purchased from AirGas (Radnor, PA, USA) in cylinders equipped with full-length eductor tube. All other solvents were purchased from Sigma-Aldrich (St. Louis, MO, USA).

2.3.4 Screening Protocol

All analytes on all columns were screened under isocratic conditions with temperatures varying between 25°C to 35°C. All the columns were screened under conditions specified in *Table 2.1*. Different additives like trifluoroacetic acid (TFA), triethylamine (TEA), ammonium formate, and water were added in different proportions. These additives helped improve peak shapes and managed to elute the peaks faster. For the tested stationary phases, a combination of the acidic TFA and the basic TEA seems to yield the best results instead of the individual use of either in most of the enantiomeric separations as has been previously observed for macrocyclic glycopeptides and also other class of chiral stationary phases[25, 26].

Table 2.1: Chiral SFC screening protocol

Chromatographic Parameters	Description
1. Carbon dioxide/modifier ratio	75/25 (% v/v)
2. Screening mobile phases	75/25 CO ₂ /Methanol 75/25 CO ₂ /Methanol-0.1(% v/v) triethylamine 75/25 CO ₂ /Methanol-0.1(% w/v) ammonium formate 75/25 CO ₂ /Methanol-0.1(% v/v) trifluoroacetic acid 75/25 CO ₂ /Methanol-0.1(% v/v) triethylamine-0.1(% v/v) trifluoroacetic acid 75/25 CO ₂ /Methanol-(0.2% v/v) triethylamine-(0.3% v/v) trifluoroacetic acid
3. Detector	UV detection at 220 and 254 nm
4. Flow rate	4 mL/min
5. Injection volume	2 µL
6. Column temperature	30°C
7. Sample concentration	Approximately 1 mg/mL
8. Backpressure	10 MPa
9. Runtime	10 mins
10. Stationary phases	TeicoShell, LarihcShell-P, NicoShell, VancoShell

2.4 Results and discussion

Chiral chromatography has undergone a paradigm shift in regards to analysis time and efficiency. Advances in instrumentation involving super/sub-critical fluid chromatography for chiral separation have played a considerable role in this regard. The following section discusses the screening protocol for TeicoShell (TS), VancoShell (VS), NicoShell (NS), and LarihcShell-P (LP) columns and the optimization of one hundred chiral analytes with different functionalities focusing on amines (primary, secondary and tertiary) due to their immense importance in the pharmaceutical industry as well as their high occurrence in natural products. The goal for all the reported separations was to achieve baseline resolution ($R_s = 1.5$) in the shortest possible time.

2.4.1 Effect of Column Backpressure

One of the key differences in instrumentation between LC and SFC is the addition of a back pressure regulator which maintains the carbon dioxide in its pressurized state. The change in backpressure regulator setting changes the overall backpressure on the SFC system thereby affecting the mobile phase density. Our results show a noticeably decreases in retention factor with increase backpressure (*Figure 2.S1*) and is in agreement with previous results where the effect has been studied in detail[27].

2.4.2 Optimized chiral separations

This study incorporates a wide range of compounds having different functionalities. The baseline separation of a variety of compounds shows the effectiveness of the tested CSPs. *Table 2.2* shows 100 compounds which have been baseline separated using the aforementioned four chiral stationary phases. Though several compounds were separated by multiple stationary phases, only the best separation with regards to time and selectivity has been reported in *Table 2.2*. As will be

discussed, in some cases a separation could only be obtained on one of the studied chiral stationary phases.

2.4.2.1 LarihcShell-P

LarihcShell-P (LP) columns use alkyl derivatized cyclofructans as the chiral selector[3]. This stationary phase possesses a crown ether core which helps in chiral recognition. However, unlike most synthetic chiral crown ethers which separate primary amines only under reversed phase conditions[28], the LarihcShell-P provides enantioseparations only with variety of polar organic and normal phase solvents[3, 29]. Further, it is not necessary for the primary amine to be protonated (ammonium ion form) to have inclusion complexation and chiral recognition as it is for synthetic chiral crown ether stationary phases in the reversed phase mode [28]. Hence this stationary phase has high potential for use in SFC conditions. To the best of our knowledge, there is no other chiral crown ether based column that provides chiral recognition and separations under SFC conditions[3, 29]. In this work, a variety of pharmaceutically relevant controlled substances containing a primary amine functional group, like norephedrine (*Figure 2.1E*), normetanephrine, and octopamine have been separated using this stationary phase (see *Table 2.2* for conditions). Also, native amino acids like tryptophan and phenylalanine were baseline separated using the derivatized cyclofructan based stationary phase (LP). Additives play a significant role in optimizing SFC enantiomeric separations. Though analytes were screened with multiple mobile phases a combination of 0.3% trifluoroacetic acid, and 0.2% triethylamine provided the best enantioselectivity and peak shapes when using LarihcShell-P stationary phase. *Figure 2.2* illustrates the effect of additives with the LarihcShell-P column using the analyte 1-(1-naphthyl) ethylamine as a representative example. *Figure 2.2A* shows that while using 0.1% triethylamine as an additive in the modifier baseline separation could not be achieved and chromatographic

efficiency was poor. The separation and peak shape improved with 0.1% trifluoroacetic acid additive but baseline separation and good peak shapes still could not be obtained as is evident from *Figure 2.2B*. The combination of 0.1% triethylamine and 0.1% trifluoroacetic acid, improved the peak shapes slightly but provided only a partial separation as shown in *Figure 2.2C*. This is possibly because carbon dioxide and methanol provide an acidic environment which protonates TEA which in turn competes with the analyte for primary adsorption sites thereby reducing analysis time and improving peak shapes. With a combination of 0.3% trifluoroacetic acid and 0.2%, triethylamine baseline separation was achieved with very good enantioselectivity, good peak shape and high efficiency along with reduced analysis time (*Figure 2.2D*). Also, it should be noted that ammonium ion (NH_4^+), should not be used with this CSP as they compete with the analyte and negate chiral recognition. Multiple analytes separated with LarihcShell-P were separated at a temperature lower than the screening temperature of 30°C in order to improve efficiency and peak shapes. Though this may be counterintuitive as common knowledge suggest faster mass transfer kinetics leading to sharper peaks at higher temperatures, the effect observed here could be a result of radial temperature gradient arising from the cooling effect of the fluid depressurization along the column. As has been seen previously with ODS bonded phases, the temperature gradient is higher for SPPs due to the higher pressure drops along columns packed with these particles resulting in lower efficiencies at higher temperature[30].

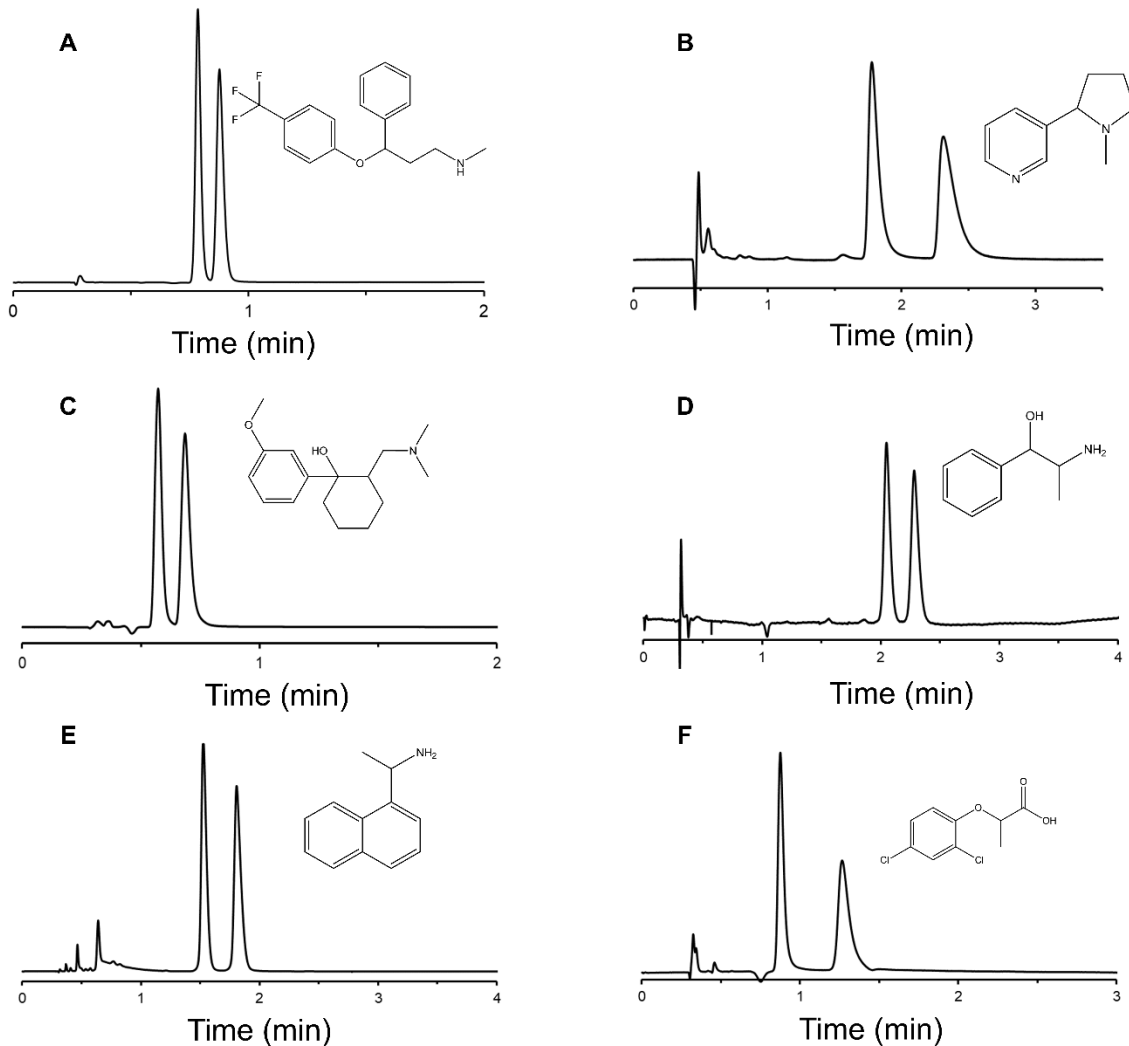


Figure 2.1. Representative chromatograms on different stationary phases (A) VancoShell (10cmX0.46cm) Analyte: Fluoxetine M.P.- 75/25 CO₂/MeOH- 3% water- 0.1% TEA- 0.1% TFA, 4 ml/min, T= 30°C (B) NicoShell (10cmX0.46cm) Analyte: Nicotine M.P.- 60/40 CO₂/MeOH- 0.1% TEA , 4 ml/min, T= 30°C (C) NicoShell (10cmX0.46cm) Analyte: Tramadol M.P.- 60/40 CO₂/MeOH- 0.2% TEA- 0.3% TFA , 4 ml/min, T= 30°C (D) LarihcShell (10cmX0.46cm) Analyte: Norephedrine M.P.- 80/20 CO₂/MeOH- 0.2% TEA- 0.3% TFA , 4 ml/min, T= 25°C (E) LarihcShell (10cmX0.46cm) Analyte: 1-(1-Naphthyl)ethylamine M.P.- 80/20 CO₂/MeOH- 0.2%

TEA- 0.3% TFA , 4 ml/min, T= 25°C (F) TeicoShell (10cmX0.46cm) Analyte: Dichloroprop M.P.-
60/40 CO₂/MeOH- 0.1% ammonium formate, 4 ml/min, T= 30°C UV detection at 254 nm

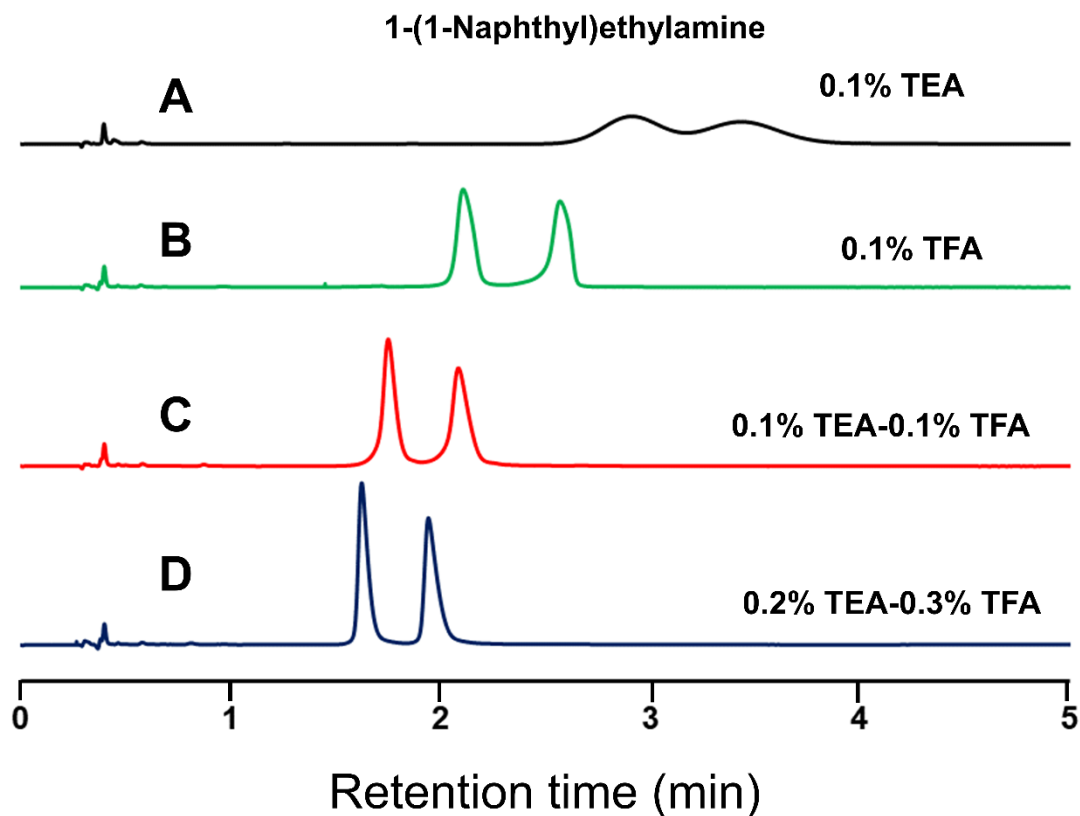


Figure 2.2. Effect of additives on the separation of the enantiomers of 1-(1-Naphthyl)ethylamine ,
Chromatographic conditions: LarihcShell-P, (10×0.46 cm), 4 ml/min, 10 MPa backpressure, 25
°C, UV detection at 254 nm. Mobile phase: (A) 80/20 CO₂/MeOH- 0.1% TEA (B) 80/20
CO₂/MeOH- 0.1% TFA (C) 80/20 CO₂/MeOH- 0.1% TEA- 0.1% TFA (D) 80/20 CO₂/MeOH-
0.2% TEA- 0.3% TFA

2.4.2.2 TeicoShell

The TeicoShell column was the stationary phase of choice in separating acidic and neutral compounds[26, 31]. TeicoShell stationary phases showed high selectivity for oxazolidinones

which are mainly used as antimicrobials. These neutral oxazolidinones did not require an additive for their baseline separation. However, the addition of a small amount of ammonium formate to methanol (0.1% w/v) as a mobile phase additive resulted in faster separations albeit with a loss of resolution. In order to achieve fast separations, up to 40% modifier in CO₂ was used which is typically regarded as high for SFC. UV detectable N-protected amino acids like N-carbobenzoxy-D, L-alanine, N-3,5-dinitro-2-pyridyl-D, L-leucine were separated with this stationary phase. With the recent increase in interest in D-amino acids and their role in biological functions effective separation of D-amino acids from their L counterparts have become immensely important[32, 33]. Other applications for this stationary phase include the separation of chlorophenoxy herbicides like dichlorprop (*Figure 2.1F*), mecoprop, and haloxyprop, and also the commonly used non-steroidal anti-inflammatory drug indoprofen. The TeicoShell stationary phase showed unique selectivity for these analytes amongst the tested stationary phases. Along with these acidic and neutral analytes excellent selectivity was achieved with TeicoShell for some basic analytes especially β -blockers like propranolol, alprenolol, esmolol, and other amino alcohols.

2.4.2.3 NicoShell

The NicoShell stationary phase uses a synthetically modified macrocyclic glycopeptide as the chiral selector[34]. Macrocyclic glycopeptides have multiple chiral centers in their structure and employ different mechanisms including but not limited to ionic interactions, hydrogen bonding, π - π interactions, dipole-dipole interactions for the separation of enantiomeric pairs[35]. The NicoShell column has been recently commercialized and therefore there is no substantial literature on the applications of the column. The NicoShell has shown novel selectivity for liquid chromatography separations and was the only macrocyclic glycopeptide based stationary phase that was easily able to baseline separate the enantiomers of nicotine[36]. In this study, NicoShell

was able to baseline separate the enantiomers of nicotine even under SFC conditions (*Figure 2.1B*). This is the first reported chiral separation of nicotine by SFC. The NicoShell also effectively separated many other pharmaceutically relevant compounds and separated important stimulants like cathinone, 4-methylethcathinone, methadone, and showed high selectivity for the enantiomers of secondary and tertiary amines used in this study. Most of the separations were obtained within 5 mins, and some compounds like tramadol (*Figure 2.1C*) were baseline separated within a minute. Enantioseparation of these analytes is important from both pharmacological and toxicological points of view as it can lead to a better understanding of the properties of individual enantiomers on the biological systems. These separations are also of significant importance in forensic investigations. All separations with this stationary phase required some additive, and the highest number of separations were obtained while using 0.1% (w/v) ammonium formate in methanol. A combination of 0.1% TEA and 0.1% TFA also worked well for multiple enantioseparations (See *Table 2.2*).

2.4.2.4 VancoShell

The native macrocyclic glycopeptide vancomycin (in VancoShell) also efficiently separated enantiomers of compounds containing amine functionalities. Pharmaceutically important small molecules like tranylcypromine, venlafaxine, fluoxetine and a variety of other drugs were baseline separated using VancoShell (See *Table 2.2*). Interestingly, drugs of abuse like MDMA and methamphetamine had high separation factors with the VancoShell stationary phase. Analytes like fluoxetine (*Figure 2.1A*) were separated under a minute on a 10 cm column at flow rate of 4 ml/min and fall under the traditional definition of ‘ultrafast’ chromatography[37]. The best choice of additive for VancoShell stationary phase turned out to be a combination of 0.1% TEA and 0.1% TFA (v/v) in methanol. Though TEA and TFA would be the primary choice of additives, using a

slightly stronger base like diethylamine (DEA) and a slightly weaker acid like acetic acid (AA) helped increasing retention as was necessary to obtain baseline resolution for tulobuterol. Addition of small amounts of water to the mobile phase provided an increase in efficiency and decrease in retention times in some analytes such as trimebutine and venlafaxine (See *Table 2.2*). This is in agreement with previous reports of separations of polar compounds using SFC[38]. The exact details of the effect of water on enantioseparations will be discussed in a later study.

Table 2.2: Optimized chiral separations at backpressure 10 MPa

Sr. No.	Name	CSP	Mobile phase	k ₁	F(mL/min)/T°C	α	R _s
1)	4-methylethcathinone	NS	70/30 CO ₂ /Methanol-3% Water-0.1% Ammonium Formate	5.83	4 / 30	1.34	3.26
2)	Midodrine	NS	70/30 CO ₂ /Methanol-3% Water-0.1% Ammonium Formate	15.2	4 / 30	1.21	1.83
3)	Thioradizine	NS	70/30 CO ₂ /Methanol-3% Water-0.1% Ammonium Formate	8.13	4 / 30	1.61	3.67
4)	Bupivacaine	NS	75/25 CO ₂ /Methanol-0.1% TEA-0.1% TFA	2.70	4 / 30	1.47	3.43
5)	2-amino-1-phenyl-1,3-propanediol	NS	75/25 CO ₂ /Methanol-3% Water-0.1% Ammonium Formate	18.7	4 / 30	1.20	2.82
6)	Cathinone	NS	75/25 CO ₂ /Methanol-3% Water-0.1% Ammonium Formate	6.70	4 / 30	1.30	3.28
7)	Methadone	NS	75/25 CO ₂ /Methanol-3% Water-0.1% Ammonium Formate	3.40	4 / 30	1.14	1.69
8)	Nefopam	NS	75/25 CO ₂ /Methanol-3% Water-0.1% Ammonium Formate	6.73	4 / 30	1.19	1.94

9)	Proglumide	NS	75/25 CO ₂ /Methanol-3% Water-0.1% Ammonium Formate	0.90	4 / 30	1.33	1.85
10)	Promethazine	NS	75/25 CO ₂ /Methanol-0.1% Ammonium Formate	5.83	4 / 30	1.24	2.23
11)	Propafenone	NS	75/25 CO ₂ /Methanol-0.1% TEA-0.1% TFA	3.40	4 / 30	1.67	1.75
12)	Tramadol	NS	60/40 CO ₂ /Methanol-0.2% TEA-0.3% TFA	0.90	4 / 30	1.41	1.90
13)	Nicotine	NS	60/40 CO ₂ /Methanol-0.1% TEA	4.93	4 / 30	1.36	3.40
14)	p-synephrine	NS	75/25 CO ₂ /Methanol-0.2% TEA-0.3% TFA	12.2	4 / 30	1.21	2.57
15)	Ephedrine	NS	75/25 CO ₂ /Methanol-0.1% TEA-0.1% TFA	13.8	4 / 30	1.16	1.83
16)	2-chloronicotine	NS	60/40 CO ₂ /Methanol-0.1% TEA-0.1% TFA	0.80	4 / 30	1.42	2.49
17)	Fenfluramine	NS (15c m)	80/20 CO ₂ /Methanol-3% Water-0.1% Ammonium Formate	3.86	4 / 25	1.1	1.78
18)	Naftopidil	NS (15c m)	80/20 CO ₂ /Methanol-3% Water-0.1% Ammonium Formate	6.61	4 / 25	1.18	1.90
19)	Prilocaine	NS (15 cm)	80/20 CO ₂ /Methanol-3% Water-0.1% Ammonium Formate	4.38	4 / 25	1.15	2.18
20)	Tetrahydrozoline	NS (15c m)	80/20 CO ₂ /Methanol-3% Water-0.1% Ammonium Formate	19.6	4 / 25	1.09	2.21
21)	Bamethane	NS (15 cm)	80/20 CO ₂ /Methanol-0.1% TFA-0.1% TEA	6.31	4 / 25	1.09	1.72
22)	Oxybutynin	NS (15 cm)	85/15 CO ₂ /Methanol-0.1% Ammonium Formate	5.37	4 / 30	1.08	1.82
23)	1-(4-methylphenyl) butylamine	LP	80/20 CO ₂ /Methanol-0.2% TEA-0.3% TFA	2.51	4 / 25	1.17	2.27

24)	2-amino-1-(4-nitrophenyl) propane-1,3-diol	LP	80/20 CO ₂ /Methanol-0.2% TEA-0.3% TFA	6.66	4 / 25	1.24	2.27
25)	2-amino-3-phenyl-1-propanol	LP	80/20 CO ₂ /Methanol-0.2% TEA-0.3% TFA	4.89	4 / 25	1.16	3.07
26)	4-chlorophenyl alaninol	LP	80/20 CO ₂ /Methanol-0.2% TEA-0.3% TFA	5.57	4 / 25	1.16	2.95
27)	6-methoxy-1,2,3,4-tetrahydro-1-naphthylamine	LP	80/20 CO ₂ /Methanol-0.2% TEA-0.3% TFA	2.97	4 / 25	1.25	3.87
28)	1-(1-naphthyl) ethylamine	LP	80/20 CO ₂ /Methanol-0.2% TEA-0.3% TFA	3.37	4 / 25	1.24	3.06
29)	1,2-Diphenyl ethylamine	LP	80/20 CO ₂ /Methanol-0.2% TEA-0.3% TFA	2.63	4 / 25	1.33	4.08
30)	2-amino-1-phenylethanol	LP	80/20 CO ₂ /Methanol-0.2% TEA-0.3% TFA	8.37	4 / 25	1.16	3.02
31)	1,2-naphthyl ethylamine	LP	80/20 CO ₂ /Methanol-0.2% TEA-0.3% TFA	3.80	4 / 25	1.21	3.32
32)	1,2,2-triphenyl ethylamine	LP	80/20 CO ₂ /Methanol-0.2% TEA-0.3% TFA	1.83	4 / 25	1.33	4.11
33)	α -aminoethyl-4-hydroxy benzylalcohol	LP	80/20 CO ₂ /Methanol-0.2% TEA-0.3% TFA	10.0	4 / 25	1.12	3.37
34)	α -methyl benzylamine	LP	80/20 CO ₂ /Methanol-0.2% TEA-0.3% TFA	2.77	4 / 25	1.19	2.58
35)	α -methyl-4-nitrobenzylamine	LP	80/20 CO ₂ /Methanol-0.2% TEA-0.3% TFA	5.25	4 / 25	1.15	2.60
36)	Norephedrine	LP	80/20 CO ₂ /Methanol-0.2% TEA-0.3% TFA	4.86	4 / 25	1.14	2.26
37)	Normetanephine	LP	80/20 CO ₂ /Methanol-0.2% TEA-0.3% TFA	17.7	4 / 25	1.12	3.27
38)	Norphenylephrine	LP	80/20 CO ₂ /Methanol-0.2% TEA-0.3% TFA	15.9	4 / 25	1.16	2.79
39)	Octopamine	LP	80/20 CO ₂ /Methanol-0.2% TEA-0.3% TFA	18.1	4 / 25	1.14	2.48
40)	Tryptophan	LP	80/20 CO ₂ /Methanol-0.2% TEA-0.3% TFA	11.6	4 / 25	1.16	2.97

41)	2-amino-1,2-diphenylethanol	LP	75/25 CO ₂ /Methanol-0.2% TEA-0.3% TFA	2.08	4 / 30	1.30	2.25
42)	Chloro-indan-1-ylamine	LP	75/25 CO ₂ /Methanol-0.2% TEA-0.3% TFA	2.03	4 / 30	1.46	3.93
43)	1-(4-chlorophenyl)ethylamine	LP	75/25 CO ₂ /Methanol-0.2% TEA-0.3% TFA	2.03	4 / 30	1.17	1.93
44)	1-(1,1-biphenyl-4-yl)ethanamine	LP	75/25 CO ₂ /Methanol-0.2% TEA-0.3% TFA	2.40	4 / 30	1.18	1.99
45)	N-p-tosyl-1,2-diphenylethylenediamine	LP	75/25 CO ₂ /Methanol-0.2% TEA-0.3% TFA	1.71	4 / 30	1.20	2.32
46)	Phenylalanine	LP	80/20 CO ₂ /Methanol-0.2% TEA-0.3% TFA	2.80	4 / 30	1.16	1.70
47)	Trans-1-amino-2-indanol	LP	75/25 CO ₂ /Methanol-0.2% TEA-0.3% TFA	2.60	4 / 30	1.31	2.73
48)	Tryptophanamide	LP	75/25 CO ₂ /Methanol-0.2% TEA-0.3% TFA	11.3	4 / 30	1.18	2.39
49)	Tryptophanol	LP	75/25 CO ₂ /Methanol-0.2% TEA-0.3% TFA	5.48	4 / 30	1.24	2.80
50)	Fluoxetine	VS	75/25 CO ₂ /Methanol-3% water-0.1% TEA-0.1% TFA	1.60	4 / 30	1.19	1.94
51)	Mexiletine	VS	80/20 CO ₂ /Methanol-3% water-0.1% TEA-0.1% TFA	3.40	4 / 25	1.16	2.27
52)	Tranlycypromine	VS	80/20 CO ₂ /Methanol-3% water-0.1% TEA-0.1% TFA	5.57	4 / 25	1.20	1.86
53)	Venlafaxine	VS	75/25 CO ₂ /Methanol-3% water-0.1% TEA-0.1% TFA	3.30	4 / 25	1.17	1.94
54)	MDMA	VS	80/20 CO ₂ /Methanol-0.2% TEA-0.3% TFA	4.20	4 / 25	1.09	1.51
55)	Tolperisone	VS	80/20 CO ₂ /Methanol-3% water-0.1% TEA-0.05% TFA	5.57	4 / 30	1.21	2.60
56)	Trimebutine	VS	80/20 CO ₂ /Methanol-3% water-0.1% TEA-0.05% TFA	18.2	4 / 30	1.16	1.94
57)	4-methoxy- α -methylbenzylamine	VS	75/25 CO ₂ /Methanol-0.1% TEA-0.1% TFA	3.50	4 / 30	1.39	3.14

58)	Amphetamine	VS	75/25 CO ₂ /Methanol-0.1% TEA-0.1% TFA	3.90	4 / 30	1.19	1.90
59)	Mepivacaine	VS	75/25 CO ₂ /Methanol-0.1% TEA-0.1% TFA	5.23	4 / 30	1.40	2.67
60)	Methoxyphenamine	VS	75/25 CO ₂ /Methanol-0.1% TEA-0.1% TFA	2.43	4 / 30	1.22	1.60
61)	Methylphenidate	VS	75/25 CO ₂ /Methanol-0.1% TEA-0.1% TFA	1.93	4 / 30	1.69	4.22
62)	Mianserin	VS	75/25 CO ₂ /Methanol-0.1% Ammonium Formate-0.2% NH ₄ OH	1.67	4 / 30	1.44	4.45
63)	Nicardipine	VS	75/25 CO ₂ /Methanol-0.1% Ammonium Formate	1.93	4 / 30	1.47	2.02
64)	p-methoxy amphetamine	VS	75/25 CO ₂ /Methanol-0.2% TEA-0.3% TFA	3.20	4 / 30	1.24	1.97
65)	Trihexylphenidyl	VS	75/25 CO ₂ /Methanol-0.1% TEA-0.1% TFA	2.33	4 / 30	1.27	2.13
66)	Metoprolol	VS	80/20 CO ₂ /Methanol-0.1% TEA-0.05% TFA	9.68	4 / 30	1.16	1.76
67)	Pseudoephedrine	VS	75/25 CO ₂ /Methanol-0.1% Ammonium Formate	7.97	4 / 30	1.13	1.66
68)	Butylone	VS	75/25 CO ₂ /Methanol-0.1% TEA-0.1% TFA	4.27	4 / 30	1.15	1.94
69)	Ethylone	VS	75/25 CO ₂ /Methanol-0.1% TEA-0.1% TFA	8.40	4 / 30	1.11	1.63
70)	Tulobuterol	VS (15c m)	75/25 CO ₂ /Methanol-0.1% DEA- 0.1% AA	13.9	3 / 30	1.21	3.06
71)	Methorphan	VS (15c m)	80/20 CO ₂ /Methanol-0.1% TEA-0.1% TFA	9.57	3 / 30	1.13	1.56
72)	Methamphetamine	VS (15c m)	75/25 CO ₂ /Methanol-0.1% TEA-0.1% TFA	6.83	3 / 30	1.14	1.85
73)	4-methyl-5-phenyl-2- oxazolidinone	TS	60/40 CO ₂ /Methanol-0.1% Ammonium Formate	0.75	4 / 30	2.36	3.65

74)	5,5-diphenyl-4-benzyl oxazolidinone	TS	60/40 CO ₂ /Methanol-0.1% Ammonium Formate	1.01	4 / 30	2.42	3.33
75)	5,5-diphenyl-4-methyl oxazolidinone	TS	60/40 CO ₂ /Methanol-0.1% Ammonium Formate	2.19	4 / 30	1.86	3.64
76)	1,5-dimethyl-4-phenyl-2-imidazolidinone	TS	60/40 CO ₂ /Methanol	1.41	4 / 35	1.14	1.58
77)	Chlorthalidone	TS	60/40 CO ₂ /Methanol-0.1% TEA-0.1% TFA	2.47	4 / 30	1.35	2.29
78)	Methoxamine	TS	80/20 CO ₂ /Methanol-0.1% Ammonium Formate-0.1% NH ₄ OH	9.69	4 / 30	1.13	1.75
79)	Dichlorprop	TS	60/40 CO ₂ /Methanol-0.1% Ammonium Formate	1.75	4 / 30	1.70	4.18
80)	Haloxypop	TS	60/40 CO ₂ /Methanol-0.1% Ammonium Formate	1.09	4 / 30	2.09	4.94
81)	Mecoprop	TS	60/40 CO ₂ /Methanol-0.1% Ammonium Formate	3.78	4 / 30	1.31	3.00
82)	Terbutaline	TS	60/40 CO ₂ /Methanol-0.1% Ammonium Formate	8.06	4 / 30	1.33	3.50
83)	Metaproterenol	TS	60/40 CO ₂ /Methanol-0.1% TEA-0.1% TEA	3.63	4 / 30	1.16	1.57
84)	Alprenolol	TS	60/40 CO ₂ /Methanol-0.1% TEA-0.1% TFA	1.68	4 / 30	1.11	1.74
85)	Pindolol	TS	60/40 CO ₂ /Methanol-0.1% TEA-0.1% TFA	7.01	4 / 30	1.15	1.75
86)	Propranolol	TS	75/25 CO ₂ /Methanol-0.1% TEA-0.1% TFA	3.00	4 / 30	1.20	2.04
87)	Esmolol	TS	60/40 CO ₂ /Methanol-0.1% TEA-0.1% TFA	2.72	4 / 30	1.17	2.41
88)	Sotalol	TS	60/40 CO ₂ /Methanol-0.1% TEA-0.1% TFA	3.65	2 / 30	1.17	2.15
89)	Clenbuterol	TS	75/25 CO ₂ /Methanol-0.1% TEA-0.1% TFA	9.71	4 / 30	1.24	2.60
90)	N-(3,5-Dinitrobenzoyl)-D, L-Leucine	TS	75/25 CO ₂ /Methanol	1.47	4 / 30	2.06	1.78

91)	N-3,5-Dinitro-2-Pyr-D, L-Leucine	TS	80/20 CO ₂ /Methanol	0.62	4 / 30	1.46	1.53
92)	N-carbobenzoxy alanine	TS	60/40 CO ₂ /Methanol-0.1% TEA	0.91	4 / 30	1.55	2.83
93)	Lorazepam	TS	60/40 CO ₂ /Methanol-0.1% Ammonium Formate	1.68	4 / 35	3.19	8.04
94)	Oxazepam	TS	60/40 CO ₂ /Methanol-0.1% Ammonium Formate	1.97	4 / 35	2.70	7.83
95)	5-Methyl-5-phenyl hydantoin	TS	60/40 CO ₂ /Methanol-0.1% Ammonium Formate	0.90	4 / 30	2.07	4.13
96)	Keterolac	TS	75/25 CO ₂ /Methanol-0.1% Ammonium Formate-0.05% Formic Acid	2.50	4 / 30	1.35	2.24
97)	2,4-chlorophenoxy propionic acid	TS	75/25 CO ₂ /Methanol-0.1% Ammonium Formate-0.05% Formic Acid	2.38	4 / 30	1.61	3.67
98)	3-Phenylphthalide	TS	75/25 CO ₂ /Methanol	0.57	4 / 30	1.48	3.00
99)	Indoprofen	TS	85/15 CO ₂ /Methanol-0.1% TFA	7.38	4 / 25	1.17	2.17
100)	α -Methyl- α -phenylsuccinimide	TS	75/25 CO ₂ /Methanol	2.24	4 / 30	1.28	3.55

Chiral Stationary Phase (CSP): NicoShell (NS), LarihcShell-P (LS), VancoShell (VS), TeicoShell (TS). k_1 = retention factor of the first enantiomer, F = flow rate in ml/min, T = temperature in °C, α =separation factor, R_s = resolution= $2(t_2-t_1)/w_1+w_2$ where t_1 and t_2 are the retention times and w_1 and w_2 are the peak widths at baseline for the first and second peaks respectively

2.4.3 van Deemter plots

van Deemter plots provide useful data regarding heights equivalent to a theoretical plate (H), the optimum flow rate for separation and allows estimation of contribution from the A, B and C terms to band broadening by plotting plate height (H) vs. volumetric flow rate[39]. With increasing focus on high throughput separations, columns being operated at flow rates much higher than optimal is now commonplace[6]. As per Darcy's law, low viscosity mobile phases comprising of super/subcritical carbon dioxide and methanol allow columns to be operated at high flow rates

with less backpressures[40]. We have compared two of the four tested stationary phases- a representative macrocyclic glycopeptide (TeicoShell) and derivatized cyclofructan (LarihcShell-P). *Figure 2.3 and 2.4* show the van Deemter plots on 2.7 μm SPP TeicoShell, 5 μm FPP Chirobiotic T, 2.7 μm SPP LarihcShell-P and 5 μm FPP Larihc-P respectively using SFC. The analyte used for teicoplanin stationary phase was 3-phenylphthalide, and for Larihc-P it was 1-(1-naphthyl) ethylamine. The minimum for the 5 μm FPP Chirobiotic T column was at 0.8 ml/min and corresponds to an efficiency of ~ 53800 plates per meter as calculated from the first eluted enantiomer of 3-phenylphthalide. On the other hand, the 2.7 μm SPPs the minimum was at 1 ml/min, and the corresponding efficiency was ~ 80000 plates per meter. For the 5 μm FPP LP column and the 2.7 μm LarihcShell-P column the minimum was at 0.6 ml/min and 1 ml/min respectively. The corresponding plate count calculated from the first eluted enantiomer of 1-(1-naphthyl)ethylamine was ~ 73800 plates m^{-1} for the fully porous particles whereas for the superficially porous particles it was ~ 108200 plates m^{-1} . Owing to the smaller particle diameter, the superficially porous particles provided higher theoretical plates (N) or lower plate height (H) compared to the 5 μm FPPs as was expected. It is interesting to note that at higher flow rates the loss of efficiency for the superficially porous particles is much less than its fully porous counterpart. This observation reinforces the findings by Gritti and Guichon[12]. Also, it should be noted that the retention time is significantly lower with the superficially porous particles at all tested flow rates. This is due to the significantly decreased amount of chiral selector on the SPPs[6, 14].

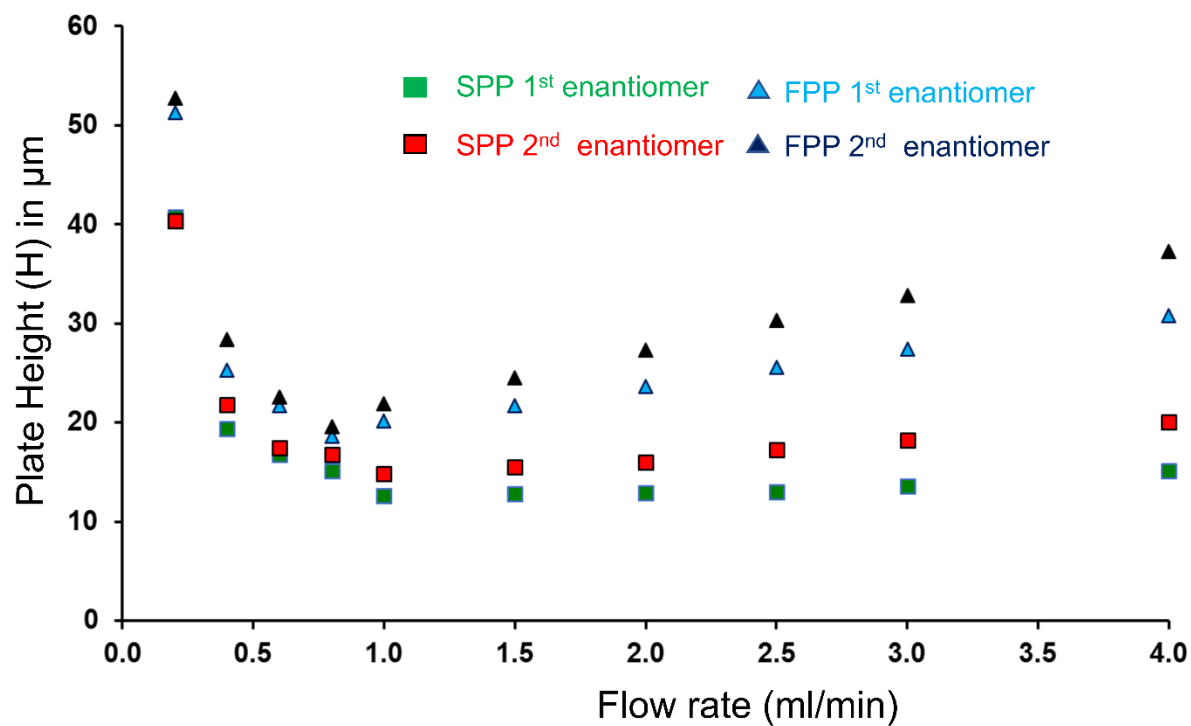


Figure 2.3. The van Deemter plot showing plate height (H) in mm versus flow rate in SFC on TeicoShell ($2.7\ \mu\text{m}$) and Chirobiotic T ($5\ \mu\text{m}$) chiral columns. SFC van Deemter with analyte 3-phenylphthalide. Chromatographic conditions: 75/25 CO_2/MeOH ; Backpressure regulator maintained at 8 MPa and temperature at 30°C . UV detection at 254 nm.

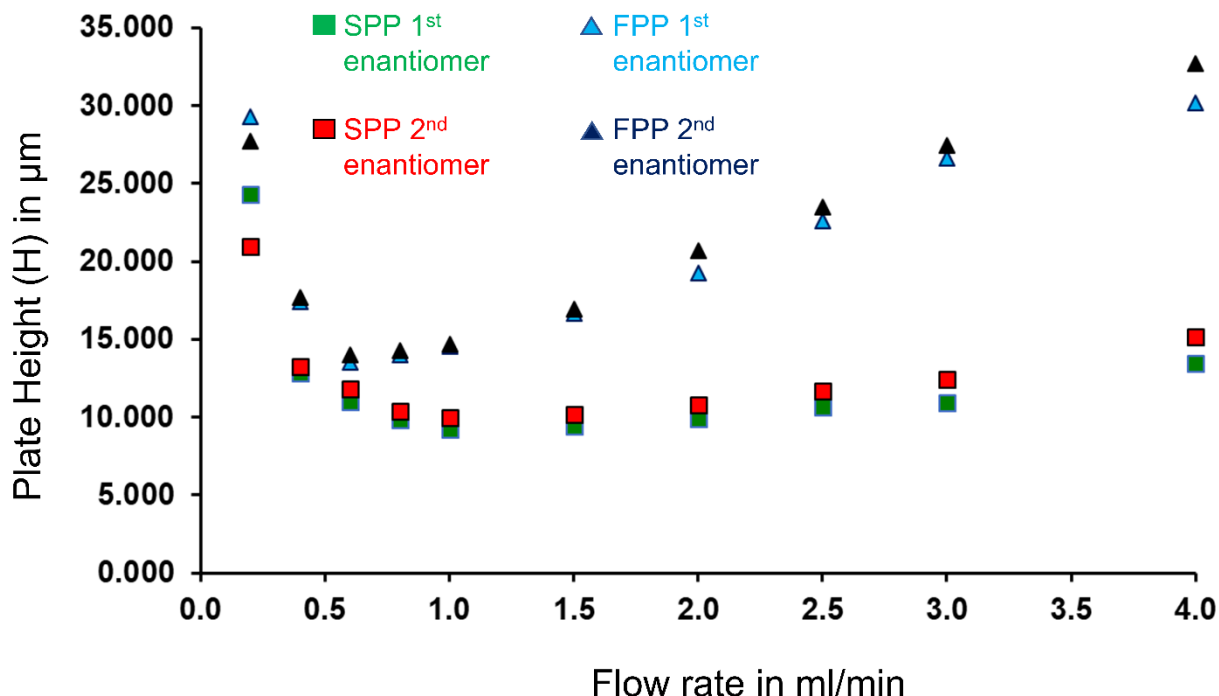


Figure 2.4. The van Deemter plot showing plate height (H) in μm versus flow rate in SFC on LarihcShell-P ($2.7\ \mu\text{m}$) and Larihc-CF6-P ($5\ \mu\text{m}$) chiral columns. SFC van Deemter with analyte 1-(1-naphthyl)ethylamine. Chromatographic conditions: 80/20 CO_2/MeOH -0.2% TEA-0.3% TFA; Backpressure regulator maintained at 8 MPa and temperature at 25°C . UV detection at 254 nm.

2.4.4 Ultrafast chromatography

Using the high efficiency SPP chiral stationary phases, we performed ultrafast chiral separations under SFC conditions for multiple analytes. Short columns of 5 cm length with 4.6 mm internal diameter were run at flow rates as high as 14 ml/min to obtain separations of 1-(1-naphthyl)ethylamine (Figure 2.5A), and 1,2,2-triphenylethylamine (Figure 2.5B) with the LarihcShell-P stationary phase. 3-phenylphthalide (Figure 2.5C), and 5,5-diphenyl-4-methyl-2-oxazolidinone (Figure 2.5D) were separated with TeicoShell columns of 5 cm length with flow

rates of 10 ml/min. All mentioned analytes were baseline separated under 30 seconds. Efficiencies for the ultrafast separation ranged from 10000 to 50000 plates m^{-1} . Extra column band broadening is detrimental to ultrafast separations on shorter columns and hence to reduce the extra column volume shorter tubing was used and the column oven was bypassed. It was clear that the instrumentation in SFC could be better engineered to further decrease extra column volumes and increase pressure capabilities in order to provide optimal ultrafast proficiency. Such instrumentals would produce higher efficiency and even faster separations[6, 7, 23, 24, 41]

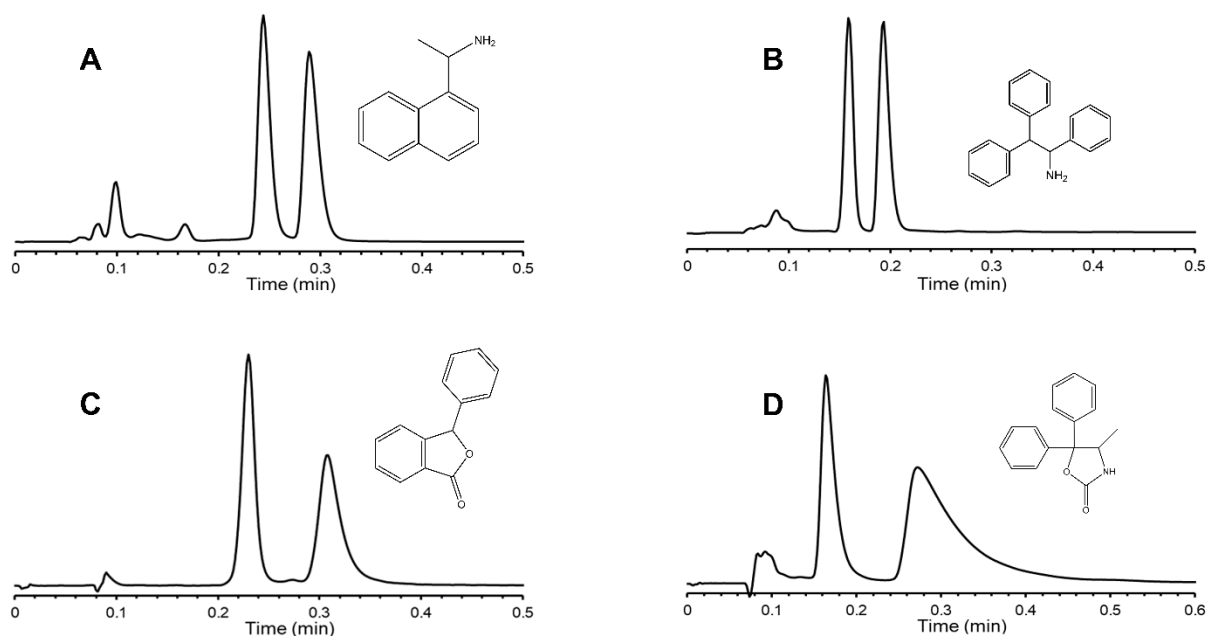


Figure 2.5. Ultrafast chiral separations on SFC. (A) 1-(1-naphthyl)ethylamine, M.P. 80/20 CO₂/Methanol-0.2% TEA-0.3% TFA, 14 mL/min (B) 1,2,2- triphenylethylamine, M.P. 80/20 CO₂/Methanol-0.2% TEA-0.3% TFA, 14 mL/min (C) 3-phenylphthalide M.P. 95/5 CO₂/Methanol, 10 mL/min (D) 5,5-diphenyl-4-methyl-2-oxazolidinone M.P. 60/40 CO₂/Methanol, 10 mL/min. All separations were performed at a backpressure of 10 Mpa and under ambient temperature.

2.5. Conclusions

The use of superficially porous particles as chromatographic supports for SFC has led to higher efficiencies and shorter retention times compared to the widely used fully porous particles. The advantages provided by SFC regarding speed has led to all separations being performed within 10 mins with some analytes separated under a minute on a 10 cm column with no special instrumental modification. Efficiencies under SFC conditions were somewhat lower than under HPLC conditions usually due to the significantly larger extra column volumes in the system. This work shows the ability of the macrocyclic glycopeptide and cyclofructan based stationary phases to perform enantiomeric separations under SFC conditions. The LarihcShell-P stationary phase effectively separated primary amines and some other compounds with very high efficiency, VancoShell and NicoShell were best in separating basic drugs, and the TeicoShell stationary phase was most successful with acidic and neutral analytes. Van Deemter plots obtained in this study point to the significant advantage offered by the SPPs when operating at high flow rates thereby making it the morphology of choice for ultrafast SFC.

2.6 Acknowledgements

The authors would like to acknowledge Dr. M. Farooq Wahab, Dr. J.T. Lee, Garrett Hellinghausen and Dr. Michael Wey for their assistance in the project. This work was supported by the Robert A. Welch Foundation (Y0026).

2.7 References

- [1] D.W. Armstrong, W. DeMond, Cyclodextrin bonded phases for the liquid chromatographic separation of optical, geometrical, and structural isomers, *Journal of Chromatographic Science*, 22 (1984) 411-415.
- [2] D.W. Armstrong, Y. Tang, S. Chen, Y. Zhou, C. Bagwill, J.-R. Chen, Macrocyclic antibiotics as a new class of chiral selectors for liquid chromatography, *Analytical Chemistry*, 66 (1994) 1473-1484.

- [3] P. Sun, C. Wang, Z.S. Breitbach, Y. Zhang, D.W. Armstrong, Development of new HPLC chiral stationary phases based on native and derivatized cyclofructans, *Analytical Chemistry*, 81 (2009) 10215-10226.
- [4] A. Ichida, T. Shibata, I. Okamoto, Y. Yuki, H. Namikoshi, Y. Toga, Resolution of enantiomers by HPLC on cellulose derivatives, *Chromatographia*, 19 (1984) 280-284.
- [5] M. Lämmerhofer, W. Lindner, Quinine and quinidine derivatives as chiral selectors I. Brush type chiral stationary phases for high-performance liquid chromatography based on cinchonan carbamates and their application as chiral anion exchangers, *Journal of Chromatography A*, 741 (1996) 33-48.
- [6] D.C. Patel, Z.S. Breitbach, M.F. Wahab, C.L. Barhate, D.W. Armstrong, Gone in seconds: praxis, performance, and peculiarities of ultrafast chiral liquid chromatography with superficially porous particles, *Analytical Chemistry*, 87 (2015) 9137-9148.
- [7] M.F. Wahab, R.M. Wimalasinghe, Y. Wang, C.L. Barhate, D.C. Patel, D.W. Armstrong, Salient sub-second separations, *Analytical Chemistry*, 88 (2016) 8821-8826.
- [8] C.L. Barhate, E.L. Regalado, N.D. Contrella, J. Lee, J. Jo, A.A. Makarov, D.W. Armstrong, C.J. Welch, Ultrafast chiral chromatography as the second dimension in two-dimensional liquid chromatography experiments, *Analytical Chemistry*, 89 (2017) 3545-3553.
- [9] D. Kottoni, A. Ciogli, C. Molinaro, I. D'Acquarica, J. Kocergin, T. Szczerba, H. Ritchie, C. Villani, F. Gasparrini, Introducing enantioselective ultrahigh-pressure liquid chromatography (eUHPLC): Theoretical inspections and ultrafast separations on a new sub-2- μm Whelk-O1 stationary phase, *Analytical Chemistry*, 84 (2012) 6805-6813.
- [10] C.G. Horvath, B. Preiss, S.R. Lipsky, Fast liquid chromatography. Investigation of operating parameters and the separation of nucleotides on pellicular ion exchangers, *Analytical Chemistry*, 39 (1967) 1422-1428.
- [11] J.J. Kirkland, Controlled surface porosity supports for high-speed gas and liquid chromatography, *Analytical Chemistry*, 41 (1969) 218-220.
- [12] F. Gritti, G. Guiochon, Possible resolution gain in enantioseparations afforded by core-shell particle technology, *Journal of Chromatography A*, 1348 (2014) 87-96.
- [13] F. Gritti, Quantification of individual mass transfer phenomena in liquid chromatography for further improvement of column efficiency, *LC-GC North America* 2014, 32, 928-940.
- [14] D.A. Spudeit, M.D. Dolzan, Z.S. Breitbach, W.E. Barber, G.A. Micke, D.W. Armstrong, Superficially porous particles vs. fully porous particles for bonded high performance liquid chromatographic chiral stationary phases: isopropyl cyclofructan 6, *Journal of Chromatography A*, 1363 (2014) 89-95.
- [15] L.T. Taylor, Supercritical fluid chromatography for the 21st century, *The Journal of Supercritical Fluids*, 47 (2009) 566-573.
- [16] E.L. Regalado, C.J. Welch, Pushing the speed limit in enantioselective supercritical fluid chromatography, *Journal of Separation Science*, 38 (2015) 2826-2832.
- [17] A.G.-G. Perrenoud, W.P. Farrell, C.M. Aurigemma, N.C. Aurigemma, S. Fekete, D. Guillarme, Evaluation of stationary phases packed with superficially porous particles for the analysis of pharmaceutical compounds using supercritical fluid chromatography, *Journal of Chromatography A*, 1360 (2014) 275-287.
- [18] V. Desfontaine, G.L. Losacco, Y. Gagnebin, J. Pezzatti, W.P. Farrell, V. González-Ruiz, S. Rudaz, J.-L. Veuthey, D. Guillarme, Applicability of supercritical fluid chromatography-mass spectrometry to metabolomics. I-Optimization of separation conditions for the simultaneous

analysis of hydrophilic and lipophilic substances, *Journal of Chromatography A*, 1562 (2018) 96-107.

[19] E. Lesellier, C. West, The many faces of packed column supercritical fluid chromatography—a critical review, *Journal of Chromatography A*, 1382 (2015) 2-46.

[20] R. De Pauw, K. Shoykhet, G. Desmet, K. Broeckhoven, Exploring the speed-resolution limits of supercritical fluid chromatography at ultra-high pressures, *Journal of Chromatography A*, 1374 (2014) 247-253.

[21] T.A. Berger, Characterization of a 2.6 μm Kinetex porous shell hydrophilic interaction liquid chromatography column in supercritical fluid chromatography with a comparison to 3 μm totally porous silica, *Journal of Chromatography A*, 1218 (2011) 4559-4568.

[22] D.C. Patel, Z.S. Breitbach, J. Yu, K.A. Nguyen, D.W. Armstrong, Quinine bonded to superficially porous particles for high-efficiency and ultrafast liquid and supercritical fluid chromatography, *Analytica Chimica Acta*, 963 (2017) 164-174.

[23] C.L. Barhate, M.F. Wahab, D. Tognarelli, T.A. Berger, D.W. Armstrong, Instrumental idiosyncrasies affecting the performance of ultrafast chiral and achiral sub/supercritical fluid chromatography, *Analytical Chemistry*, 88 (2016) 8664-8672.

[24] M.F. Wahab, P.K. Dasgupta, A.F. Kadjo, D.W. Armstrong, Sampling frequency, response times and embedded signal filtration in fast, high efficiency liquid chromatography: A tutorial, *Analytica Chimica Acta*, 907 (2016) 31-44.

[25] K. De Klerck, Y. Vander Heyden, D. Mangelings, Generic chiral method development in supercritical fluid chromatography and ultra-performance supercritical fluid chromatography, *Journal of Chromatography A*, 1363 (2014) 311-322.

[26] Y. Liu, A. Berthod, C.R. Mitchell, T.L. Xiao, B. Zhang, D.W. Armstrong, Super/subcritical fluid chromatography chiral separations with macrocyclic glycopeptide stationary phases, *Journal of Chromatography A*, 978 (2002) 185-204.

[27] C. Wang, Y. Zhang, Effects of column back pressure on supercritical fluid chromatography separations of enantiomers using binary mobile phases on 10 chiral stationary phases, *Journal of Chromatography A*, 1281 (2013) 127-134.

[28] M. Hilton, D.W. Armstrong, Evaluation of a chiral crown etherlc column for the separation of racemic amines, *Journal of Liquid Chromatography*, 14 (1991) 9-28.

[29] D.W. Armstrong, R.M. Woods, Z.S. Breitbach, Comparison of enantiomeric separations and screening protocols for chiral primary amines by SFC and HPLC, *LC-GC North America*, 32 (2014) 742-752.

[30] E. Lesellier, Efficiency in supercritical fluid chromatography with different superficially porous and fully porous particles ODS bonded phases, *Journal of Chromatography A*, 1228 (2012) 89-98.

[31] D.W. Armstrong, Y. Liu, K.H. Ekborgott, A covalently bonded teicoplanin chiral stationary phase for HPLC enantioseparations, *Chirality*, 7 (1995) 474-497.

[32] A. Berthod, Y. Liu, C. Bagwill, D.W. Armstrong, Facile liquid chromatographic enantioresolution of native amino acids and peptides using a teicoplanin chiral stationary phase, *Journal of Chromatography A*, 731 (1996) 123-137.

[33] I. Livnat, H.-C. Tai, E.T. Jansson, L. Bai, E.V. Romanova, T.-t. Chen, K. Yu, S.-a. Chen, Y. Zhang, Z.-y. Wang, A D-amino acid-containing neuropeptide discovery funnel, *Analytical Chemistry*, 88 (2016) 11868-11876.

[34] G. Hellinghausen, D. Roy, J.T. Lee, Y. Wang, C.A. Weatherly, D.A. Lopez, K.A. Nguyen, J.D. Armstrong, D.W. Armstrong, Effective methodologies for enantiomeric separations of 150

pharmacology and toxicology related 1°, 2°, and 3° amines with core-shell chiral stationary phases, *Journal of Pharmaceutical and Biomedical Analysis*, 155 (2018) 70-81.

[35] I. Ilisz, R. Berkecz, A. Péter, Retention mechanism of high-performance liquid chromatographic enantioseparation on macrocyclic glycopeptide-based chiral stationary phases, *Journal of Chromatography A*, 1216 (2009) 1845-1860.

[36] G. Hellinghausen, D. Roy, Y. Wang, J.T. Lee, D.A. Lopez, C.A. Weatherly, D.W. Armstrong, A comprehensive methodology for the chiral separation of 40 tobacco alkaloids and their carcinogenic E/Z-(R, S)-tobacco-specific nitrosamine metabolites, *Talanta*, 181 (2018) 132-141.

[37] L.R. Snyder, J.J. Kirkland, J.W. Dolan, Introduction to modern liquid chromatography, John Wiley & Sons, 2011.

[38] J. Liu, E.L. Regalado, I. Mergelsberg, C.J. Welch, Extending the range of supercritical fluid chromatography by use of water-rich modifiers, *Organic & Biomolecular Chemistry*, 11 (2013) 4925-4929.

[39] J.J. Van Deemter, F. Zuiderweg, A.v. Klinkenberg, Longitudinal diffusion and resistance to mass transfer as causes of nonideality in chromatography, *Chemical Engineering Science*, 5 (1956) 271-289.

[40] J. Giddings, Dynamics of Chromatography. Part I, Principles and Theory. New York, NY, USA: M, in, Dekker, Inc, 1965.

[41] D.C. Patel, M.F. Wahab, T.C. O'Haver, D.W. Armstrong, Separations at the Speed of Sensors, *Analytical Chemistry*, 90 (2018) 3349-3356.

2.8 Supporting Information

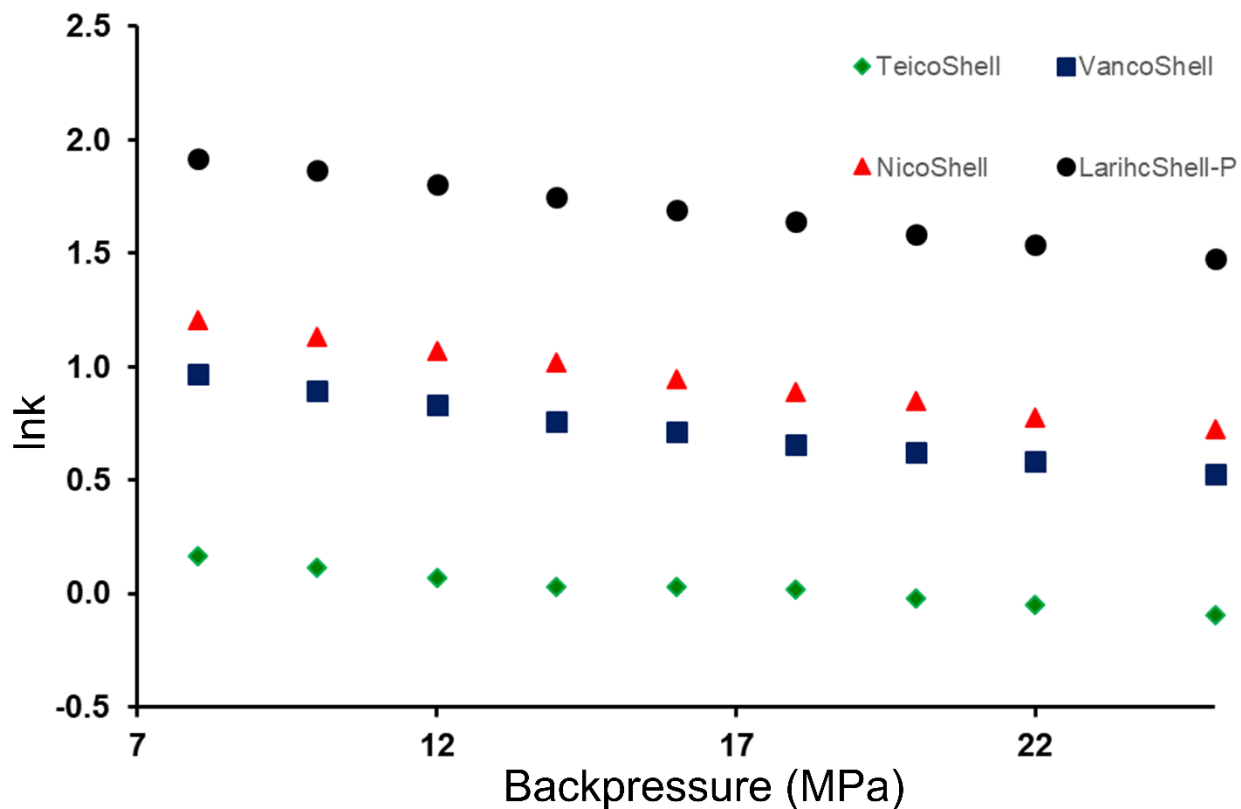


Figure 2.S1. Natural logarithm of experimental retention factor versus backpressure measured in MPa for chiral columns TeicoShell, NicoShell, VancoShell and LarihcShell-P.

Chromatographic conditions for different columns: TeicoShell (10 X 0.46 cm), 5-Methyl-5-phenyl hydantoin 60/40 CO₂/Methanol-0.1% ammonium formate; NicoShell (10 X 0.46 cm), Mepivacaine, 75/25 CO₂/Methanol-0.1% TEA-0.1% TFA; VancoShell (10 X 0.46 cm), Methylphenidate, 80/20 CO₂/Methanol-0.1% TEA-0.1% TFA; LarihcShell (10 X 0.46 cm), 4-chlorophenyl alaninol, 80/20 CO₂/Methanol-0.2% TEA-0.3% TFA. Flow rate 4 mL/min and UV detection at 254 nm

Chapter 3
Ramifications and Insights on the Role of Water in Chiral Sub/Supercritical Fluid
Chromatography

3.1 Abstract

More than forty co-solvents have been used with carbon dioxide to alter its solvation strength. Among the most interesting systems is the sub/supercritical CO₂/alkanol eluents. Using small amounts of water in CO₂/MeOH is known to be beneficial in chiral SFC. However, the ramifications of introducing water as a co-solvent component is not entirely understood. In this work, we demonstrate important aspects of CO₂/MeOH/H₂O system on nine chiral stationary phases with very different surface chemistries encompassing derivatized polysaccharides, macrocyclic glycopeptides, iso-butylmercaptoquinine, isopropyl macrocyclic oligosaccharides, and π -electron acceptor/ π -electron donor phases. A hydrophilicity scale has been shown to be useful in predicting if a given chiral column chemistry would show a significant enhancement in separation efficiency in the presence of water in CO₂/MeOH system. We demonstrate up to 8-fold enhancements in plate counts of chiral separations with a concomitant decrease in retention times as predicted by the qualitative test. The same chiral analysis can now be completed in almost 1/3rd of the time with the addition of small amounts of water thereby decreasing organic solvent consumption by a considerable amount. Hydrophobic stationary phases show a minimal increase in efficiency and decrease in analysis times and optimized separations show much larger reduced plate heights as compared to more hydrophilic stationary phase. Furthermore, the presence of water can alter the nature of the adsorption isotherm under non-linear conditions. Small amounts of water can be used to tune non-linear tailing peaks into fronting ones, significantly improving preparative enantiomeric separations.

3.2 Introduction

The solubility parameter of a fluid near the supercritical region changes over a large magnitude with a small change in pressure and temperature, which allows a convenient regulation of solvation strength of the fluid. Consequently, sub/supercritical fluids are considered as the solvents of the future.¹ This aspect makes sub/supercritical chromatography (SFC) a versatile technology for analytical and preparative separations. Gases with safely accessible critical temperatures and pressures such as CO₂, N₂O, NH₃, C₂H₆, can be employed as mobile phases.² The use of gases like N₂O and NH₃ have led to serious accidents in the past; hence CO₂ is the gas of choice in modern-day SFC.³ Chiral SFC separations, are now an integrated part of drug discovery protocols for analytical and purification purposes.⁴⁻⁶ Carbon dioxide can interact with analytes via a large number of interactions such as acid-base and induced dipole. Compressed CO₂ near or above the critical region has weak solvation power for a majority of analytes encountered in research. SFC with pure CO₂ as the mobile phase often results in infinitely retained analytes, clogged columns/tubings, or distorted peak shapes. Consequently, co-solvent(s) must be employed to have acceptable retention, resolution, and peak shapes. Additionally, acids, bases and salts in small concentrations are often added to the SFC mobile phase. These additives prevent unwanted interactions of the analytes with the stationary phase and thereby elute at reasonable times and symmetry.⁷ Additives are often important in providing selectivity between enantiomeric pairs.⁸ It is a common practice to use CO₂ with co-solvents in the sub-critical region. More than 40 co-solvents have been successfully employed in SFC including pure water;⁹⁻¹⁴ yet a majority of the modifiers such as acetone, dimethylsulfoxide, dimethylformamide are not suitable for chromatography due to UV-cut off issues, and mass spectrometry incompatibility with chlorinated solvents and alkanes.

Among the most common solvents, CO₂/alcohol mixtures have been well studied and thermodynamically characterized.¹⁵ A small amount of water can be added to the alcohol, e.g., CO₂/Alkanol/H₂O to generate a ternary mobile phase.¹⁶⁻¹⁹ The presence of alcohol is necessary since pure water has a limited solubility of 3x10⁻³ g dm⁻³ in supercritical CO₂ at 25 MPa and given the fact that phase separation also occurs.^{10, 11} The amount of water can be considerably increased with 2-propanol vs. methanol before phases separate.¹⁶ Methanol is still the most popular co-solvent because of its roughly four-fold lower viscosity (0.543 vs. 2.04 mPa.s for 2-propanol). The ternary systems are sometimes used to elute achiral hydrophilic analytes that are difficult to solubilize under SFC conditions.¹⁸⁻²⁰ This has been attributed to chaotropic effects in a recent publication when dealing with hydrophilic analytes.²¹

Little information is available on the specific role of water in chiral SFC separations although a few recent studies have indicated that it could be advantageous in some cases.^{6, 17, 22, 23} The most common observation is that the retention time of the enantiomeric pair decreases in the presence of water. It is not known if there are any general trends regarding added water and its utility in SFC. In this work, the effect of mobile phase “polarity” on the addition of water is studied with a solvatochromic dye. Some trends are noted where certain chiral stationary phases show a significant increase in efficiency and decrease in retention times, thereby providing predictive capabilities. A detailed phenomenological analysis on the separation behavior of chiral stationary phases with a ternary CO₂/MeOH/H₂O system is presented. Acidic, basic and neutral analytes were included with a wide variety of structures to generalize the phenomenon. A wide range of chiral stationary phase chemistries including derivatized polysaccharides, three types of macrocyclic glycopeptides, iso-butylmercaptoquinine, an isopropyl macrocyclic oligosaccharide, and a π -electron acceptor/ π -electron donor phases are evaluated. A simple predictive test is proposed,

which allows one to estimate the relative degree of efficiency gain and retention time decrease for different column chemistries. This paper also demonstrates for the first time, the tuning of peak shapes by changing the adsorption isotherm under chiral non-linear SFC conditions. Since SFC remains the method of choice for preparative chiral separations,²⁴ the ability to tune peak shapes from tailing to fronting conditions has enormous implications. Dramatic gains in efficiency, along with large reductions in analysis time, can be predictably achieved by judicious use of small amounts of water.

3.3 Experimental

3.3.1 Materials

All organic solvents, reagents, and analytes used were purchased from Sigma Aldrich (St. Louis, MO, U.S.A.) or Alfa Aesar (Ward Hill, MA, U.S.A.). Carbon dioxide was purchased from Airgas (UN1013, Radnor, PA) in cylinders equipped with a full-length educator tube. Distilled deionized water (18.2 M Ω .cm) was obtained from a Milli-Q purification system (EMD Millipore, Billerica, MA, U.S.A.). Superficially porous 2.7 μ m columns TeicoShell, LarihcShell-P, VancoShell, Q-Shell and NicoShell (10 x 0.46 cm) were synthesized by AZYP, LLC. (Arlington, TX, U.S.A.), Chiralpak IA-3 (3 μ m fully porous, 15 x 0.46 cm), Chiral OD-H (3 μ m fully porous, 5x0.46 cm) and Chiralpak IC (5 μ m fully porous, 25 x 0.46 cm) columns were purchased from Chiral Technologies (West Chester, PA, U.S.A.). (S, S)-Whelk-O1 column (5 μ m fully porous, 25 x 0.46 cm) was from Regis Technologies (Morton Grove, IL, U.S.A.). All analytes were dissolved in methanol.

3.3.2 Mobile phase preparation protocol

All SFC mobile phases were prepared using HPLC grade methanol and Milli-Q water. The reported percentage of water represents the percent water added to a given volume of modifier before mixing, e.g., 6% v/v H₂O in MeOH was made by adding 12 mL H₂O to 200 mL MeOH. The volume of methanol was measured using a mass balance (3 kg balance) and dividing it by the density at that particular temperature. Water was then added to the mobile phase using a 50 mL Class-A buret. The additives were either weighed or added using a micropipette. The mobile phase used for the construction of the selectivity plot was identical to the previously reported composition^{25, 26}, i.e., 80/20 ACN/25 mM ammonium acetate buffer (v/v).

3.3.3 Instrumentation

All separations were performed on a Jasco 2000 series SFC (SFC-2000-7) equipped with carbon dioxide and modifier pumps (PU-2086). The CO₂ pump head was chilled at -10 °C. A back-pressure regulator (BP-2080) was set at 8 MPa with a heat controller at 60 °C (HC-2068-01). The autosampler (AS-2059-SFC) had a 5 µL stainless steel injection loop, and the detection was conducted with a variable-wavelength high-pressure compatible UV detector (UV-2075). Column oven was also bypassed. All column connections were made with silica lined pre-cut PEEK and had an internal diameter of 254 µm as they provide maximum efficiency as reported in previous studies.²⁷ The efficiency values reported in this paper are calculated from the peak width at half height.

Nile red experiments and van Deemter plots were constructed on a custom modified Agilent Infinity II SFC modified to perform modifier stream injections. The Nile Red experiment was performed by plumbing the injection valve between the modifier pump and mixing tee. Nile Red was dissolved in the modifier used (either pure methanol or methanol and 6% water) hence there is no other change in the mobile phase apart from the introduction of Nile Red. Nile Red was

retained onto a 50 x 4.6 mm, 3.5 μm RX-Sil column in order to separate it from injection disturbances and avoid any discrepancies occurring from the wash solvent. An ultralow dispersion heat exchanger was connected to the mixer with a 34 cm long and 75 μm internal diameter tubing to keep the density of the CO_2 constant and independent of modifier concentration. Detection was conducted with Agilent DAD UV 13 μL 10 mm detector flow cell at 40 $^\circ\text{C}$ and 120 bar outlet pressure. The slit was set to 1 nm. Spectra were collected at 5 Hz between 350 nm and 650 nm with a spacing of 1 nm.

3.4 Results & Discussion

3.4.1 Solvatochromic Characterization of the Sub/Supercritical Eluents.

One of the most convenient ways to characterize the nature of SFC solvents is to use a solvatochromic probe where the wavelength of maximum absorption (λ_{max}) correlates approximately to the polarity of a given solvent system.^{28,29} Several probes such as 2-nitroanisole, methyl red, azo-dyes have been used for solvatochromic studies in compressed (liquid, sub/supercritical) carbon dioxide.^{7, 30} Nile Red, which is a lipophilic dye, was chosen for this experiment because unlike Reichardt's dye, it has sufficient solubility in pure and compressed carbon dioxide and co-solvent mixtures.²⁸ Nile red shows sensitive and large bathochromic shifts with an increase in solvent polarity.²⁹ In the following discussion, we use some of the data from a previous detailed Nile Red study for comparative purposes with this work.²⁹ Pure carbon dioxide (8.75 MPa), MeOH and water show a λ_{max} of 480.2 nm, 549.6 nm and 593.2 nm respectively at room temperature and ambient pressure.²⁹ The corresponding transition energy of Nile Red (E_{NR}) in pure CO_2 matches very closely with pentane (483.6 nm) and n-hexane (484.4 nm). A similar polarity scale with the 2-nitroanisole probe, confirms the same polarity trend. When MeOH was progressively added at 1, 2, 3, 4 and 5 %; the λ_{max} of the dye in CO_2 shifted from 480.2 to 488,

494, 498, 500 and 504 nm respectively confirming an increase in polarity. A recent study used 0.02% H₂O and acetic acid in MeOH and saw no substantial change in the λ_{max} of Nile Red dye due to the presence of the additives until the modifier reached 60%.⁷ The authors attributed this behavior to the low concentration of the water additive in carbon dioxide. In this work, a ternary mobile phase (CO₂/ MeOH/ H₂O) was characterized with Nile Red in the working range of 90% to 60% CO₂ with and without water using a 300-fold higher concentration of water than the previous study.⁷ *Table 3.S1* summarizes the results showing the E_{NR} and λ_{max} shifts. The addition of 10% MeOH to CO₂ causes a redshift to 511 nm, which confirms the increase in the solvent strength of the SFC mobile phase in terms of higher polarity. This shift is close to the “polarity” of solvents like *N,N*-diethylamine, and tetramethylethylenediamine. However, the remarkable observation is that the addition of 6% water to the MeOH modifier does not further shift the λ_{max} of Nile Red. Increasing the MeOH concentration in CO₂ decreases the E_{NR} as a quadratic function of % MeOH (*Figure 3.S1*). In each case, there was no change in the λ_{max} of the dye with the addition of small amounts of water to the methanol modifier. There is a minor change of +2 nm with 40% MeOH. At this concentration, the $\lambda_{max} = 532$ nm falls in the solvent polarity range of acetonitrile. There are two possibilities for the observed lack of a bathochromic shift in the presence of water. First, the amount of water in the bulk mobile phase is still minimal (2.3% H₂O final concentration in a 60:40 CO₂: MeOH composition). Another reason may be related to the concept of the existence of a cybotatic region, which is the area in the vicinity of the probe molecule and which has been modified by the local arrangement of the solvent molecules around the solute.³⁰ It is possible that at higher concentrations of MeOH ($\geq 10\%$),³⁰ the cybotatic region is so enriched in methanol relative to the bulk solvent system that a trace of water does not cause a spectral shift. The cybotatic phenomenon has been observed in supercritical fluids with 2-

nitroanisole, and thus it is not unique to Nile Red.³⁰ Clearly the mobile phase polarity provides an incomplete picture of what happens in SFC with water containing mobile phases. Clearly, the sorption of water by the stationary phase must be taken into account.

3.4.2 Prediction and Correlation of Chiral Stationary Phase Affinity for Water with Hydrophilic Probe Molecules.

The affinity of nine chiral stationary phases for water was examined, with reference to bare silica. The relative retention of cytosine and uracil has been suggested as a measure for the ‘hydrophilic’ character of a stationary phase and the relative retention of benzyl trimethylammonium chloride (BTMA) and cytosine as a measure of its ion-exchange character.^{25, 26} Based on previous works, we constructed a selectivity plot of ion-exchange behavior ($\alpha_{\text{BTMA/cytosine}}$) on the y-axis vs. hydrophilicity ($\alpha_{\text{cytosine/uracil}}$) on the x-axis for multiple chiral stationary phases used under super/subcritical conditions (*Figure 3.1*).^{25, 26} A higher value of the $\alpha_{\text{cytosine/uracil}}$ suggests an increased hydrophilic character of the stationary phase whereas a higher value of the $\alpha_{\text{BTMA/cytosine}}$ suggests higher ion exchange capacity as shown in *Figure 3.1A*). If we project this data onto the $\alpha_{\text{cytosine/uracil}}$ axis, we get an ordering of the hydrophilicity for these columns (*Figure 3.1B*). This plot can serve as a predictive tool to determine how a given stationary phase would interact with the aqueous portion of the mobile phase, *vide infra*.

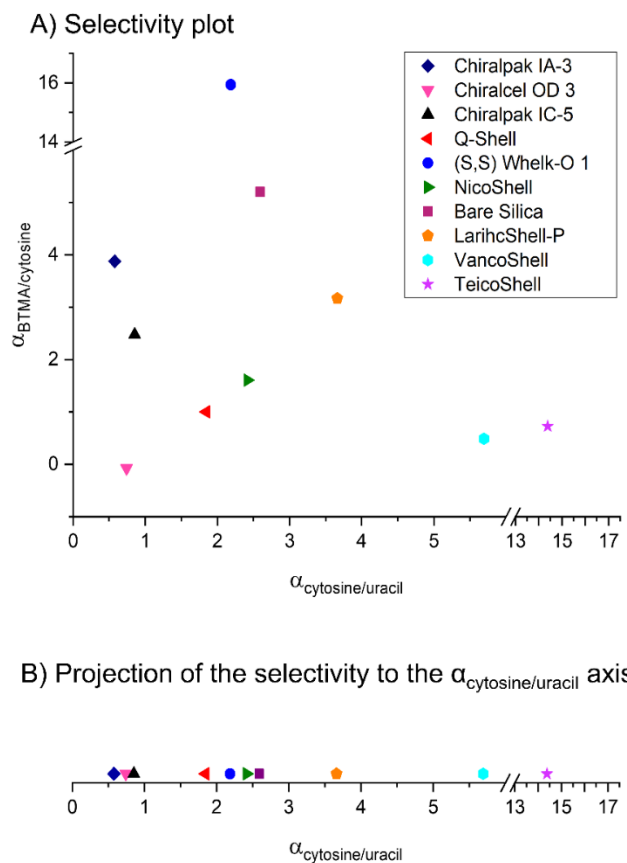


Figure 3.1. A) Plot of electrostatic character (y-axis) and the hydrophilic character (x-axis) for the chiral stationary phases used in SFC. B) Projection of selectivity on the $\alpha_{\text{cytosine/uracil}}$ axis.

Experimental conditions: 80/20 (v/v) ACN/ 25 mM ammonium acetate pH 6.8, flow rate: 1 mL/min and UV detection at 254 nm. The dead time was measured with water or acetone.

According to values obtained from the Figure 3.1B plot, the order for hydrophilicity is: TeicoShell >> VancoShell > LarihcShell > Bare Silica ~ NicoShell > (S,S) Whelk-O 1 > QShell > Chiralpak IC-5 > Chiralcel OD-3 > Chiralpak IA-3. TeicoShell is by far the most hydrophilic of the tested stationary phases followed by VancoShell. This is expected as these stationary phases employ naturally occurring macrocyclic glycopeptides for chiral recognition and have multiple glucose moieties, carboxylate, amine, and amide groups in their structure. The modified macrocyclic

glycopeptide NicoShell and the LarihcShell-P, an isopropyl derivatized cyclofructan-6, also possess multiple -OH groups. These stationary phases, therefore, have a high selectivity value for cytosine and uracil pair. The QShell (iso-butyl mercapto quinine) and the (S,S) Whelk O-1 (1-(3,5-dinitrobenzamido)-1,2,3,4-tetrahydrophenanthrene) have a $\alpha_{\text{cytosine/uracil}}$ value of 1.8 and 2.1 respectively. Though the chiral selectors for these two columns lack hydrophilic sites, the apparent hydrophilicity may be due to the residual silanols since neither of these columns is end-capped as is the case with all bonded stationary phases used in this study. The Chiralpak IC-5 and Chiralcel OD-3 use cellulose tris(3,5-dimethylphenylcarbamate) and have very low value (<1) for $\alpha_{\text{cytosine/uracil}}$ pair as is the case with Chiralpak IA-3 which uses amylose tris(3,5-dimethylphenylcarbamate).

3.4.3 Types of Stationary Phases which Show a Gain in Efficiency with Water in the Mobile Phase.

As shown in the previous sections, small amounts of water do not cause any major change in the solvatochromism of Nile red. On the other hand, the selectivity plot of chiral phases and the projection of the data on the cytosine/uracil axis reveals that there is a definite ordering of stationary phases according to their affinity for water. The next question to be explored is, what is the effect of water in SFC once it is sorbed on the stationary phase. A systematic study was conducted on the effect of small amounts of water on the separation efficiency. *Figure 3.2A* illustrates the changes in the efficiency of a representative neutral analyte, hydrobenzoin, on a ChiralPak-IA column, which is a stationary phase of low hydrophilicity. As is evident from the 3D plot of % water added to the modifier, the % modifier in the mobile phase and plates/m, the presence of water causes only a small change in the efficiency (from 48800/m to a maximum of 58500/m). A similar study was conducted with (\pm) cis-4,5-diphenyl-2-oxazolidinone on the Chiralpak-IA stationary phase. The gain in efficiency with added water was small and similar to

hydrobenzoin though it had lesser number of theoretical plates than hydrobenzoin both with and without water. Hence, hydrobenzoin was chosen as a model neutral analyte for the Chiralpak-IA. Note that there is a concomitant reduction in retention factor which will be discussed in a subsequent section. *Figure 3.2B*, on the other hand, represents the behavior of a neutral compound with a hydrophilic stationary phase, TeicoShell, with the neutral analyte (+) cis-4,5-diphenyl-2-oxazolidinone. With increasing water percentage from 0 to 15% (v/v) water in the methanol modifier (0% to a maximum of 6% added water to the total mobile phase), an approximate 8-fold efficiency change ($N/m \approx 12000$ to $N/m \approx 104,000$) was recorded at the point of maximum efficiency. It is worth noting that the effect of water is much more profound at lower methanol concentrations. At 40% methanol concentration increasing the water amount from 0 to 6% (v/v) results in an increase in plates per meter from 35500/m to 64100/m for the first enantiomer. However, at methanol concentration of 5%, increasing the water content by the same amount resulted in a substantial increase in the number of plates from $N/m = 12,830$ ($h = 28.8$) to $N/m = 104,330$ ($h = 3.5$). As shown previously, the amount of water that can be added at lower modifier concentrations is limited since phase separation occurs at higher water concentrations.^{22, 31} In general, one can increase the efficiency by simply increasing the methanol percentage. Water at low methanol concentrations has such a significant impact on separation efficiency that it surpasses efficiencies at high MeOH concentrations both with and without water (*Figure 3.2B*). The decrease in peak width is due to the improved sorption-desorption kinetics, as will be discussed in the following section. Water also acts as a sorption competitor to the analyte on hydrophilic stationary phases. This will be demonstrated with non-linear chiral chromatography in later sections.

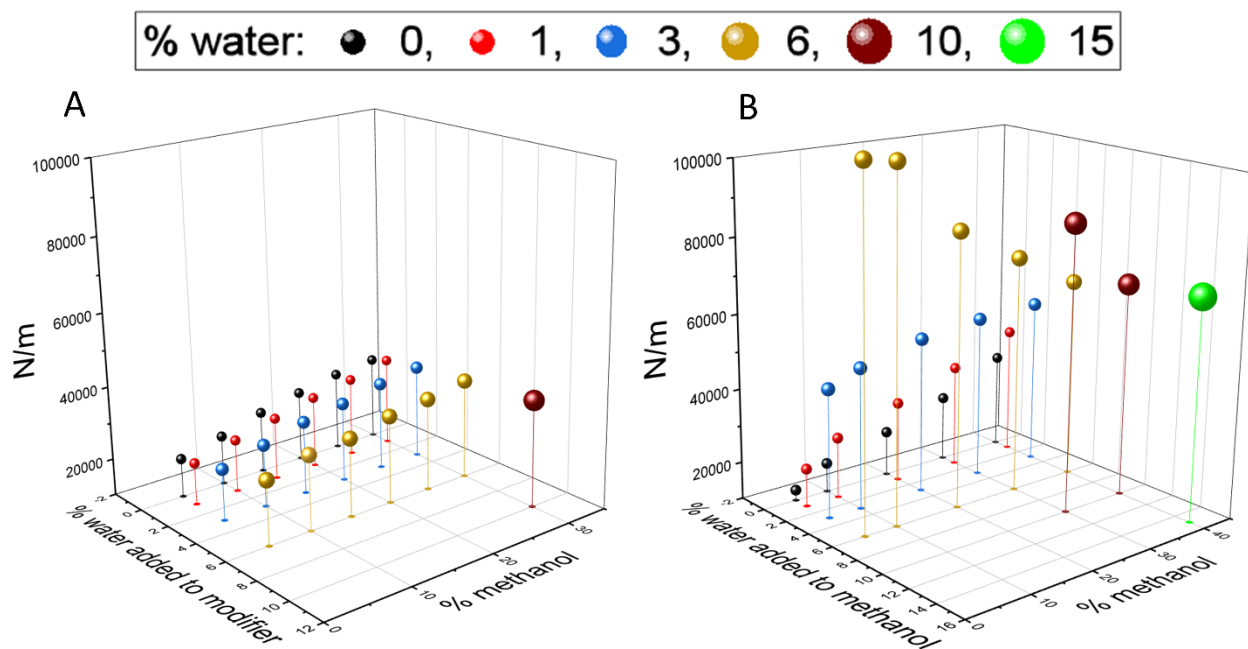


Figure 3.2. 3D plot for efficiency gains with water addition under different modifier concentrations (A) Gain in efficiency for Chiralpak IA-3 column with neutral analyte: hydrobenzoin. (B) Gain in efficiency for TeicoShell column with neutral analyte: (\pm) cis-4,5-diphenyl-2-oxazolidinone. Experimental condition: 60-95/40-5 CO₂/ MeOH with 0-15% H₂O, flow rate: 4 mL/min, temp.: 25°C, outlet pressure: 8 MPa. UV detection at 220 nm

To test the generality of efficiency trends with added water, the TeicoShell column was further tested with an acidic and basic analyte namely 2-(4-chlorophenoxy)propionic acid and metoprolol, respectively (Table 3.1 & Figures 3.S2 and 3.S3). These analytes are enantiomerically separated with different additives using ammonium formate for the former and a combination of triethylamine (TEA) and trifluoroacetic acid (TFA) for the latter. Even with these additives, substantial improvements in efficiency are obtained with the addition of small amounts of water in the mobile phase (Figure 3.S2 and 3.S3). Furthermore, three analytes tryptophanamide (neutral), tryptophan (amphoteric) and 1-(1-naphthyl)ethylamine (basic) were separated on the LarihcShell-

P column with and without water in the mobile phase. As predicted from the selectivity plot (*vide supra*) since the stationary phase is comparatively hydrophilic, large increases in efficiency (> 300%) are seen with the addition of small quantities of water (*Table 3.1, Figure 3.S4, 3.S5, and 3.S6*). All the columns mentioned in the selectivity plot have been tested with a range of analytes with different functionalities, which are baseline separated on said stationary phases, with and without water, and the results are summarized in *Table 3.1*. The change in efficiency after water addition is quantified as ΔN ($N_{\text{with water}} - N_{\text{without water}}$) and a positive value of ΔN signifies an efficiency gain which is omnipresent for all tested compounds with all stationary phases. The results from the *Table 3.1* highlight the fact that stationary phases with low $\alpha_{\text{cytosine/uracil}}$ values such as Chiralpak IA and IC, ChiralCel-OD, Q-shell and (S,S) Whelk-O 1 show small increases in plate counts as compared to highly hydrophilic stationary phase like VancoShell, NicoShell, LarihcShell-P, and TeicoShell. This observation is consistent with the ordering seen on the projection axis of *Figure 3.1B*. Representative chromatograms from *Table 3.1* are also shown in the Supporting Information (*Figure 3.S7-3.S10*). The results on randomly chosen compounds (*Table 3.1*) advocate for the incorporation of small amounts of water in all SFC method development performed protocols, especially when using hydrophilic stationary phases or when analysis time has to be reduced without using an excessive amount of MeOH.

Table 3.1: Effect of water on enantioseparation under super/subcritical conditions

Analyte	Stationary Phase	Mobile Phase	ΔN ($N_{\text{with water}} - N_{\text{without water}}$)	Δt_R (min) ($t_{R \text{ with water}} - t_{R \text{ without water}}$)	ΔR_s ($R_{s \text{ with water}} - R_{s \text{ without water}}$)
(±) cis-4,5-diphenyl-2-oxazolidinone	TeicoShell (10x0.46cm)	95/5 CO ₂ /MeOH 95/5 CO ₂ /MeOH + 6% (v/v) water	+9320 (~837%)	-11.68	+2.07

2-(4-chlorophenoxy) propionic acid	TeicoShell (10x0.46cm)	80/20 CO ₂ /MeOH- 0.1% (w/v) ammonium formate 80/20 CO ₂ /MeOH- 0.1% (w/v) ammonium formate + 6% (v/v) water	+6319 (~154%)	-1.23	+1.18
Metoprolol	TeicoShell (10x0.46cm)	80/20 CO ₂ /MeOH- 0.1% TEA-0.1% TFA 80/20 CO ₂ /MeOH- 0.1% TEA-0.1% TFA + 6% (v/v) water	+6512 (~91%)	-3.49	-0.43
Tryptophan	LarihcShell-P (10x0.46cm)	80/20 CO ₂ /MeOH- 0.2% TEA-0.3% TFA 80/20 CO ₂ /MeOH- 0.2% TEA-0.3% TFA + 6% (v/v) water	+7593 (~330%)	-1.605	+0.09
Tryptophanamide	LarihcShell-P (10x0.46cm)	80/20 CO ₂ /MeOH- 0.2% TEA-0.3% TFA 80/20 CO ₂ /MeOH- 0.2% TEA-0.3% TFA + 6% (v/v) water	+4700 (~84%)	-3.859	-0.33
Fluoxetine	VancoShell (10x0.46cm)	85/15 CO ₂ /MeOH- 0.1% TEA-0.1% TFA 85/15 CO ₂ /MeOH- 0.1% TEA-0.1% TFA + 6% (v/v) water	+5634 (~277%)	-1.913	+1.42
Nicardipine	VancoShell (10x0.46cm)	80/20 CO ₂ /MeOH- 0.1% (w/v) ammonium formate 80/20 CO ₂ /MeOH- 0.1% (w/v) ammonium formate + 6% (v/v) water	+3067 (~160%)	-0.152	+0.39
Bupivacaine	NicoShell (10x0.46cm)	80/20 CO ₂ /MeOH- 0.1% TEA-0.1% TFA 80/20 CO ₂ /MeOH- 0.1% TEA-0.1% TFA + 6% (v/v) water	+3650 (~181%)	-0.588	+0.33

Proglumide	NicoShell (10x0.46cm)	80/20 CO ₂ /MeOH- 0.1% (w/v) ammonium formate 80/20 CO ₂ /MeOH- 0.1% (w/v) ammonium formate + 6% (v/v) water	+10516 (~286%)	-0.158	+1.66
Trans-Stilbene oxide	(S,S) Whelk O 1 (25x0.46cm)	80/20 CO ₂ /MeOH 80/20 CO ₂ /MeOH + 6% (v/v) water	+2555 (~30%)	-0.088	-0.44
Ketoprofen	(S,S) Whelk O 1 (25x0.46cm)	80/20 CO ₂ /MeOH- 0.1% DEA 80/20 CO ₂ /MeOH- 0.1% DEA + 6% (v/v) water	+274 (~4%)	-1.122	+0.06
Bendroflumethazi de	Chiralpak IC-5 (25x0.46cm)	80/20 CO ₂ /MeOH 80/20 CO ₂ /MeOH + 6% (v/v) water	+1427 (~29%)	-0.636	-0.84
Warfarin	Chiralpak IC-5 (25x0.46cm)	90/10 CO ₂ /MeOH 90/10 CO ₂ /MeOH + 6% (v/v) water	+1090 (~14%)	-1.856	-0.93
N-benzoyl-dl- valine	Qshell (10x0.46cm)	70/30 CO ₂ /MeOH- 0.1% ammonium formate-0.3% formic acid 70/30 CO ₂ /MeOH- 0.1% ammonium formate-0.3% formic acid + 6% (v/v) water	+1594 (~13%)	-0.049	-0.36
Dansyl serine	Qshell (10x0.46cm)	70/30 CO ₂ /MeOH- 0.1% ammonium formate-0.3% formic acid 70/30 CO ₂ /MeOH- 0.1% ammonium formate-0.3% formic acid + 6% (v/v) water	1682 (~21%)	-1.787	+0.15

Hydrobenzoin	Chiralpak (15x0.46cm)	IA-3	80/20 CO ₂ /MeOH 80/20 CO ₂ /MeOH + 6% (v/v) water	+699 (~16%)	-0.221	+0.19
Mianserin	Chiralpak (15x0.46cm)	IA-3	80/20 CO ₂ /MeOH- 0.1% DEA 80/20 CO ₂ /MeOH- 0.1% DEA + 6% (v/v) water	+416 (~16%)	-0.037	-0.04
Coumachlor	Chiralcel (5x0.46cm)	OD-H	90/10 CO ₂ /MeOH 90/10 CO ₂ /MeOH + 6% (v/v) water	+680 (~31%)	-0.181	+0.51
Trans-stilbene oxide	Chiralcel (5x0.46cm)	OD-H	90/10 CO ₂ /MeOH 90/10 CO ₂ /MeOH + 6% (v/v) water	+49 (~1%)	-0.046	-1.86

* Resolution (R_s) = $2(t_2 - t_1)/(w_1 + w_2)$ where w_1 and w_2 are the baseline peak widths of the first and second eluted enantiomers; TEA = triethylamine, TFA = trifluoroacetic acid, DEA = diethylamine

3.4.4 Kinetic Evaluation in Chiral SFC with and without Water.

The effects of water on SFC in terms of plate counts, as well as other nuances, can further be examined by linear velocity vs. reduced plate height (h) curves. Chiral separations often show non-classical behavior despite the familiar “van Deemter like” appearance.²⁷ Figure 3.3 shows such a curve for (\pm) cis-4,5-diphenyl-2-oxazolidinone enantiomers in the absence (Figure 3.3A) and in the presence (Figure 3.3B) of water using a CO₂/MeOH mobile phase and a teicoplanin bonded column. This curve was made on a custom modified SFC in which extra-column effects and especially detector-based band broadening is negligible (see Experimental). Several interesting observations regarding water in the co-solvent can be made. In the absence of water, the van Deemter plot shows large h values of approximately 4 and 10 for the first and the second eluting enantiomers respectively. Once water is added, both analyte enantiomers show a dramatic change in efficiency, reaching the ideal reduced plate heights (h) of 2 to 3 for both the first and the

second eluted enantiomers.³² In the presence of water, the change in h for the second enantiomer is considerably larger as compared to the change in h for the first enantiomer. The more highly retained enantiomer is believed to have the highest resistance to stationary phase mass transfer as it is subject to a higher number of associative stereochemical interactions and often is subjected to molecular/diastereomeric reorientation effects on the chiral stationary phase.³³ Indeed, water assists in decreasing mass transfer contributions to the plate height in SFC. One can compare this result with the effect of methyl tert-butyl ether (MTBE) in the mobile phase under reversed phase conditions consisting of methanol-water on α -cyclodextrin columns.³⁴ In the absence of MTBE, monoterpenes appeared as broad peaks with longer retention. With small amount of MTBE in the eluent, the retention time of the analyte decreases, and peak widths are significantly reduced due MTBE acting as a competitor for the hydrophobic cavity of the cyclodextrin. It appears that water produces a similar effect with hydrophilic stationary phases under SFC conditions. Secondly, the absence of minima in the h vs. u curve is notable, this effect is also seen in chiral liquid chromatography on chiral stationary phases.³²

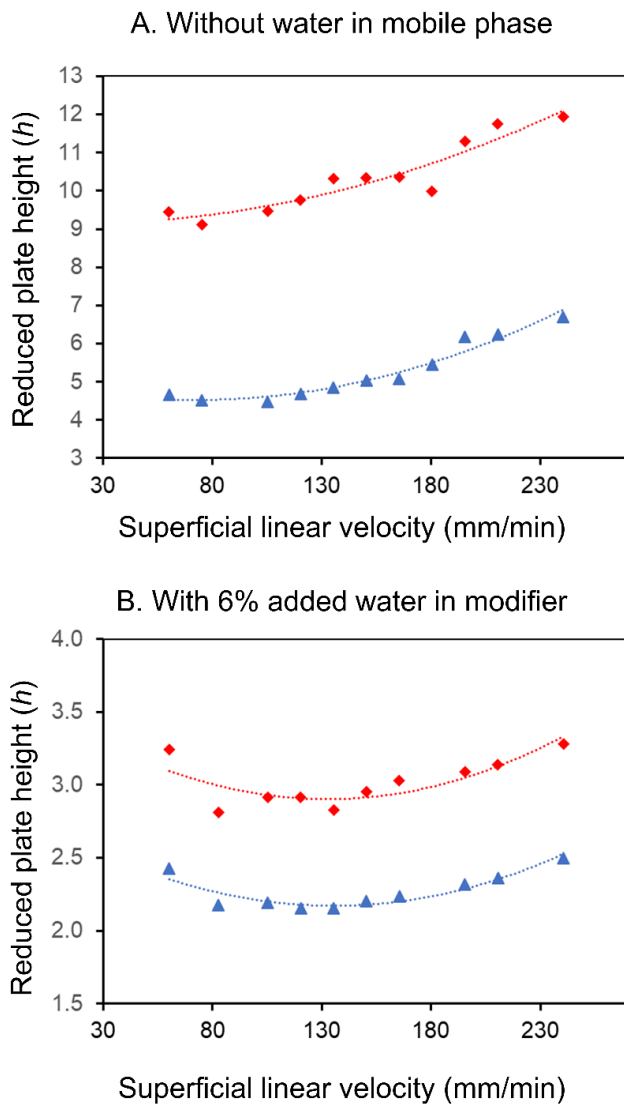


Figure 3.3. Superficial linear velocity vs. reduced plate height curves for (\pm) *cis*-4,5-diphenyl-2-oxazolidinone enantiomers with and without water in the mobile phase. Experimental conditions: TecioShell 10x0.46 cm (A) 82/18 CO₂/ MeOH and (B) 82/18 CO₂/ MeOH+6% H₂O, temp.: 40°C, outlet pressure: 12 MPa. UV detection at 254 nm

3.4.5 Making SFC Greener: Reduction of Analysis Times with the Help of Water.

A common bottleneck in drug discovery research is the generation of hundreds of samples for enantiomeric purity analyses. For high-throughput chiral screening, SFC is the method of choice

where high flow rates can be routinely employed due to low mobile phase viscosity. The reduction in the analysis time in chiral LC has made excellent progress where the separations now take less than 1 second to 1 min on 0.5 to 3 cm columns.^{35, 36} SFC has unfortunately lagged behind in terms of hardware development. As a result, shorter columns cannot be conveniently used without hurting the peak width via extra-column effects.³⁷ Pressure limitations are another shortcoming of the SFC instrumentation, something which has been long overcome in liquid chromatography by the introduction of ultrahigh pressure liquid chromatographs. As dictated by the equation, $R_s = [N^{1/2}/4][(\alpha-1)/\alpha][k_2/(1+k_2)]$, the resolution (R_s) shows maximum dependency on the selectivity, α , whereas efficiency N and retention factor k play relatively smaller roles. Despite a loss in selectivity and a smaller retention factor with the enhanced N , as shown in the previous section, the ΔR_s in many cases is positive as shown in *Table 3.1*; however Δt_r is always < 0 . In the case of the hydrobenzoin separation on the Chiralpak IA column (hydrophobic) the retention time of the first eluted enantiomer decreased from 1.03 to 0.95 min when 0% and 6% water was added to the modifier (30% methanol) in the mobile phase respectively. With 10% modifier concentration, retention times of the first eluted enantiomers with 0% and 6% water changed from 3.54 to 2.88 min. Water in the co-solvent clearly increases the eluotropic strength of the SFC mobile phase. The decreasing retention with the non-polar stationary phases in the presence of water has been attributed to the lowering of the extent of interactions like dipole-dipole and charge transfer.³⁸ On the other hand, separation of (\pm) cis-4,5-diphenyl-2-oxazolidinone on the TeicoShell column (hydrophilic) resulted in a decrease of retention of the first eluted enantiomer from 0.83 to 0.59 min with 40% modifier in the mobile phase and 0% and 6% water added respectively. When the modifier concentration is changed to 10% of the total mobile phase, retention with 0% water of the first enantiomer was 5.52 min, and with 6% water, it decreased almost half to 2.29 min. The

entire separation with water was completed even before the elution of the first enantiomer without water. The relative retention change under different modifier concentrations is illustrated in *Figure 3.4*. *Figure 3.4A* represents the retention time change with increasing quantities of water using 40% methanol concentration, while *Figure 3.4B* illustrates the retention changes upon water addition when using 10% methanol. The decrease in selectivity and retention factor was more than compensated by the increase in efficiency. Also, the resolution between enantiomers was maintained, pointing to the fact that water offers a kinetic advantage as confirmed by the *u* vs. *h* curves of *Figure 3.3*.

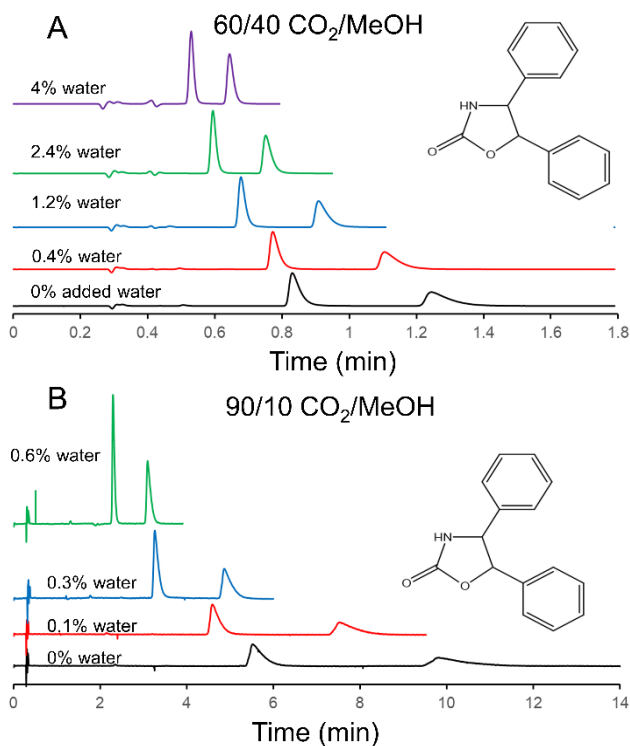


Figure 3.4. Reduction in analysis times with the introduction of increasing amount of water under different modifier compositions. Experimental condition: TecioShell 10 x 0.46 cm (A) 60/40 CO₂/ MeOH and (B) 90/10 CO₂/ MeOH, flow rate: 4 mL/min, temp.: 25°C and outlet

pressure: 8 MPa. Amounts of water recorded are the amount present in the entire mobile phase.

Analyte: (+) cis-4,5-diphenyl-2-oxazolidinone and UV detection at 220 nm.

The hydrophilic columns are much more sensitive to small amounts of water in the methanolic modifier. The large reductions in analysis times with hydrophilic stationary phases point to the advantages of water in SFC co-solvents, especially in the case of fast screening. In the aforementioned example, above the separation at 10% methanol modifier concentration and no added water is completed at about 11 min at a flow rate of 4 mL/min, and the total amount of methanol consumed in the process was 4.4 mL. Whereas with 0.6% water in the total mobile phase (6% added water in the methanol modifier), the same separation is now completed within 3.2 min, and the amount of modifier consumed at the same flow rate is 1.3 mL. It is common knowledge that increasing the amount of modifier leads to a decrease in the SFC retention time of an analyte. However, with the aim of minimizing the volume of organic solvents owing to their environmental impact, the addition of small amounts of water can be a beneficial alternative. Water being the most environmentally benign solvent, replacing the organic modifier is a step towards making SFC greener. This is combined with the fact that efficiencies of CO₂-MeOH-H₂O mobile phases are intrinsically higher than those of CO₂-MeOH mobile phases.

3.4.6 Ramifications of Using Water in Preparative SFC Under Non-Linear Conditions: Tuning Peak Shapes.

SFC is often operated under non-linear adsorption conditions for preparative chiral separations. Changing the adsorption isotherm in chiral chromatography under overload conditions can result in an advantageous situation when one of the eluted enantiomers is fronting, and the other peak shows classical tailing. One of the successful models in predicting non-linear peaks shapes in liquid chromatography is the competitive adsorption isotherm, where the overloaded peak shape

is dependent on the retention of the more strongly adsorbed component of the mobile phase.³⁹ If the more strongly adsorbed mobile phase component is more retained than the analyte, then fronting peaks may be observed. Based on the information from the selectivity plot, it can be deduced that water must be strongly sorbed on the hydrophilic stationary phases. Therefore, in the presence of water, chiral analytes can be tuned to a fronting shape under preparative conditions. As a proof of concept, the changing adsorption isotherm of the analyte 2-(4-chlorophenoxy) propionic acid is shown with and without water in *Figure 3.5*. The mobile phase consists of 90% CO₂ and 10% MeOH with 0.1% (w/v) ammonium formate. Under this condition, both enantiomers display classical nested tailing (*Figure 3.5A*). With 0.6% water in the total mobile phase (*Figure 3.5B*), the first eluted enantiomer shows pronounced fronting and a very steep rear slope, while the second eluted enantiomer continues to tail (albeit with a much-improved peak shape). Such a situation is highly beneficial in preparative SFC as it greatly increases the enantiomeric resolution of peaks in overloaded solute conditions. This is a general phenomenon. Previous reports^{40, 41} employed various mobile phase conditions to achieve the same type of peak shape tuning; however, the present method is simpler, in that it requires only small amounts of water in the co-solvent. At low water concentrations (e.g., 1%) in the above stated mobile phase, both the peaks continue to tail similar to the situation without water (*Figure 3.S11*). However, at somewhat higher water concentrations in the methanolic modifier, we can successfully tune the overloaded peak shapes.

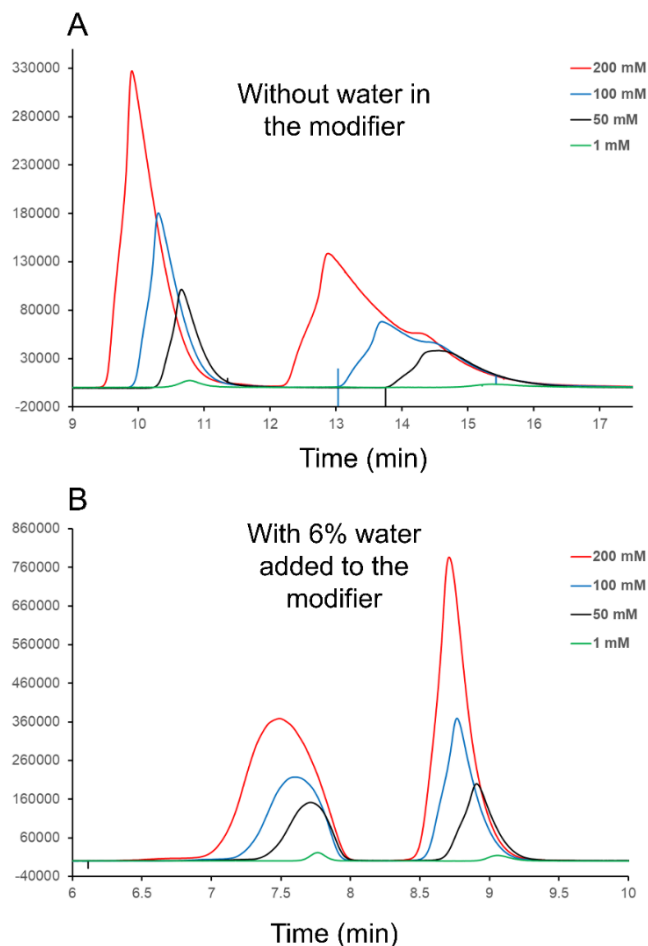


Figure 3.5. Modulating peak shapes by varying adsorption isotherm with water under SFC conditions. Experimental condition: TecioShell 10 x 0.46 cm (A) 90/10 CO₂/ MeOH-0.1% (w/v) ammonium formate and (B) 90/10 CO₂/ MeOH-0.1% (w/v) ammonium formate+ 6% H₂O, flow rate: 4 mL/min, temp.:25°C and outlet pressure: 8 MPa. Analyte: 2-(4-chlorophenoxy)propionic acid and UV detection at 220 nm.

3.5 Conclusions

Herein we demonstrate substantial efficiency gains using small amounts of water in the SFC mobile phase. We develop a predictive test based on stationary phase hydrophilicity to understand which chiral stationary phases will show the greatest efficiency gains and a simultaneous reduction

of the separation window with the addition of water. Slight gains in efficiency are noticeable with hydrophobic chiral stationary phases; however, there can be ≥ 8 -fold improvements in efficiency with hydrophilic stationary phases. Under optimized conditions, hydrophilic phases perform much better than hydrophobic stationary phases in SFC. Significant reduction in analysis times observed in the case of hydrophilic columns in the presence of water results in decreased consumption of environmentally unwanted organic modifier, thereby making SFC greener. Finally, tuning of peak shapes under overload conditions by varying the adsorption isotherm is demonstrated for the first time in chiral SFC, using water. The implications of this phenomenon are immense for preparative chiral SFC, which remains one of the primary purification applications in the pharmaceutical industry. The results herein clearly advocate for the use of small amounts of water in analytical as well as preparative separations by chiral SFC.

3.6 Acknowledgments.

The authors would like to thank Robert A Welch Foundation (Y-0026) for financial support. We would acknowledge AZYP LLC Arlington, TX for providing chiral columns.

3.7 References

1. Knez, Ž.; Pantić, M.; Cör, D.; Novak, Z.; Knez Hrnčič, M., *Chem. Eng. Process. (Process Intensification)* **2019**, *141*, 107532.
2. Wright, B. W.; Kalinoski, H. T.; Smith, R. D., *Anal. Chem.* **1985**, *57* (14), 2823-2829.
3. Raynie, D. E., *Anal. Chem.* **1993**, *65* (21), 3127-3128.
4. White, C., *J. Chromatogr. A* **2005**, *1074* (1), 163-173.
5. Barhate, C. L.; Joyce, L. A.; Makarov, A. A.; Zawatzky, K.; Bernardoni, F.; Schafer, W. A.; Armstrong, D. W.; Welch, C. J.; Regalado, E. L., *Chem. Comm.* **2017**, *53* (3), 509-512.
6. Liu, Y.; Berthod, A.; Mitchell, C. R.; Xiao, T. L.; Zhang, B.; Armstrong, D. W., *J. Chromatogr. A* **2002**, *978* (1-2), 185-204.
7. West, C.; Melin, J.; Ansouri, H.; Metogo, M. M., *J. Chromatogr. A* **2017**, *1492*, 136-143.
8. Stringham, R. W., *J. Chromatogr. A* **2005**, *1070* (1-2), 163-170.
9. Page, S. H.; Sumpter, S. R.; Lee, M. L., *J. Microcolumn Sep.* **1992**, *4* (2), 91-122.
10. Pyo, D., *J. Biochem. Bioph. Methods* **2000**, *43* (1-3), 113-123.
11. Pyo, D.; Ju, D., *Analyst* **1993**, *118* (3), 253-255.
12. Miller, L., *J. Chromatogr. A* **2012**, *1256*, 261-266.

13. DaSilva, J. O.; Coes, B.; Frey, L.; Mergelsberg, I.; McClain, R.; Nogle, L.; Welch, C. J., *J. Chromatogr. A* **2014**, *1328*, 98-103.
14. Gritti, F.; Fogwill, M.; Gilar, M.; Jarrell, J. A., *J. Chromatogr. A* **2016**, *1468*, 217-227.
15. Strubinger, J. R.; Song, H.; Parcher, J. F., *Anal. Chem.* **1991**, *63* (2), 104-108.
16. Li, J.; Thurbide, K. B., *Can. J. Anal. Sci. Spectros.* **2008**, *53* (2), 59-65.
17. Liu, J.; Regalado, E. L.; Mergelsberg, I.; Welch, C. J., *Org. Biomol. Chem.* **2013**, *11* (30), 4925-4929.
18. Taylor, L. T., *J. Chromatogr. A* **2012**, *1250*, 196-204.
19. West, C.; Lemasson, E., *J. Chromatogr. A* **2019**, *1593*, 135-146.
20. Patel, M.; Riley, F.; Ashraf-Khorassani, M.; Taylor, L., *J. Chromatogr. A* **2012**, *1233*, 85-90.
21. Liu, J.; Makarov, A. A.; Bennett, R.; Haidar Ahmad, I. A.; DaSilva, J.; Reibarkh, M.; Mangion, I.; Mann, B. F.; Regalado, E. L., *Anal. Chem.* **2019**, *91*, 13907-13915.
22. Bennett, R.; Biba, M.; Liu, J.; Ahmad, I. A. H.; Hicks, M. B.; Regalado, E. L., *J. Chromatogr. A* **2019**, *1595*, 190-198.
23. Roy, D.; Armstrong, D., *J. Chromatogr. A* **2019**.
24. West, C., *Anal. and Bioanal. Chem.* **2018**, *410* (25), 6441-6457.
25. Ibrahim, M. E.; Liu, Y.; Lucy, C. A., *J. Chromatogr. A* **2012**, *1260*, 126-131.
26. Dinh, N. P.; Jonsson, T.; Irgum, K., *J. Chromatogr. A* **2011**, *1218* (35), 5880-5891.
27. Barhate, C. L.; Wahab, M. F.; Tognarelli, D.; Berger, T. A.; Armstrong, D. W., *Anal. Chem.* **2016**, *88* (17), 8664-8672.
28. Bright, F. V.; McNally, M. E. P., *Supercritical Fluid Technology: Theoretical and Applied Approaches to Analytical Chemistry*. ACS Publications: Atlanta GA, 1992.
29. Deye, J. F.; Berger, T. A.; Anderson, A. G., *Anal. Chem.* **1990**, *62* (6), 615-622.
30. Squires, T. G., *Supercritical Fluids: Chemical and Engineering Principles and Applications Application of solvatochromic probes to supercritical and mixed fluid solvents*. ACS Publications: Chicago, 1987; p 304.
31. Lee, S. T.; Reighard, T. S.; Olesik, S. V., *Fluid Phase Equilib.* **1996**, *122* (1-2), 223-241.
32. Patel, D. C.; Breitbach, Z. S.; Wahab, M. F.; Barhate, C. L.; Armstrong, D. W., *Anal. Chem.* **2015**, *87* (18), 9137-9148.
33. Boehm, R. E.; Martire, D. E.; Armstrong, D. W., *Anal. Chem.* **1988**, *60* (6), 522-528.
34. Armstrong, D. W.; Zukowski, J., *J. Chromatogr. A* **1994**, *666* (1), 445-448.
35. Wahab, M. F.; Wimalasinghe, R. M.; Wang, Y.; Barhate, C. L.; Patel, D. C.; Armstrong, D. W., *Anal. Chem.* **2016**, *88* (17), 8821-8826.
36. Kotoni, D.; Ciogli, A.; Molinaro, C.; D'Acquarica, I.; Kocergin, J.; Szczerba, T.; Ritchie, H.; Villani, C.; Gasparrini, F., *Anal. Chem.* **2012**, *84* (15), 6805-6813.
37. Berger, T. A., *Chromatographia* **2019**, *82* (2), 537-542.
38. Lesellier, E., *J. Chromatogr. A* **2009**, *1216* (10), 1881-1890.
39. Golshan-Shirazi, S.; Guiochon, G., *J. Phys. Chem.* **1989**, *93* (10), 4143-4157.
40. Arnell, R.; Forssén, P.; Fornstedt, T., *Anal. Chem.* **2007**, *79* (15), 5838-5847.
41. Wahab, M. F.; Anderson, J. K.; Abdelrady, M.; Lucy, C. A., *Anal. Chem.* **2013**, *86* (1), 559-566.

3.8 Supporting Information

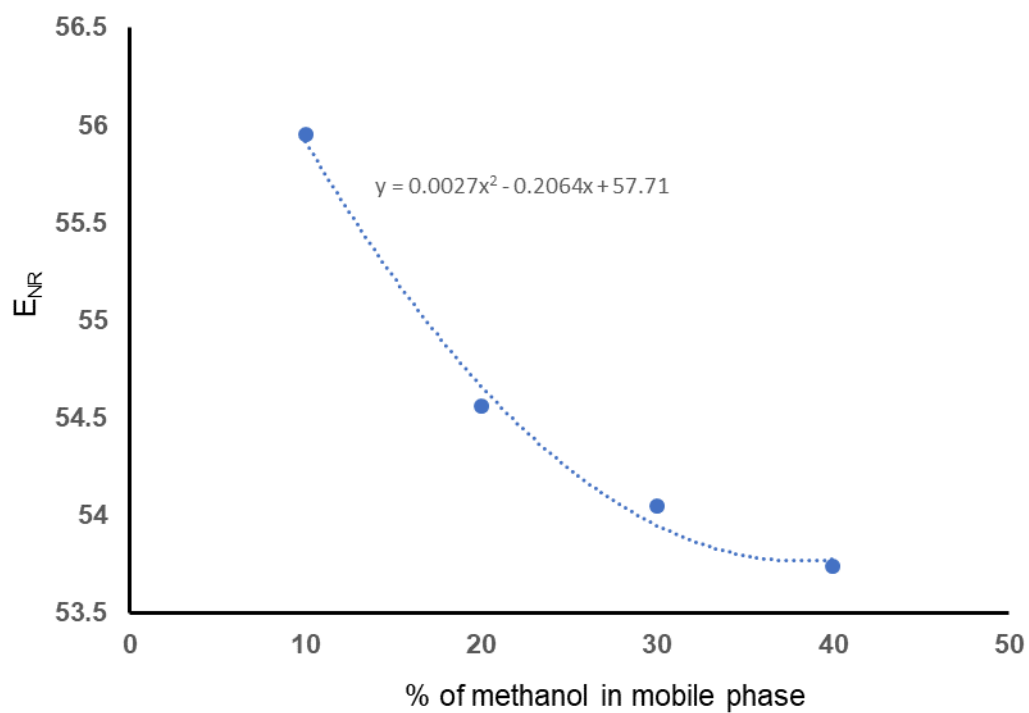


Figure 3.S1. Plot of energy of transition of Nile red dye vs. methanol percentage in the mobile phase. Transition energy calculated by $E_{NR} = 28591.44/\text{wavelength}(\text{nm})$

Table 3.S1. Solvatochromism effects in SFC with Nile Red Dye.

	Composition	E_{NR} (kcal/mol)	Wavelength (nm)
1.	a. 90% CO ₂ - 10% methanol	55.95	511
	b. 90% CO ₂ - 10% methanol containing 6% water	55.95	511
2.	a. 80% CO ₂ - 20% methanol	54.56	524
	b. 80% CO ₂ - 20% methanol containing 6% water	54.56	524
3.	a. 70% CO ₂ - 30% methanol	54.05	529
	b. 70% CO ₂ - 30% methanol containing 6% water	54.05	529
4.	a. 60% CO ₂ - 40% methanol	53.74	532
	b. 60% CO ₂ - 40% methanol containing 6% water	53.44	535

*all values at 40 °C and 12 MPa outlet pressure. The flow cell temperature was measured at 40°C using a thermocouple

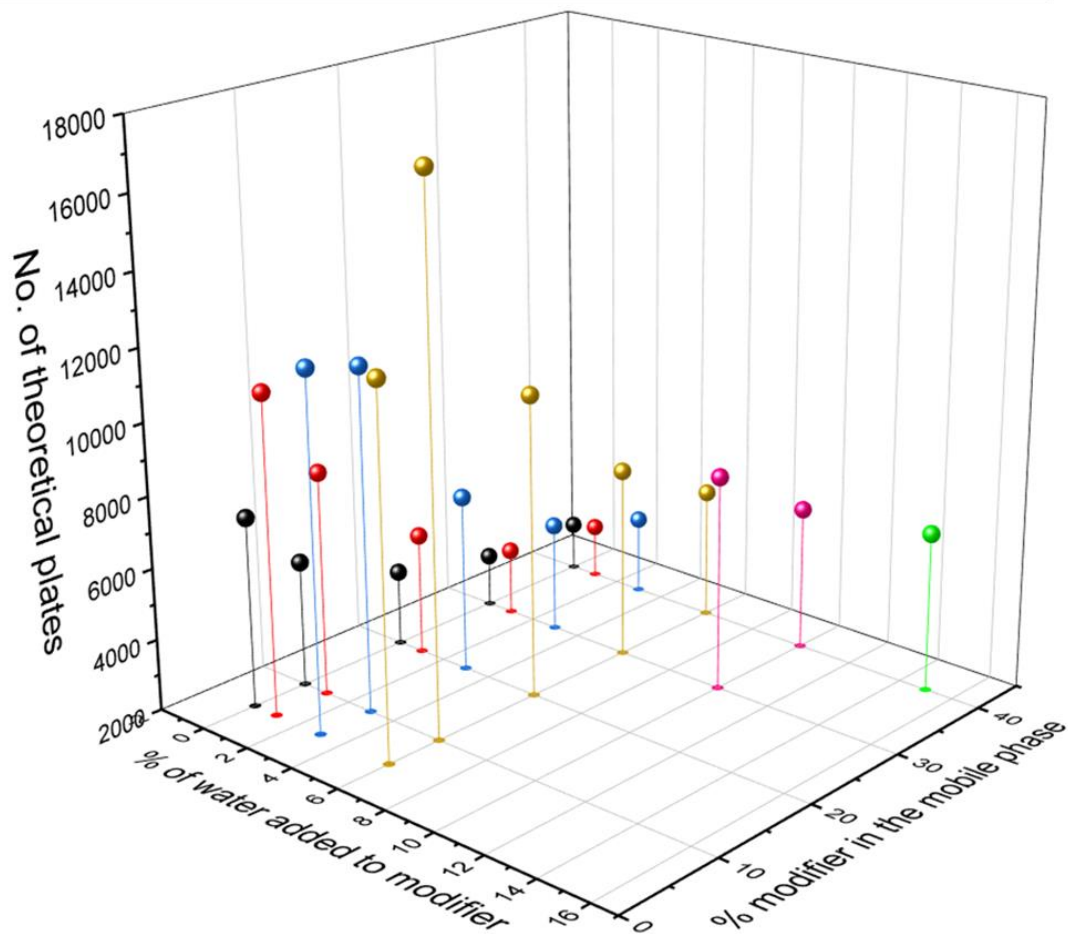


Figure 3.S2: 3D plot representing % water in the modifier, % modifier in the mobile phase and number of theoretical plates for 2-(4-chlorophenoxy)propionic acid on TeicoShell (10 x 0.46 cm). Experimental condition: 60-95/40-5 CO₂/ MeOH-0.1% (w/v) ammonium formate+ 0-15% H₂O. Flow rate: 4 mL/min, temperature: ambient and outlet pressure: 8 MPa. UV detection at 220 nm

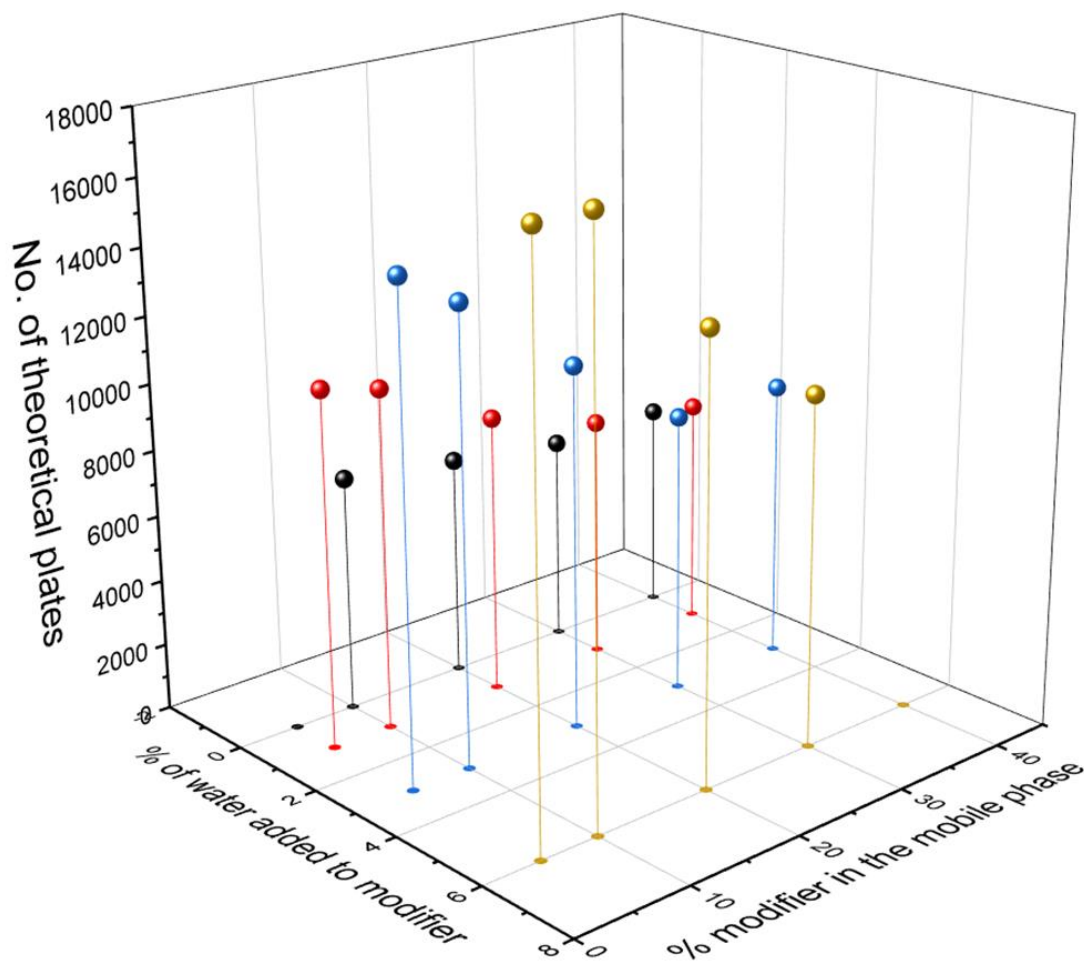


Figure 3.S3: 3D plot representing % water in the modifier, % modifier in the mobile phase and number of theoretical plates for metoprolol on TeicoShell (10 x 0.46 cm). Experimental condition: 75-95/25-5 CO₂/ MeOH-0.1% (v/v) triethylamine-trifluoroacetic acid+ 0-6% H₂O. Flow rate: 4 mL/min, temperature: ambient and outlet pressure: 8 MPa. UV detection at 220 nm

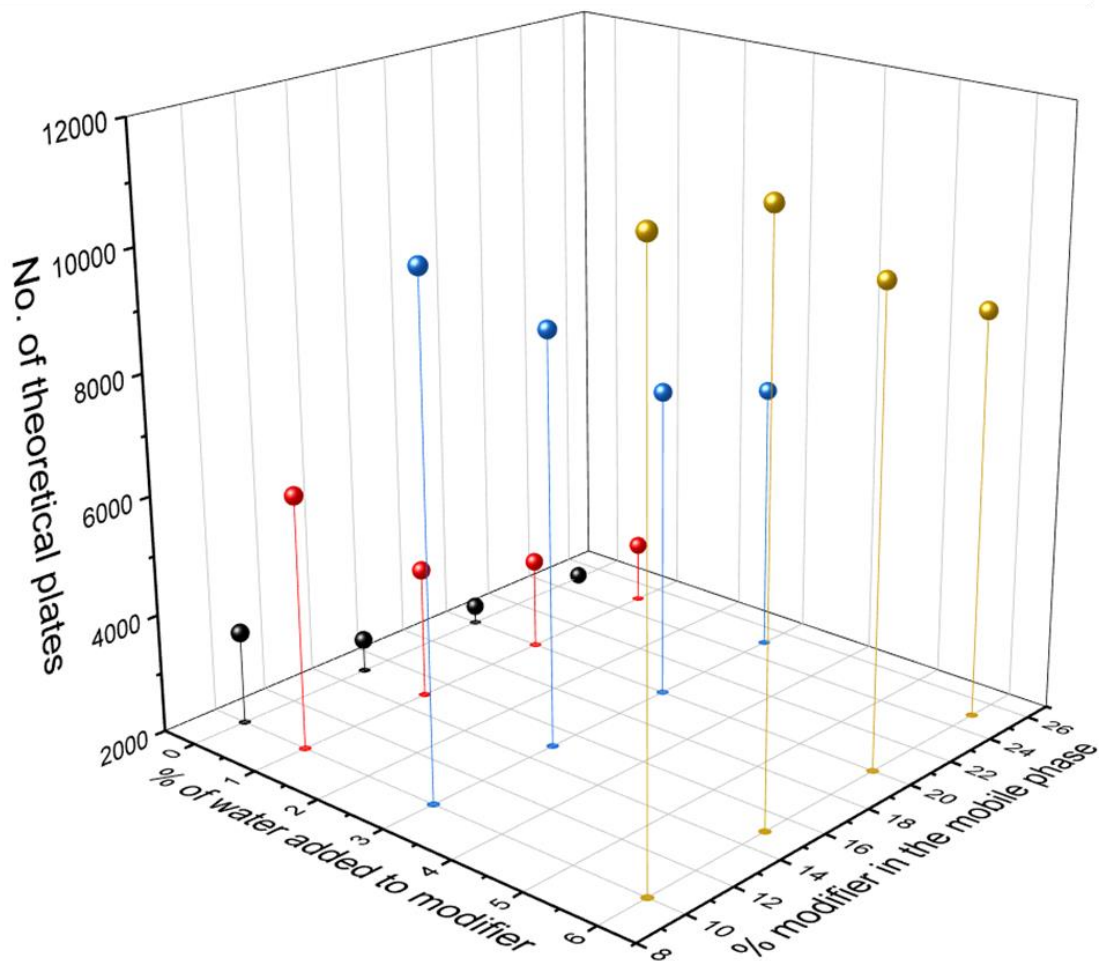


Figure 3.S4: 3D plot representing % water in the modifier, % modifier in the mobile phase and number of theoretical plates for tryptophan on LarihcShell-P (10 x 0.46 cm). Experimental condition: 75-95/25-5 CO₂/MeOH-0.2% (v/v) triethylamine-0.3% (v/v) trifluoroacetic acid+ 0-6% H₂O. Flow rate: 4 mL/min, temperature: ambient and outlet pressure: 8 MPa. UV detection at 220 nm

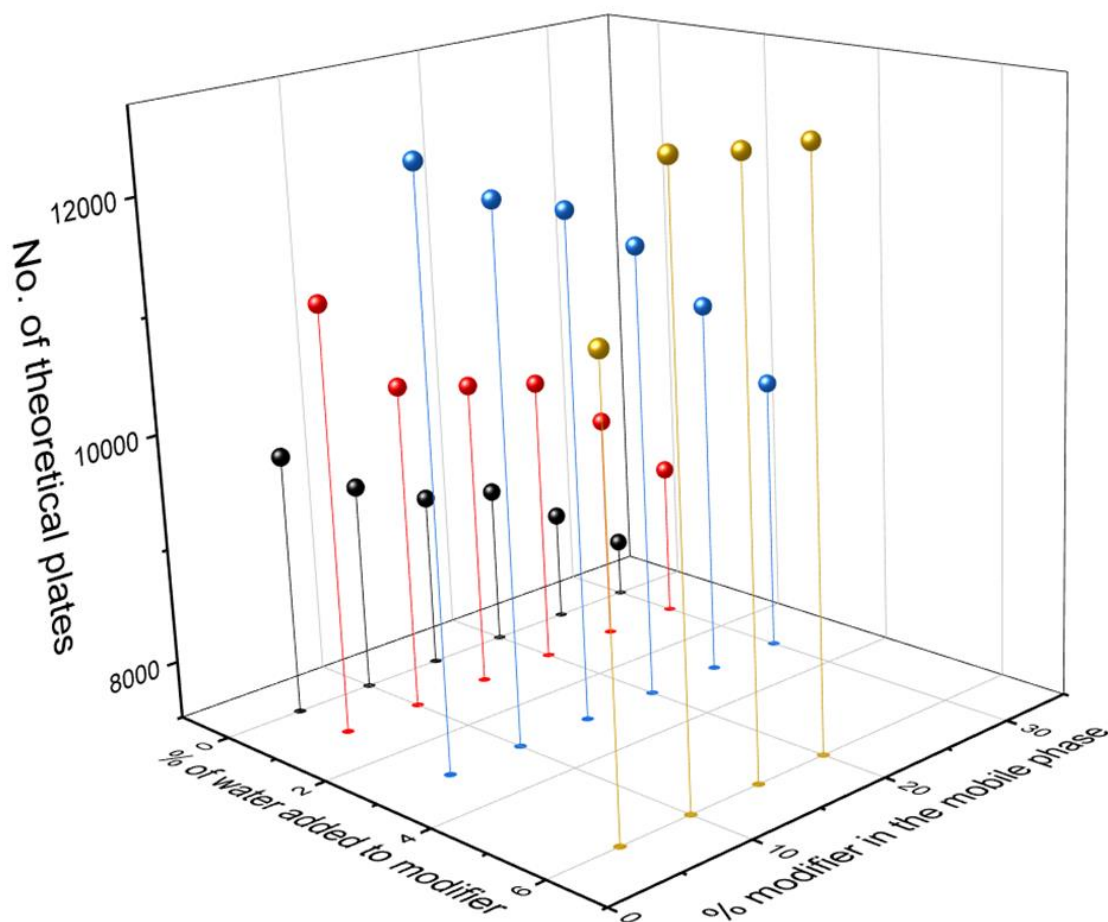


Figure 3.S5: 3D plot representing % water in the modifier, % modifier in the mobile phase and number of theoretical plates for 1-(1-naphthyl)ethylamine on LarihcShell-P (10 x 0.46 cm).
 Experimental condition: 70-95/30-5 CO₂/ MeOH-0.2% (v/v) triethylamine-0.3% (v/v) trifluoroacetic acid+ 0-6% H₂O. Flow rate: 4 mL/min, temperature: ambient and outlet pressure: 8 MPa. UV detection at 220 nm

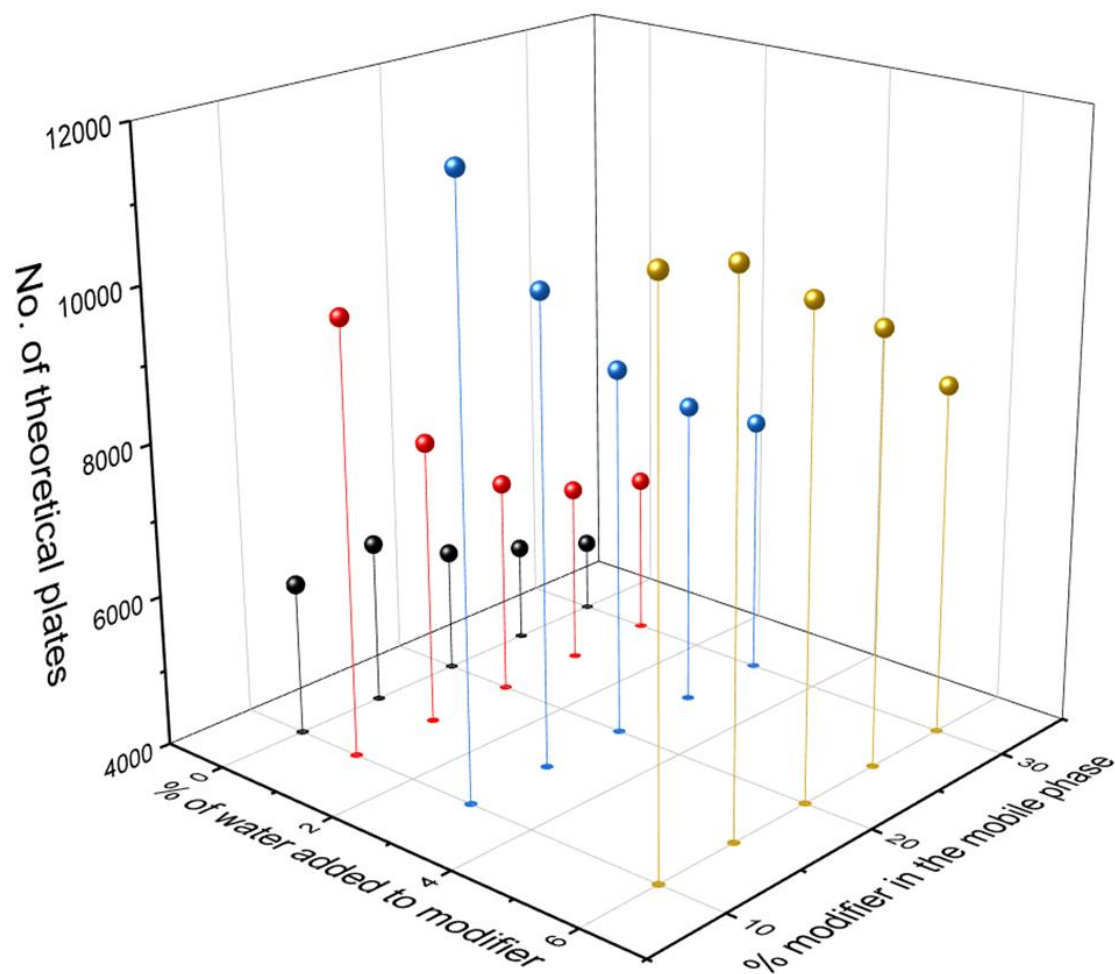


Figure 3.S6: 3D plot representing % water in the modifier, % modifier in the mobile phase and number of theoretical plates for tryptophanamide on LarihcShell-P (10 x 0.46 cm). Experimental condition: 70-95/30-5 CO₂/ MeOH-0.2% (v/v) triethylamine-0.3% (v/v) trifluoroacetic acid+ 0-6% H₂O. Flow rate: 4 mL/min, temperature: ambient and outlet pressure: 8 MPa. UV detection at 220 nm

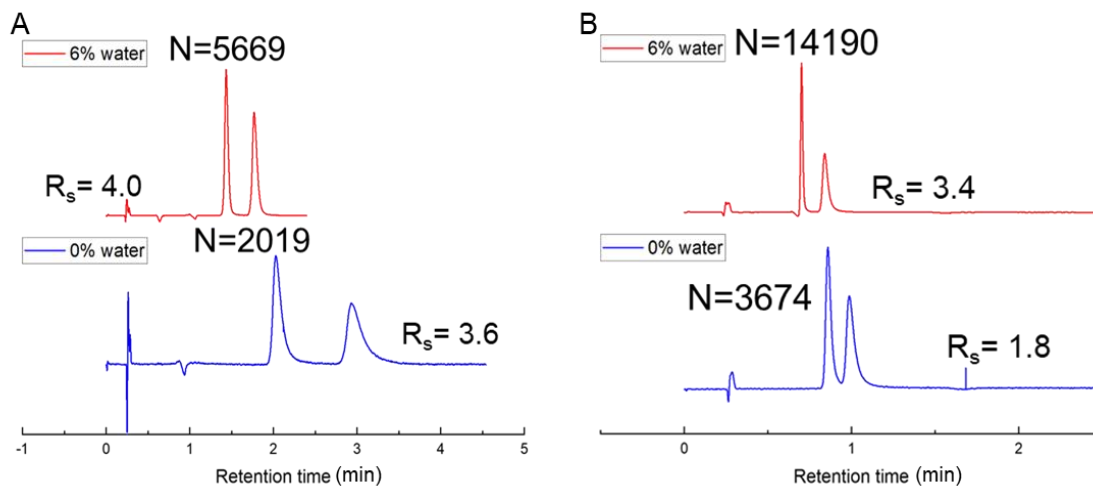


Figure 3.S7: Effect of water on enantiomeric separations with NicoShell (10 x 0.46 cm). Experimental conditions: A. Analyte: Bupivacaine; Mobile phase: 80/20 CO₂/ MeOH- 0.1% (v/v) triethylamine-0.1% (v/v) trifluoroacetic acid. B. Analyte: Proglumide; Mobile phase: 80/20 CO₂/ MeOH- 0.1% (w/v) ammonium formate. Temperature: ambient, Flow rate: 4 mL/min, Outlet pressure: 8 MPa, UV detection at 220 nm.

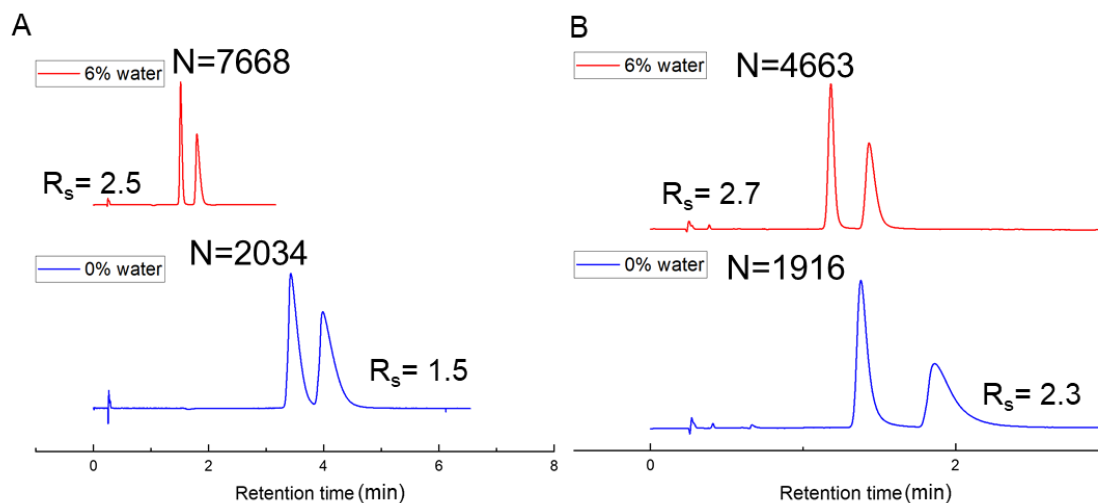


Figure 3.S8: Effect of water on enantiomeric separations with VancoShell (10 x 0.46 cm). Experimental conditions: A. Analyte: Fluoxetine; Mobile phase: 85/15 CO₂/ MeOH- 0.1% (v/v) triethylamine-0.1% (v/v) trifluoroacetic acid. B. Analyte: Nicardipine; Mobile phase: 80/20 CO₂/ MeOH- 0.1% (w/v) ammonium formate. Temperature: ambient, Flow rate: 4 mL/min, Outlet pressure: 8 MPa, UV detection at 220 nm.

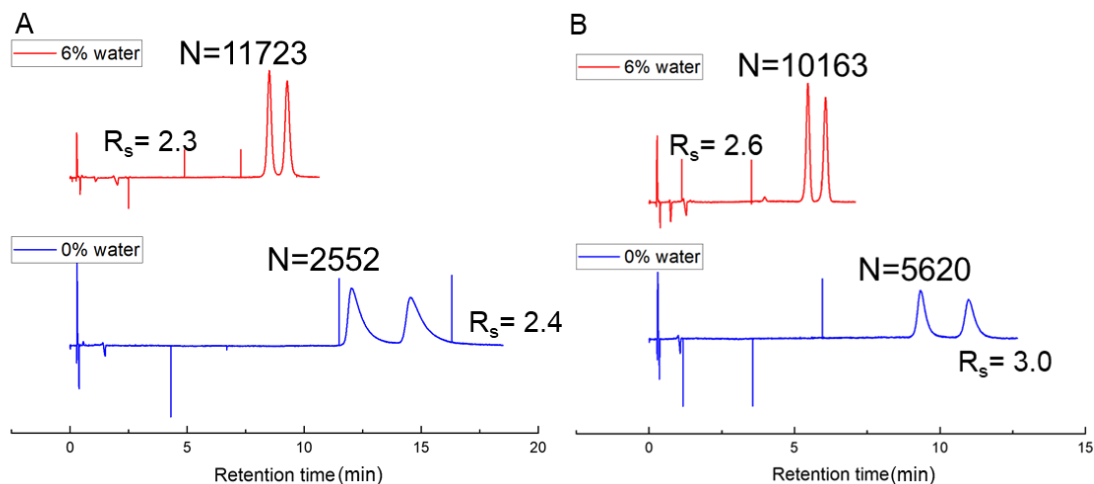


Figure 3.S9: Effect of water on enantiomeric separations with LarihcShell-P (10 x 0.46 cm). Experimental conditions: A. Analyte: Tryptophan; Mobile phase: 85/15 CO₂/ MeOH- 0.2% (v/v) triethylamine-0.3% (v/v) trifluoroacetic acid. B. Analyte: Tryptophanamide; Mobile phase: 80/20 CO₂/ MeOH- 0.2% (v/v) triethylamine-0.3% (v/v) trifluoroacetic acid. Temperature: ambient, Flow rate: 4 mL/min, Outlet pressure: 8 MPa, UV detection at 220 nm.

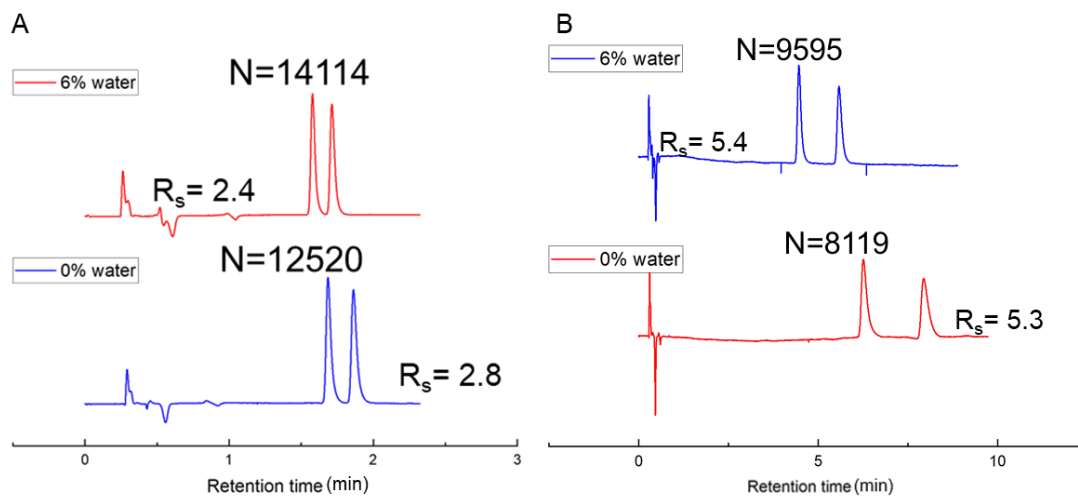


Figure 3.S10: Effect of water on enantiomeric separations with Qshell (10 x 0.46 cm). Experimental conditions: A. Analyte: N-benzoyl-d,l-valine; Mobile phase: 80/20 CO₂/ MeOH- 0.1% (w/v) ammonium formate-0.3% (v/v) formic acid. B. Analyte: Dansyl-d,l-serine; Mobile phase: 80/20 CO₂/ MeOH- 0.1% (w/v) ammonium formate-0.3% (v/v) formic acid. Temperature: ambient, Flow rate: 4 mL/min, Outlet pressure: 8 MPa, UV detection at 220 nm.

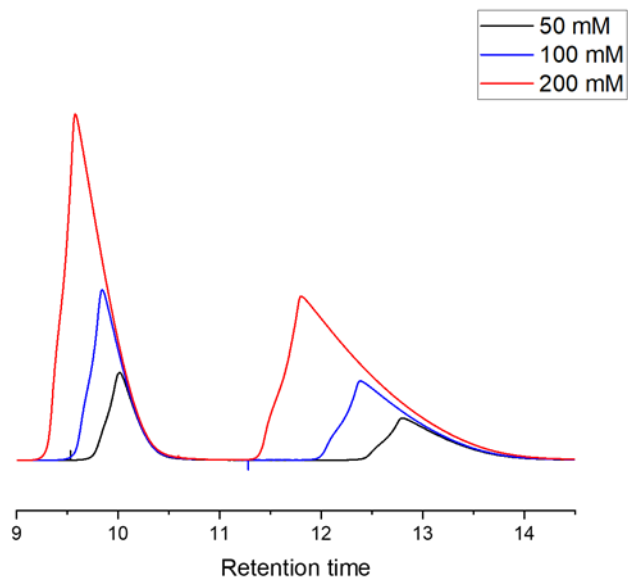


Figure 3.S11: Chromatogram under non-linear condition. Experimental conditions: Column TeicoShell 10 x 0.46 cm. Analyte: 2-(4-chlorophenoxy)propionic acid; Mobile phase: 90/10 CO₂/MeOH-1% water. Temperature: ambient, Flow rate: 4 mL/min, Outlet pressure: 8 MPa, UV detection at 220 nm.

Chapter 4

Greener Super/subcritical Fluid Chromatography: Replacing Methanol as the Co-solvent for Chiral Separations

4.1 Abstract

Supercritical and near supercritical fluids are considered as the green solvents of the future because they decrease the need for toxic organic solvents and are easily recyclable. Consequently, supercritical fluid chromatography, SFC, has emerged as an environment-friendly technique especially for analytical and preparative scale enantiomeric separations. In order to separate a wide range of analytes with differing polarities, most SFC systems employ super- or subcritical carbon dioxide mixed with 5-40% organic solvents. More than 40 chlorinated or non-chlorinated co-solvents have been employed in SFC so far. However, methanol is far and away the dominant SFC mobile phase component as it outperforms most of the other solvents. Given the relatively high cost, non-renewable source of manufacture, and toxicity of methanol in humans, we propose elimination of methanol as a component of the SFC mobile phase by replacing with a biomass derived solvent, i.e., minimum boiling azeotropic ethanol. Azeotropic ethanol contains ~ 4.6% water (aka '190 proof'). It is less expensive and easy to recycle as it distills off at constant composition. This work demonstrates, for the first time, that one can obtain better chiral SFC separations by using '190 proof' ethanol instead of methanol. This solvent choice is shown to be favorable and compatible with a wide range of macrocyclic and chiral polysaccharide column chemistries. In chiral analyses, we show efficiency enhancement up to an order of magnitude and reduced retention by using azeotropic ethanol. In general, SFC separations with azeotropic ethanol can provide enhanced separation performance in a more economical and environmentally friendly format and hopefully change the status quo of current analytical and preparative SFC.

4.2 Introduction

With advances in instrumentation, super/subcritical fluid chromatography (SFC) has been rapidly gaining prominence.^{1, 2} SFC is considered a 'greener' alternative to high performance liquid chromatography (HPLC) especially normal phase liquid chromatography (NPLC), owing to its use of supercritical carbon dioxide (sCO₂) as the major component of the mobile phase.^{3, 4} Carbon dioxide is easy to remove, non-toxic and nonflammable. However, an SFC mobile phase consisting of pure carbon dioxide is an extremely weak eluent with an elutropic strength comparable to n-pentane.⁵ Hence, the addition of a polar organic solvent is necessary to elute analytes commonly encountered in both academia and industry. Some quantity of additive is added to elute peaks faster and with good peak shapes.⁶⁻⁸ The higher diffusivity and lower viscosity of the mobile phase in SFC allow the use of flow rates typically considered high for HPLC. SFC leads to lower consumption of toxic organic solvents and reduced post separation isolation times in preparative SFC which also contributes in making SFC a greener alternative to HPLC.^{3, 9, 10} The better diffusivity of the SFC mobile phase has made enantiomeric separations one of the primary applications for this technique since these separations have inherently slow mass transfer kinetics.¹¹ However, with high throughput screening becoming the norm, the use of higher amounts of organic co-solvents are often used to reduce analysis times.¹²

The most commonly used mobile phase component in chiral SFC is methanol.¹³ Methanol is the most polar alcohol and leads to the higher polarity of the bulk mobile phase, which results in lower retention of most analytes.⁵ The use of higher alcohols often leads to longer retention times and reduced chromatographic performance.¹⁴ Methanol is predominantly produced from natural gas which is a nonrenewable source. Methanol is highly toxic when ingested, and cases of methanol poisoning may also occur through skin exposure and breathing in fumes.^{15, 16} Methanol is broken

down by the body to form formaldehyde, formic acid and formate which produces adverse effects.¹⁷ Hence according to Prat et al.'s solvent selection guide ranking of 51 solvents, methanol is not listed under the recommended solvents category. Thus, it is evident that methanol needs to be replaced by a better alternative.¹⁸

The holy grail for a greener analytical technique revolves around the three 'R' principle namely (i) reduction of solvent consumed and waste generated, (ii) replacement of commonly used solvent with greener alternatives and (iii) recycle.¹⁹⁻²¹ The replacement of methanol with ethanol seems to be an obvious choice given the lower toxicity and the fact that ethanol is most commonly produced from biomass via fermentation, i.e. a renewable source. However, as mentioned earlier such a switch often leads to lower chromatographic performance under SFC conditions.

The macrocyclic glycopeptides and cyclofructans are important classes of chiral stationary phase often used to separate analytes which are different or impossible to separate with the derivatized cellulose and amylose (polysaccharide) stationary phases.²²⁻²⁴ They contain a substantial number of ionizable groups like hydroxyls, carboxylic acids and amines thereby making the stationary phases polar. The polysaccharide phases which are generally hydrophobic are more useful for neutral compounds compared to the macrocyclic glycopeptides. The macrocyclic glycopeptides and derivatized cyclofructan on the other hand are extremely effective in separating analytes with ionizable groups especially amines.²⁵⁻²⁷ It is telling that out of the 59 new drugs approved by the FDA in 2018, 38 were small molecules and out of those 38 all but 5 molecules had either an aromatic or an aliphatic amine functionality. This makes polar chiral stationary phases indispensable for enantiomeric separations.²⁸

In this work, we provide a viable alternative to methanol for enantiomeric separations using SFC. A simple switch from methanol to ethanol will not provide the desired efficiency and increases

retention times for enantiomeric separations. We propose the use of the minimum boiling azeotrope of 95.63% ethanol and 4.37% water instead of methanol. The azeotropically derived ethanol (also loosely defined as ‘190 proof’ ethanol) typically costs as little as \$8/L compared to ~\$120/L for HPLC-grade absolute ethanol and \$32/L for HPLC grade methanol.²⁹ Water has been as an additive in SFC for achiral separation mainly for solubilizing hydrophilic analytes like nucleobases, peptides and polar drug molecules.^{30, 31} A recent study conclusively proved that in presence of ammonium hydroxide and water in the mobile phase chaotropic effects leading to better peak shapes and enabling separations of hydrophilic analytes.³² A previous work demonstrated that adding water to the methanol resulted in increased efficiency and decreased retention time with different classes of chiral stationary phases.^{33, 34} The most common observation with the addition of water to the SFC mobile phase is a decrease in retention time and better peak shapes.^{8, 31} The decrease in retention time with hydrophilic chiral selectors such as macrocyclic glycopeptides and derivatized cyclofructans was much more significant compared to non-polar stationary phases. In this work we exploited the previously observed phenomenon and hypothesized the advantage of using azeotropic ethanol for SFC enantiomeric separations since it inherently contains a small amount of water. To the best of our knowledge, azeotropic ethanol has not been explored or proposed in chiral SFC separations. We examine the efficiency, separation times and loadability in order to evaluate the efficacy of ‘190 proof’ ethanol in SFC.

4.3 Experimental

4.3.1 Materials

Additives, solvatochromic dyes and analytes used were purchased from Sigma Aldrich (St. Louis, MO, U.S.A.) or Alfa Aesar (Ward Hill, MA, U.S.A.). Absolute ethanol and ‘190 proof’ ethanol were purchased from Decon Laboratories (King of Prussia, PA, USA). Carbon dioxide was

purchased from Airgas (UN1013, Radnor, PA) in cylinders equipped with a full-length eductor tube. TeicoShell, LarihcShell-P, VancoShell, Q-Shell and NicoShell (10 x 0.46 cm) were obtained from AZYP, LLC. (Arlington, TX, U.S.A.). The structures of these chiral selectors is given in the Supporting Information (*Figure 4.SI*).^{23, 35, 36} Chiralpak IA-3 (3 μm fully porous, 15 x 0.46 cm), and Chiralpak IC (5 μm fully porous, 25 x 0.46 cm) columns were purchased from Chiral Technologies (West Chester, PA, U.S.A.). (S, S)-Whelk-O1 column (5 μm fully porous, 25 x 0.46 cm) was from Regis Technologies (Morton Grove, IL, U.S.A.). All analytes were dissolved in methanol with an approximate concentration of 1 mg/mL.

Hamilton syringes were acquired from Restek (Bellefonte, PA). WatercolTM 1910 capillary column (30 m \times 0.25 mm I.D. \times 0.2 μm d_f), NIST[®] SRM[®] 8509, and OMI[®] purifier tube were acquired from Sigma Aldrich (St. Louis, MO). Autosampler vials (2 mL) were purchased from VWR, USA.

4.3.2 Instrumentation

All separations were performed on a Jasco 2000 series SFC (SFC-2000-7) equipped with carbon dioxide and modifier pumps (PU-2086). The CO₂ pump head was chilled at -10 °C. A back-pressure regulator (BP-2080) was set at 8 MPa with a heat controller at 60 °C (HC-2068-01). The autosampler (AS-2059-SFC) had a 5 μL stainless steel injection loop, and the detection was conducted with a variable-wavelength high-pressure compatible UV detector (UV-2075). The column oven was also bypassed in order to reduce extra column band broadening.

Manual injections of water-containing solvents were carried out on the Agilent 6890 gas chromatograph (GC) equipped with a thermal conductivity detector (TCD). WatercolTM 1910 with diameters of 30 m \times 0.25 mm I.D. \times 0.2 μm d_f was utilized for separation of water from solvent peak. The oven temperature was held isothermally at 70 °C for water analysis in methanol, and at

80 °C to analyze water content in ethanol samples. Helium was used as carrier gas with flow rate of 1.5 mL/min. The helium was purified with a high-capacity gas purifier and an OMI[®] purifier tube. Injection port and detector temperature were both set at 200 °C. A 5 µL injection was made with split ratio of 10:1 to introduce absolute ethanol and HPLC grade methanol into the GC. Regarding the azeotropically derived ethanol samples, a 1 µL sample injection with a split ratio of 100:1 achieved satisfactory peak areas for integration.

Spectrophotometric measurements were performed using an HP 8453 UV-Visible spectrophotometer.

4.3.3 Sample Preparation for water measurement

All vials along with Hamilton syringes were oven-dried overnight and then cooled back to room temperature in a desiccator. Two separate calibration curves were constructed, one for anhydrous solvents and the other for ‘190 proof’ ethanol. For anhydrous ethanol, and HPLC grade methanol, standard addition was performed by preparing 20, 50, 100, 200, and 500 ppm (v/v) solutions of water in solvents. In case of azeotropically derived ‘190 proof’ ethanol, 1%, 2%, 4%, 5%, 6%, and 10% water in ethanol solutions were prepared to produce standard addition calibration curve. To determine method accuracy, 1 mL of NIST[®] SRM[®] 8509 was pipetted out in the dried 2 mL autosampler vials. For standard addition 80-300 nL volumes of water were spiked into SRM[®] 8509 using 0.5 µL Hamilton syringe. This process is required to be quick as methanol may absorb water while it is exposed to the atmosphere. The cover was immediately placed on the vial. All samples were prepared in quadruplicate and immediately injected into GC.

4.3.4 Quantifying of water content in different organic solvents

The choice of a proper column is one of the key elements in the GC separation. The Watercol™ 1910 capillary column provides more symmetric peak shapes and shorter retention times for water peak compared to other commercially available stationary phases. It is also completely stable in the presence of water.³⁷ Table 4.1 illustrates the water content found in methanol and ethanol samples.

Table 4.1: Comparison between methanol, ethanol and '190 proof' ethanol

Properties	HPLC grade Methanol	Absolute Ethanol	'190 proof' Ethanol
1. Water content (in ppm)	36 + 5	240 + 4	56200 + 10
2. Wavelength for Nile Red transition	553 nm	549 nm	553 nm
3. Energy for Nile Red transition (in Kcal/mol)	51.70	52.08	51.70
4. Wavelength for Reichardt's dye transition	515 nm	552 nm	547 nm
5. Energy for Reichardt's dye transition (in kcal/mol)	55.52	51.80	52.27
6. Toxicity by inhalation (Threshold limit value in ppm) ¹⁶	200	1000	~1000

The precision of this method was determined by evaluating relative standard deviation (RSTD%) of multiple injections. The RSTDs were all <5%, indicating a precise method for analysis of moisture residue in organic solvents. The method validation was assessed by analyzing NIST[®] Standard Reference Material (SRM[®] 8509). As depicted in *Table 4.1*, the water content of 103.7 + 1.7 ppm was found via described protocol which was identical to the NIST[®] values (93 + 13) within experimental error.

4.4 Results and Discussion

4.4.1 Estimation of solvent polarity

Solvatochromic dyes Nile Red and Reichardt's dye were used to estimate the polarity of methanol, absolute ethanol and '190 proof' ethanol. With a change in polarity of the solvent, the wavelength for maximum absorption (λ_{max}) of the solvatochromic dye changes.^{5, 38} Hence these dyes provide a convenient method for estimating polarity. Reichardt's dye is insoluble in supercritical carbon dioxide hence cannot be used to measure the polarity of the mobile phase in SFC. Nile Red is used as an alternative to Reichardt's dye. However, when water is introduced into the system spectral shifts do not occur as has been reported previously.³⁴ It has been theorized that this occurs due to the low amount of water present in the mobile phase and may also be due to the existence of a cybotactic region around the probe molecule which is so enriched by the non-polar part of the mobile phase that the influence of small water amounts is unnoticeable.³⁹ Hence, we estimated the polarity of the different organic solvents separately i.e., without carbon dioxide. For measurements with Nile Red it is interesting to note that λ_{max} for methanol is 553 nm and for absolute ethanol it is 549 nm. When 190 proof ethanol (containing ~4.6% water) is used the λ_{max} is red shifted to 553 nm indicating that according to Nile Red solvatochromism, azeotropic ethanol and neat methanol

have about the same polarity in terms of the solvatochromic scale of Nile Red. The values of λ_{\max} and E_{NR} are summarized in *Table 4.1*. The change in the absorption maxima going from methanol to ethanol is small with Nile Red hence studies with a different solvatochromic dye is essential. Studies with Reichardt's dye were thus conducted and the values of λ_{\max} for methanol was 515 nm, 552 nm for absolute ethanol and 547 nm for '190 proof ethanol' (*Table 4.1*). It is important to note that Reichardt's dye is negatively solvatochromic i.e. it shows a hypsochromic shift in maximum absorption wavelength with increasing polarity. This indicates that the addition of small amounts of water does not significantly increase the polarity of ethanol and methanol remains much more polar compared to both azeotropic ethanol and absolute ethanol according to Reichardt's dye.

4.4.2 Comparison of methanol and ethanol as SFC mobile phase components

The lower polarity of absolute ethanol has been known to reduce chromatographic performance and increase retention times. *Figure 4.1a* shows the separation of (+) cis-4,5-diphenyl-2-oxazolidinone, with 20% methanol as the co-solvent, on a polar TeicoShell stationary phase under ambient temperature, a flow rate of 4 mL/min and 8 MPa backpressure. When methanol is replaced with absolute ethanol the efficiency falls from ~22000 plates/m to 7000 plates/m for the first enantiomer under the same chromatographic conditions (*Figure 4.1b*). Along with lower efficiency, the ethanol increases the elution time of both enantiomers from ~4 min with methanol co-solvent to ~9 min with absolute ethanol. As a consequence of the reduced plate count the resolution (R_s) between the two enantiomers for the mobile phase containing absolute ethanol also is lowered to 3.7 compared to 4.9 for the traditionally used methanol. The total organic solvent consumption in this for the separation with methanol is about 3.6 mL whereas the separation with absolute ethanol uses about 9.6 mL. Similarly, in the case of enantiomeric separation of bupivacaine with NicoShell column with 10% methanol, retention times for the first and second

peaks are 6.43 and 10 min respectively with 19440 plates/m for the first enantiomer and 12180 plates/m for the second enantiomer (*Figure 4.1d*). When switching to a neat ethanol, the retention times for the same increase to 8.72 min and 13.69 min and the efficiency drops to 6520 plates/m and 5560 plates/m (*Figure 4.1e*) under the same conditions of temperature, flow rate and backpressure.

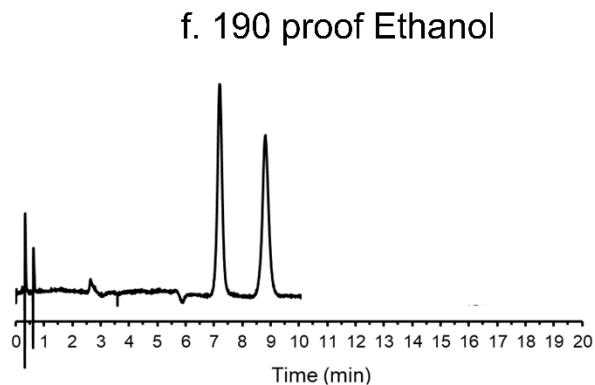
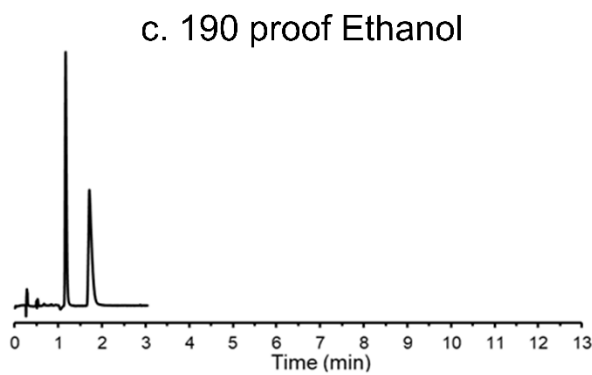
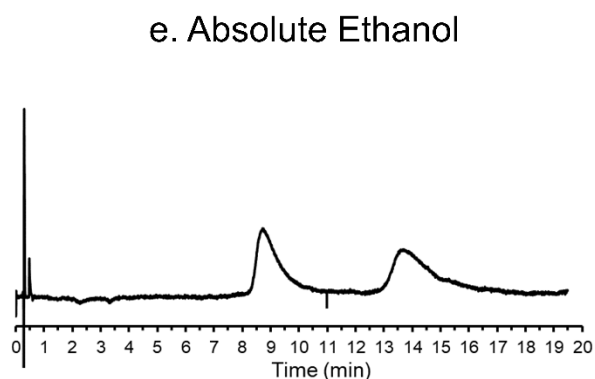
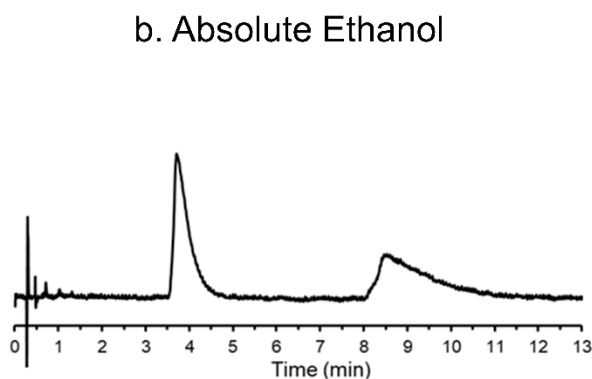
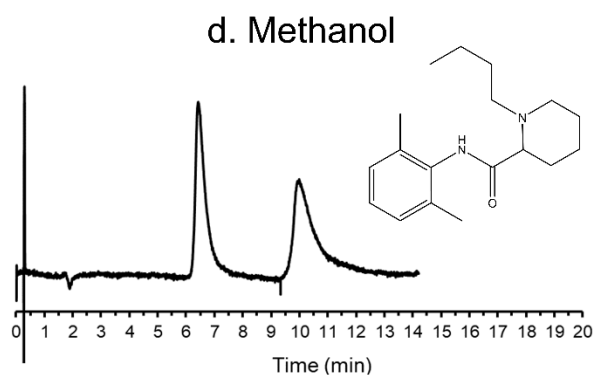
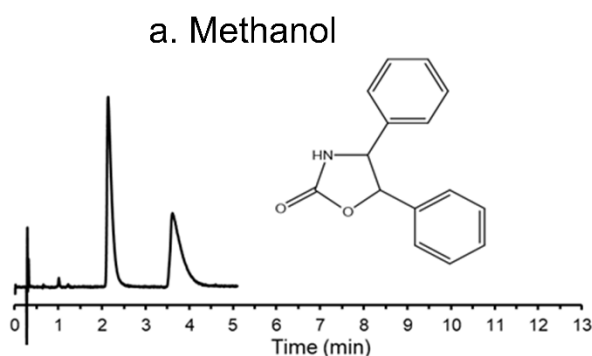


Figure 4.1: Effect of methanol (a,d), absolute ethanol (b,e), and '190 proof' ethanol (c,f) on the separation of cis-4,5-diphenyl-2-oxazolidinone (left) and bupivacaine (right) with TeicoShell and NicoShell stationary phase respectively. Mobile Phase: (a,b,c) 80/20 CO₂/modifier, (d,e,f) 90/10 CO₂/modifier-0.1% TEA-TFA (v/v). All separations were performed using Flow rate: 4 mL/min, Temperature: Ambient, Backpressure: 8 MPa

For non-polar stationary phases, the effect of changing the solvent from methanol to ethanol does not adversely affect the separation and may yield better peak efficiencies. Separation of hydrobenzoin on a ChiralPak-IA 3 column with 25% methanol as the co-solvent yields ~31000 plates/m (*Figure 4.S2 a*). Switching to absolute ethanol the plate count increases to ~36000 plates/m (*Figure 4.S2 b*). The retention time increased from 1.19 min to 1.26 min. Separations with other hydrophobic columns like Whelk-O 1 and Chiralpak IC yielded similar results i.e. switching from methanol to ethanol had little effect of the separation (*Figure 4.S3*). All experiments were performed with 4mL/min flow rate, ambient temperature and 8 MPa backpressure.

4.4.3 Using azeotropic ethanol in SFC

As shown in the previous section the increase in polarity of ethanol due to the presence of small amounts of water is minimal. Too high concentrations of water in ethanol to match the polarity of methanol cannot be used since this results in phase separation in the SFC chromatographic system.⁴⁰ When 20% azeotropic ethanol is used as co-solvent with a 4mL/min flow rate (same as that used for separation with methanol and absolute ethanol) for the separation of (+) cis-4,5-diphenyl-2-oxazolidinone with TeicoShell column, a dramatic increase in efficiency was obtained (*Figure 4.1c*). The first eluted enantiomer had an efficiency of ~72300 plates/m which is approximately a 10-time gain compared to absolute ethanol and a 3-fold gain when compared to

methanol. The retention times were considerably reduced with the first enantiomer eluting at 1.67 min and the second enantiomer was eluted at 1.77 min with a R_s of 5.95. This is due to the small amount of water in the mobile phase competing for the active sites on the stationary phase and enhancing the rate of mass transfer kinetics. Both the peaks eluted within 2 min, hence the total organic solvent consumed was 0.8 mL which is significantly lower than the amount of organic solvent consumed in the case of separation with methanol or absolute ethanol. The separation of bupivacaine on the NicoShell column showed a similar trend. With 10% 190 proof ethanol co-solvent, the retention time of the first and second eluted enantiomers were 7.20 min and 8.82 min respectively (*Figure 4.1f*). The first eluted peak had an efficiency of ~91100 plates/m which is a 15-fold gain compared to absolute ethanol and a 4-fold gain compared to a methanol. Total separation time was significantly less than that required for absolute ethanol. The separation time was slightly less than that with a methanol. However, the significant increase in efficiency even with comparable retention times leads to substantial decrease in the limit of detection (LOD) with 190 proof ethanol. The decrease in LOD is especially useful for detecting and quantifying pharmaceutical impurities or for forensic detection of controlled substances. For example, the separation of amphetamine a Schedule II drug using a VancoShell column with methanol and azeotropic ethanol have similar retention times but the efficiency with ‘190 proof ethanol’ is almost 3 times higher (*Figure 4.2 a and b*). Other analytes separated using both azeotropic ethanol and methanol had somewhat similar retention and were always accompanied by higher efficiencies when using ‘190 proof ethanol’. (*Figure 4.2 and Table 4.2*).

Table 4.2: Representative separations with methanol and azeotropic ethanol as modifiers

Analyte	Chromatographic conditions	t_{R1}	t_{R2}	N_1	N_2	R_s

cis-4,5-diphenyl-2-oxazolidinone	TeicoShell						
	(i) 80/20 CO ₂ /MeOH	2.14	3.62	2210	1195	4.93	
	(ii) 80/20 CO ₂ /190 EtOH	1.17	1.71	7227	2834	5.95	
Chlorthalidone	TeicoShell						
	(i) 75/25 CO ₂ /MeOH	5.54	8.08	1958	612	2.81	
	(ii) 75/25 CO ₂ /190 EtOH	3.30	3.82	5044	2252	2.05	
5,5-diphenyl-4-benzyl-2-oxazolidinone	TeicoShell						
	(i) 75/25 CO ₂ /MeOH	2.35	5.87	391	275	3.73	
	(ii) 75/25 CO ₂ /190 EtOH	1.02	2.11	1360	608	4.81	
Nicotine	NicoShell						
	(i) 60/40 CO ₂ /MeOH-0.1% TEA (v/v)	1.35	1.82	920	676	2.07	
	(ii) 60/40 CO ₂ /190 EtOH-0.1% TEA (v/v)	1.29	1.76	1136	1115	2.53	
Bupivacaine	NicoShell						
	(i) 80/20 CO ₂ /MeOH-0.1% TEA-TFA (v/v)	1.82	2.63	2339	1701	3.99	
	(ii) 80/20 CO ₂ /190 EtOH-0.1% TEA-TFA (v/v)	1.98	2.46	5669	4785	3.89	

Prilocaine	NicoShell							
	(i) 60/40 CO ₂ /MeOH-0.05% NH ₄ CO ₂ H (w/v)	2.26	2.73	1050	825	1.43		
	(ii) 60/40 CO ₂ /190 EtOH-0.1% NH ₄ CO ₂ H (w/v)	1.69	1.94	2766	2210	1.72		
Tranylcypromine	VancoShell							
	(i) 80/20 CO ₂ /MeOH-0.1% TEA-TFA (v/v)	3.74	4.24	2370	1681	1.40		
	(ii) 80/20 CO ₂ /190 EtOH-0.1% TEA-TFA (v/v)	2.48	2.71	7342	5291	1.78		
Amphetamine	VancoShell							
	(i) 75/25 CO ₂ /MeOH-0.1% TEA-TFA (v/v)	1.48	1.74	3200	2266	2.07		
	(ii) 75/25 CO ₂ /190 EtOH-0.1% TEA-TFA (v/v)	1.42	1.59	8140	5517	2.27		
Venlafaxine	VancoShell							
	(i) 75/25 CO ₂ /MeOH-0.1% TEA-TFA (v/v)	1.97	2.33	2345	1540	1.80		
		2.11	2.40	4834	3600	2.13		

	(ii) 75/25 CO ₂ /190 EtOH- 0.1% TEA-TFA (v/v)							
Tryptophan	LarihcShell-P							
	(i) 75/25 CO ₂ /MeOH-0.2% TEA-0.3% TFA (v/v)	6.24	7.35	5546	5450	2.75		
	(ii) 75/25 CO ₂ /190 EtOH- 0.2% TEA-0.3% TFA (v/v)	5.62	6.06	10987	10106	1.92		
1,2,2- triphenylethylamine	LarihcShell-P							
	(i) 85/15 CO ₂ /MeOH-0.2% TEA-0.3% TFA (v/v)	1.97	2.46	7150	4608	4.13		
	(ii) 85/15 CO ₂ /190 EtOH- 0.2% TEA-0.3% TFA (v/v)	1.87	2.06	8107	10073	2.35		
2-chloro-indan-1- ylamine	LarihcShell-P							
	(i) 80/20 CO ₂ /MeOH-0.2% TEA-0.3% TFA (v/v)	1.81	2.40	6795	6462	6.01		
	(ii) 80/20 CO ₂ /190 EtOH- 0.2% TEA-0.3% TFA (v/v)	1.37	1.59	8341	8648	3.75		
Disopyramide	ChiralPak IA							
		6.25	11.37	1520	476	3.76		

	(i) 80/20 CO ₂ /MeOH-0.1% TEA (v/v)	5.14	7.08	2204	1349	3.23
	(ii) 80/20 CO ₂ /190 EtOH- 0.1% TEA (v/v)					
Tetramisole	ChiralPak IC					
	(i) 70/30 CO ₂ /MeOH-0.1% TEA (v/v)	3.28	3.94	7497	6826	3.86
	(ii) 70/30 CO ₂ /190 EtOH- 0.1% TEA (v/v)	3.22	3.97	8097	6944	4.48
Fenoprofen	Whelk-O 1					
	(i) 85/15 CO ₂ /MeOH-0.5% AA (v/v)	2.15	2.59	8032	8300	4.16
	(ii) 85/15 CO ₂ /190 EtOH- 0.5% AA (v/v)	2.44	2.86	8071	8405	3.68

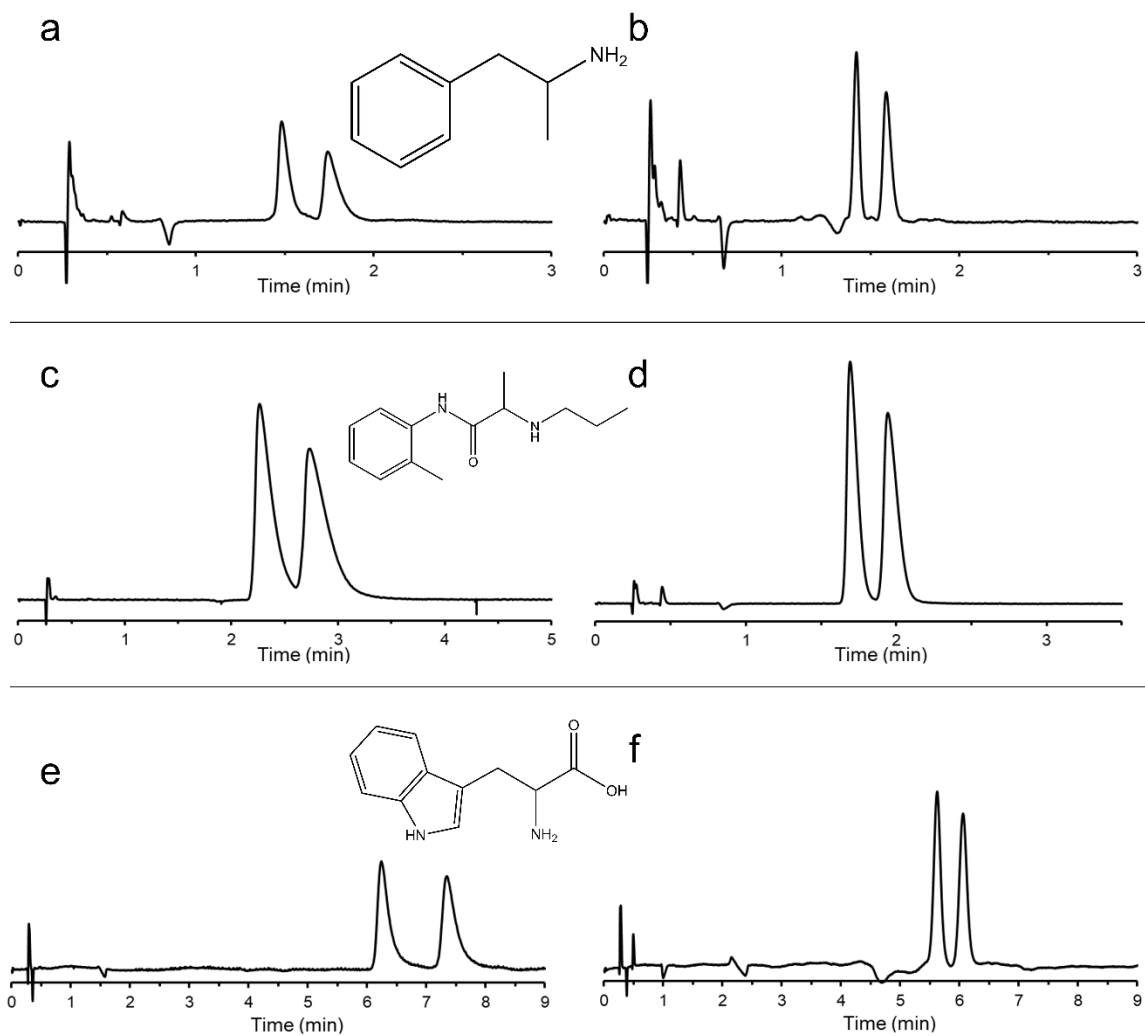


Figure 4.2: Representative chromatograms: Analyte: Amphetamine Conditions: Stationary phase: VancoShell Mobile Phase: (a) 75/25 CO₂/MeOH-0.1% TEA-TFA (v/v) and (b) 75/25 CO₂/'190 proof' EtOH-0.1% TEA-TFA (v/v). Analyte: Prilocaine Conditions: Stationary Phase: NicoShell Mobile Phase: (c) 80/20 CO₂/MeOH-0.05% ammonium formate (w/v) and (d) 80/20 CO₂/'190 proof' EtOH-0.05% ammonium formate (w/v). Analyte: Tryptophan Conditions: Stationary Phase: LarihcShell-P Mobile Phase: (a) 75/25 CO₂/MeOH-0.2% TEA-0.3% TFA

(v/v) and (b) 75/25 CO₂/‘190 proof’ EtOH-0.2% TEA-0.3% TFA (v/v). All separations were performed using Flow rate: 4 mL/min, Temperature: Ambient, Backpressure: 8 MPa

When ‘190 proof’ ethanol is used for separations on hydrophobic chiral stationary phases, a smaller improvement in efficiency is found (*Table 4.2*). In the case of hydrobenzoin separation, the azeotropic ethanol yielded a higher number of theoretical plates than methanol (rising to ~39000 plates/m from ~32000 plates/m) (*Figure 4.S2 c*) when using 25% organic solvent and from ~24000 plates/m to ~41000 plates/m while using a mobile phase with 10% modifier.

4.4.4 Effect of solvent concentration in CO₂

It is well known that decreasing the polar solvent concentration in the mobile phase leads to higher retention factor in SFC.⁴¹ *Figure 4.3a and 4.3b* shows the change in retention factor of the second eluted enantiomer (k) and efficiency (N) as a function of organic solvent concentration for (+) cis-4,5-diphenyl-2-oxazolidinone and bupivacaine respectively. Methanol, absolute ethanol and ‘190 proof ethanol’ were tested. The increase in retention factor with a decreasing amount of organic solvent is well known due to reduced eluotropic strength of the mobile phase. It is, however, interesting to note that there is steepest rise in retention factor with absolute ethanol as compared to other solvents. The lowest slope is that for azeotropic ethanol indicating smaller increases in retention times compared to both methanol and absolute ethanol especially at low modifier concentrations. At higher co-solvent concentrations, the differences in retention factors are lower.

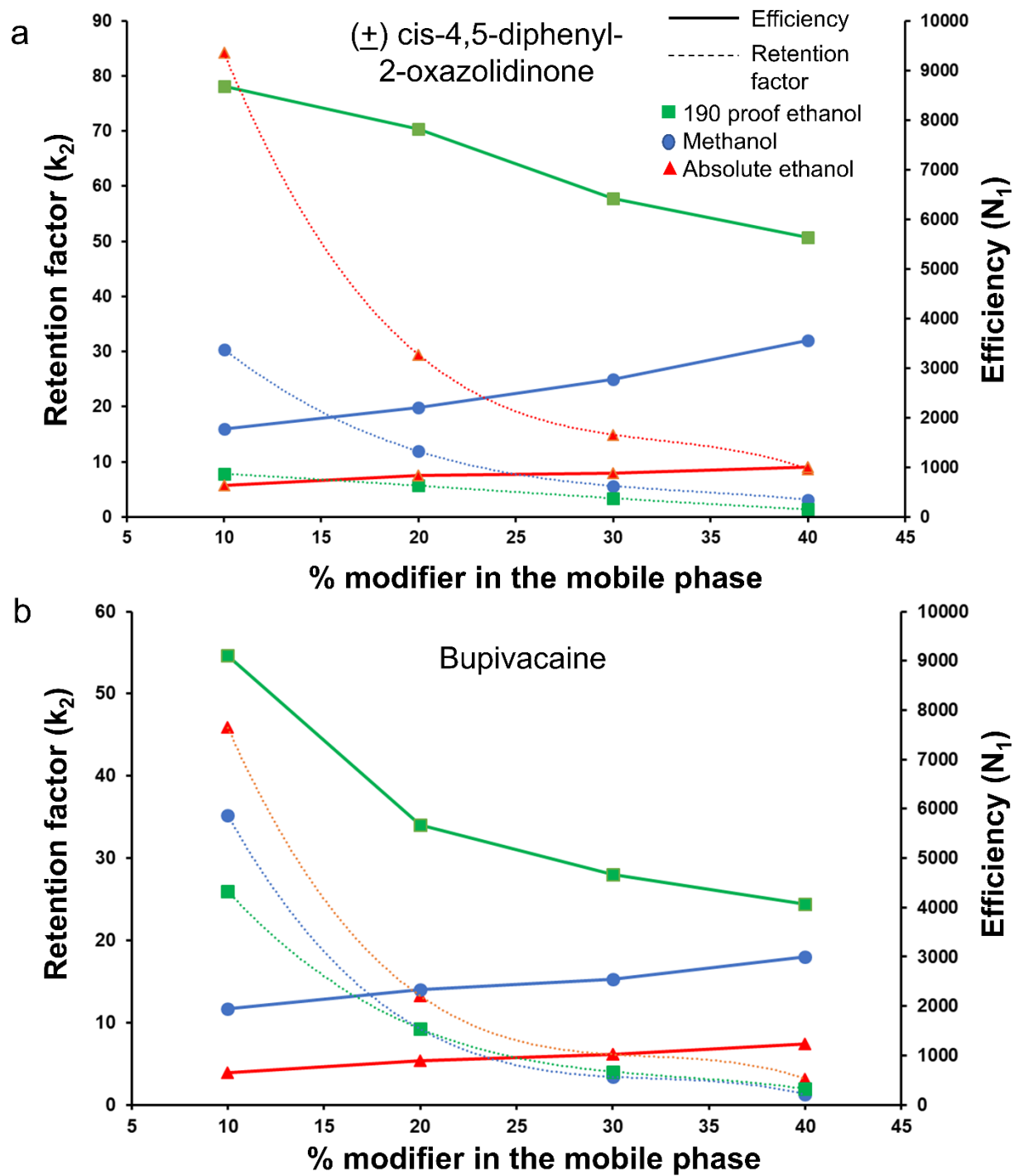


Figure 4.3: Effect of variation of modifier concentration on retention factor of the second eluted enantiomer and the efficiency on **a.** *cis-4,5-diphenyl-2-oxazolidinone* and **b.** *bupivacaine*

For both analytes with methanol and absolute ethanol as mobile phase components, the efficiency is directly proportional to their concentration in the mobile phase. However, when using 190 proof ethanol, the efficiency trend is reversed, i.e. the efficiency increases with lower concentration. Efficiencies with '190 proof ethanol' at low concentrations in the mobile phase significantly exceed efficiencies recorded with methanol even with high co-solvent concentrations. Higher efficiencies lead to higher peak capacities which is a fundamental aspect of high throughput separations. The higher efficiencies with lower concentrations can lead to significant reduction in solvent consumption in SFC.

4.4.5 Benefitting from altered selectivity with ethanol-water

In very specific cases methanol is known to show unique selectivity. One such case is the separation of carprofen on ChiralPak IA column (15 x 0.46 cm) (*Figure 4.4*). With 30% methanol co-solvent, the selectivity (α) between the two enantiomers is 1.23. However, with 30% absolute ethanol as the co-solvent, the ' α ' between the two enantiomers decreased to 1, which corresponds to a full overlap of the peaks. When azeotropic ethanol-water is used, the selectivity between the two enantiomers increases considerably to 1.14. Though a baseline separation is not afforded by '190 proof ethanol' with additional water (5% added water to the solvent) in this case, a longer column or chemometrics will allow the baseline separation and quantitation of the individual enantiomers which cannot be attained by using absolute ethanol as no chemometric technique would work for completely overlapped peaks in the case of enantiomers.^{42, 43}

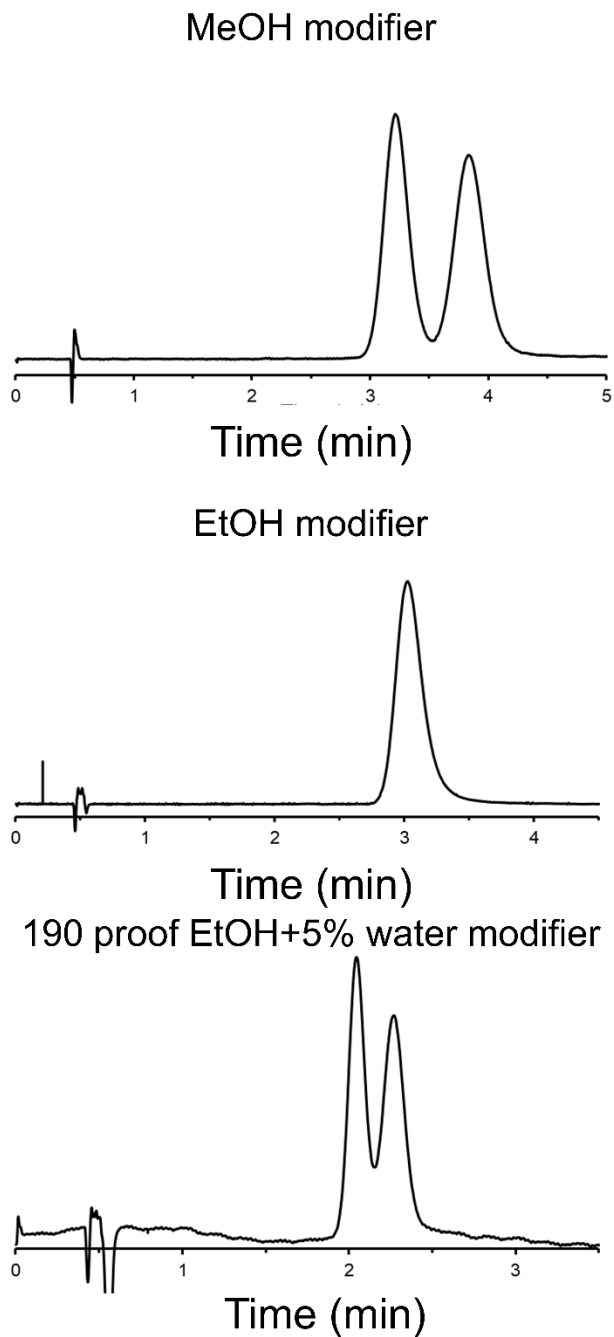


Figure 4.4: Enantiomeric separation of carprofen on ChiralPak IA column (15 x 0.46 cm) with different modifiers **a.** methanol **b.** absolute ethanol **c.** '190 proof' ethanol. Mobile Phase: 70/30

CO₂/modifier. All separations were performed using Flow rate: 4 mL/min, Temperature:

ambient, Backpressure: 8 MPa.

Similarly, the separation of four β -blockers can also be performed with a ‘190 proof ethanol’ (Figure 4.5a). With both absolute ethanol (Figure 4.5b) and methanol (Figure 4.5c) there is complete coelution of the second eluted enantiomer of alprenolol and the first eluted enantiomer of metoprolol. Using a 20% azeotropic ethanol in the bulk mobile phase, all enantiomers of the four β -blockers namely alprenolol, metoprolol, propranolol, and pindolol are baseline separated with high efficiency and lower retention times compared to the other neat alcohols.

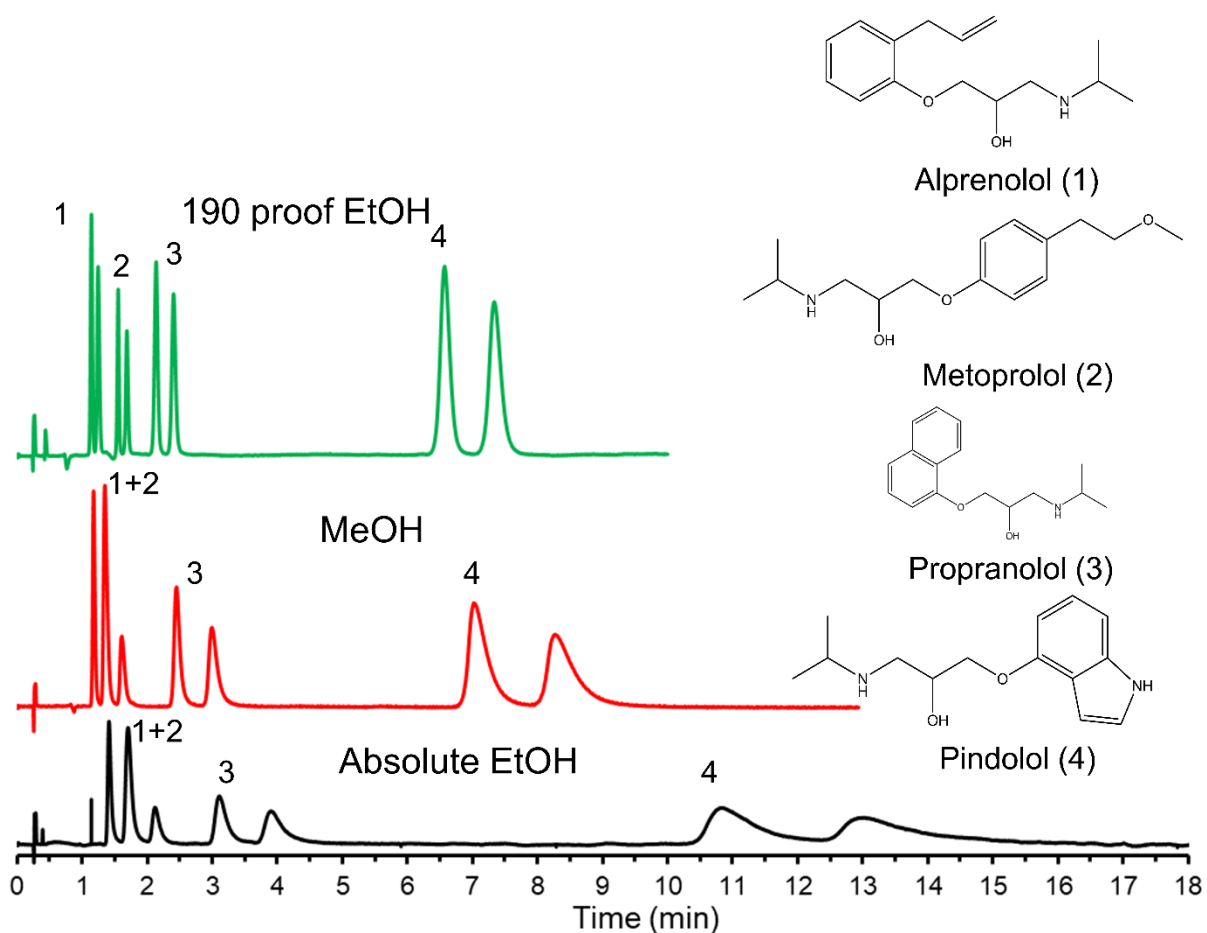


Figure 4.5: Separation of 4 β blockers namely alprenolol, metoprolol, propranolol and pindolol with methanol, absolute ethanol and ‘190 proof’ ethanol. Conditions: Stationary Phase:

NicoShell, Mobile Phase: 80/20 CO₂/modifier-0.1% (v/v) TEA-0.1% (v/v) TFA. All separations were performed using Flow rate: 4 mL/min, Temperature: ambient, Backpressure: 8 MPa.

4.4.6 Increased loadability for preparative chromatography

Preparative chiral separations are an essential part of drug discovery and drug development. Supercritical fluid chromatography is increasingly becoming the technique of choice for preparative chiral separations due to solvent saving. Though selectivity is an essential factor when determining the loading capacity of an analyte on a column, parameters such as the composition of the mobile phase and time of analysis must be taken into account while scaling up a separation.⁴⁴ It is desirable to have lower peak distortion at high analyte concentrations. Herein the advantage of high efficiencies offered by ‘190 proof’ ethanol is shown for the enantiomeric separation of venlafaxine with the VancoShell stationary phase. With a 20% methanol, a sample with 6.25 mM concentration of venlafaxine can be baseline separated into its constituent enantiomers (*Figure 4.6a*). As soon as the concentration is doubled the baseline resolution is lost because of increasing tailing of the first eluted enantiomer. At higher concentrations the separation gets progressively worse with decreasing resolution. However, with azeotropic ethanol, the increased efficiency allows separation at concentrations as high as 50 mM which is an 8 times improvement compared to the commonly used methanol (*Figure 4.6b*). The detrimental effect of increased analyte loading on the peak shapes is significantly reduced when using 190 proof ethanol thereby allowing higher loadability on the same stationary phase.

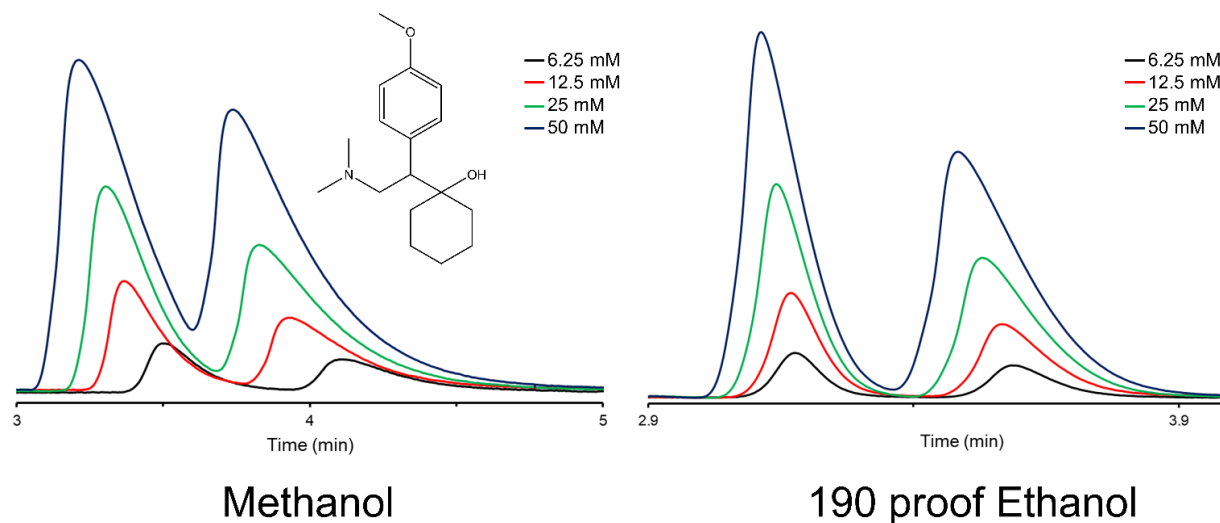


Figure 4.6: Increasing column loadability with ‘190 proof’ ethanol in chiral SFC. Conditions: Stationary Phase: VancoShell, Mobile Phase: a. 80/20 CO₂/MeOH-0.1% (v/v) TEA-0.1% (v/v) TFA b. 80/20 CO₂/‘190 proof’ ethanol-0.1% (v/v) TEA-0.1% (v/v) TFA. Separations were performed using Flow rate: 4 mL/min, Temperature: ambient. Backpressure: 8 MPa

4.5 Conclusions

Azeotropic ethanol water (aka “190 proof”) was tested as a substitute for methanol in chiral supercritical/subcritical fluid chromatography. The ‘190 proof’ ethanol produced better chromatographic efficiencies and often decreased retention times as compared to methanol. However, relative to absolute ethanol, the azeotropic ethanol had far better performance especially with more polar chiral/hydrophilic stationary phases. Substituting methanol for azeotropic ethanol did not adversely affect separations when using non-polar chiral stationary phases. Advantages are prevalent even in preparative SFC where the use of ‘190 proof’ ethanol to increase loadability of a chiral stationary phase has been demonstrated. Since the water-ethanol azeotrope boils at a lower temperature than absolute ethanol hence post-separation purification step is easier when using azeotropic ethanol. The three ‘R’ principle in green chemistry is satisfied by the Replacement of

methanol with '190 proof' ethanol since it is a less toxic alternative, results in comparable or lower retention times thereby Reducing solvent consumption and finally the '190 proof' ethanol can be obtained by simple distillation and doesn't require additional steps of purification and hence Recycling is much easier compared to absolute ethanol. The results demonstrated herein are of significant interest for users trying to reduce the environmental impact resulting from the chemical analysis by chromatography both in industry and academia.

4.6 Acknowledgment

The authors would like to acknowledge AZYP LLC. for providing chiral column. We would also like to acknowledge Dr. Terry Berger for a helpful discussion. This work was funded by the Robert A. Welch Foundation (No. Y-0026).

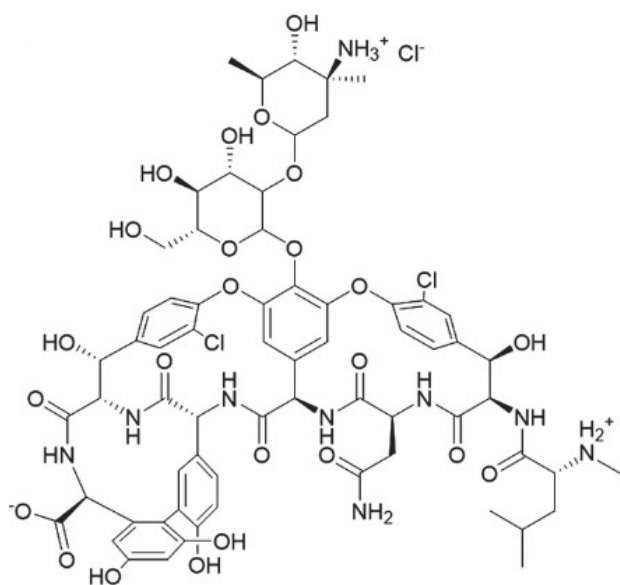
4.7 References

1. E. L. Regalado and C. J. Welch, *J. Sep. Sci.*, 2015, **38**, 2826-2832.
2. C. L. Barhate, M. F. Wahab, D. Tognarelli, T. A. Berger and D. W. Armstrong, *Anal. Chem.*, 2016, **88**, 8664-8672.
3. M. B. Hicks, W. Farrell, C. Aurigemma, L. Lehmann, L. Weisel, K. Nadeau, H. Lee, C. Moraff, M. Wong and Y. Huang, *Green Chem.*, 2019, **21**, 1816-1826.
4. E. A. Peterson, B. Dillon, I. Raheem, P. Richardson, D. Richter, R. Schmidt and H. F. Sneddon, *Green Chem.*, 2014, **16**, 4060-4075.
5. J. F. Deye, T. A. Berger and A. G. Anderson, *Anal. Chem.*, 1990, **62**, 615-622.
6. J. A. Blackwell, R. W. Stringham and J. D. Weckwerth, *Anal. Chem.*, 1997, **69**, 409-415.
7. C. West, J. Melin, H. Ansouri and M. M. Metogo, *J. Chromatogr. A*, 2017, **1492**, 136-143.
8. C. West and E. Lemasson, *J. Chromatogr. A*, 2019, **1593**, 135-146.
9. L. Miller, *J. Chromatogr. A*, 2012, **1250**, 250-255.
10. R. E. Majors, *LC GC North America*, 2005, **23**, 16-29.
11. T. Fornstedt, P. Sajonz and G. Guiochon, *Chirality*, 1998, **10**, 375-381.
12. C. L. Barhate, L. A. Joyce, A. A. Makarov, K. Zawatzky, F. Bernardoni, W. A. Schafer, D. W. Armstrong, C. J. Welch and E. L. Regalado, *Chem. Comm.*, 2017, **53**, 509-512.
13. C. West, *Anal. Bioanal. Chem.*, 2018, **410**, 6441-6457.
14. D. W. Armstrong, R. M. Woods and Z. S. Breitbach, *LC-GC North Am.*, 2014, **32**, 742-752.
15. N. Permpalung, W. Cheungpasitporn, D. Chongnarungsin and T. M. Hodgdon, *N. Am. J. Med. Sci.*, 2013, **5**, 623.
16. J. E. Amooore and E. Hautala, *J. Appl. Toxicol.*, 1983, **3**, 272-290.

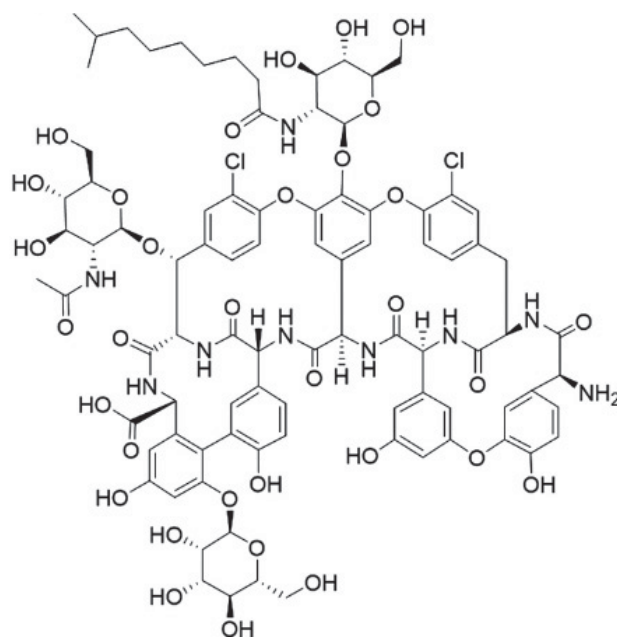
17. L. J. Schep, R. J. Slaughter, J. A. Vale and D. M. G. Beasley, *Bmj*, 2009, **339**, b3929.
18. D. Prat, J. Hayler and A. Wells, *Green Chem.*, 2014, **16**, 4546-4551.
19. M. Koel, *Green Chem.*, 2016, **18**, 923-931.
20. M. de la Guardia and S. Garrigues, *Handbook of green analytical chemistry*, Wiley Online Library, 2012.
21. X. Yuan, B. Richter, K. Jiang, K. Boniface, A. Cormier, C. Sanders, C. Palmer, P. Jessop, M. Cunningham and R. Oleschuk, *Green Chem.*, 2018, **20**, 440-448.
22. P. Sun, C. Wang, Z. S. Breitbach, Y. Zhang and D. W. Armstrong, *Anal. Chem.*, 2009, **81**, 10215-10226.
23. D. W. Armstrong, Y. Tang, S. Chen, Y. Zhou, C. Bagwill and J.-R. Chen, *Anal. Chem.*, 1994, **66**, 1473-1484.
24. Y. Liu, A. W. Lantz and D. W. Armstrong, *J. Liq. Chromatogr. Relat. Technol.*, 2004, **27**, 1121-1178.
25. S. Khater and C. West, *J. Chromatogr. A*, 2019, **1604**, 460485.
26. Y. Liu, R. V. Rozhkov, R. C. Larock, T. L. Xiao and D. W. Armstrong, *Chromatographia*, 2003, **58**, 775-779.
27. Y. Liu, A. Berthod, C. R. Mitchell, T. L. Xiao, B. Zhang and D. W. Armstrong, *J. Chromatogr. A*, 2002, **978**, 185-204.
28. A. M. Ebied, J. Na and R. M. Cooper-DeHoff, *Am. J. Med.*, 2019.
29. C. J. Welch, T. Nowak, L. A. Joyce and E. L. Regalado, *ACS Sustain. Chem. Eng.*, 2015, **3**, 1000-1009.
30. L. T. Taylor, *J. Chromatogr. A*, 2012, **1250**, 196-204.
31. J. Liu, E. L. Regalado, I. Mergelsberg and C. J. Welch, *Org. Biomol. Chem.*, 2013, **11**, 4925-4929.
32. J. Liu, A. A. Makarov, R. Bennett, I. A. Haidar Ahmad, J. DaSilva, M. Reibarkh, I. Mangion, B. F. Mann and E. L. Regalado, *Anal. Chem.*, 2019, **91**, 13907-13915.
33. D. Roy and D. W. Armstrong, *J. Chromatogr. A*, 2019, 360339.
34. D. Roy, M. F. Wahab, T. A. Berger and D. W. Armstrong, *Anal. Chem.*, 2019, **91**, 14672-14680.
35. M. F. Wahab, C. A. Weatherly, R. A. Patil and D. W. Armstrong, in *Chiral Analysis*, Elsevier, 2018, pp. 507-564.
36. G. Hellinghausen, J. T. Lee, C. A. Weatherly, D. A. Lopez and D. W. Armstrong, *Drug Test Anal.*, 2017, **9**, 944-948.
37. C. A. Weatherly, R. M. Woods and D. W. Armstrong, *J. Agric. Food Chem.*, 2014, **62**, 1832-1838.
38. C. Reichardt, *Chem. Soc. Rev.*, 1992, **21**, 147-153.
39. S. Frye, C. Yonker, D. Kalkwarf and R. Smith, *Application of Solvatochromic Probes to Supercritical and Mixed Fluid Solvents*. In *Supercritical Fluids: Chemical and Engineering Principles and Applications*; Squires, T. G., Paulitis, M. E., Eds.; ACS Symposium Series, Vol. 329; American Chemical Society: Washington, DC, 1987; Chapter 3, pp 29-41.
40. R. Bennett, M. Biba, J. Liu, I. A. H. Ahmad, M. B. Hicks and E. L. Regalado, *J. Chromatogr. A*, 2019, **1595**, 190-198.
41. S. Khater and C. West, *J. Chromatogr. A*, 2014, **1373**, 197-210.
42. M. F. Wahab, A. Berthod and D. W. Armstrong, *J. Sep. Sci.*, 2019.

43. D. C. Patel, M. F. Wahab, T. C. O'Haver and D. W. Armstrong, *Anal. Chem.*, 2018, **90**, 3349-3356.
44. P. Franco, C. Minguillón and L. Oliveros, *J. Chromatogr. A*, 1998, **793**, 239-247.

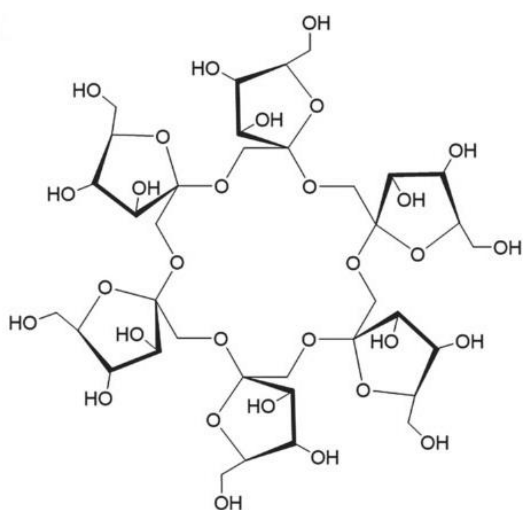
4.8 Supporting Information



Vancomycin



Teicoplanin



Larihc-P (Cyclofructan based stationary phase)

Figure 4.S1: Structures of chiral selectors

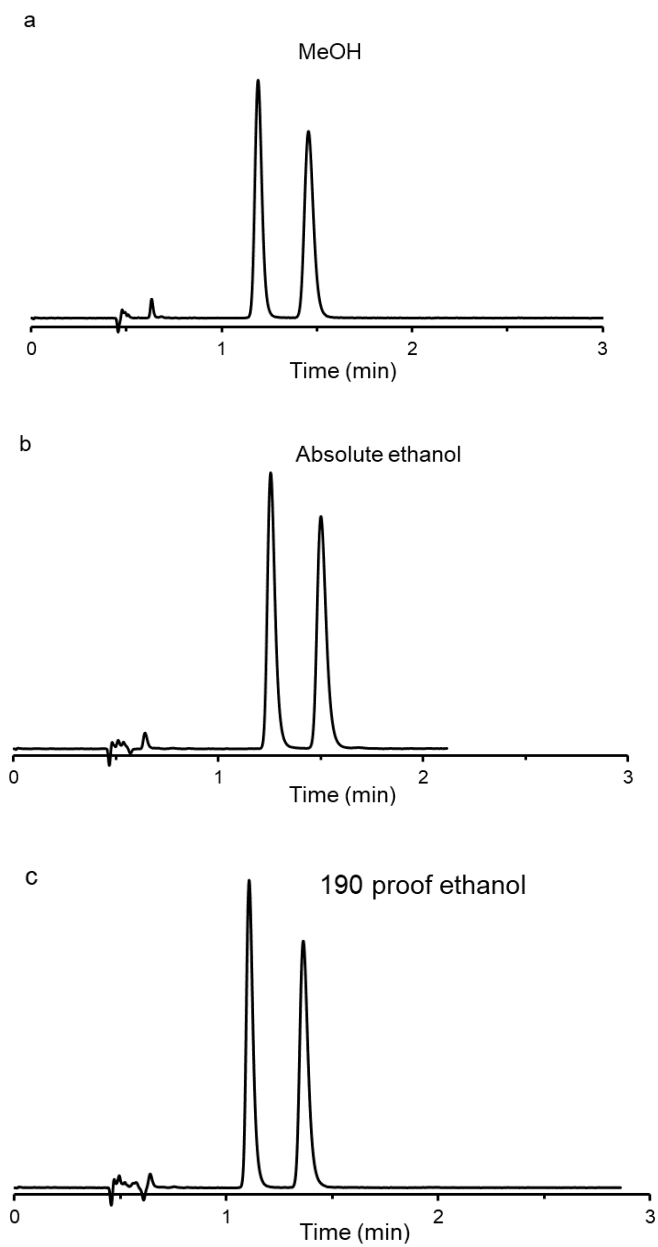


Figure 4.S2: Effect of methanol (a), absolute ethanol (b), and “190 proof” ethanol (c) on the separation of hydrobenzoin with ChiralPak IA stationary phase respectively. Mobile Phase: 75/25 CO₂/modifier. All separations were performed using Flow rate: 4 mL/min, Temperature: Ambient, Backpressure: 8 MPa

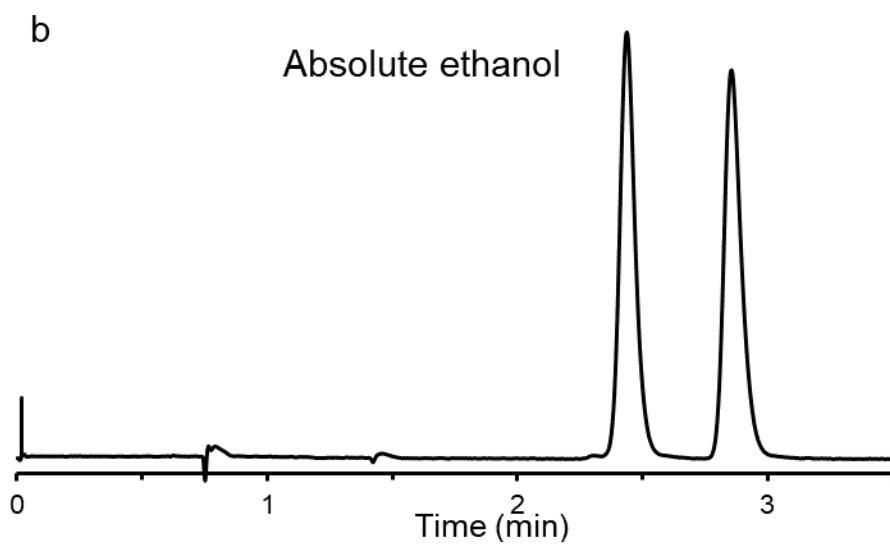
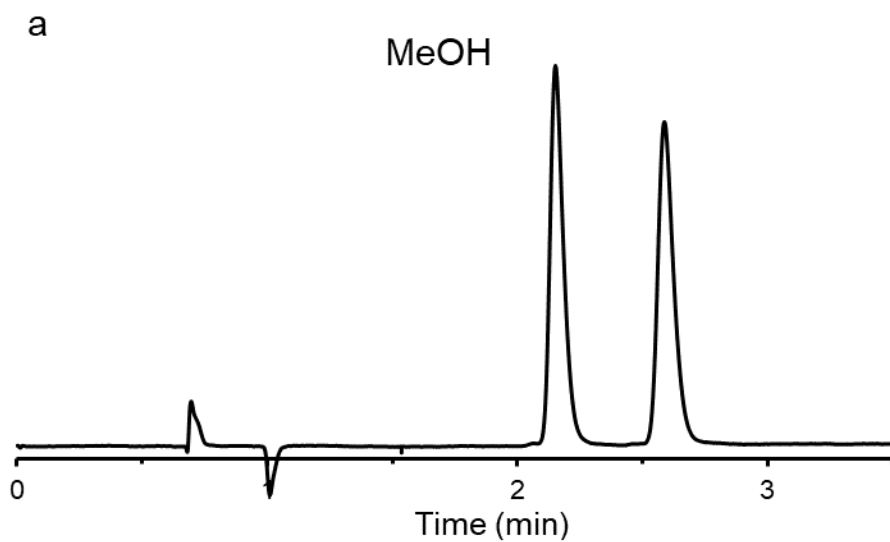


Figure 4.S3: Representative chromatograms: Analyte: Fenoprofen Conditions: Stationary phase: Whelk O1 Mobile Phase: (a) 80/20 CO₂/MeOH-0.1% TEA-TFA (v/v) and (b) 80/20 CO₂/Ethanol -0.1% TEA-TFA (v/v).

Chapter 5

Enhancing Supercritical Fluid Chromatographic Efficiency: Predicting Effects of Small Aqueous Additives

5.1 Abstract

Supercritical fluid chromatography is becoming more prevalent, particularly in industry. This is due to the inexpensive, and more importantly, environmentally benign carbon dioxide that is used as the major component of the mobile phase. Water is minimally miscible with carbon dioxide at temperatures and pressures commonly used in SFC. However, the introduction of a polar alcohol modifier component increases the solubility of water in carbon dioxide. Previously, the addition of small amounts of water in the mobile phase was shown to provide significant gains in efficiency in chiral supercritical fluid chromatography, especially with polar stationary phases. In this work, we report the effect of the addition of small amounts of water on efficiency and retention factor with four different SFC stationary phases used for achiral analysis namely FructoShell-N (native cyclofructan-6), SilicaShell (bare silica), PoroShell 120 EC C18 (octadecyl silica) and Xselect C18 SB. This is the first reported use of FructoShell-N, a cyclofructan derivatized phase for SFC applications. We devised a predictive test to determine which analytes show an increase in efficiency using their known chemical constants ($\log K_{ow}$, pK_a , PSA and H_{sum}). We also use discriminant analysis to elucidate the most important analyte parameters that contribute to “water enhanced” efficiency gains.

5.2 Introduction

Analytical supercritical fluid chromatography (SFC) has been known since the late 1960s [1, 2]. Significant improvements in instrumentation and column packing technology in the last few

decades resulted in a renewed interest in packed column SFC [3]. Achiral SFC has become a judicious choice for replacing liquid chromatographic separations in the normal phase mode, non-aqueous reversed-phase mode, and hydrophilic interaction mode (HILIC) due to its low organic solvent consumption and compatibility with mass spectrometry [4]. Supercritical carbon dioxide is used as the major component of the mobile phase since it has an easily accessible critical point, low cost, low toxicity, and ease of recycling [5]. Because of the low polarity and modest eluting strength of fluid CO₂ (similar to liquid pentane or liquid hexane), different organic modifiers like alcohols or acetonitrile can be mixed with CO₂ in order to decrease retention times and improve the peak shapes of analytes. The effects of the polar organic co-solvents in SFC include (i) changing the density of mobile phase [6-8]; (ii) changing the polarity of stationary phase and mobile phase [7-11]; (iii) changing the volume of stationary phase [7-11]; and (iv) deactivation of active sites on the surface of stationary phase [7, 8].

Small amounts (~1%) of very polar additives can be added to the modifier in order to obtain better peak shapes and affect the retention of analytes. In 1991, Berger and Deye concluded that polar additives work by covering the active sites on the stationary phases and, in some cases, by suppressing solute ionization and ion-pairing [12]. The solubility of water in supercritical CO₂ is very low (~0.1% w/w) [13]. However, upon addition of a polar organic modifier, the solubility of water is significantly increased [14, 15], for instance up to 10% water has been used in SFC mobile phases [16-18]. Water provides an additional source of hydrogen bonds, besides methanol [4, 19]. Also, it is well known that water can interact with carbon dioxide forming carbonic acid [20].

A recent study focused on the effects of incorporating small amounts of water in the mobile phase and elucidated the role of water in SFC enantiomeric separations [16]. It was observed that the presence of water in the mobile phase greatly enhanced separation efficiencies and decreased

retention times when polar stationary phases were used. Decreased retention times and increased efficiencies also were observed with non-polar chiral stationary phases, but these effects were less pronounced. The use of water in achiral SFC separation has been reported, but its exact role and effects were not clearly understood [21-23]. A recent study, incorporating water and ammonium hydroxide in the SFC mobile phase, reportedly increased efficiencies for hydrophilic analytes and this was attributed to “chaotropic effects” [24]. However, the relation between the polarity of the stationary phase and the presence of water in the mobile phase has not been established.

This work studies the effect of water in SFC for four different stationary phases. The polar FructoShell-N is cyclofructan-6 bonded to silica, SilicaShell is bare silica, Poroshell 120-EC C18 is an end-capped C18 stationary phase and Xselect C18 SB is a nonendcapped C18 stationary phase. In the first three cases, the silica support has a core-shell structure whereas for the Xselect C18 SB has a fully porous silica support. These three stationary phases have vastly different surface chemistries and are expected to behave differently under SFC conditions. Acidic, neutral and basic analytes were tested with the different stationary phases and their behaviors with respect to retention time and efficiency were studied. Discriminant analysis was performed with the tested analytes to further elucidate the factors that produced increased efficiencies with the addition of water. To the best of our knowledge, this work is also the first reported use of FructoShell-N (a HILIC material) as an SFC stationary phase for achiral analytes.

5.3 Experimental

5.3.1 SFC Instrumentation

The chromatographic system used was a Jasco chromatograph (2000 series SFC SFC-2000-7)) with a carbon dioxide pump (PU-2086), a modifier pump (PU-2086), an autosampler (AS-2059-SFC) with 5 μ l injection loop, a variable-wavelength high-pressure compatible UV

detector (UV-2075), a back-pressure regulator (BP-2080) was used in all SFC analyses. A carbon dioxide pump was chilled by Julabo chiller to -10°C. Backpressure was set up to 8MPa while the heat controller was maintained at 60°C. Data analysis was performed by ChromNAV (1.17.01 Build 8) connected via an LC-NET II/ADC.

5.3.2 Stationary Phases and Analytes

FructoShell-N (2.7 µm particles, 10 x 0.46 cm), SilicaShell (2.7 µm particles, 10 x 0.46 cm) columns were obtained from AZYP LLC (Arlington, TX, USA) and Poroshell 120 EC-C18 (2.7 µm particles, 10 x 0.46 cm) column was obtained from Agilent Technologies (Santa Clara, CA, USA) and Waters Xselect C18 (3.0 µm particles, 10 x 0.46 cm) was obtained from Waters Corporation (Milford, MA).

Analytes used in this study were obtained from Sigma-Aldrich (St. Louis, MO, USA), Cerilliant Corporation (Round Rock, TX, USA) and LKT Laboratories (Minneapolis, MN, USA). They are listed in *Table 5.1*. For the dissolving of all analytes to the concentration (~1 mg/mL), methanol was used. Analytes used in the study, their logarithms of octanol/water partition coefficient, negative logarithms of the acid dissociation constant, polar surface area and the sum of hydrogen bonds that molecule can provide are presented in *Table 5.1*.

5.3.3 Other Chemicals

SFC-grade carbon dioxide was purchased from AirGas (Radnor, PA, USA) in cylinders equipped with a full-length eductor tube. Methanol was purchased from Sigma-Aldrich (St. Louis, MO, USA), distilled water was further purified with Milli-Q water purification system to 18 MΩ (Millipore, Billerica, MA, USA). Trifluoroacetic acid (TFA) and triethylamine (TEA) were

purchased from Sigma-Aldrich (St. Louis, MO, USA). These additives helped in peak shape improvement.

5.3.4 Water-rich modifier preparation

All water-rich modifiers were prepared by use HPLC grade methanol and Milli-Q water. For the preparation of modifier with water, the reported percent of water was added to a given volume before mixing, e.g., ~ 6% v/v H₂O in MeOH was made by adding 6 mL H₂O to 100 mL MeOH. For calculating of MeOH volume, the mass of MeOH was divided by the density of MeOH at the specific temperature. After that, water was added by the use of a 50 mL Class-A burette. The additives (TEA and TFA) were added using a micropipette.

5.3.5 Determination of water “retention factor”

The water “disturbance” was measured by injecting 5 µL of Millipore water with a flow rate of 4 mL/min and with different modifier concentrations (See *Figure 5.S1*). The measurement was conducted at 210 nm. The dead time was measured by the injection disturbance.

5.3.6 Discriminant analysis

Discriminant analysis was performed by XLSTAT software. Discriminant analysis for all four columns utilized the logarithm of octanol/water partition coefficient ($\log K_{ow}$), negative logarithm of acid dissociation constant (pK_a), polar surface area (PSA), sum of hydrogen bonds that molecule can provide (H_{sum}) and retention factor of compounds with use of mobile phases without water were used as variables. The $\log K_{ow}$, pK_a , PSA and H_{sum} values were taken from SciFinder, PubChem and DrugBank databases.

Table 5.1. Analytes and their characteristics used in study

Sr. No.	Name	^a log K _{ow}	^b pK _{a1}	^c PSA, Å ²	^d H _{sum}
1	Ibuprofen	3.97	5.3	37.30	3.00
2	2-Phenylbutyric acid	2.21	4.3	37.30	3.00
3	5-Phenylvaleric acid	2.94	4.7	37.30	3.00
4	<i>m</i> -Toluic acid	2.37	4.3	37.30	3.00
5	<i>p</i> -Toluic acid	2.27	4.4	37.30	3.00
6	Benzoic acid	1.88	4.5	37.30	3.00
7	4-Vinylbenzoic acid	2.18	4.2	37.30	3.00
8	4-Nitrobenzoic acid	1.89	3.4	83.10	6.00
9	Fenoprofen	3.10	4.5	46.50	4.00
10	Flurbiprofen	4.16	4.4	37.30	3.00
11	Naproxen	3.18	4.2	46.50	4.00
12	Ketoprofen	3.00	4.5	54.40	4.00
13	1-Naphthylacetic acid	2.24	4.2	37.30	3.00
14	3,5-Dinitrobenzoic acid	1.54	3.9	129.00	9.00
15	Nicotinic acid	0.36	4.8	50.20	4.00
16	Phenylsuccinic acid	-0.01	3.6	74.60	6.00
17	2,3-Naphthalenedicarboxylic acid	2.06	3.0	74.60	6.00
18	Diphenylacetic acid	3.09	4.7	37.30	3.00
19	Suprofen	2.20	3.9	82.60	4.00
20	Thymol	3.30	10.6	20.20	2.00
21	Phenol	1.46	10.0	20.20	2.00
22	4-Benzyl-5,5-dimethyl-2-oxazolidinone	1.16	12.9	38.30	4.00
23	5,5-Diphenyl-4-benzyl-2-oxazolidinone	4.22	11.8	38.30	4.00
24	4,5,5-Triphenyl-2-oxazolidinone	2.19	11.1	38.30	4.00
25	5,5-Diphenyl-4-methyl-2-oxazolidinone	1.78	11.9	38.30	4.00
26	4-Phenyl-2-oxazolidinone	-0.20	12.5	38.30	4.00

27	4-(Diphenylmethyl)-2-oxazolidinone	1.53	12.3	38.30	4.00
28	3-Aminoquinoline	1.63	5.0	38.90	4.00
29	Theophylline	-0.02	8.8	69.30	7.00
30	Benzenesulfonamide	0.31	10.1	68.50	5.00
31	Benzamide	0.64	16.0	43.10	4.00
32	N-Benzylbenzamide	2.26	14.9	29.10	3.00
33	Thymine	-0.62	9.7	58.20	6.00
34	Nicotinamide	-0.38	3.4	56.00	5.00
35	2-Phenylbenzimidazole	3.24	5.0	28.10	3.00
36	1-Benzylimidazole	1.60	6.7	17.80	2.00
37	2-Methylimidazole	0.24	7.9	28.70	3.00
38	Imidazole	-0.08	7.0	28.70	3.00
39	Adenosine	-1.05	3.6	140.00	14.00
40	1-(2-Hydroxyethyl)imidazole	-0.45	6.8	38.00	4.00
41	1,2-Dimethylimidazole	0.03	7.8	17.80	2.00
42	2,6-Dimethylaniline	1.84	4.0	26.00	3.00
43	2-Nitroaniline	1.85	-0.2	71.80	6.00
44	3-Nitroaniline	1.37	2.5	71.80	6.00
45	4-Nitroaniline	1.39	1.0	71.80	6.00
46	2-Aminoanthracene	3.50	4.3	26.00	3.00
47	α ,4-Dimethylbenzylamine	2.15	9.2	26.00	3.00
48	1,2,2-Triphenylethylamine	3.96	8.5	26.00	3.00
49	1-Methyl-3-phenylpropylamine	2.26	10.0	26.00	3.00
50	α -Methylbenzylamine	1.72	9.0	26.00	3.00
51	Triphenylamine	5.74	-3.0	3.24	1.00
52	Melamine	-1.37	5.0	117.00	12.00
53	Benzylamine	1.09	9.3	26.00	3.00
54	Atropine	1.83	9.4	49.80	5.00

55	1-(2-Naphthyl)ethylamine	2.90	9.4	26.00	3.00
56	3-Phenyl-1-propylamine	1.83	10.1	26.02	2.00
57	Sotalol	0.37	10.1	86.80	8.00
58	Acebutolol	1.19	13.9	87.70	9.00
59	Metoprolol	1.88	9.7	50.70	6.00
60	Propranolol	3.48	9.4	41.50	5.00
61	4-(1H-imidazol-1-yl)-aniline	0.49	6.1	43.80	5.00
62	Atenolol	0.16	9.6	84.60	9.00
63	N-allylaniline	2.06	4.0	12.00	2.00
64	1,1'-Binaphthyl-2,2'-diamine	4.06	3.8	52.00	6.00
65	Nebivolol	4.04	14.3	71.00	8.00
66	N-Tert-butylbenzamide	2.06	14.99	29.1	3.00
67	Caffeine	-0.07	14.0	58.4	6.00
68	4-Butylbenzylamine	3.42	9.20	26.0	3.00

a: log K_{ow} – logarithm of octanol/water partition coefficient; b: pK_{a1} – negative logarithm of acid dissociation constant; c: PSA – polar surface area, Å²; d: H_{sum} – sum of hydrogen bonds that molecule can provide

5.4. Results and Discussion

Four stationary phases with different hydrophilicity and ion exchange behavior were examined. A semi-qualitative estimation of the polarities and ion exchange behavior of these stationary phases have been made previously using a plot with the relative retention of cytosine and uracil on the x-axis and the relative retention of BTMA and cytosine on the y-axis (*Figure 5.S2*) [25, 26]. Cyclofructan based stationary phase lies towards the right of the plot indicating it has the highest hydrophilicity among the tested stationary phases, followed by SilicaShell. The value of endcapped C18 column is very close to zero on the x-axis. However, the non-endcapped C18 shows both x and y axes values even higher than bare silica.

Acidic, neutral, and basic compounds with different chemical functionality and hydrophilicity were selected for the study. Methanol is the most widely used co-solvent in SFC as it is completely miscible with carbon dioxide over a wide range of temperatures and pressures and dramatically increases the eluotropic strength of the mobile phase [4]. Also, in order to obtain acceptable retention times and peak shapes for acidic and basic compounds, 0.1% (v/v) TEA and TFA with and without water were used for all separations. A methanolic modifier concentration of 10% and 20% was used since lower modifier percentages gave a higher percentage change in efficiency with chiral separations, according to a previous report [16]. The retention, peak shape and efficiency of each separation were compared for mobile phases without and with 6% (v/v) of water in the modifier. Higher amounts of water in the 90/10 CO₂/methanol lead to phase separation [15].

5.4.1 Effect of water on FructoShell-N

5.4.1.1 Effect of water as an additive

The plots in *Figures 5.1 and 5.2* show how the addition of a small amount of water to the SFC mobile phase affects retention (*k*) and efficiency (*N*) on the FructoShell-N column for a variety of neutral and basic analytes, respectively. The red line parallel to the x-axis indicates the retention factor of water (*k_w*=1.91) in the 80/20, CO₂/methanol eluent system. Analogous plots for the 90/10, CO₂/methanol system are shown in *Figure 5.S3 and 5.S4* of the Supplementary Material.

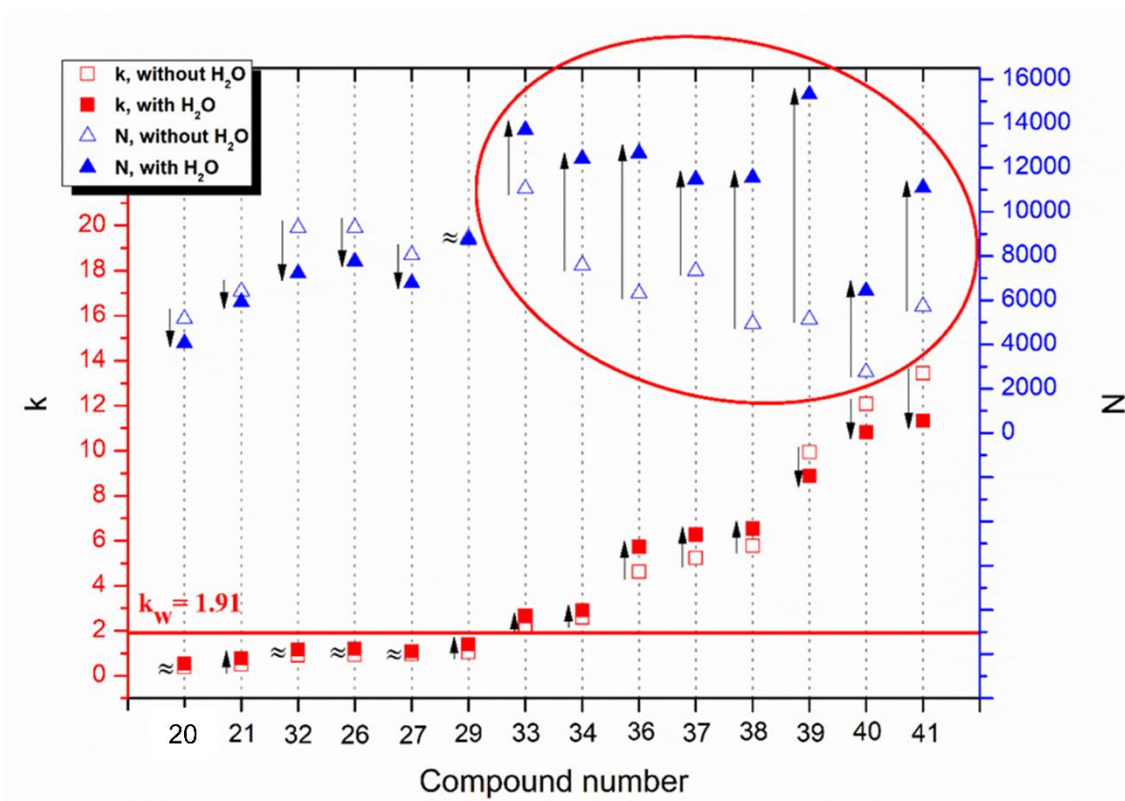


Figure 5.1: Influence of water on the separation of neutral compounds on FructoShell-N column (2.7 μm particles, 10 x 0.46 cm). Conditions: 80/20 CO_2/MeOH + 0.1% (v/v) TEA + 0.1% (v/v) TFA (empty squares and triangles); 80/20 CO_2/MeOH + 0.1% (v/v) TEA + 0.1% (v/v) TFA + 6% (v/v) H_2O (full squares and triangles); flow rate 4 ml/min, back pressure 8 MPa; detection: UV, 220nm. Compounds numbers are same as that in Table 5.1. X-axis denotes compound numbers; the left y-axis denotes retention factor and the right y-axis denotes efficiency.

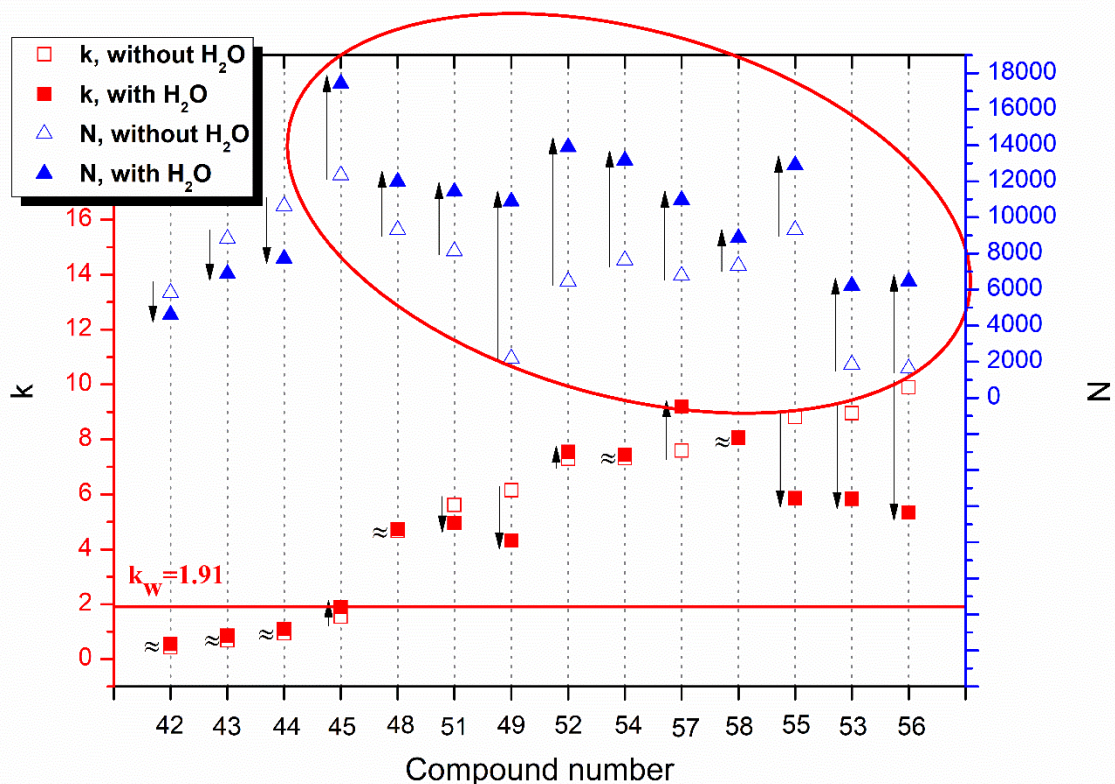


Figure 5.2: Influence of water on the separation of basic compounds on FructoShell-N column (2.7 μm particles, 10 x 0.46 cm). Conditions: 80/20 CO_2/MeOH + 0.1% (v/v) TEA + 0.1% (v/v) TFA (empty squares and triangles); 80/20 CO_2/MeOH + 0.1% (v/v) TEA + 0.1% (v/v) TFA + 6% (v/v) H_2O (full squares and triangles); flow rate 4 ml/min, back pressure 8 MPa; detection: UV, 220nm. Compounds numbers are same as that in Table 5.1. X-axis denotes compound numbers; the left y-axis denotes retention factor and the right y-axis denotes efficiency.

As can be seen, added water affects the efficiency of analyte peaks that have retention factors less than that of k_w very differently than analytes that have retention factors higher than k_w (i.e., the circled points in Figures 5.1 and 5.2). The presence of water significantly enhances the efficiency of all compounds with retention factors $>k_w$, while slightly decreasing the efficiency of

compounds with retention factors $<k_w$. The same trend was found for 90/10, CO₂/MeOH (*Figures 5.S3 and 5.S4* of the Supplementary Material). More highly retained compounds undergo a greater number of interactive and/or stronger interactions with the stationary phase, some of which can give rise to unwanted peak tailing. Water can act competitively for some adsorption sites since the polar stationary phase has a high affinity for water. The net result is that a very small amount of water in the mobile phase provides better peak shapes and higher efficiencies for most analytes (*Figures 5.1, 5.2, 5.S3, 5.S4*). A somewhat similar effect was observed when a competitive adsorbing molecule, methyl tert-butyl ether (MTBE), was added to a methanol-water reversed-phase separation with a cyclodextrin stationary phase [27]. The effect of water on analyte retention (*Figures 5.1 and 5.2*) is less pronounced than what has been reported for enantiomeric separations on chiral stationary phases, where the addition of water often significantly decreased retention [16]. Added water had little effect on the retention of analytes with retention factors less than k_w . Analytes with retention factors higher than k_w showed either increased or decreased retention but with no discernible pattern (*Figures 5.1, 5.2, 5.S3 and 5.S4*). Presumably, those analytes showing decreased retention did so because the added water competitively associated to a strong binding site. The increase in the retention factor of some analytes may appear to be anomalous. However, such behavior has been previously observed in normal-phase liquid chromatography [28]. It was attributed to the formation of adsorbed multi-layers of modifier and water on the surface of the stationary phase [29].

For acidic compounds, a decrease in efficiency was typical for both of the used mobile phases (*Figures 5.S5 and 5.S6* in Supplementary Material). Thus, all acidic analytes have retention factors less than that of k_w . Only nicotinic acid and 3,5-dinitrobenzoic acid with the use of 90/10,

CO₂/methanol system show increasing efficiency with the addition of water to the co-solvent (Figures 5.3A, 5.3B, 5.S5 and 5.S6).

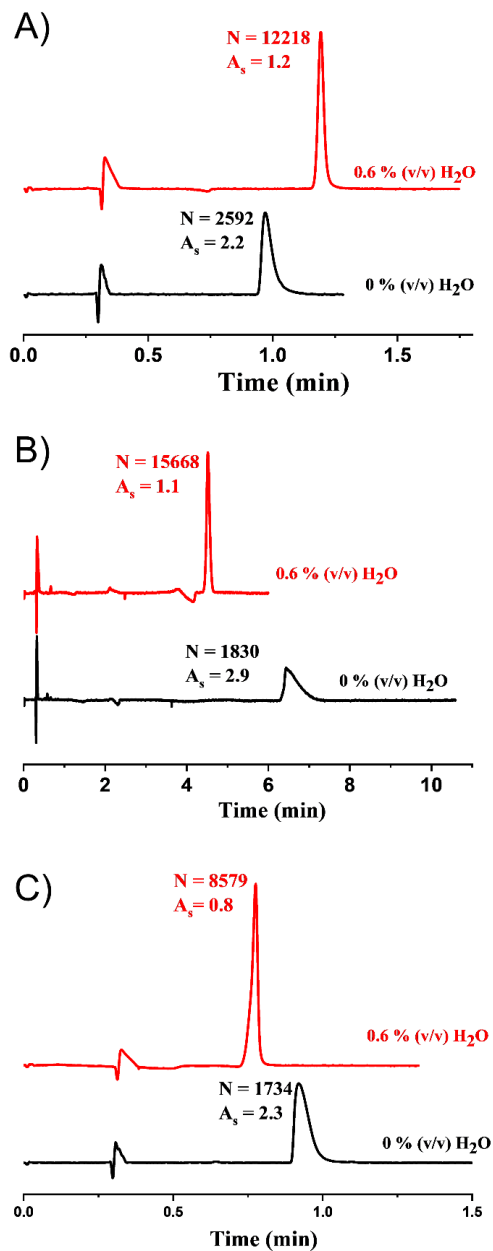


Figure 5.3: SFC chromatograms of nicotinic acid (A) and 1-methyl-3-phenylpropylamine (B) and 3,5-dinitrobenzoic acid (C) on FructoShell-N column with 90/10 CO₂/MeOH + 0.1% (v/v) TEA + 0.1% (v/v) TFA mobile phase without and with addition of 6% (v/v) H₂O to modifier.

So far, a peak width reduction has been discussed (*vide supra*) in the presence of water, but the addition of water can also change peak shapes. The tailing peak of 3,5-dinitrobenzoic acid can change its shape to fronting after the addition of water to the mobile phase (*Figure 5.3C*). This observation shows that the presence of water can change the symmetry of the peak. Also, this indicates the likelihood of a competing mechanism of analyte and water adsorption on the stationary phase as the peak shape of the analyte is dependent on the strongly adsorbed component, in this case, water. This phenomenon has also been seen in different modes of chromatography like polar organic mode, achiral and chiral SFC, and ion chromatography where the presence of a competing ion in the mobile phase altered the asymmetry from fronting to tailing [16, 30-32]. It is seen that when a strongly adsorbed component of the mobile phase is more retained than the analyte, and only in this case, may fronting peaks be observed. Polar stationary phases can demonstrate such changes in adsorption isotherms in the presence of water in the co-solvent. This phenomenon is important and could be highly useful for preparative SFC separations.

5.4.2 Effect of water on SilicaShell

Unmodified silica columns are used in normal phase chromatography (NPLC). These columns are problematic in NPLC due to the complexity in obtaining a constant surface activity leading to irreproducibility in chromatographic separations. There are a few methods of maintaining constant silica surface activity: (i) control of water concentration in the mobile phase which, in turn controls the amount of water adsorbed onto the silica surface, and (ii) use of protic co-solvents (e.g., methanol, propanol) [29].

SFC is often considered as an alternative to NPLC, so it can be assumed that there is a need for the deactivation of active sites in the case of unmodified silica columns. As was mentioned above, this can be accomplished by the use of modifiers and additives under SFC conditions. Also,

methanol reacts with silanols to form methyl silyl ethers (*Figure 5.S7* of Supplementary Material) [33]. However, the addition of water, quickly depletes the methyl silyl ethers. This results in altered selectivity in the presence of water.

An unmodified silica surface provides inhomogeneous adsorption arising from non-homogeneity of surface silanols. Three main types of silanols on the surface of unmodified silica are known: free silanols, geminal silanols, and associated silanols (*Figure S7* of Supplementary Material) [29]. Free silanols are more acidic and cause broad and poorly shaped peaks for polar analytes. Geminal silanols and associated silanols are less acidic in comparison with free silanols and cause more narrow peaks for polar analytes [29, 34]. The non-homogeneity would, in turn, result in differential water adsorption and multilayer formation. This fact can explain the specific behavior of silica under SFC conditions with the use of water as an additive.

To study the influence of water on the SFC separations when using a “bare” silica gel stationary phase, 48 compounds with different functionalities, acidity and hydrophilicity were analyzed (*Tables 5.S3 and 5.S4* of Supplementary Material).

5.4.2.1 Effect of water as an additive on efficiency

Figure 5.4 shows how the addition of a small amount of water (0.6%-1.2% in the total mobile phase) for achiral SFC affects retention (k) and efficiency (N) for a variety of basic analytes with the use of the SilicaShell column and the 80/20 CO₂/methanol mobile phase. An analogous plot for the 90/10, CO₂/methanol system is shown in *Figure 5.S8* of the Supplementary Material. Plots for acidic and neutral compounds are shown in *Figures 5.S9-S12* of the Supplementary Material. The red line parallel to the x-axis indicates the retention factor of water ($k_w=4.55$ in the

80/20, CO₂/methanol mobile phase system and $k_w=10.60$ in the 90/10, CO₂/methanol mobile phase system).

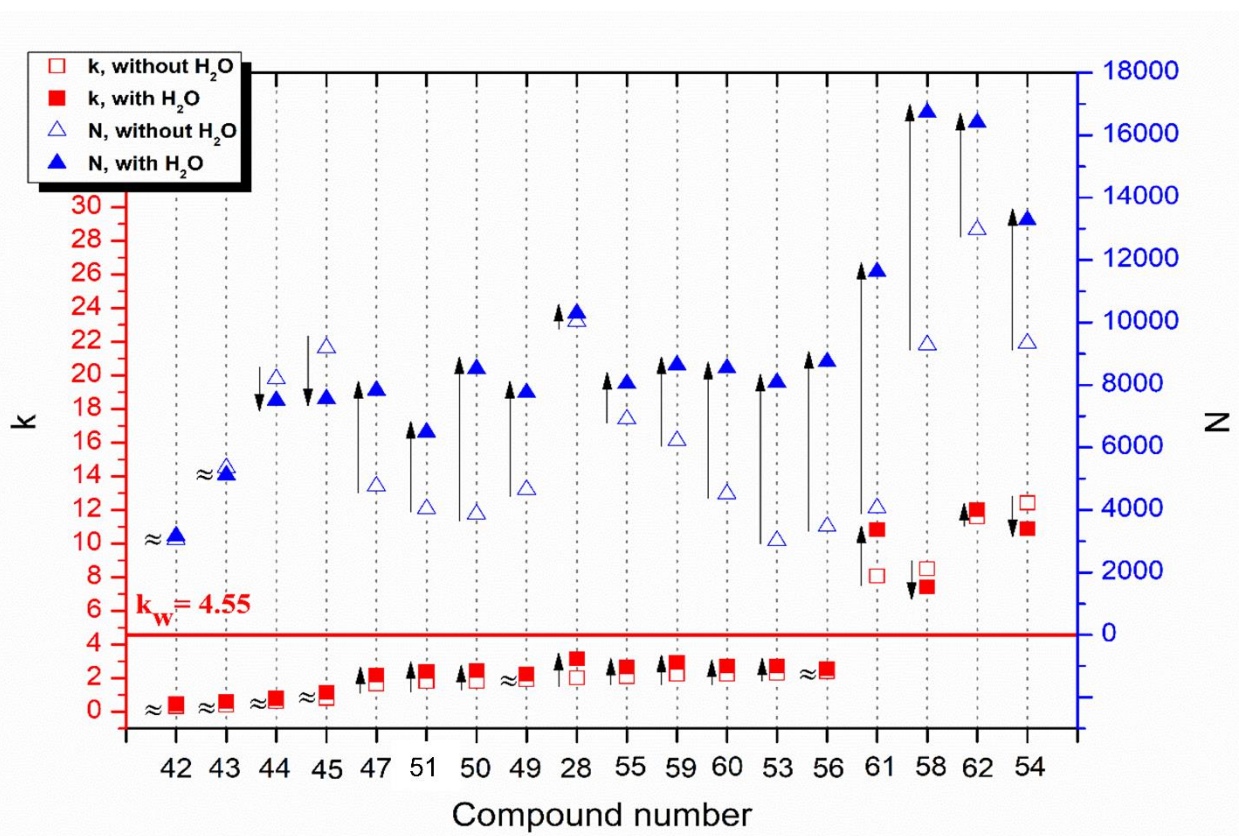


Figure 5.4: Influence of water on the separation of basic compounds on SilicaShell column.

Conditions: 80/20 CO₂/MeOH + 0.1% (v/v) TEA + 0.1% (v/v) TFA (empty squares and triangles); 80/20 CO₂/MeOH + 0.1% (v/v) TEA + 0.1% (v/v) TFA + 6% (v/v) H₂O (full squares and triangles); flow rate 4 ml/min, back pressure 8 MPa; detection: UV, 220nm. Compounds numbers are same as that in Table 5.1. X-axis denotes compound numbers; the left y-axis denotes retention factor and the right y-axis denotes efficiency.

As can be seen, the addition of a small amount of water increased the separation efficiency for most of the studied compounds. Interestingly, there was no correlation between the changes in efficiency and retention of analytes, as was observed for the FructoShell-N column. The effect of

added water on retention times was generally small and any increase or decrease in retention appears to be random (*Figure 5.4, Figures 5.S8-S12* of Supplementary Material). The presence of water in the mobile phase shifts the equilibria of methyl silyl ether formation to almost complete removal of methyl silyl ethers, which can result in changes in selectivity as discussed in the previous section. Differences in the behavior of FructoShell-N and SilicaShell columns also may result from the higher cation exchange property of SilicaShell (*Figure 5.S1*). These changes point to an important role of water in method development with silica stationary phases.

Figure 5.5 shows the effect of water on the efficiency and retention of phenylsuccinic acid with the silica stationary phase. An approximately 4-fold increase in efficiency is obtained with an increase in retention. However, there seemed to be a much smaller effect of water on retention times for neutral compounds. Neutral compounds have far weaker interactions with surface silanols due to the lack of ionic interactions which is inherently stronger than hydrogen bonding or dispersion interactions.

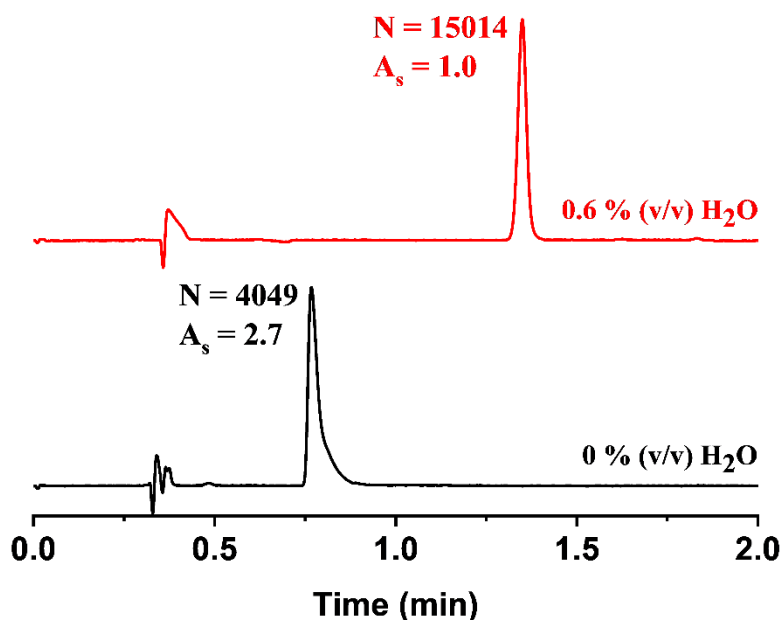


Figure 5.5: SFC chromatogram of phenylsuccinic acid on SilicaShell column with 90/10 CO₂/MeOH + 0.1% (v/v) TEA + 0.1% (v/v) TFA mobile phase without (bottom) and with (top) addition of 6% (v/v) H₂O to modifier.

5.4.3 Octadecylsilica stationary phase

Octadecylsilica stationary phases contain hydrophobic alkyl chains. Therefore, they cannot introduce any polar interactions (such as dipole-dipole or hydrogen bonding interactions) to the overall mechanism of separation. The end-capping process ensures that the remaining silanol activities are minimized (as is the case for Poroshell C18 EC). Non endcapped C18 stationary phases can have a significant number of residual surface silanols which can contribute to polar interactions thereby changing selectivity of the column (as is the case for Xselect C18 SB, *vide infra*). For the study of water influence on the SFC separations on a Poroshell C18 EC column, 19 compounds with different functionalities and acidity were analyzed. These compounds, their relevant properties and retention factors are presented in *Table 5.S5*. For the study of the effect of water presence in mobile phase 10% modifier concentration was used since higher amounts of co-solvent resulted in practically no retention of the analytes. To study the influence of water on Water Xselect C18, a total of 41 different analytes with different functionalities were analyzed for the effect of water on retention factor and efficiency with modifier concentrations of 10% and 20% methanol.

5.4.3.1 Effect of water as an additive

Figure 5.6 shows the effect of the addition of a small amount of water on retention (k) and efficiency (N) for a variety of analytes eluted from an endcapped octadecyl (Poroshell C18 EC)

substituted silica column with a 90/10, CO₂/methanol system. The red line parallel to the x-axis indicates the retention factor of water ($k_w=0.13$) with 90/10, CO₂/methanol.

A slight increase in efficiency with added water was observed (~ 200-500 theoretical plates) regardless of the acidity of the compounds (*Figure 5.6*). Efficiency gains for most analytes having retention factors higher than k_w were observed. However, the magnitude of increase in plate count was significantly lower than was found for the FructoShell-N column. Such smaller increases in efficiency with the use of water-rich modifiers are also typical for nonpolar stationary phases for chiral separations under SFC conditions [16]. A small increase in retention was observed for most of the studied analytes with the use of water as an additive. For some analytes, changes in retention were insignificant (*Figure 5.6*). The increased retention of the tested analytes can be attributed to a preferential partitioning of the nonpolar analytes into the stationary phase in the presence of water.

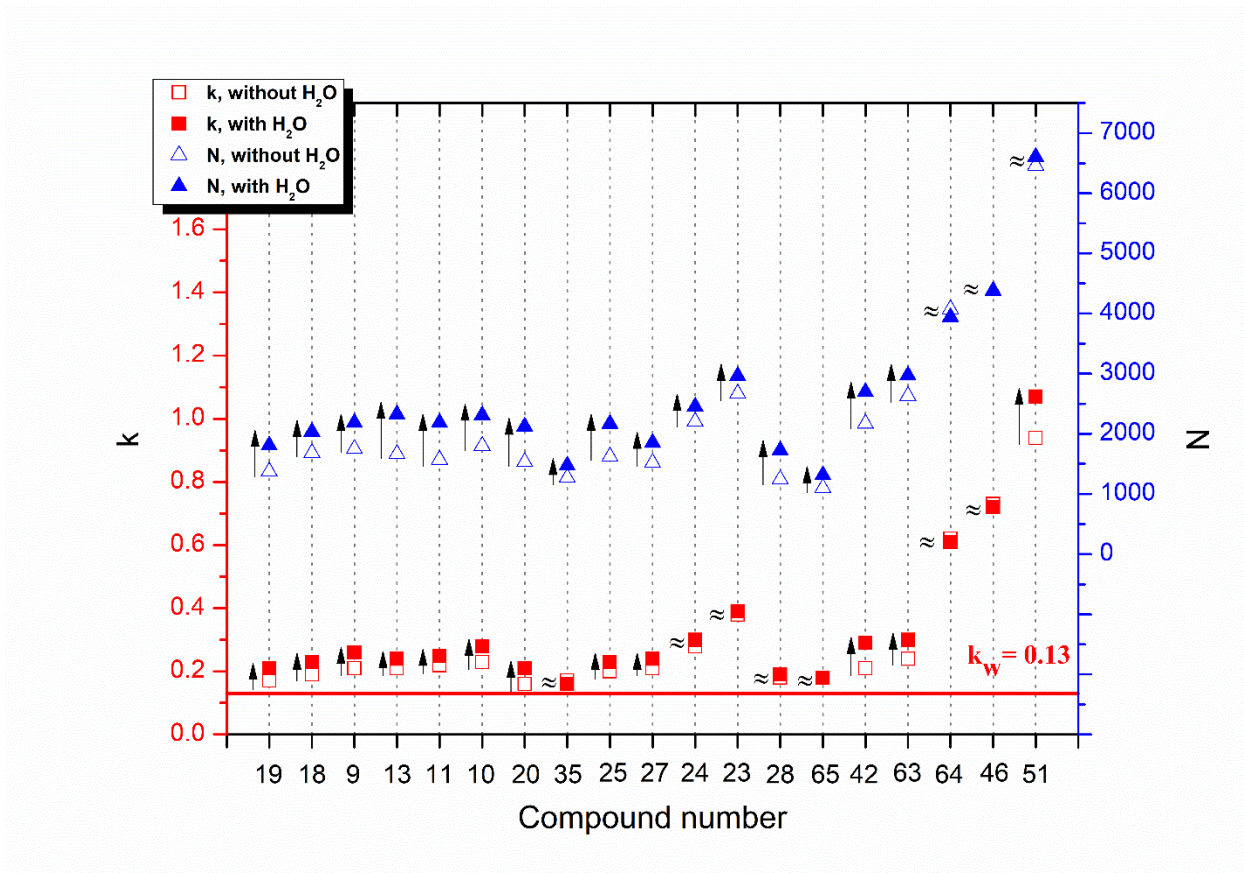


Figure 5.6: Influence of water on the separation of analytes on C18 column. Conditions: 90/10 $\text{CO}_2/\text{MeOH} + 0.1\%$ (v/v) TEA + 0.1% (v/v) TFA (empty squares and triangles); 90/10 $\text{CO}_2/\text{MeOH} + 0.1\%$ (v/v) TEA + 0.1% (v/v) TFA + 6% (v/v) H_2O (full squares and triangles); flow rate 4 ml/min, back pressure 8 MPa, detection: UV, 220nm. Compounds numbers are same as that in Table 5.1. X-axis denotes compound numbers; the left y-axis denotes retention factor and the right y-axis denotes efficiency.

On the contrary, when non-encapped C18 (Xselect C18 SB) is used as the stationary phase, the results are quite different. Some analytes show a gain in efficiency whereas some analytes show a decrease in efficiency (Figure 5.7, 5.S13-S17, Table 5.S6 & S7). As mentioned previously, unlike encapped C18 which has primarily a single mode of retention. The

nonendcapped C18 can also retain analytes due to polar interactions resulting from the residual surface silanols. This stationary phase can retain analytes much more than its endcapped counterpart. These multiple modes of retention, however, lead to somewhat unpredictable behavior of the analytes when water is added to the mobile phase. As discussed for silica the interaction of water with the surface silanols can cause changes in selectivity, thus a predictive test eludes us. However, unlike the bare silica stationary phase the magnitude of gain or loss in efficiency was far lower with added water. Also, like the other tested stationary phases there was no correlation between mobile phase composition and the changes in retention factor.

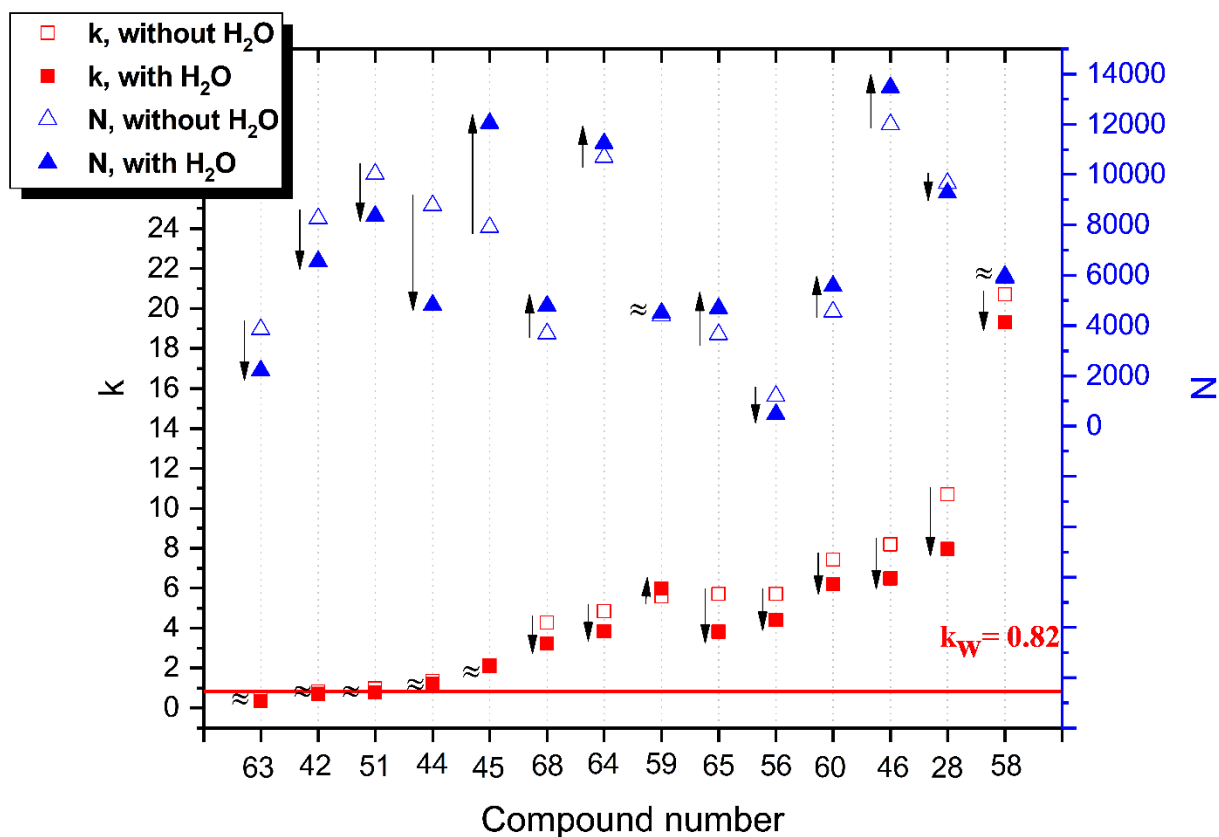


Figure 5.7: Influence of water on the separation of basic compounds on Xselect C18 SB column.

Conditions: 80/20 CO₂/MeOH + 0.1% (v/v) TEA + 0.1% (v/v) TFA (empty squares and triangles); 90/10 CO₂/MeOH + 0.1% (v/v) TEA + 0.1% (v/v) TFA + 6% (v/v) H₂O (full squares

and triangles); flow rate 4 ml/min, back pressure 8 MPa; detection: UV, 220nm. Compounds numbers are same as that in Table 5.1. X-axis denotes compound numbers; the left y-axis denotes retention factor and the right y-axis denotes efficiency.

5.4.4 Discriminant Analysis

Besides using k_w , a more robust approach to predict the behavior of various columns can be achieved with the help of discriminant analysis. This statistical approach allows one to determine which structural parameters of the analyte, can be used to predict efficiency gains[35]. For this purpose, all compounds included in the study were separated into two classes according to the positive or negative impact of the presence of water on the efficiency of separation. The positive or negative impact was evaluated according to the formula: $\Delta N = N_{water} - N$, where N_{water} is the efficiency of separation with the use of water-rich co-solvent and N is the efficiency of separation without the addition of water.

The discriminant method determines which variables can "discriminate" the two classes of data i.e., efficiency gain with water corresponding to $\Delta N > 0$, and efficiency loss corresponds to $\Delta N < 0$ [36, 37]. Since there are only two observable parameters only a single dimension is sufficient for representing the variables as well as the observations i.e. F1 represents 100% of the variance whereas F2 represents 0% (*Figure 5.8*). Also, by the use of discriminant analysis, it is possible to predict which class a new analyte will belong to. Data used for discriminant analysis should be grouped into classes and for all samples ("observations"), identical variables must be used. Results of discriminant analysis are presented by a score plot on which the centroid of the groups of observations is as spread out as far as possible in the space.

5.4.4.1 FructoShell-N

Results of discriminant analysis for the FructoShell-N column with the use of 20% modifier concentration with and without water in the mobile phase are presented in *Figure 5.8A*. There is a distinct group of compounds that show a gain in efficiency or losses in efficiency after adding water. The question is which parameter is best able to discriminate the two classes of compounds. As shown in the circle *Figure 5.8A*, the retention factor (k) has the highest ability to distinguish the $\Delta N > 0$ or $\Delta N < 0$ classes of compounds. This information is supported by *Figures 5.1 and 5.2*, which show that compounds with larger retention factors show a gain in theoretical plates with water. On the other hand, higher values of the log octanol-water partition coefficient mostly correlated with decreasing efficiencies. It is interesting to note that the polar surface area (PSA) has little discriminating ability when using FructoShell- N stationary phase. Since the centroid of the two classes ($\Delta N > 0$ and $\Delta N < 0$) are far apart, this indicates good discrimination between these two classes. With the use of discriminant analysis on FructoShell-N, there is predictive power which indicates that when the retention factor of a compound is large, with $k > \sim 2$, the addition of water to the SFC mobile phase will be beneficial in terms of plate count. Discriminant analysis performed under 10% methanolic modifier also showed similar results with retention factor (k) being the most important parameter for discrimination between the two groups (See *Figure 5.S18A*).

5.4.4.2 SilicaShell

Results of discriminant analysis for the SilicaShell column with the use of a 20% modifier concentration with and without water in the mobile phase are presented in *Figure 5.8B*. In the majority of the cases, there is a gain the plate count in the presence of water, i.e., 39 of 48 analytes show an increased plate count with the addition of water (See Supporting Information *Tables 5.S3 and 5.S4*). In terms of discriminant analysis, bare silica does not show any distinct grouping of

data. The centroids which represent the means of the two classes are closely placed along with significant overlap in the scatter of the two classes. The five studied parameters are not good predictive variables for the examined observable ($\Delta N > 0$ and $\Delta N < 0$). In addition, it should be noted that silanols will interact via H-bonding and polar interactions explaining the contributions from PSA and H_{sum} in the plot. It is likely that silica offers a variety of interactions for retention which must be analyte dependent. Thus, predicting the behavior of silica is significantly more challenging than FructoShell-N column, where the retention factor could be conveniently used for the prediction of efficiency gains. However, it is interesting to note that when SilicaShell is used with a mobile phase of 10% methanolic modifier, the retention factor (k) again is the most important parameter for analytes which show a gain in efficiency (See *Figure 5.S18B*).

5.4.4.3 Octadecylsilica

Results of discriminant analysis for the Poroshell C18 column EC with the use of a 10% modifier concentration with and without water in the mobile phase are presented in *Figure 8C*. Like bare silica and the FructoShell column, the majority of the analytes (18 out of 20) show an increase in efficiency in the presence of water. However, unlike the FructoShell-N and SilicaShell columns the increases in efficiency are not as prominent for the C18 phase. As shown in the variables plot in *Figure 5.7C*, the retention factor is the main contributing factor to grouping for C18, like the FructoShell-N stationary phase. But unlike Fructoshell-N the high retention factors lead to a decrease in the plate count on the C18 albeit by a very small amount. The low discriminating ability of the polar surface area is obvious in this case, since the C18 column is highly nonpolar and doesn't participate in polar interactions.

Discriminant analysis with the tested analytes on Xselect C18 SB using 20% modifier in the mobile phase reveals that the octanol-water partition coefficient is the predominant parameter

for analytes showing a decrease in efficiency with added water whereas pK_a is the most important parameter in grouping the analytes which show a gain in efficiency (*Figure 5.8D*). However, there is significant overlap between the two groups suggesting that the chosen parameters are not good variables for discriminating between the two groups ($\Delta N > 0$ and $\Delta N < 0$). When 10% methanolic mobile phase is used, polar surface area closely followed by sum of hydrogen bonding ability provides best grouping ability for the analytes showing a gain in efficiency (*Figure 5.S18C*). This is expected from previous results (*vide supra*) as polar interactions with the stationary phase are of utmost importance for gain in efficiency. However, a good grouping of the observable is still not achieved and significant overlap between the groups are present even with 10% modifier concentration in the mobile phase.

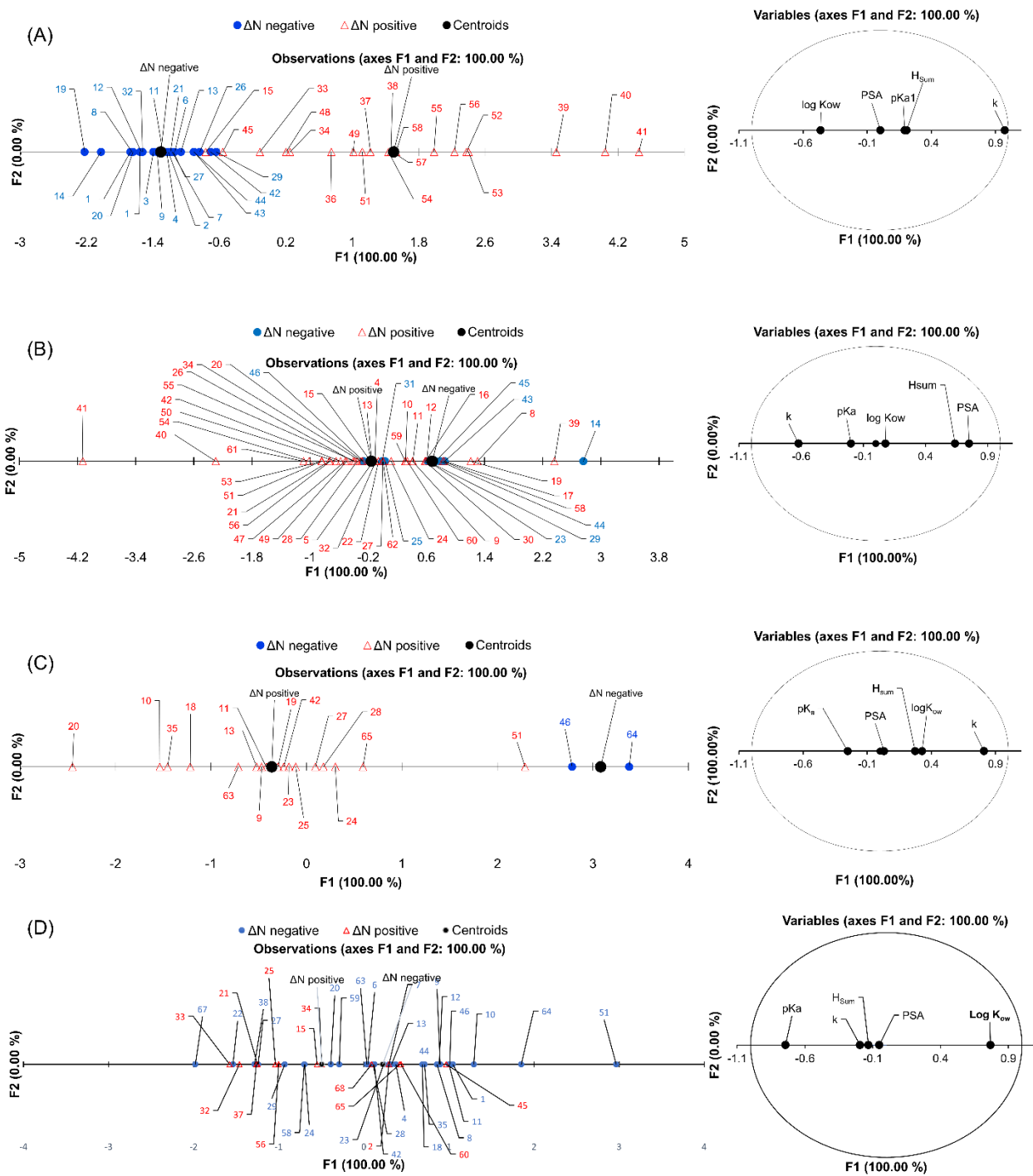


Figure 5.8: Discriminant analysis for FructoShell-N column with use of 80/20 CO₂/MeOH + 0.1% (v/v) TEA + 0.1% (v/v) TFA without and with addition of 6% (v/v) H₂O (A); SilicaShell column with use of 80/20 CO₂/MeOH + 0.1% (v/v) TEA + 0.1% (v/v) TFA without and with

addition of 6% (v/v) H₂O (B); and C18 column with use of 90/10 CO₂/MeOH + 0.1% (v/v) TEA + 0.1% (v/v) TFA without and with addition of 6% (v/v) H₂O (C). Compounds numbers are same as that in Table 5.1.

5.5 Conclusions

Four stationary phases with different polarities have been evaluated to help understand the role of added water in SFC. For most of the studied compounds on different stationary phases, the presence of a small amount of water in the mobile phase improves efficiency. For FructoShell-N and C18 stationary phases, a predictive test of using the water system peak as a marker is proposed: if the retention factor of a compound is bigger than retention factor of water system peak, then the presence of the water will lead to improvements in efficiency. For the SilicaShell stationary phase for most of the studied compounds, a gain in efficiency was observed with the use of water-rich modifiers; however a simple predictive test remains elusive due to changes in selectivity resulting from the changes in column chemistry in the presence of water. Similarly, for Xselect C18 SB, a similar test was also found to be inadequate since there were multiple retention mechanisms at play. The discriminant analysis further confirms that for FructoShell-N stationary phases, the more highly retained analytes show the most gains in efficiency and this can be especially helpful since generally highly retained analyte peaks often have lower efficiency. The increase in efficiency for the highly retained compounds also allows for lower detection limits with analytical SFC. Finally, this study indicates the beneficial role of water in achiral SFC method development.

5.6 Acknowledgments

The authors would like to thank Robert A. Welch Foundation (Y-0026) and Erasmus+International Credit Mobility program (Grant Agreement No. 2018-1-SK01-KA107-

045949) for financial support. We would acknowledge AZYP LLC Arlington, TX for providing FructoShell-N columns. The authors would also like to acknowledge Dr. Charles A. Lucy, Dr. M.E.A. Ibrahim and Dr. Knut Irgum for providing the raw data for HILIC selectivity chart.

5.7 References

- [1] N.M. Karayannis, A.H. Corwin, E.W. Baker, E. Klesper, J.A. Walter, Apparatus and materials for hyperpressure gas chromatography of nonvolatile compounds, *Analytical Chemistry* 40(11) (1968) 1736-1739.
- [2] F.I. Stalkup, R. Kobayashi, High-pressure phase-equilibrium studies by gas-liquid partition chromatography, *AIChE Journal* 9(1) (1963) 121-128.
- [3] C. West, Current trends in supercritical fluid chromatography, *Analytical and bioanalytical chemistry* 410(25) (2018) 6441-6457.
- [4] L. Novakova, A.G.-G. Perrenoud, I. Francois, C. West, E. Lesellier, D. Guillarme, Modern analytical supercritical fluid chromatography using columns packed with sub-2 μm particles: a tutorial, *Analytica Chimica Acta* 824 (2014) 18-35.
- [5] T.A. Berger, Instrumentation for analytical scale supercritical fluid chromatography, *Journal of Chromatography A* 1421 (2015) 171-183.
- [6] C.R. Yonker, R.D. Smith, Pressure and composition gradients in capillary supercritical fluid chromatography, *Analytical Chemistry* 59(5) (1987) 727-731.
- [7] E. Lesellier, K. Gurdale, A. Tchaplal, Phase ratio and eluotropic strength changes on retention variations in subcritical fluid chromatography (SubFC) using packed octadecyl columns, *Chromatographia* 55(9-10) (2002) 555-563.
- [8] T.A. Berger, Separation of polar solutes by packed column supercritical fluid chromatography, *Journal of Chromatography A* 785(1-2) (1997) 3-33.
- [9] C. Lochmüller, L. Mink, Adsorption isotherms on silica for methanol and 1-hexanol modifiers from supercritical carbon dioxide, *Journal of Chromatography A* 471 (1989) 357-366.
- [10] J.R. Strubinger, H. Song, J.F. Parcher, High-pressure phase distribution isotherms for supercritical fluid chromatographic systems. 1. Pure carbon dioxide, *Analytical Chemistry* 63(2) (1991) 98-103.
- [11] J.R. Strubinger, H. Song, J.F. Parcher, High-pressure phase distribution isotherms for supercritical fluid chromatographic systems. 2. Binary isotherms of carbon dioxide and methanol, *Analytical Chemistry* 63(2) (1991) 104-108.
- [12] T.A. Berger, J.F. Deye, Role of additives in packed column supercritical fluid chromatography: suppression of solute ionization, *Journal of Chromatography A* 547 (1991) 377-392.
- [13] D. Pyo, Separation of vitamins by supercritical fluid chromatography with water-modified carbon dioxide as the mobile phase, *Journal of Biochemical and Biophysical Methods* 43(1) (2000) 113-123.
- [14] D. Pyo, D. Ju, Addition and measurement of water in carbon dioxide mobile phase for supercritical fluid chromatography, *Analyst* 118(3) (1993) 253-255.

- [15] S.T. Lee, T.S. Reighard, S.V. Olesik, Phase diagram studies of methanol H₂O-CO₂ and acetonitrile-H₂O CO₂ mixtures, *Fluid Phase Equilibria* 122(1-2) (1996) 223-241.
- [16] D. Roy, M.F. Wahab, T.A. Berger, D.W. Armstrong, Ramifications and Insights on the Role of Water in Chiral Sub/Supercritical Fluid Chromatography, *Analytical Chemistry* 91 (22), (2019), 14672-14680.
- [17] D. Roy, M.F. Wahab, M. Talebi, D.W. Armstrong, Replacing methanol with azeotropic ethanol as the co-solvent for improved chiral separations with supercritical fluid chromatography (SFC), *Green Chemistry* 10.1039/C9GC04207E (2020).
- [18] D. Roy, D.W. Armstrong, Fast super/subcritical fluid chromatographic enantioseparations on superficially porous particles bonded with broad selectivity chiral selectors relative to fully porous particles, *Journal of Chromatography A* 1605 (2019) <https://doi.org/10.1016/j.chroma.2019.06.060>.
- [19] O. Bonner, Y. Choi, A spectroscopic investigation of the structure of alcohol-water solutions, *Journal of Solution Chemistry* 4(5) (1975) 457-469.
- [20] S. Wang, S. Elshani, C. Wai, Selective extraction of mercury with ionizable crown ethers in supercritical carbon dioxide, *Analytical Chemistry* 67(5) (1995) 919-923.
- [21] L.T. Taylor, Packed column supercritical fluid chromatography of hydrophilic analytes via water-rich modifiers, *Journal of Chromatography A* 1250 (2012) 196-204.
- [22] M. Ashraf-Khorassani, L.T. Taylor, Subcritical fluid chromatography of water soluble nucleobases on various polar stationary phases facilitated with alcohol-modified CO₂ and water as the polar additive, *Journal of Separation Science* 33(11) (2010) 1682-1691.
- [23] J. Liu, E.L. Regalado, I. Mergelsberg, C.J. Welch, Extending the range of supercritical fluid chromatography by use of water-rich modifiers, *Organic & Biomolecular chemistry* 11(30) (2013) 4925-4929.
- [24] J. Liu, A.A. Makarov, R. Bennett, I.A. Haidar Ahmad, J. DaSilva, M. Reibarkh, I. Mangion, B.F. Mann, E.L. Regalado, Chaotropic Effects in Sub/Supercritical Fluid Chromatography via Ammonium Hydroxide in Water-Rich Modifiers: Enabling Separation of Peptides and Highly Polar Pharmaceuticals at the Preparative Scale, *Analytical Chemistry* 91(21) (2019) 13907-13915.
- [25] Y. Wang, M.F. Wahab, Z.S. Breitbach, D.W. Armstrong, Carboxylated cyclofructan 6 as a hydrolytically stable high efficiency stationary phase for hydrophilic interaction liquid chromatography and mixed mode separations, *Analytical Methods* 8(31) (2016) 6038-6045.
- [26] N.P. Dinh, T. Jonsson, K. Irgum, Probing the interaction mode in hydrophilic interaction chromatography, *Journal of Chromatography A* 1218(35) (2011) 5880-5891.
- [27] D. Armstrong, J. Zukowski, Direct enantiomeric resolution of monoterpene hydrocarbons via reversed-phase high-performance liquid chromatography with an α -cyclodextrin bonded stationary phase, *Journal of Chromatography A* 666(1-2) (1994) 445-448.
- [28] J.E. Paanakker, J.C. Kraak, H. Poppe, Some aspects of the influence of the mobile phase composition in normal-phase liquid-solid chromatography, with special attention to the role of water present in binary organic mixtures, *Journal of Chromatography A* 149 (1978) 111-126.
- [29] J.J. Kirkland, C.H. Dilks, J.J. DeStefano, Normal-phase high-performance liquid chromatography with highly purified porous silica microspheres, *Journal of Chromatography A* 635(1) (1993) 19-30.
- [30] M.F. Wahab, J.K. Anderson, M. Abdelrady, C.A. Lucy, Peak distortion effects in analytical ion chromatography, *Analytical Chemistry* 86(1) (2014) 559-566.

- [31] R. Arnell, P. Forssén, T. Fornstedt, Tuneable Peak Deformations in Chiral Liquid Chromatography, *Analytical Chemistry* 79(15) (2007) 5838-5847.
- [32] E. Glenne, H. Leek, M. Klarqvist, J. Samuelsson, T. Fornstedt, Peak deformations in preparative supercritical fluid chromatography due to co-solvent adsorption, *Journal of Chromatography A* 1468 (2016) 200-208.
- [33] J.N. Fairchild, D.W. Brousmiche, J.F. Hill, M.F. Morris, C.A. Boissel, K.D. Wyndham, Chromatographic evidence of silyl ether formation (SEF) in supercritical fluid chromatography, *Analytical Chemistry* 87(3) (2015) 1735-1742.
- [34] J. Köhler, J.J. Kirkland, Improved silica-based column packings for high-performance liquid chromatography, *Journal of Chromatography A* 385 (1987) 125-150.
- [35] S. Khater, Y. Zhang, C. West, Insights into chiral recognition mechanism in supercritical fluid chromatography IV. Chlorinated polysaccharide stationary phases, *Journal of Chromatography A* 1363 (2014) 294-310.
- [36] M.D. Jones, B. Avula, Y.-H. Wang, L. Lu, J. Zhao, C. Avonto, G. Isaac, L. Meeker, K. Yu, C. Legido-Quigley, Investigating sub-2 μm particle stationary phase supercritical fluid chromatography coupled to mass spectrometry for chemical profiling of chamomile extracts, *Analytica Chimica Acta* 847 (2014) 61-72.
- [37] C. West, G. Guenegou, Y. Zhang, L. Morin-Allory, Insights into chiral recognition mechanisms in supercritical fluid chromatography. II. Factors contributing to enantiomer separation on tris-(3, 5-dimethylphenylcarbamate) of amylose and cellulose stationary phases, *Journal of Chromatography A* 1218(15) (2011) 2033-2057.

5.8 Supplementary Information

Table 5.S1 Characteristics and measured data for compounds used for study on FructoShell-N stationary phase with use 90/10 CO₂/MeOH + 0.1% (v/v) TEA + 0.1% (v/v) TFA and 90/10 CO₂/MeOH + 0.1% (v/v) TEA + 0.1% (v/v) TFA + 5.7% (v/v) H₂O mobile phases

Name	^a log K _{ow}	^b pKa	^c PSA, Å ²	^d H _{sum}	^e k	^f k _{water}	^g N	^h N _{water}	ⁱ A _s	^j A _{s water}
Ibuprofen	3.97	5.30	37.30	3.00	0.57	0.50	7609	3517	1.0	0.9
2-Phenylbutyric acid	2.21	4.34	37.30	3.00	0.68	0.73	6485	5476	1.0	0.9
5-Phenylvaleric acid	2.94	4.74	37.30	3.00	0.69	0.72	5967	4801	1.0	0.9
m-Toluic acid	2.37	4.27	37.30	3.00	0.70	0.85	7134	6999	1.0	1.0
Benzoic acid	1.88	4.50	37.30	3.00	0.75	1.00	7697	7519	1.1	0.9
4-Vinylbenzoic acid	2.18	4.24	37.30	3.00	0.82	0.98	7530	6742	1.1	0.9
4-Nitrobenzoic acid	1.89	3.44	83.10	6.00	0.95	1.13	6776	6512	1.2	1.0
Fenoprofen	3.10	4.50	46.50	4.00	0.95	1.01	7914	6868	1.0	1.0
Flurbiprofen	4.16	4.42	37.30	3.00	1.00	1.02	8624	6785	1.0	1.0
Naproxen	3.18	4.15	46.50	4.00	1.31	1.46	9089	8269	1.1	1.0
Ketoprofen	3.00	4.45	54.40	4.00	1.47	1.75	8800	8024	1.0	0.9
1-Naphthylacetic acid	2.24	4.23	37.30	3.00	1.56	1.62	9191	8811	1.1	1.0

3,5-Dinitrobenzoic acid	1.54	3.90	129.00	9.00	2.04	1.43	1734	8579	2.3	0.8
Nicotinic acid	0.36	4.75	50.20	4.00	2.20	2.74	2592	12218	2.2	1.2
Suprofen	2.20	3.91	82.60	4.00	2.37	2.96	12382	10590	1.1	1.0
Thymol	3.30	10.60	20.20	2.00	0.68	0.64	6724	4728	0.9	0.9
Phenol	1.46	10.00	20.20	2.00	0.90	1.17	8703	8235	1.0	1.0
4-Phenyl-2-oxazolidinone	-0.20	12.50	38.30	4.00	1.96	2.18	11553	10396	1.0	1.0
4-(Diphenylmethyl)-2-oxazolidinone	1.53	12.29	38.30	4.00	2.12	1.85	9654	8314	0.8	1.0
Theophylline	-0.02	8.81	69.30	7.00	2.20	2.88	9972	13513	1.2	1.0
N-Benzylbenzamide	2.26	14.86	29.10	3.00	2.36	2.43	10852	7906	1.0	1.0
Thymine	-0.62	10.02	58.20	6.00	5.99	7.63	11721	14639	1.2	1.0
Nicotinamide	-0.38	3.35	56.00	5.00	7.25	8.00	9952	14707	1.6	1.0
2-Phenylbenzimidazole	3.24	5.00	28.10	3.00	10.70	19.33	12152	13029	1.0	0.9
1-Benzylimidazole	1.60	6.70	17.80	2.00	14.28	19.45	10213	14985	1.7	1.1
2-Methylimidazole	0.24	7.86	28.70	3.00	21.74	29.92	7282	12904	2.4	1.3
Imidazole	-0.08	6.95	28.70	3.00	21.90	28.13	5422	13296	2.7	1.2

Adenosine	-1.05	3.60	140.00	14.00	39.66	39.24	6948	16486	1.5	0.9
1-(2-Hydroxyethyl)imidazole	-0.45	6.78	38.00	4.00	52.98	50.00	3590	8659	2.6	1.7
1,2-Dimethylimidazole	0.03	7.76	17.80	2.00	54.14	48.15	8543	13266	1.8	1.2
2,6-Dimethylaniline	1.84	3.95	26.00	3.00	0.49	0.57	6813	6449	1.0	1.0
2-Nitroaniline	1.85	-0.23	71.80	6.00	1.24	1.27	11518	9157	1.0	0.9
3-Nitroaniline	1.37	2.47	71.80	6.00	1.83	1.86	13149	9772	1.1	1.1
4-Nitroaniline	1.39	1.01	71.80	6.00	4.06	4.31	14532	15503	1.0	1.0
1,2,2-Triphenylethylamine	3.96	8.52	26.00	3.00	16.44	15.83	10317	12717	1.0	0.8
1-Methyl-3-phenylpropylamine	2.26	10.00	26.00	3.00	19.83	13.21	1830	15668	2.9	1.1
Triphenylamine	5.74	-3.04	3.24	1.00	20.26	16.92	8292	13059	1.6	0.8
Melamine	-1.37	5.00	117.0	12.00	27.72	28.39	7346	16630	2.2	1.1
Benzylamine	1.09	9.33	26.00	3.00	28.29	18.26	2230	8922	3.2	1.7
Atropine	1.83	9.43	49.80	5.00	30.53	34.24	7990	15753	2.0	1.1

1-(2-Naphthyl)ethylamine	2.90	9.36	26.00	3.00	30.88	19.20	10137	16589	1.5	1.0
3-Phenyl-1-propylamine	1.83	10.05	26.02	2.00	34.61	15.39	1791	10096	3.0	1.6
Sotalolol	0.37	10.07	86.80	8.00	40.69	59.98	7176	12900	1.8	1.1
Acebutolol	1.19	13.91	87.70	9.00	49.16	56.91	9506	13216	1.2	1.0

a: $\log K_{ow}$ – logarithm of octanol/water partition coefficient; b: pKa – negative logarithm of acid dissociation constant for the first ionization; c: PSA – polar surface area, Å²; d: H_{sum} – sum of hydrogen bonds that molecule can provide; e,g,i: k, N, A_s – retention factor, number of theoretical plates and peak symmetry factor respectively with use of 90/10 CO₂/MeOH + 0.1% (v/v) TEA + 0.1% (v/v) TFA mobile phase ; f,h,j: k_{water}, N_{water}, A_{swater} – retention factor, number of theoretical plates and peak symmetry factor respectively with use of 90/10 CO₂/MeOH + 0.1% (v/v) TEA + 0.1% (v/v) TFA + 5.7% (v/v) H₂O mobile phase.

Table 5.S2 Characteristics and measured data for compounds used for study on FructoShell-N stationary phase with use 80/20 CO₂/MeOH + 0.1% (v/v) TEA + 0.1% (v/v) TFA and 80/20 CO₂/MeOH + 0.1% (v/v) TEA + 0.1% (v/v) TFA + 5.7% (v/v) H₂O mobile phases

Name	^a log K _{ow}	^b pKa	^c PSA, Å ²	^d H _{sum}	^e k	^f k _{water}	^g N	^h N _{water}	ⁱ A _s	^j A _{swater}
Ibuprofen	3.97	5.30	37.30	3.00	0.32	0.43	4245	2992	1.0	0.9
2-Phenylbutyric acid	2.21	4.34	37.30	3.00	0.40	0.57	5330	4314	1.0	1.0
5-Phenylvaleric acid	2.94	4.74	37.30	3.00	0.39	0.56	4387	3625	1.0	1.0
<i>m</i> -Toluic acid	2.37	4.27	37.30	3.00	0.42	0.61	5592	4855	1.0	1.0
Benzoic acid	1.88	4.50	37.30	3.00	0.46	0.67	5973	5555	1.0	0.9
4-Vinylbenzoic acid	2.18	4.24	37.30	3.00	0.48	0.66	5903	5294	1.1	1.0
4-Nitrobenzoic acid	1.89	3.44	83.10	6.00	0.51	0.69	5988	5286	1.1	0.9
Fenoprofen	3.10	4.50	46.50	4.00	0.51	0.65	6509	5408	1.0	1.0
Flurbiprofen	4.16	4.42	37.30	3.00	0.54	0.66	6589	5601	1.1	1.0
Naproxen	3.18	4.15	46.50	4.00	0.66	0.83	7448	6312	1.0	1.0
Ketoprofen	3.00	4.45	54.40	4.00	0.68	0.88	7568	6514	1.0	1.0
1-Naphthylacetic acid	2.24	4.23	37.30	3.00	0.78	0.96	7511	6362	1.0	1.0
3,5-Dinitrobenzoic acid	1.54	3.90	129.0	9.00	1.03	0.88	5968	4889	1.6	1.1
Nicotinic acid	0.36	4.75	50.20	4.00	0.99	1.31	4878	6812	1.7	1.2
Suprofen	2.20	3.91	82.60	4.00	0.97	1.24	9283	7690	1.1	1.0
Thymol	3.30	10.60	20.20	2.00	0.39	0.53	5161	4056	1.0	1.0

Phenol	1.46	10.00	20.20	2.00	0.49	0.76	6410	5926	1.0	1.0
N-Benzylbenzamide	2.26	14.86	29.10	3.00	0.91	1.15	9269	7219	1.1	1.0
4-Phenyl-2-oxazolidinone	-0.20	12.50	38.30	4.00	0.93	1.19	9286	7761	1.1	1.0
4-(Diphenylmethyl)-2-oxazolidinone	1.53	12.29	38.30	4.00	0.96	1.09	8044	6778	0.9	1.0
Theophylline	-0.02	8.81	69.30	7.00	1.04	1.39	8816	8718	1.2	1.0
Thymine	-0.62	10.02	58.20	6.00	2.16	2.66	11054	13714	1.2	1.1
Nicotinamide	-0.38	3.35	56.00	5.00	2.59	2.91	7581	12413	1.3	1.1
1-Benzylimidazole	1.60	6.70	17.80	2.00	4.63	5.73	6311	12661	0.9	1.3
2-Methylimidazole	0.24	7.86	28.70	3.00	5.23	6.27	7324	11472	2.0	1.3
Imidazole	-0.08	6.95	28.70	3.00	5.77	6.54	4941	11557	2.9	1.4
Adenosine	-1.05	3.60	140.0	14.00	9.93	8.87	5140	15318	1.7	1.0
1-(2-Hydroxyethyl)imidazole	-0.45	6.78	38.00	4.00	12.08	10.81	2750	6424	3.0	2.0
1,2-Dimethylimidazole	0.03	7.76	17.80	2.00	13.44	11.32	5730	11097	2.0	1.3
2,6-Dimethylaniline	1.84	3.95	26.00	3.00	0.42	0.54	5805	4599	1.0	1.0
2-Nitroaniline	1.85	-0.23	71.80	6.00	0.67	0.85	8807	6874	1.0	1.0
3-Nitroaniline	1.37	2.47	71.80	6.00	0.93	1.10	10632	7718	1.1	1.0
4-Nitroaniline	1.39	1.01	71.80	6.00	1.55	1.90	12345	17413	1.1	0.9

1,2,2-Triphenylethylamine	3.96	8.52	26.00	3.00	4.67	4.73	9310	11991	1.4	0.9
Triphenylamine	5.74	-3.04	3.24	1.00	5.61	4.96	8122	11430	1.6	1.0
1-Methyl-3-phenylpropylamine	2.26	10.00	26.00	3.00	6.15	4.31	2189	10882	2.8	1.3
Melamine	-1.37	5.00	117.0	12.00	7.29	7.55	6452	13907	2.1	1.2
Atropine	1.83	9.43	49.80	5.00	7.32	7.45	7630	13171	1.8	1.2
Sotalol	0.37	10.07	86.80	8.00	7.59	9.19	6771	10966	1.7	1.3
Acebutolol	1.19	13.91	87.70	9.00	8.07	8.04	7321	8857	1.2	1.0
1-(2-Naphthyl)ethylamine	2.90	9.36	26.00	3.00	8.82	5.86	9313	12898	1.5	1.0
Benzylamine	1.09	9.33	26.00	3.00	8.95	5.83	1850	6221	3.6	1.9
3-Phenyl-1-propylamine	1.83	10.05	26.02	2.00	9.89	5.33	1637	6460	3.3	1.9

Table 5.S3 Characteristics and measured data for compounds used for study on SilicaShell stationary phase with use 90/10 CO₂/MeOH + 0.1% (v/v) TEA + 0.1% (v/v) TFA and 90/10 CO₂/MeOH + 0.1% (v/v) TEA + 0.1% (v/v) TFA +5.7% (v/v) H₂O mobile phases

Name	^a log Kow	^b pKa	^c PSA, Å ²	^d H _{sum}	^e k	^f k _{water}	^g N	^h N _{water}	ⁱ A _s	^j A _{swater}
<i>m</i> -Toluic acid	2.37	4.27	37.30	3.00	0.34	0.55	2662	4844	1.3	1.0
<i>p</i> -Toluic acid	2.27	4.37	37.30	3.00	0.35	0.57	2746	4839	1.4	0.9
4-Nitrobenzoic acid	1.89	3.44	83.10	6.00	0.40	0.73	5532	4688	1.0	1.0
Fenoprofen	3.10	4.50	46.50	4.00	0.43	0.67	5007	5161	1.0	1.0
Flurbiprofen	4.16	4.42	37.30	3.00	0.44	0.67	5414	5556	1.1	1.0
Naproxen	3.18	4.15	46.50	4.00	0.55	0.94	6280	7158	1.0	1.0
3,5-Dinitrobenzoic acid	1.54	3.90	129.0	9.00	0.60	0.98	8608	3370	1.2	0.8
1-Naphthylacetic acid	2.24	4.23	37.30	3.00	0.63	0.94	5124	8488	1.5	0.9
Ketoprofen	3.00	4.45	54.40	4.00	0.70	1.14	5235	8343	1.4	0.9
Suprofen	2.20	3.91	82.60	4.00	0.91	1.83	7280	10656	1.1	1.0
Nicotinic acid	0.36	4.75	50.20	4.00	1.06	2.04	10968	9523	1.3	1.1
Phenylsuccinic acid	-0.01	3.60	74.60	6.00	1.30	2.72	4049	15014	2.7	1.0
2,3-Naphthalenedi carboxylic acid	2.06	2.95	74.60	6.00	9.30	6.20	6590	19338	2.2	1.0
Thymol	3.30	10.60	20.20	2.00	0.33	0.43	3444	3353	1.1	1.0
Phenol	1.46	10.00	20.20	2.00	0.42	0.74	4827	6756	1.0	1.0
4-Benzyl-5,5-dimethyl-2-oxazolidinone	1.16	12.86	38.30	4.00	0.59	0.8	5298	5923	1.0	1.0

5,5-Diphenyl-4-benzyl-2-oxazolidinone	4.22	11.80	38.30	4.00	0.75	0.98	6661	6688	1.1	1.0
4-(Diphenylmethyl)-2-oxazolidinone	1.53	12.29	38.30	4.00	0.84	1.15	8712	8819	1.0	1.0
4-Phenyl-2-oxazolidinone	-0.20	12.50	38.30	4.00	0.89	1.37	8280	10057	1.0	0.9
N-Benzylbenzamide	2.26	14.86	29.10	3.00	0.97	1.53	8328	9837	1.0	1.0
4,5,5-Triphenyl-2-oxazolidinone	2.19	11.07	38.30	4.00	1.14	1.44	9160	8934	1.0	1.0
5,5-Diphenyl-4-methyl-2-oxazolidinone	1.78	11.87	38.30	4.00	1.15	1.50	8927	8775	1.0	1.0
Theophylline	-0.02	8.81	69.30	7.00	1.39	2.02	12271	13462	1.1	1.0
Benzenesulfonamide	0.31	10.08	68.50	5.00	1.43	2.82	9687	15499	1.1	1.1
Benzamide	0.64	16.00	43.10	4.00	1.74	2.40	10947	14000	1.2	1.0
Nicotinamide	-0.38	3.35	56.00	5.00	4.46	5.72	15577	16800	1.3	1.0
Adenosine	-1.05	3.60	140.0	14.00	14.52	20.63	17723	18628	1.7	0.9
1(2-Hydroxyethyl)imidazole	-0.45	6.78	38.00	4.00	52.49	56.27	4997	8581	6.0	2.2
1,2-Dimethylimidazole	0.03	7.76	17.80	2.00	83.26	72.21	14765	18755	1.8	0.9
2,6-Dimethylaniline	1.84	3.95	26.00	3.00	0.34	0.29	4666	2831	1.1	1.1
2-Nitroaniline	1.85	-0.23	71.80	6.00	0.62	0.77	7747	8402	1.0	1.0

3-Nitroaniline	1.37	2.47	71.80	6.00	1.05	1.17	12083	11169	1.0	1.1
4-Nitroaniline	1.39	1.01	71.80	6.00	1.84	2.52	11015	13288	1.0	1.0
2-Aminoanthracene	3.50	4.32	26.00	3.00	1.91	2.02	11290	8318	1.1	0.9
α ,4-Dimethylbenzylamine	2.15	9.2	26.00	3.00	4.70	6.53	10326	12012	1.2	0.8
1-Methyl-3-phenylpropylamine	2.26	10.00	26.00	3.00	4.88	6.82	8893	12657	1.5	0.7
α -Methylbenzylamine	1.72	9.04	26.00	3.00	4.92	7.55	8765	12578	1.2	0.8
Triphenylamine	5.74	-3.04	3.24	1.00	5.12	7.78	7255	7274	0.9	0.7
3-Aminoquinoline	1.63	4.98	38.90	4.00	5.43	6.34	9317	11131	1.2	0.9
Benzylamine	1.09	9.33	26.00	3.00	5.65	8.52	6510	11497	1.3	0.9
1-(2-Naphthyl)ethylamine	2.90	9.36	26.00	3.00	5.89	8.64	11478	13191	1.5	0.9
Metoprolol	1.88	9.70	50.70	6.00	6.23	9.92	11361	12535	1.3	0.9
3-Phenyl-1-propylamine	1.83	10.05	26.02	2.00	6.51	7.76	7459	13888	2.1	0.9
Propranolol	3.48	9.42	41.50	5.00	6.82	8.78	10988	11616	1.3	1.0
4-(1H-imidazol-1-yl)-aniline	0.49	6.05	43.80	5.00	29.00	46.54	10100	12934	1.6	1.3
Acebutolol	1.19	13.91	87.70	9.00	40.75	43.25	14095	17509	2.4	1.1
Atropine	1.83	9.43	49.80	5.00	43.85	40.01	11401	15491	3.9	1.5
Atenolol	0.16	9.6	84.60	9.00	65.31	89.64	15667	15897	2.1	1.0

Table 5.S4 Characteristics and measured data for compounds used for study on SilicaShell stationary phase with use 80/20 CO₂/MeOH + 0.1% (v/v) TEA + 0.1% (v/v) TFA and 80/20 CO₂/MeOH + 0.1% (v/v) TEA + 0.1% (v/v) TFA + 5.7% (v/v) H₂O mobile phases

Name	^a log Kow	^b pKa	^c PSA, Å ²	^d H _{sum}	^e k	^f k _{water}	^g N	^h N _{water}	ⁱ A _s	^j A _{swater}
<i>m</i> -Toluic acid	2.37	4.27	37.30	3.00	0.23	0.47	1509	2658	1.4	1.2
<i>p</i> -Toluic acid	2.27	4.37	37.30	3.00	0.24	0.49	1693	2594	1.3	1.2
Fenopropfen	3.10	4.50	46.50	4.00	0.27	0.50	1942	3211	1.3	1.1
Flurbiprofen	4.16	4.42	37.30	3.00	0.28	0.51	2092	3702	1.3	1.0
4-Nitrobenzoic acid	1.89	3.44	83.10	6.00	0.30	0.51	3407	3504	1.6	1.0
Naproxen	3.18	4.15	46.50	4.00	0.32	0.61	2940	4400	1.4	1.0
Ketoprofen	3.00	4.45	54.40	4.00	0.34	0.65	2825	4997	1.3	1.1
1-Naphthylacetic acid	2.24	4.23	37.30	3.00	0.34	0.62	3026	4636	1.4	1.0
Suprofen	2.20	3.91	82.60	4.00	0.48	0.82	4761	6244	1.3	1.1
Phenylsuccinic acid	-0.01	3.60	74.60	6.00	0.50	1.02	4341	6960	1.5	1.2
3,5-Dinitrobenzoic acid	1.54	3.90	129.0	9.00	0.59	0.58	5555	2772	2.1	1.0
Nicotinic acid	0.36	4.75	50.20	4.00	0.63	0.97	5511	8004	1.7	1.2
2,3-Naphthalene dicarboxylic acid	2.06	2.95	74.60	6.00	2.33	1.96	4198	12015	1.8	1.4
Thymol	3.30	10.60	20.20	2.00	0.22	0.41	1543	2225	1.3	1.1
Phenol	1.46	10.00	20.20	2.00	0.27	0.53	2283	3986	1.2	1.0

4-Benzyl-5,5-dimethyl-2-oxazolidinone	1.16	12.86	38.30	4.00	0.34	0.59	3355	3364	1.2	1.1
5,5-Diphenyl-4-benzyl-2-oxazolidinone	4.22	11.80	38.30	4.00	0.41	0.65	4236	4137	1.1	1.1
4-(Diphenylmethyl)-2-oxazolidinone	1.53	12.29	38.30	4.00	0.44	0.70	5096	5650	1.1	1.0
N-Benylbenzamide	2.26	14.86	29.10	3.00	0.45	0.76	4831	5928	1.1	1.0
4-Phenyl-2-oxazolidinone	-0.20	12.50	38.30	4.00	0.47	0.79	5330	6045	1.1	1.0
4,5,5-Triphenyl-2-oxazolidinone	2.19	11.07	38.30	4.00	0.49	0.79	5307	5695	1.0	1.0
5,5-Diphenyl-4-methyl-2-oxazolidinone	1.78	11.87	38.30	4.00	0.56	0.80	6360	5854	1.0	1.0
Benzenesulfonamide	0.31	10.08	68.50	5.00	0.63	1.17	7280	9141	1.1	1.2
Theophylline	-0.02	8.81	69.30	7.00	0.77	1.08	9697	8311	1.1	1.1
Benzamide	0.64	16.00	43.10	4.00	0.80	1.13	9645	7855	1.1	1.1

Nicotinamide	-0.38	3.35	56.00	5.00	1.97	2.31	13345	15113	1.3	1.1
Adenosine	-1.05	3.60	140.0	14.00	4.53	5.14	12006	14596	1.8	1.1
1(2-Hydroxyethyl)imidazole	-0.45	6.78	38.00	4.00	14.55	14.14	5555	6843	4.3	3.0
1,2-Dimethylimidazole	0.03	7.76	17.80	2.00	25.02	19.76	13166	15077	2.4	1.7
2,6-Dimethylaniline	1.84	3.95	26.00	3.00	0.30	0.46	3053	3172	1.1	1.1
2-Nitroaniline	1.85	-0.23	71.80	6.00	0.38	0.60	5357	5125	1.1	1.1
3-Nitroaniline	1.37	2.47	71.80	6.00	0.59	0.79	8200	7505	1.1	1.1
4-Nitroaniline	1.39	1.01	71.80	6.00	0.79	1.13	9187	7562	1.0	1.1
α ,4-Dimethylbenzylamine	2.15	9.2	26.00	3.00	1.65	2.16	4767	7833	1.0	0.9
Triphenylamine	5.74	-3.04	3.24	1.00	1.79	2.38	4041	6494	0.9	0.9
α -Methylbenzylamine	1.72	9.04	26.00	3.00	1.81	2.43	3873	8518	1.1	1.0
1-Methyl-3-phenylpropylamine	2.26	10.00	26.00	3.00	1.91	2.24	4660	7753	1.1	1.0
3-Aminoquinoline	1.63	4.98	38.90	4.00	2.01	3.16	10035	10299	1.2	1.0
1-(2-Naphthyl)ethylamine	2.90	9.36	26.00	3.00	2.08	2.64	6911	8045	1.2	0.95

Metoprolol	1.88	9.70	50.70	6.00	2.22	2.92	6218	8641	1.3	1.0
Propranolol	3.48	9.42	41.50	5.00	2.22	2.71	4518	8537	1.2	1.0
Benzylamine	1.09	9.33	26.00	3.00	2.26	2.73	3024	8083	1.0	1.1
3-Phenyl-1-propylamine	1.83	10.05	26.02	2.00	2.36	2.57	3471	8741	1.2	1.1
4-(1H-imidazol-1-yl)-aniline	0.49	6.05	43.80	5.00	8.07	10.81	4067	11628	1.2	1.7
Acebutolol	1.19	13.91	87.70	9.00	8.49	7.42	9286	16772	2.1	1.2
Atenolol	0.16	9.6	84.60	9.00	11.58	12.02	12967	16405	2.2	1.4
Atropine	1.83	9.43	49.80	5.00	12.42	10.87	9344	13277	2.9	1.9
2-Aminoanthracene	3.50	4.32	26.00	3.00	1.06	1.23	9505	5531	1.2	1.1

Table 5.S5 Characteristics and measured data for compounds used for study on Poroshell 120 EC-C18 stationary phase with use 90/10 CO₂/MeOH + 0.1% (v/v) TEA + 0.1% (v/v) TFA and 90/10 CO₂/MeOH + 0.1% (v/v) TEA + 0.1% (v/v) TFA +5.7% (v/v) H₂O mobile phases

Name	^a log Kow	^b pKa	^c PSA, Å ²	^d H _{sum}	^e k	^f k _{wat} er	^g N	^h N _{wate} r	ⁱ A _s	^j A _{swate} r
Suprofen	2.20	3.91	82.60	4.00	0.17	0.21	1376	1809	1.0	1.1
Diphenylacetic acid	3.09	4.72	37.30	3.00	0.19	0.23	1682	2035	1.1	1.1
Fenoprofen	3.10	4.50	46.50	4.00	0.21	0.26	1750	2185	1.1	1.2
1-Naphthylacetic acid	2.24	4.23	37.30	3.00	0.21	0.24	1668	2323	1.2	1.1
Naproxen	3.18	4.15	46.50	4.00	0.22	0.25	1570	2186	1.1	1.1
Flurbiprofen	4.16	4.42	37.30	3.00	0.23	0.28	1803	2309	1.2	1.1
Thymol	3.30	10.60	20.20	2.00	0.16	0.21	1531	2122	1.0	1.0
2-Phenylbenzimidazole	3.24	5.00	28.10	3.00	0.17	0.16	1271	1472	1.1	1.2
5,5-Diphenyl-4-methyl-2-oxazolidinone	1.78	11.87	38.30	4.00	0.2	0.23	1625	2167	1.1	1.1
4-(Diphenylmethyl)-2-oxazolidinone	1.53	12.29	38.30	4.00	0.21	0.24	1519	1851	1.2	1.4
4,5,5-Triphenyl-2-oxazolidinone	2.19	11.07	38.30	4.00	0.28	0.30	2205	2454	1.2	1.1
5,5-Diphenyl-4-benzyl-2-	4.22	11.80	38.30	4.00	0.38	0.39	2671	2963	1.2	1.2

oxazolidino ne										
3- Aminoquino line	1.63	4.98	38.90	4.00	0.18	0.19	1242	1726	1.2	1.2
Nebivolol	4.04	14.29	71.00	8.00	0.18	0.18	1102	1313	1.4	1.3
2,6- Dimethylani line	1.84	3.95	26.00	3.00	0.21	0.29	2171	2696	1.1	1.1
N- allylaniline	2.06	4.04	12.00	2.00	0.24	0.30	2632	2972	1.1	1.1
1,1'- Binaphthyl- 2,2'- diamine	4.06	3.79	52.00	6.00	0.62	0.61	4073	3941	1.5	1.5
2- Aminoanthr acene	3.50	4.32	26.00	3.00	0.73	0.72	4382	4378	1.5	1.4
Triphenyla mine	5.74	-3.04	3.24	1.00	0.94	1.07	6461	6606	1.4	1.4

Table 5.S6 Characteristics and measured data for compounds used for study on Xselect C18 SB stationary phase with use 80/20 CO₂/MeOH + 0.1% (v/v) TEA + 0.1% (v/v) TFA and 80/20 CO₂/MeOH + 0.1% (v/v) TEA + 0.1% (v/v) TFA +5.7% (v/v) H₂O mobile phases

Name	^a log Kow	^b pKa	^c PSA, Å ²	^d H _{sum}	^e k	^f k _{wat} er	^g N	^h N _{water}	ⁱ A _s	^j A _{swat} er
Thymine	-0.62	9.7	58.2	6.00	0.91	1.11	6072	6454	1.1	1.0
Nebivolol	4.04	14.3	71.00	8.00	1.48	1.22	3498	4433	1.1	1.1
Fenoprofen	3.10	4.50	46.50	4.00	0.42	0.66	4572	4496	1.1	1.1
Flurbiprofen	4.16	4.42	37.30	3.00	0.46	0.64	5201	4548	1.1	1.2
Benzoic acid	1.80	4.50	37.30	3.00	0.31	0.50	3076	2837	1.1	1.2
Naproxen	3.18	4.15	46.50	4.00	0.52	0.72	4936	3726	1.1	1.0
Ketoprofen	3.00	4.45	54.40	4.00	0.43	0.63	3974	3601	0.8	1.2
1-Naphthylacetic acid	2.24	4.23	37.30	3.00	0.51	0.72	5447	4336	1.2	1.3
Caffeine	-0.07	14.00	58.40	6.00	1.85	1.88	8622	8009	1.3	1.3
2-Phenylbutyric acid	2.21	4.30	37.30	3.00	0.29	0.47	2204	2235	1.1	1.1
m-Toluic acid	2.37	4.30	37.30	3.00	0.28	0.52	3002	2734	1.2	1.2
Nicotinic acid	0.36	4.75	50.20	4.00	0.62	0.88	1382	1793	1.4	1.0
2-Aminoanthracene	3.50	4.30	26.00	3.00	3.60	3.46	1136 2	8903	1.0	1.0
Thymol	3.30	10.60	20.20	2.00	0.35	0.53	3267	3050	1.2	1.1
Phenol	1.46	10.00	20.20	2.00	0.25	0.48	2539	2697	1.2	1.2
4-Benzyl-5,5-dimethyl-2-oxazolidinone	1.16	12.86	38.30	4.00	0.38	0.61	4124	3542	1.1	1.2

5,5-Diphenyl-4-benzyl-2-oxazolidinone	4.22	11.80	38.30	4.00	0.41	0.65	4236	4137	1.0	1.1
4-(Diphenylmethyl)-2-oxazolidinone	1.53	12.29	38.30	4.00	0.67	0.89	5906	4965	1.1	0.8
N-Benylbenzamide	2.26	14.86	29.10	3.00	0.60	0.76	5460	3290	1.1	1.2
1,1'-Binaphthyl-2,2'-diamine	4.06	3.80	52.00	6.00	2.04	2.09	9010	8642	1.2	1.2
4,5,5-Triphenyl-2-oxazolidinone	2.19	11.07	38.30	4.00	0.67	0.88	6079	5371	1.0	0.8
5,5-Diphenyl-4-methyl-2-oxazolidinone	1.78	11.87	38.30	4.00	0.73	0.91	6420	10372	1.0	1.0
4-Vinylbenzoic acid	2.18	4.20	37.30	3.00	0.34	0.58	3799	3440	1.2	1.2
Theophylline	-0.02	8.81	69.30	7.00	1.20	1.33	7557	7141	1.1	1.1
Imidazole	-0.08	7.00	28.70	3.00	3.92	3.18	4290	4218	1.5	1.2
Nicotinamide	-0.38	3.35	56.00	5.00	2.47	2.31	6286	6383	1.6	1.3
Ibuprofen	3.97	5.3	37.30	3.00	0.34	0.52	2934	2736	1.1	1.2
2,6-Dimethylaniline	1.84	3.95	26.00	3.00	0.60	0.72	7136	4042	1.1	1.3

2-Methylimidazole	0.24	7.90	28.70	3.00	4.04	3.33	3547	4068	2.0	1.4
3-Nitroaniline	1.37	2.47	71.80	6.00	0.66	0.80	6918	1933	1.1	1.0
4-Nitroaniline	1.39	1.01	71.80	6.00	0.81	0.96	7335	9736	1.1	1.1
3-Aminoquinoline	1.63	5.00	38.90	4.00	3.70	3.17	7959	7058	1.2	1.0
Triphenylamine	5.74	-3.04	3.24	1.00	0.76	0.93	9043	8985	1.1	1.1
Metoprolol	1.88	9.70	50.70	6.00	1.49	1.62	3320	3168	1.0	1.0
Propranolol	3.48	9.42	41.50	5.00	2.05	2.02	3763	3792	1.1	1.1
Diphenylacetic acid	3.09	4.70	37.30	3.00	0.41	0.62	3822	3535	1.1	1.2
3-Phenyl-1-propylamine	1.83	10.05	26.02	2.00	1.72	1.51	1020	1171	1.9	1.8
4-Butylbenzylamine	3.42	9.20	26.00	3.00	1.30	1.20	3212	3952	1.0	1.1
Acebutolol	1.19	13.91	87.70	9.00	5.21	3.58	3415	2585	1.2	1.0
N-Allylaniline	2.06	4.00	12.00	2.00	0.37	0.51	3550	3114	1.1	1.2
2-phenylbenzimidazole	3.24	5.00	28.10	3.00	1.60	1.66	5117	4726	1.1	1.0
4-Nitrobenzoic acid	1.89	3.40	83.10	6.00	0.29	0.50	2661	2524	1.2	1.3

Table 5.S7 Characteristics and measured data for compounds used for study on Xselect C18 SB stationary phase with use 90/10 CO₂/MeOH + 0.1% (v/v) TEA + 0.1% (v/v) TFA and 90/10 CO₂/MeOH + 0.1% (v/v) TEA + 0.1% (v/v) TFA + 5.7% (v/v) H₂O mobile phases

Name	^a log Kow	^b pKa	^c PSA, Å ²	^d H _{sum}	^e k	^f k _{water}	^g N	^h N _{water}	ⁱ A _s	^j A _{s water}
Thymine	-0.62	9.7	58.2	6.00	2.50	2.78	7178	6922	1.1	1.0
Nebivolol	4.04	14.3	71.00	8.00	5.71	3.82	3647	4675	1.1	0.9
Fenoprofen	3.10	4.50	46.50	4.00	0.80	0.88	6537	6359	1.1	1.1
Flurbiprofen	4.16	4.42	37.30	3.00	0.87	0.95	7091	6340	1.1	1.1
Benzoic acid	1.80	4.50	37.30	3.00	0.53	0.63	4559	5330	1.1	1.2
Naproxen	3.18	4.15	46.50	4.00	1.05	1.10	7348	6996	1.1	1.1
Ketoprofen	3.00	4.45	54.40	4.00	0.96	1.14	6612	6178	1.1	1.0
1-Naphthylacetic acid	2.24	4.23	37.30	3.00	1.04	1.19	7634	7352	1.1	1.1
Caffeine	-0.07	14.00	58.40	6.00	3.52	2.90	9676	10448	1.3	1.3
2-Phenylbutyric acid	2.21	4.30	37.30	3.00	0.47	0.54	3615	4115	1.1	1.2
m-Toluic acid	2.37	4.30	37.30	3.00	0.50	0.60	5045	5303	1.2	1.3
Nicotinic acid	0.36	4.75	50.20	4.00	1.75	1.74	414	1219	1.5	1.2
2-Aminoanthracene	3.50	4.30	26.00	3.00	8.19	6.49	11997	13467	1.0	1.1
Thymol	3.30	10.60	20.20	2.00	0.63	0.69	5619	5371	1.1	1.2
Phenol	1.46	10.00	20.20	2.00	0.48	0.60	4768	4833	1.1	1.1
4-Benzyl-5,5-dimethyl-2-oxazolidinone	1.16	12.86	38.30	4.00	0.83	0.88	6027	5434	1.1	1.2
5,5-Diphenyl-4-benzyl-2-oxazolidinone	4.22	11.80	38.30	4.00	1.60	1.64	8756	6248	1.1	0.9

4-(Diphenylmethyl)-2-oxazolidinone	1.53	12.29	38.30	4.00	1.49	1.52	7836	3761	1.1	0.9
N-Benylbenzamide	2.26	14.86	29.10	3.00	1.45	1.53	8075	4369	1.1	1.0
1,1'-Binaphthyl-2,2'-diamine	4.06	3.80	52.00	6.00	4.84	3.83	10697	11250	1.2	1.2
4,5,5-Triphenyl-2-oxazolidinone	2.19	11.07	38.30	4.00	1.62	1.66	7824	6826	1.0	1.0
5,5-Diphenyl-4-methyl-2-oxazolidinone	1.78	11.87	38.30	4.00	1.78	1.75	8320	11264	1.1	1.0
4-Vinylbenzoic acid	2.18	4.20	37.30	3.00	0.62	0.77	5697	6177	1.3	1.2
Theophylline	-0.02	8.81	69.30	7.00	2.64	2.53	8753	9663	1.2	1.1
Imidazole	-0.08	7.00	28.70	3.00	15.89	11.16	6432	4963	1.6	1.4
Nicotinamide	-0.38	3.35	56.00	5.00	7.19	5.58	6548	8268	2.1	1.5
Ibuprofen	3.97	5.3	37.30	3.00	0.56	0.58	5075	4886	1.0	1.2
2,6-Dimethylaniline	1.84	3.95	26.00	3.00	0.82	0.70	8254	6556	1.2	1.2
2-Methylimidazole	0.24	7.90	28.70	3.00	18.93	13.50	6158	7355	1.7	1.1
3-Nitroaniline	1.37	2.47	71.80	6.00	1.35	1.21	8773	4819	1.1	1.1
4-Nitroaniline	1.39	1.01	71.80	6.00	2.14	2.09	7896	12050	1.5	1.1
3-Aminoquinoline	1.63	5.00	38.90	4.00	10.69	7.95	9655	9281	1.2	1.0

Triphenylamine	5.74	-3.04	3.24	1.00	0.97	0.79	10027	8350	1.1	1.1
Metoprolol	1.88	9.70	50.70	6.00	5.58	5.98	4405	4497	1.0	0.9
Propranolol	3.48	9.42	41.50	5.00	7.43	6.2	4549	5566	1.1	1.0
Diphenylacetic acid	3.09	4.70	37.30	3.00	0.80	0.90	6758	6092	1.0	1.1
3-Phenyl-1-propylamine	1.83	10.05	26.02	2.00	5.71	4.40	1189	466	1.8	1.6
4-Butylbenzylamine	3.42	9.20	26.00	3.00	4.28	3.22	3683	4780	1.1	1.0
N-Allylaniline	2.06	4.00	12.00	2.00	0.43	0.34	3839	2205	1.2	1.2
2-phenylbenzimidazole	3.24	5.00	28.10	3.00	6.19	6.34	6060	6151	1.1	1.0
4-Nitrobenzoic acid	1.89	3.40	83.10	6.00	0.66	0.73	3347	4396	1.8	1.5

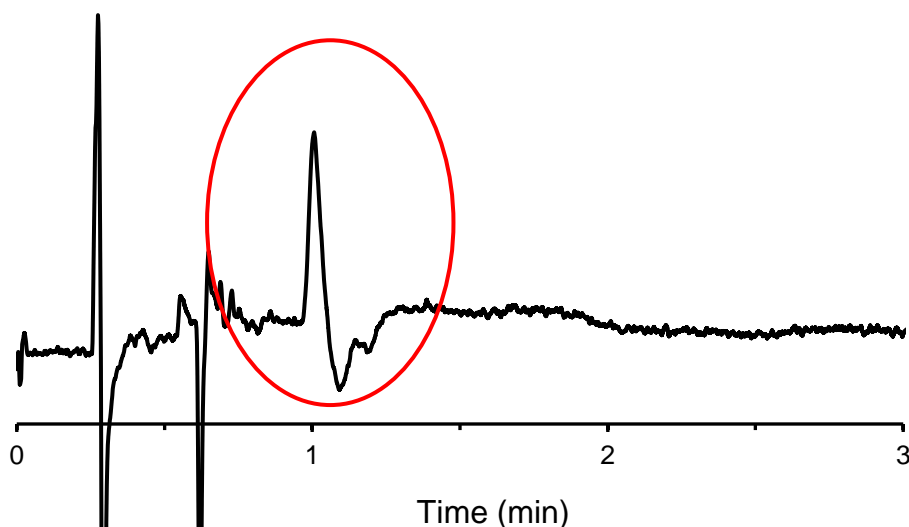


Figure 5.S1: Water disturbance peak for FructoShell-N column. Retention time of water was determined by the procedure in Experimental Section (Section 2.5). The representative disturbance peak was measured at 210 nm wavelength using 10x0.46 cm FructoShell-N column with 80/20 CO₂/MeOH mobile phase and flow rate of 4 mL/min and 8 MPa backpressure. Similar water disturbance peaks were obtained with SilicaShell at 1.87 mins using 10x0.46 cm column with 80/20 CO₂/MeOH mobile phase and flow rate of 4 mL/min and 8 MPa backpressure. Using 10x0.46 cm FructoShell-N, SilicaShell and C18 column with 90/10 CO₂/MeOH mobile phase and flow rate of 4 mL/min and 8 MPa backpressures the retention times were 2.27, 4.99 and 0.31 min. respectively.

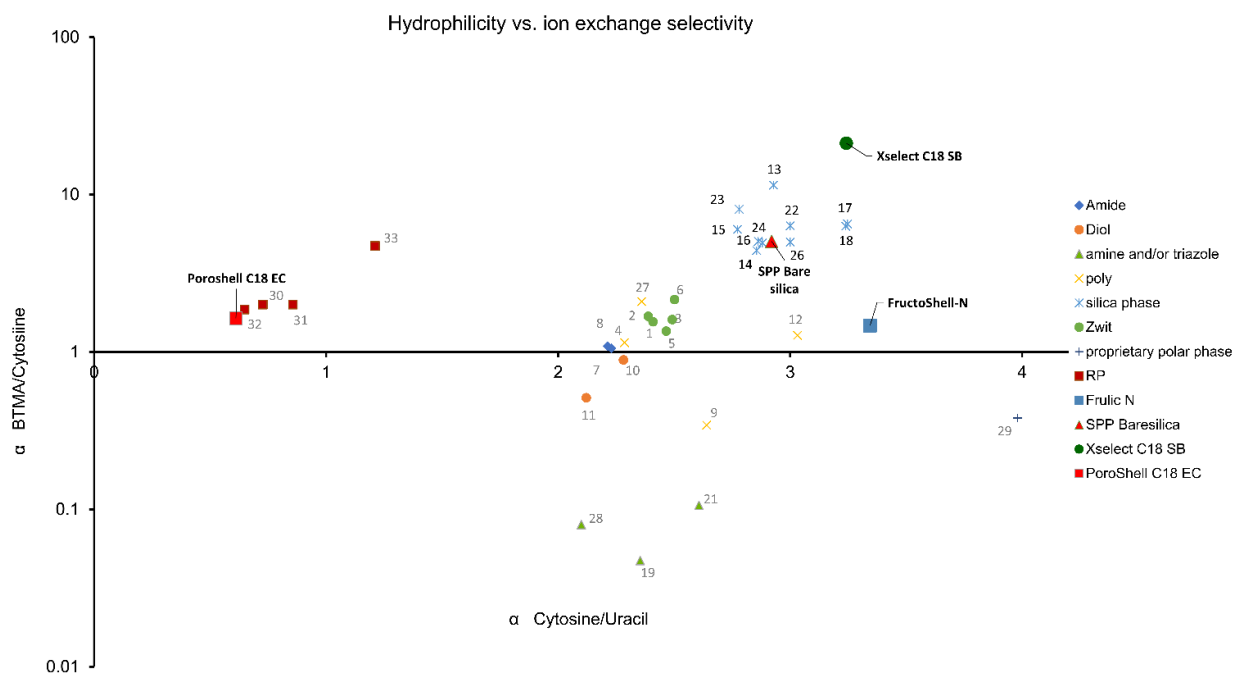


Figure 5.S2 Plot of electrostatic character vs. hydrophilicity character: CF6 – Cylofructan-6 stationary phase (FructoShell-N); Silica- silica stationary phase (SilicaShell); Reversed phase stationary phases (C18) and Xselect C18 SB.

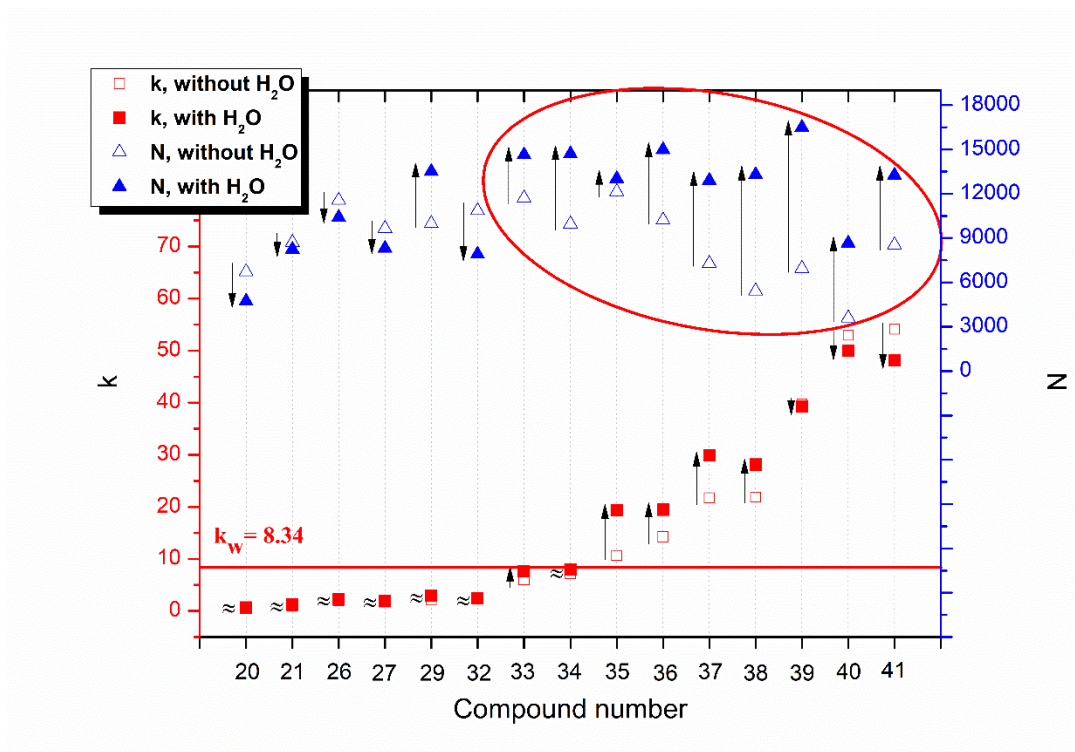


Figure 5.S3. Influence of water on the separation of neutral compounds on FructoShell-N column. Conditions: 90/10 CO₂/MeOH + 0.1% (v/v) TEA + 0.1% (v/v) TFA (empty squares and triangles); 90/10 CO₂/MeOH + 0.1% (v/v) TEA + 0.1% (v/v) TFA + 5.7% (v/v) H₂O (full squares and triangles); flow rate 4 ml/min, back pressure 8 MPa; detection: UV, 220nm.

Compound number as in Table 5.1.

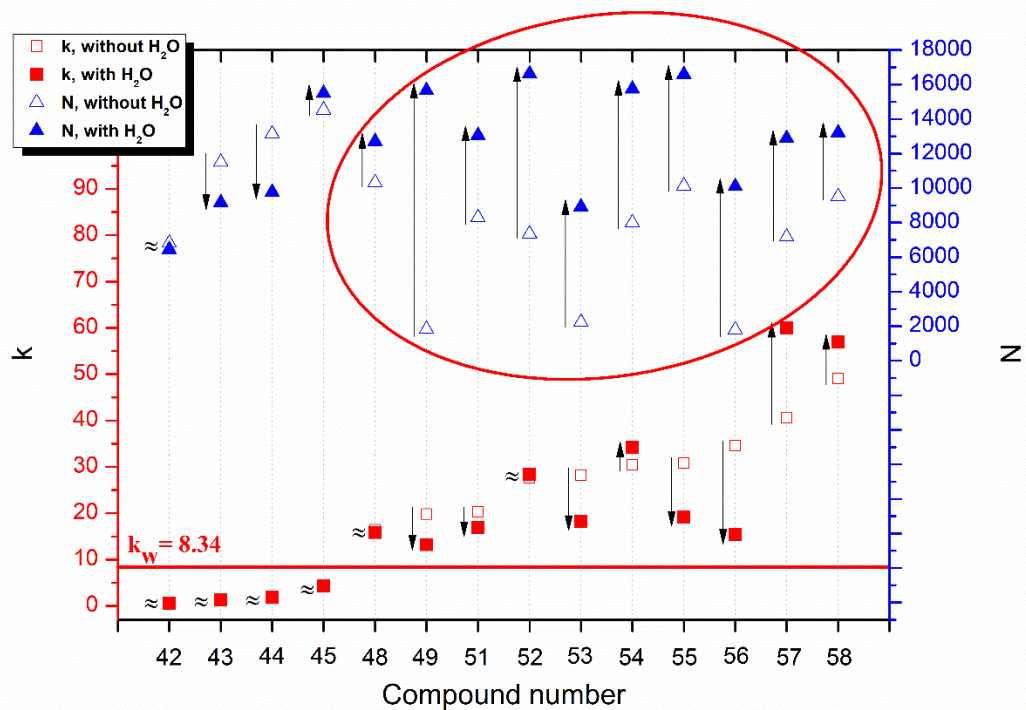


Figure 5.S4. Influence of water on the separation of basic compounds on FructoShell-N column.

Conditions: 90/10 CO₂/MeOH + 0.1% (v/v) TEA + 0.1% (v/v) TFA (empty squares and triangles); 90/10 CO₂/MeOH + 0.1% (v/v) TEA + 0.1% (v/v) TFA + 5.7% (v/v) H₂O (full squares and triangles); flow rate 4 ml/min, back pressure 8 MPa; detection: UV, 220nm.

Compound number as in Table 5.1.

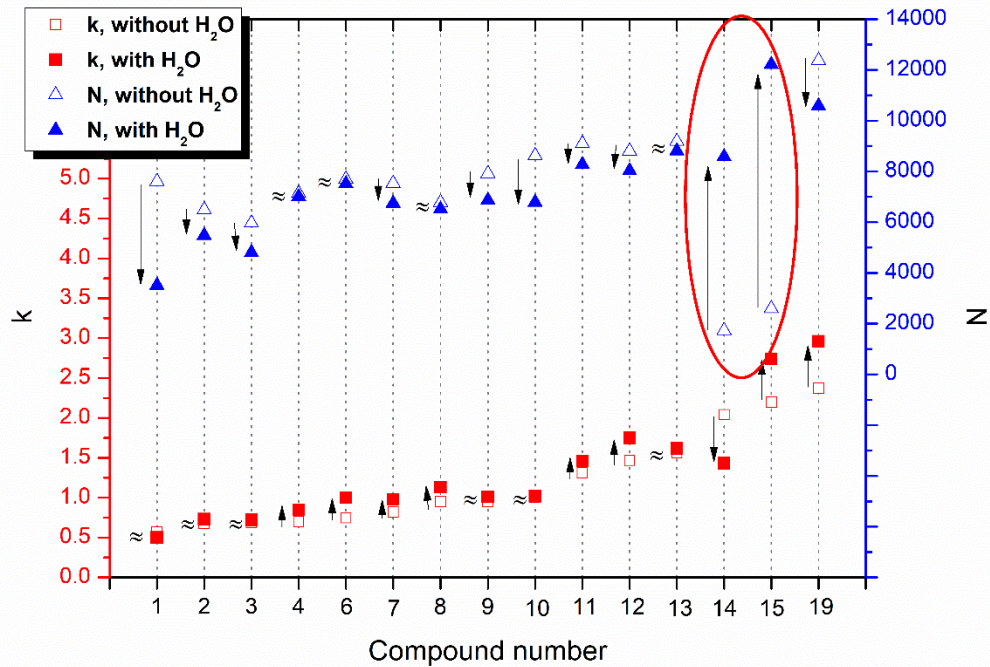


Figure 5.S5. Influence of water on the separation of acidic compounds on FructoShell-N column (2.7 μm particles, 10 x 0.46 cm). Conditions: 90/10 CO_2/MeOH + 0.1% (v/v) TEA + 0.1% (v/v) TFA (empty squares and triangles); 90/10 CO_2/MeOH + 0.1% (v/v) TEA + 0.1% (v/v) TFA + 5.7% (v/v) H_2O (full squares and triangles); flow rate 4 ml/min, back pressure 8 MPa, detection: UV 220nm. Compound number as in Table 5.1.

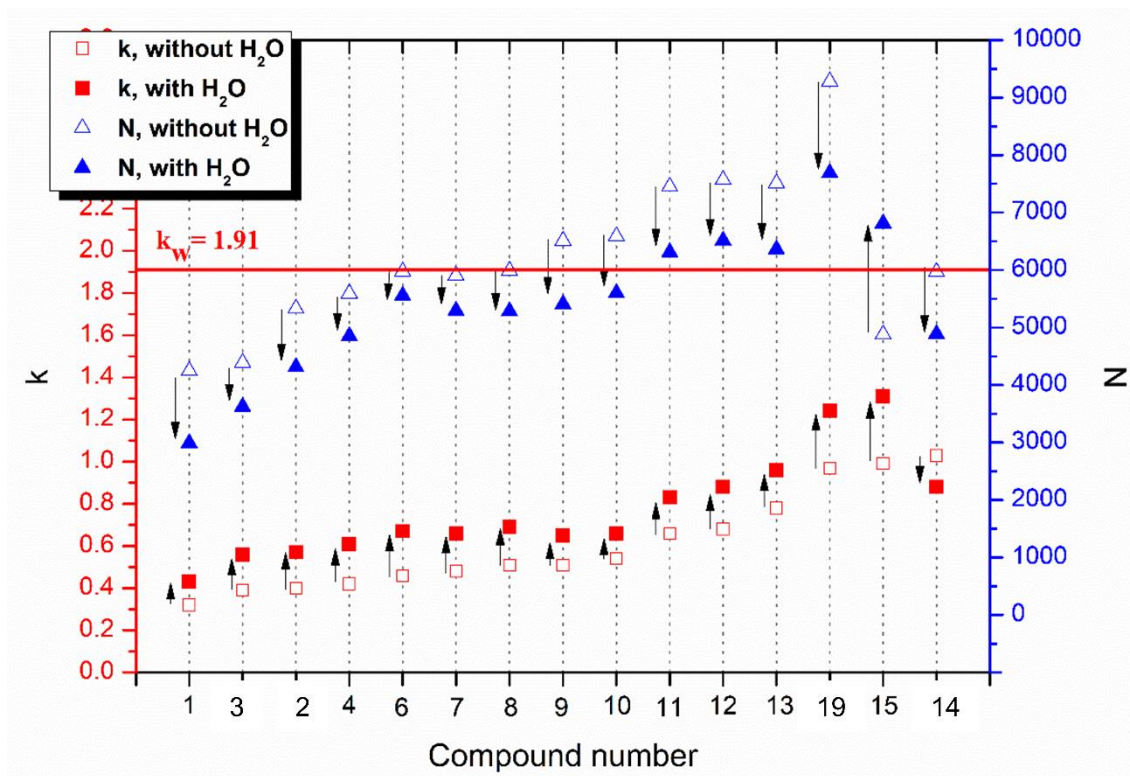
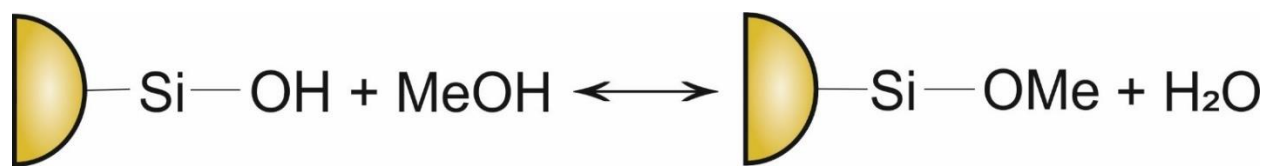
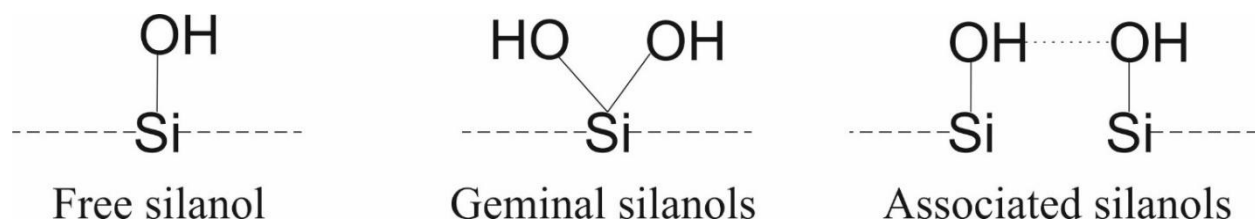


Figure 5.S6. Influence of water on the separation of acidic compounds on FructoShell-N column (2.7 μm particles, 10 x 0.46 cm). Conditions: 80/20 CO_2/MeOH + 0.1% (v/v) TEA + 0.1% (v/v) TFA (empty squares and triangles); 80/20 CO_2/MeOH + 0.1% (v/v) TEA + 0.1% (v/v) TFA + 5.7% (v/v) H_2O (full squares and triangles); flow rate 4 ml/min, back pressure 8 MPa; detection: UV, 220nm. Compound number as in Table 5.1



A)



B)

Figure 5.S7 Formation of silyl ethers on silica surface (A) and types of silanols present on silica surface (B)

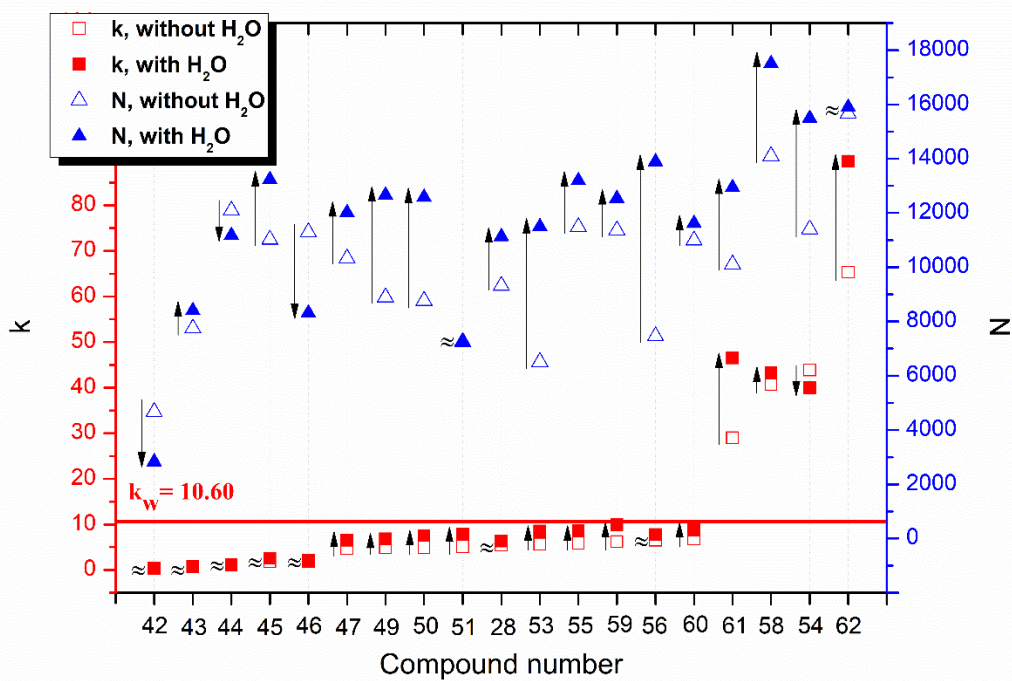


Figure 5.S8 Influence of water on the separation of basic compounds on SilicaShell column.

Conditions: 90/10 CO₂/MeOH + 0.1% (v/v) TEA + 0.1% (v/v) TFA (empty squares and triangles); 90/10 CO₂/MeOH + 0.1% (v/v) TEA + 0.1% (v/v) TFA + 5.7% (v/v) H₂O (full squares and triangles); flow rate 4 ml/min, back pressure 8 MPa; detection: UV, 220nm.

Compound number as in Table 5.1.

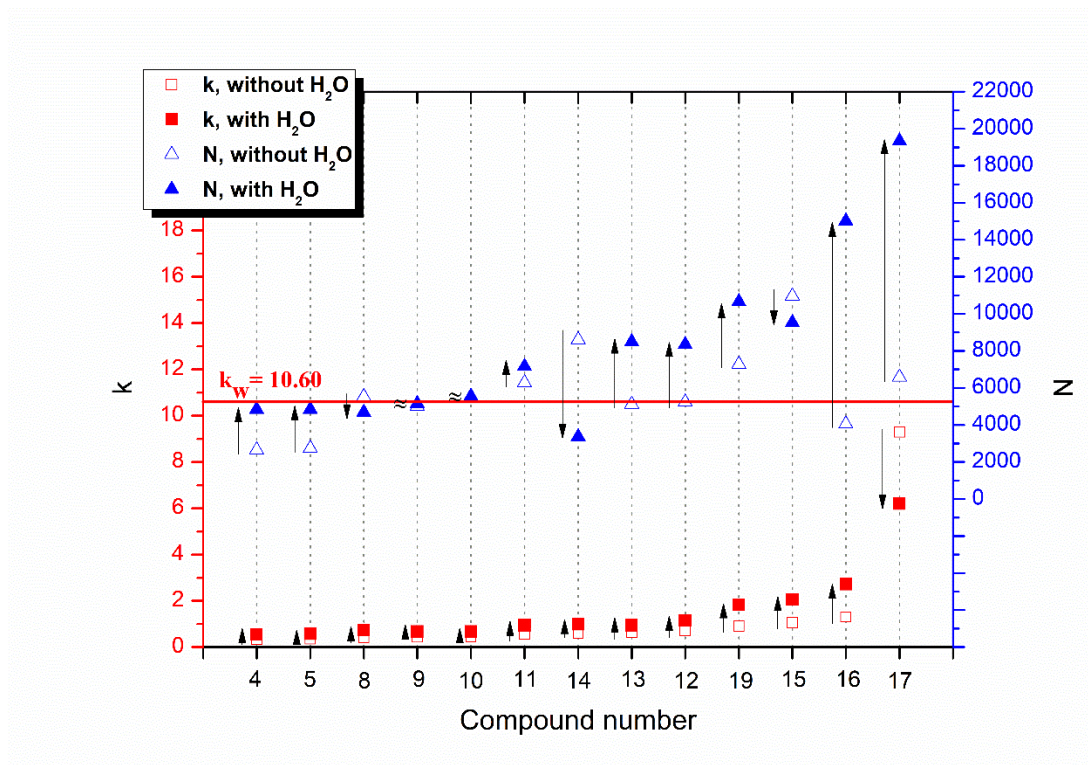


Figure 5.S9 Influence of water on the separation of acidic compounds on SilicaShell column.

Conditions: 90/10 CO₂/MeOH + 0.1% (v/v) TEA + 0.1% (v/v) TFA (empty squares and triangles); 90/10 CO₂/MeOH + 0.1% (v/v) TEA + 0.1% (v/v) TFA + 5.7% (v/v) H₂O (full squares and triangles); flow rate 4 ml/min, back pressure 8 MPa, detection: UV, 220nm.

Compound number as in Table 5.1.

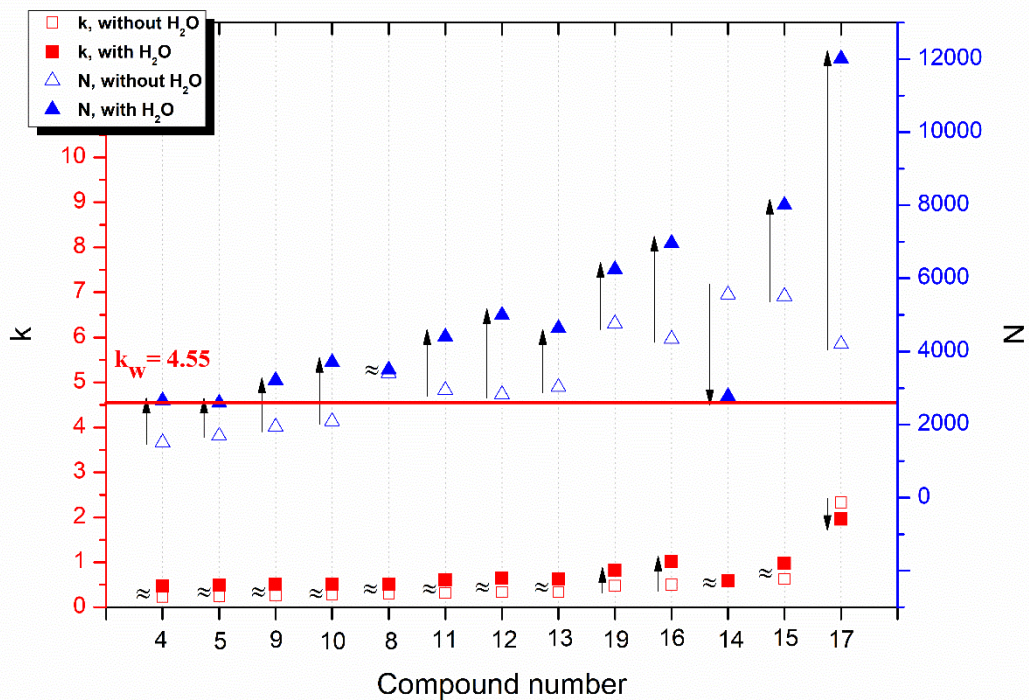


Figure 5.S10 Influence of water on the separation of acidic compounds on SilicaShell column.

Conditions: 80/20 CO₂/MeOH + 0.1% (v/v) TEA + 0.1% (v/v) TFA (empty squares and triangles); 80/20 CO₂/MeOH + 0.1% (v/v) TEA + 0.1% (v/v) TFA + 5.7% (v/v) H₂O (full squares and triangles); flow rate 4 ml/min, back pressure 8 MPa, detection: UV, 220nm.

Compound number as in Table 5.1.

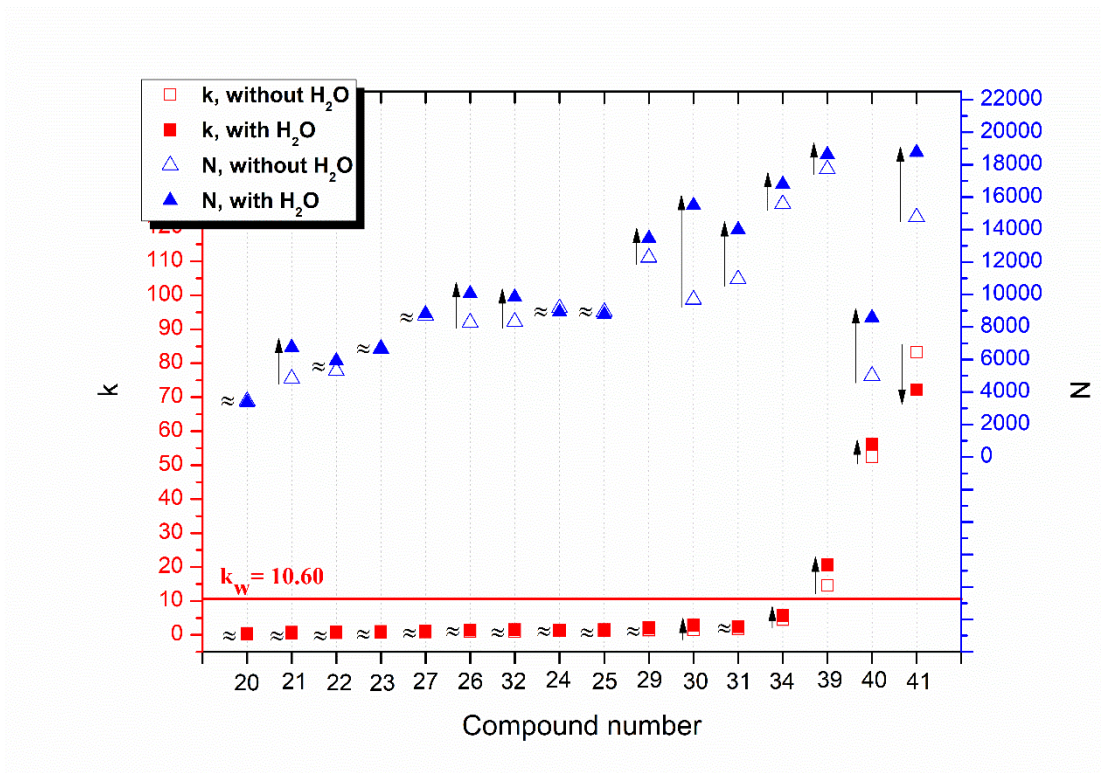


Figure 5.S11 Influence of water on the separation of neutral compounds on SilicaShell column.

Conditions: 90/10 CO₂/MeOH + 0.1% (v/v) TEA + 0.1% (v/v) TFA (empty squares and triangles); 90/10 CO₂/MeOH + 0.1% (v/v) TEA + 0.1% (v/v) TFA + 5.7% (v/v) H₂O (full squares and triangles); flow rate 4 ml/min, back pressure 8 MPa; detection: UV, 220nm.

Compound number as in Table 5.1.

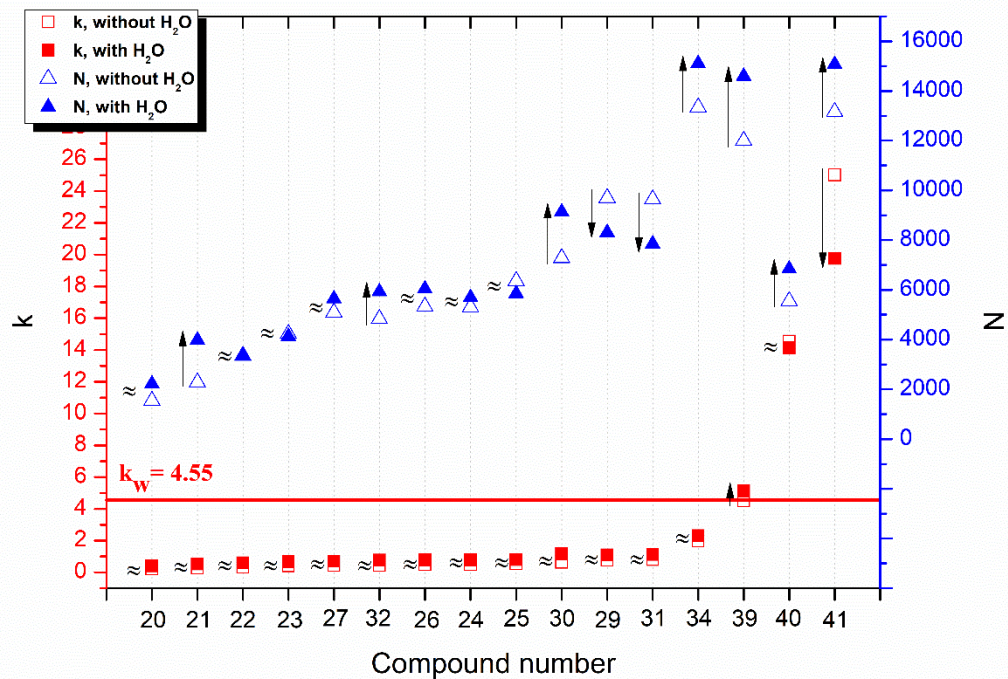


Figure 5.S12 Influence of water on the separation of neutral compounds on SilicaShell column.

Conditions: 80/20 CO₂/MeOH + 0.1% (v/v) TEA + 0.1% (v/v) TFA (empty squares and triangles); 80/20 CO₂/MeOH + 0.1% (v/v) TEA + 0.1% (v/v) TFA + 5.7% (v/v) H₂O (full squares and triangles); flow rate 4 ml/min, back pressure 8 MPa; detection: UV, 220nm.

Compound number as in Table 5.1.

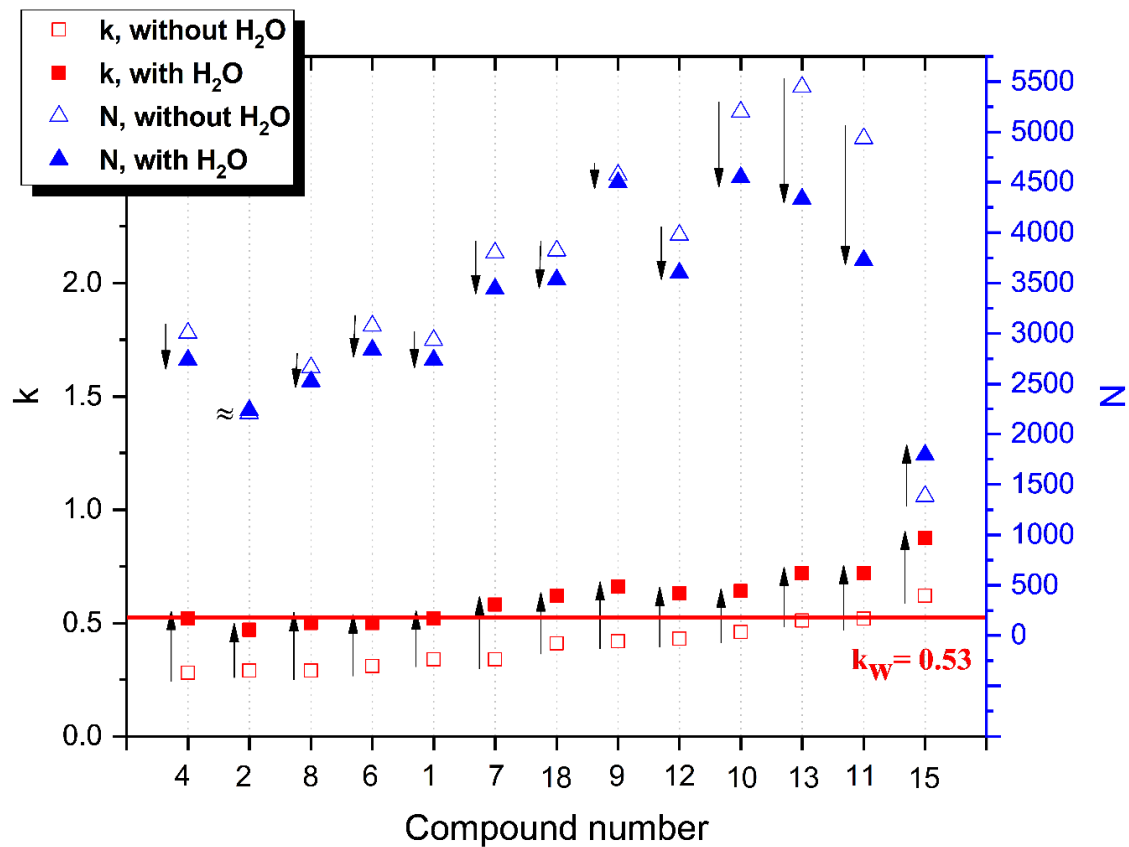


Figure 5.S13. Influence of water on the separation of acidic compounds on Xselect C18 SB column. Conditions: 80/20 CO₂/MeOH + 0.1% (v/v) TEA + 0.1% (v/v) TFA (empty squares and triangles); 80/20 CO₂/MeOH + 0.1% (v/v) TEA + 0.1% (v/v) TFA + 5.7% (v/v) H₂O (full squares and triangles); flow rate 4 ml/min, back pressure 8 MPa; detection: UV, 220nm.

Compound number as in Table 5.1.

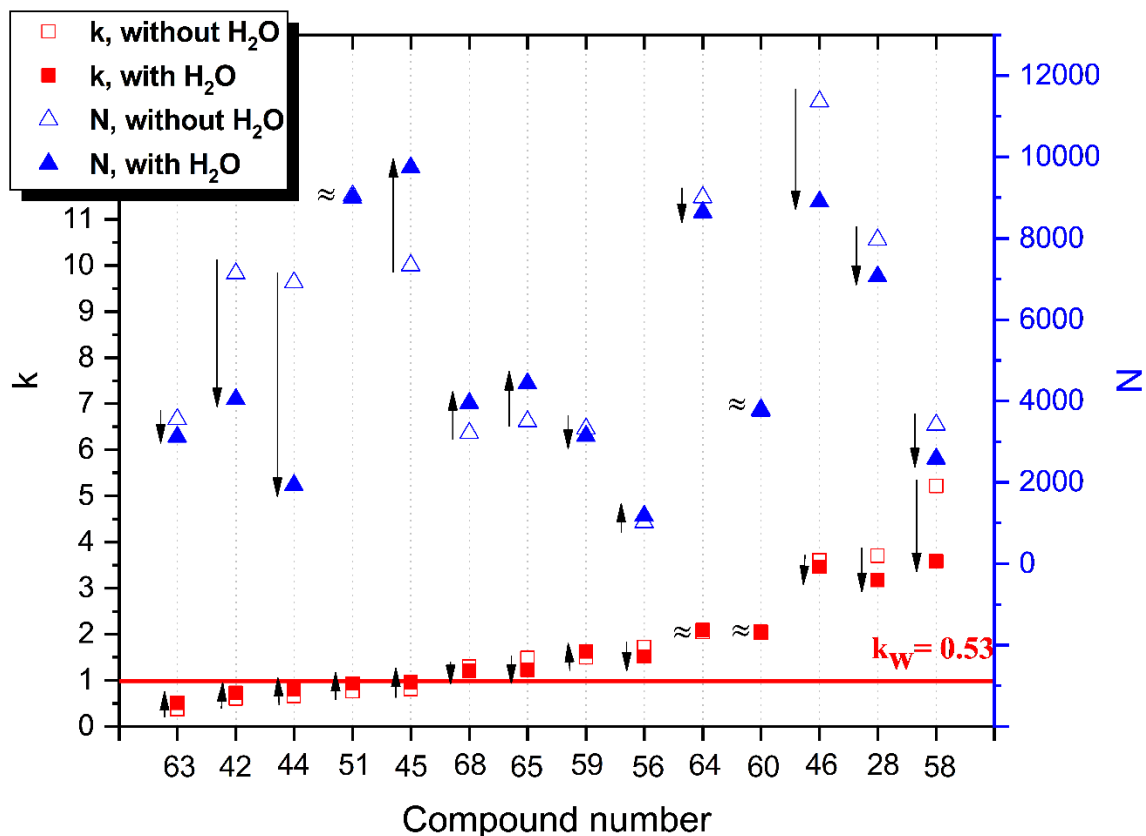


Figure 5.S14. Influence of water on the separation of basic compounds on Xselect C18 SB column. Conditions: 80/20 CO₂/MeOH + 0.1% (v/v) TEA + 0.1% (v/v) TFA (empty squares and triangles); 80/20 CO₂/MeOH + 0.1% (v/v) TEA + 0.1% (v/v) TFA + 5.7% (v/v) H₂O (full squares and triangles); flow rate 4 ml/min, back pressure 8 MPa; detection: UV, 220nm. Compound number as in Table 5.1.

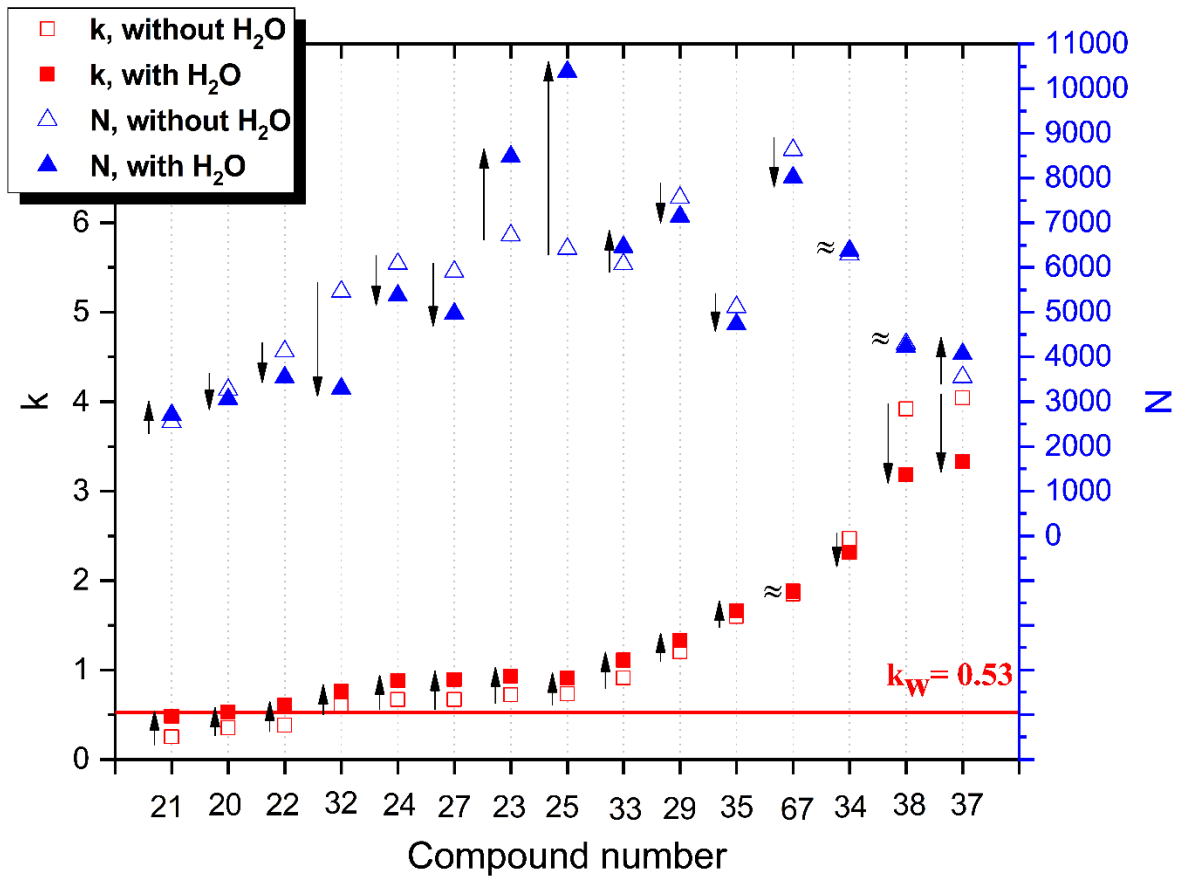


Figure 5.S15 Influence of water on the separation of neutral compounds on Xselect C18 SB column. Conditions: 80/20 CO₂/MeOH + 0.1% (v/v) TEA + 0.1% (v/v) TFA (empty squares and triangles); 80/20 CO₂/MeOH + 0.1% (v/v) TEA + 0.1% (v/v) TFA + 5.7% (v/v) H₂O (full squares and triangles); flow rate 4 ml/min, back pressure 8 MPa; detection: UV, 220nm. Compound number as in Table 5.1.

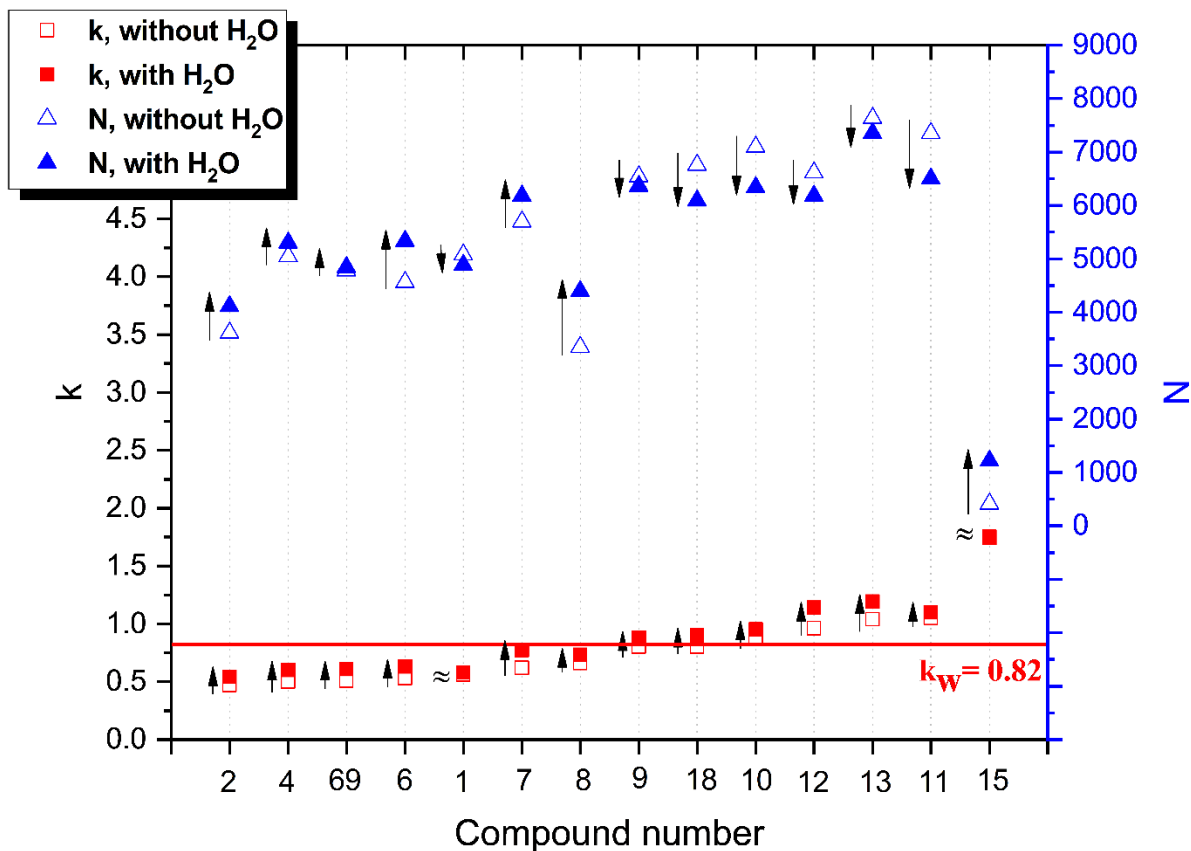


Figure 5.S16. Influence of water on the separation of acidic compounds on Xselect C18 SB column. Conditions: 90/10 CO₂/MeOH + 0.1% (v/v) TEA + 0.1% (v/v) TFA (empty squares and triangles); 90/10 CO₂/MeOH + 0.1% (v/v) TEA + 0.1% (v/v) TFA + 5.7% (v/v) H₂O (full squares and triangles); flow rate 4 ml/min, back pressure 8 MPa; detection: UV, 220nm. Compound number as in Table 5.1.

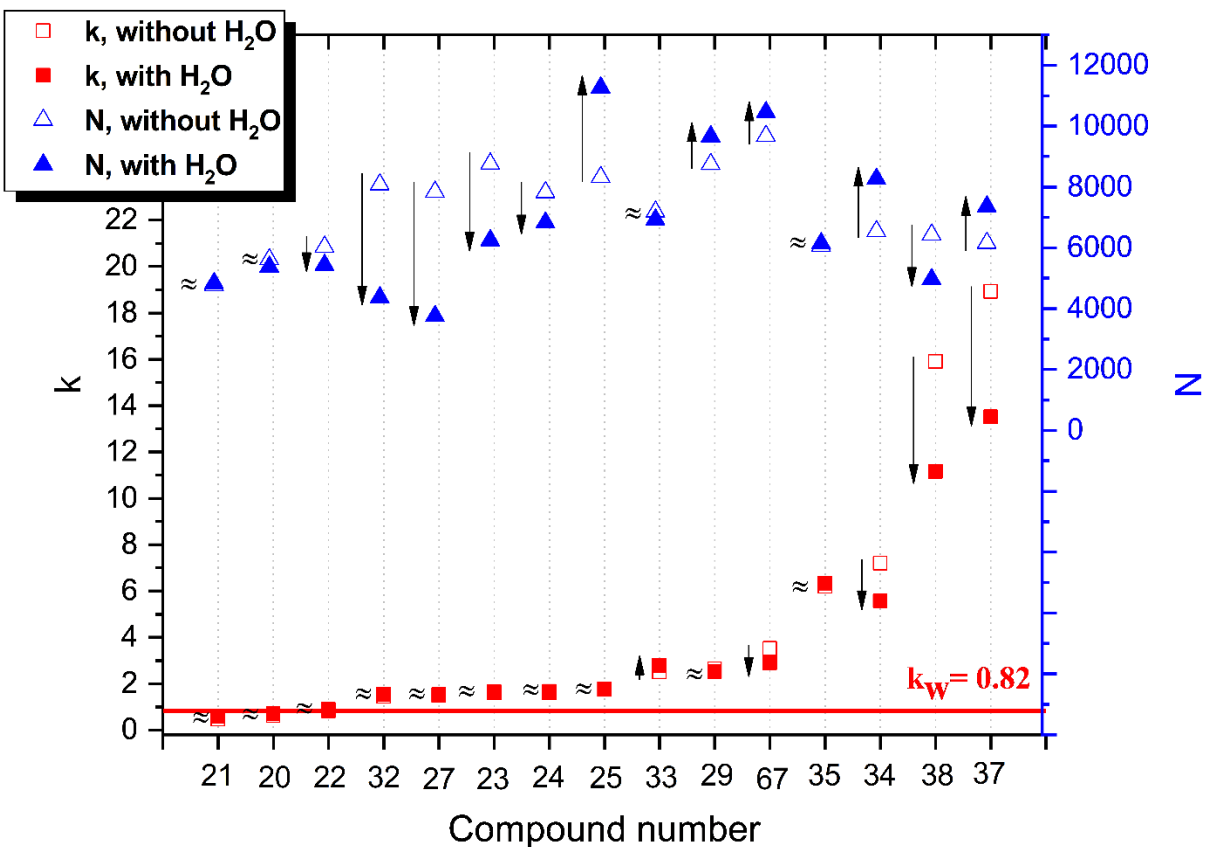


Figure 5.S17. Influence of water on the separation of neutral compounds on Xselect C18 SB column. Conditions: 90/10 CO₂/MeOH + 0.1% (v/v) TEA + 0.1% (v/v) TFA (empty squares and triangles); 90/10 CO₂/MeOH + 0.1% (v/v) TEA + 0.1% (v/v) TFA + 5.7% (v/v) H₂O (full squares and triangles); flow rate 4 ml/min, back pressure 8 MPa; detection: UV, 220nm. Compound number as in Table 5.1.

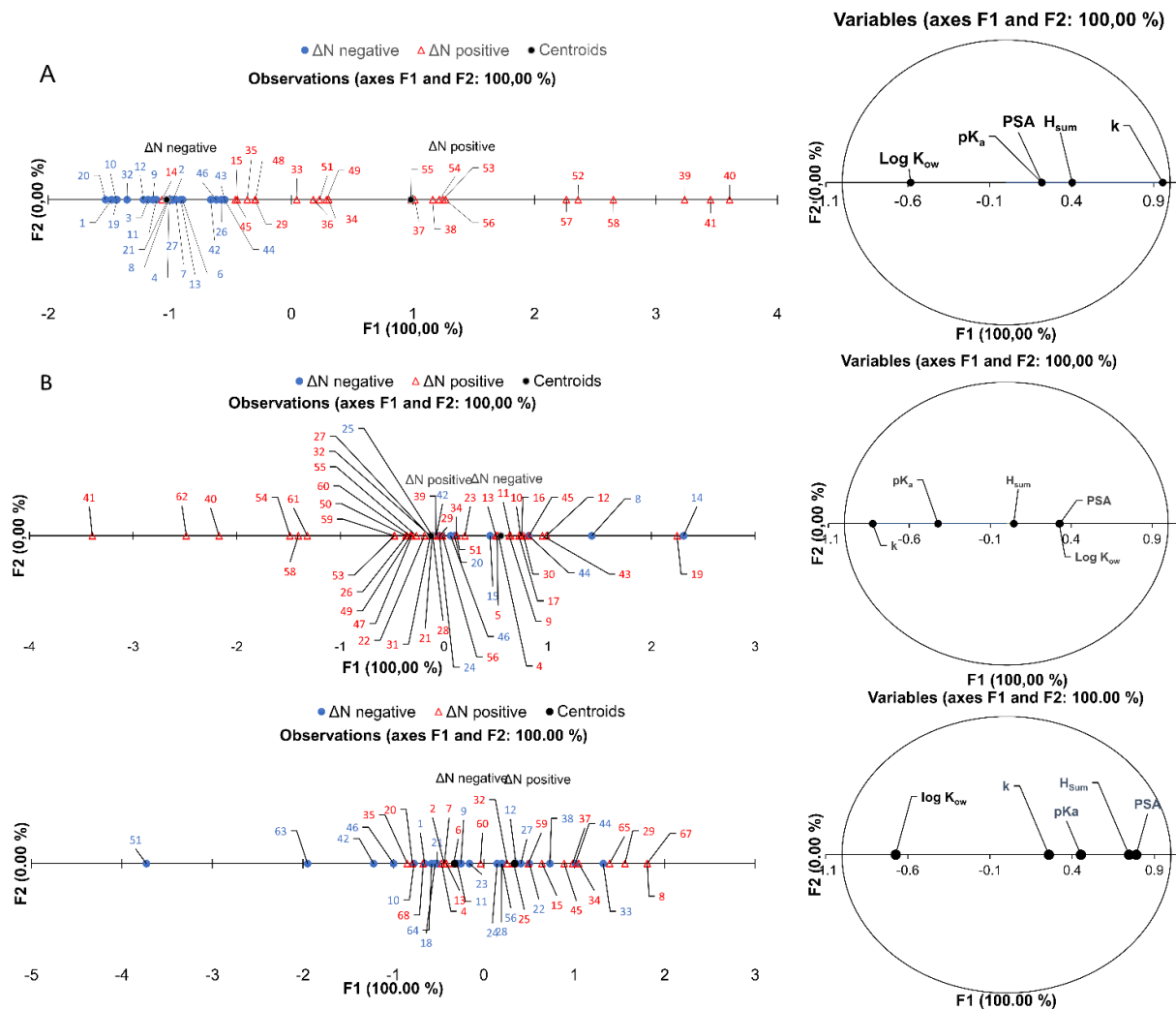


Figure 5.S18 Discriminant analysis for FructoShell-N column with use of 90/10 CO₂/MeOH + 0.1% (v/v) TEA + 0.1% (v/v) TFA without and with addition of 5.7% (v/v) H₂O (A); SilicaShell column with use of 90/10 CO₂/MeOH + 0.1% (v/v) TEA + 0.1% (v/v) TFA without and with addition of 5.7% (v/v) H₂O (B); Xselect C18 SB column with use of 90/10 CO₂/MeOH + 0.1% (v/v) TEA + 0.1% (v/v) TFA without and with addition of 5.7% (v/v) H₂O (C)

Chapter 6

Effective methodologies for enantiomeric separations of 150 pharmacology and toxicology related 1°, 2°, and 3° amines with core-shell chiral stationary phases

6.1 Abstract

Core-shell particles (superficially porous particles, SPPs) have been proven to provide high-throughput and effective separations of a variety of chiral molecules. However, due to their limited commercialization, many separations have not been reported with these stationary phases. In this study, four SPP chiral stationary phases (CSPs) were utilized for the enantiomeric separation of 150 chiral amines. These amines encompass a variety of structural and drug classes, which are particularly important to the pharmaceutical industry and in forensics. This comprehensive evaluation demonstrates the power of these CSPs and the ease of method development and optimization. The CSPs used in this study included the macro-cyclic glycopeptide-based CSPs (VancoShell and NicoShell), the cyclodextrin-based CSP (CDShell-RSP), and the cyclofructan-based CSP (LarihcShell-P). These CSPs offered versatility for a variety of applications and worked in a complementary fashion to baseline separate all 150 amines. The LarihcShell-P was highly effective for separating primary amines. VancoShell, NicoShell, and CDShellRSP were useful for separating all types of amines. These CSPs are multi-modal and can be utilized with mass spectrometry compatible solvents. Eighteen racemic controlled substances were simultaneously baseline separated in a single liquid chromatography–mass spectrometry (LC–MS) analysis. Details in high-performance liquid chromatography (HPLC) parameters will be discussed as well as the improved chromatographic performance afforded by the SPP CSPs.

6.2 Introduction

In 2017, the Food and Drug Administration (FDA) approved 22 small molecules as new molecular entities. In comparison to the last five years (2012-2016), the percentage of amines approved increased from 70% to 77%, and the percentage of chiral compounds and chiral amines remained constant at 59% and 40%, respectively [1]. Since enantiomers may possess different biological activity, chiral separation methods of amines have become routine and important for chiral pharmaceutical analysis. The FDA states that “the pharmacology and toxicology of the enantiomer should be characterized for the principal effects and any other pharmacological effect, with respect to potency, specificity, maximum effect, etc.” In some racemic mixtures, one of the enantiomers is inactive or contributes very little pharmacologically or in opposition compared to the other enantiomer [2]. In the pharmaceutical industry from 1994 to 2011, 15 “chiral switches” were made due to the inactivity of one enantiomer [2]. Additionally, some compounds have more than one set of enantiomers, which further complicates their therapeutic use. One example is ephedrine, which has two chiral centers and is used as a vasopressor. However, its diastereomer, pseudoephedrine, acts oppositely and is used as a vasoconstrictor. Also, ephedrine and pseudoephedrine are both precursors to methamphetamine [3]. Depending on which diastereomer is used, different enantiomeric compositions of methamphetamine are obtained, which is used in forensics to trace the origin of the substance if it is under investigation for illicit use [3]. Of course, the isomeric ratio of ephedrine and pseudoephedrine cannot be determined by mass spectrometry (MS) unless they are chromatographically separated because they have the same m/z [3,4].

According to the 2017 DEA Orangebook, over 70% of scheduled controlled substances are amines, including catecholamines, cathinones, and substituted amphetamines [5]. Also, over 50% and 40% are chiral compounds and chiral amines, respectively [5]. According to the DEA Orangebook list I regulated chemicals, ~40% of the precursors to controlled substances are amines [5]. Also, 37%

are chiral, and only one of the chiral chemicals is not an amine [5]. In addition, there are new designer drugs that have been derived from regulated substances to avert detection [3]. One of the most common techniques used by forensics is MS because it accurately provides sensitive identification and quantitation of target compounds in complex samples. Most reported analyses for designer drugs rely on gas chromatography (GC), which is not suited for biological analysis of nonvolatile or thermally liable samples. Liquid chromatography (LC) would be preferable for metabolic, pharmacokinetic, and pharmacodynamic studies. Also, LC can be performed at preparative scales to obtain large amounts of individual enantiomers and assess their pharmacological properties. This approach might be particularly useful for the investigation of new chiral controlled substances and designer drugs and their metabolites.

Some commercial CSPs have solvent limitations, where the optimized mobile phase is not MS compatible. Recently, isopropyl cyclofructan-6 bonded to superficially porous particles (SPPs) was shown to provide faster and higher efficiency separations, while maintaining selectively (α) at much higher flow rates in comparison to its analogous fully porous particles (FPPs) CSP [6]. The speed of chromatographic separation with SPP CSPs compared to FPP CSPs has advanced from minutes to seconds [7-8]. Merck researchers have demonstrated the power of a SPP teicoplanin CSP with highthroughput screening, estimating that over 1000 samples could be tested for enantiomeric excess within a single workday [9].

Macrocyclic glycopeptides, cyclodextrins, and cyclofructans have been investigated to achieve higher selectivities for difficult and important chiral separations [10-18]. However, few comprehensive studies, especially for controlled substances, have been performed using these chiral selectors bonded to SPPs [19-26]. The results of this study highlight new and highly improved separations of 150 chiral primary (1°), secondary (2°), and tertiary (3°) amines with

three SPP-bonded derivatized chiral selectors (hydroxypropyl β -cyclodextrin, isopropyl cyclofructan-6-P, and a modified macrocyclic glycopeptide) and one native SPP-bonded chiral selector (vancomycin). Focus was paid to the “principle of complementary separations,” which states that a partial separation with one chiral selector can be brought to baseline with one of the other related selectors [27-28]. This characteristic provides a high likelihood of baseline separating any structure within a given class of compounds. In this study, the focus is on pharmaceuticals, stimulants, and related compounds. These chiral selectors are multi-modal, so they offer ease of optimization and perform well in MS compatible solvents, which would be useful for biological and forensic analyses.

6.3 Experimental

6.3.1 Chemicals and materials

Native vancomycin (VancoShell, VS), modified macrocyclic glycopeptide (NicoShell, NS), hydroxypropyl- β -cyclodextrin (CDShell-RSP, RSP), and isopropyl-cyclofructan (LarihcShell-P, LS-P) chiral selectors were bonded to 2.7 μm SPP and obtained from AZYP, LLC. (Arlington, TX, USA) [1820]. Analytes were purchased as racemic standards or individual enantiomer standards (then mixed to form racemates) from Cerilliant Corporation (Round Rock, TX, USA), Sigma-Aldrich (St. Louis, MO, USA), and LKT Laboratories Inc (Minneapolis, MN, USA). Racemic standards were prepared in methanol (MeOH) at 1 mg/mL for analysis. Solvents and additives including HPLC grade acetonitrile (ACN), ethanol (EtOH), MeOH, hexane (Hex), heptane (Hep), trifluoroacetic acid (TFA), acetic acid (AA), ammonium hydroxide (NH_4OH), trimethylamine (TEA), formic acid (FA), ammonium acetate ($\text{NH}_4\text{CH}_3\text{CO}_2$), ammonium formate (NH_4HCO_2), and ammonium trifluoroacetate (NH_4TFA) were obtained from Sigma-Aldrich (St.

Louis, MO, USA). Water was purified by a Milli-Q water purification system (Millipore, Billerica, MA, USA).

6.3.2 Chromatographic conditions

An Agilent 1260 (Agilent Technologies, Palo Alto, CA, USA) HPLC was used. It consisted of a 1200 diode array detector, autosampler, and quaternary pump. The mass spectrometer used in this study was a Shimadzu triple quadrupole LC-MS instrument, LCMS-8040, (Shimadzu, Tokyo, Japan). All MS was operated in positive ion mode with an electron spray ionization source. The parameters were set as follows: nebulizer gas flow, 3 L/min; drying gas flow, 15 L/min; desolvation line temperature, 250 °C; heat block temperature, 400 °C. Multiple UV wavelengths of 220, 230, and 254 nm were utilized for detection and identification of enantiomers. All separations were carried out at room temperature, unless otherwise noted, using an isocratic method. Mobile phases were degassed by ultrasonication under vacuum for 5 minutes. Each analyte was screened and optimized as described in section 3.1.

When distinguishing the following mobile phases, the letters in parenthesis refer to the ratio changes in parenthesis. For example, 1(a,b): MeOH-NH₄TFA (100:(0.1,0.025), v/w) means 1a corresponds to MeOH-NH₄TFA (100:0.1, v/w) while 1b is MeOH-NH₄TFA (100:0.025, v/w). If the pH is given, it is the pH of the aqueous buffer prior to mixing with organic modifier. The optimized mobile phase conditions referring to Tables 1-3 were as follows: 1(a,b): MeOH-NH₄TFA (100:(0.1,0.025), v/w), 2(a,b,c): MeOHNH₄HCO₂ (100:(0.2,0.5,0.1), v/w), 3(a,b): MeOH-AA-TEA (100:(0.2:0.1,0.1:0.05), v/v/v), 3(c,d,e): MeOH-AA-NH₄OH (100:(0.2:0.05,0.1:0.02,0.3:0.05), v/v/v), 4(a,b,c,d,e,f,g): ACN-MeOH-AA-TEA ((60:40,50:50,30:70,10:90,70:30,80:20,95:5):0.3:0.2, v/v/v/v), 4(g): ACN-MeOH-TFA-TEA (90:10:0.3:0.2, v/v/v/v), 5(a,b,c,d,e,f): ACN-NH₄HCO₂ (pH 3.6; 16 mM)

((30:70,25:75,20:80,15:85,10:90,5:95), v/v), 5(g,h,i,j): ACN-NH₄HCO₂ (pH 3.6; 48 mM) ((20:80,15:85,10:90,5:95), v/v), 5(k): ACN-NH₄HCO₂ (pH 3.6; 80 mM) (5:95, v/v), 6(a,b,c): MeOH-NH₄HCO₂ (pH 3.6; 16 mM) ((90:10,80:20,30:70), v/v), 6(d,e): MeOH-NH₄HCO₂ (pH 3.6; 48 mM) ((90:10,30:70), v/v), 6(f): MeOH-NH₄HCO₂ (pH 6.0; 16 mM) (35:65, v/v), 6(g): MeOH-NH₄HCO₂ (pH 5.0; 16 mM) (30:70, v/v), 7(a,b): EtOH-NH₄HCO₂ (pH 3.6; 16 mM) ((95:5,90:10), v/v), 8(a,b): Hex-EtOH-TFA-TEA ((70:30,80:20):0.3:0.2, v/v/v/v), 9(a,b): Hep-EtOH-TFA-TEA ((95:5,90:10):0.3:0.2, v/v/v/v).

6.3.3 Sample categorization

In *Tables 6.1-6.3*, the 150 amines are classified by their type; 1°, 2°, or 3°, then categorized into one of the following classes: pharmaceuticals, stimulants, reagents, or amino acids and derivatives (listed alphabetically). Pharmaceuticals were distinguished based on their pharmacological effects. Stimulants were defined as any amine that increases the functional activity of an organism, such as α - and β adrenergic agonists (AAA, BAA), analgesics (ANA), antidepressants (AD), antiparasitics (AP), catecholamines (CAT), and tobacco-related compounds (TOB). Additionally, if stimulants were classified in the DEA Orangebook by a class scheduling action number (CSA #) or regulated chemical list number (RC #), they were labeled as such [5]. One non-stimulant (NS) was included with the stimulants due to its similarity in structure to amphetamine. Pharmaceuticals included α -, β -, calcium channel, and sodium channel blockers (AB, BB, CCB, SCB), anesthetics (ANE), antibiotics (ABIO), antimuscarinics (AM), antipsychotics (APC), diuretics (DIU), and hormones (HOR).

Table 6.1 Optimized chiral separations of primary (1°) amines.

a) Pharmaceuticals							
Name ¹	Class ²	CSP ³	MP ⁴	F(T) ⁵	k_1^{6a}	α^{6b}	R_s^{6c}
Amlodipine	CCB	LS-P	4g	0.7	2.7	1.09	1.9
		NS	3c	1.0	7.7	1.09	1.7
		RSP*	5e	1.0	3.1	1.10	1.5
		VS	4a	1.0	7.6	1.11	2.0
Mexitilane	SCB	LS-P	4g	1.0	7.5	1.08	1.5
		VS**	3c	0.5	1.1	1.10	2.0
Thyroxine	HOR	LS-P	4g	1.0	2.3	1.21	2.8
b) Stimulants							
Name ¹	Class ²	CSP ³	MP ⁴	F(T) ⁵	k_1^{6a}	α^{6b}	R_s^{6c}
3,4-methylenedioxyamphetamine (MDA)	CSA I	LS-P***	4g	1.0	3.1	1.06	1.7
		RSP*	5e	0.5	2.2	1.07	1.6
		VS**	7a	0.4	5.1	1.08	1.5
Amphetamine	CSA II	LS-P****	4g	0.3	5.5	1.05	1.5
		NS*****	3c	0.3	2.9	1.05	1.5

		RSP*	5f	0.5(45)	2.4	1.08	1.5
		VS	1a	1.0	1.1	1.18	2.5
Aminorex	CSA I	NS	3c	0.5	4.6	1.06	1.5
		RSP*	5d	1.0	1.7	1.10	2.2
		VS	3c	0.7	2.6	1.10	2.0
Methoxamine	AAA	LS-P**	4e	0.5	3.7	1.06	1.5
		NS	4a	1.0	7.0	1.12	2.2
		RSP	5e	1.0	0.9	1.42	3.6
		VS	4a	0.5	3.2	1.10	1.5
Midodrine	AAA	LS-P*	4g	0.5	7.7	1.07	1.5
		NS	3c	1.0	5.2	1.23	2.9
Norepinephrine (Arterenol)	CAT	LS-P	4g	1.0(45)	3.7	1.13	2.4
Normetanephrine	CAT	LS-P	4a	1.0	3.5	1.14	2.9
		NS	3c	1.0	4.0	1.10	2.0
Norphenylephrine (3-octopamine)	CAT	LS-P	4a	1.0	3.3	1.14	2.8
		VS**	8a	0.5	11.5	1.05	1.5

Octopamine	CAT	LS-P	4a	1.0	3.2	1.13	2.1
		NS	3c	1.0	5.8	1.08	1.8
p-methoxyamphetamine (PMA)	CSA I	LS-P	4g	0.3	2.6	1.05	1.5
		RSP*	5d	0.5(45)	2.2	1.06	1.5
		VS	1a	0.6	1.0	1.17	2.5
p-chloroamphetamine (PCA)	NS	LS-P***	4g	0.3	2.7	1.05	1.5
		RSP*	5d	0.5	2.3	1.06	1.5
Phenylpropanolamine (Norephedrine)	RC I	LS-P	4a	0.8	2.4	1.10	2.0
		NS	4a	0.7	3.6	1.08	1.5
Tranlycypromine	AD	LS-P**	4g	1.0	5.5	1.06	1.5
		NS	3e	1.0(10)	5.0	1.12	2.0
		RSP*	5e	1.0	1.6	1.13	2.8
		VS	6a	0.5(30)	1.5	1.15	2.5
4-hydroxynorephedrine	CAT	LS-P	4a	0.5	2.4	1.09	1.9
		NS	8a	1.0	5.8	1.25	1.5
β-keto-amphetamine (Cathinone)	CSA I	LS-P	8b	1.0	6.0	1.12	2.3

		NS	2b	2.0(45)	1.4	1.44	4.5
		RSP*	5k	0.7	2.2	1.10	2.4
		VS	1a	1.0(15)	1.0	1.22	2.6
c) Reagents							
Name ¹	CSP ³	MP ⁴	F(T) ⁵	k ₁ ^{6a}	α ^{6b}	R _s ^{6c}	
1-(1,1-biphenyl-4-yl) ethanamine	LS-P	4g	1.0	2.4	1.14	2.6	
	NS*	4a	1.0	7.4	1.12	2.5	
	VS	1a	1.0	0.8	1.24	2.6	
1-(1-naphthyl) ethylamine	LS-P	4a	1.0	1.6	1.18	3.3	
	NS	2a	1.0	1.9	1.21	3.2	
	VS	1a	1.0	1.1	1.21	2.8	
1-(2-naphthyl) ethylamine	LS-P	4a	1.0	2.3	1.14	2.9	
1-(4-chlorophenyl) ethylamine	LS-P	4g	1.0	2.9	1.13	2.6	
	VS	3c	0.5	2.1	1.09	1.8	
1-(4-methylphenyl)ethylamine	LS-P	4a	1.0	2.1	1.13	2.3	
	NS*	4a	1.0	5.8	1.08	2.5	

	VS	3c	1.0	1.4	1.15	2.4
1,1-diphenyl-2-amino-propane	LS-P	4g	1.0	0.8	1.14	2.0
	VS	1a	1.0	0.9	1.30	3.3
1,1-diphenyl-fluoro-2-aminopropane	LS-P**	9b	0.5	5.1	1.06	1.8
	RSP	5a	1.0	1.5	1.14	2.1
	VS	1a	1.0	0.5	1.39	3.2
1,2,2-triphenylethylamine	LS-P	4g	1.0	0.6	1.25	2.8
	NS***	3c	0.3	1.3	1.07	1.5
	VS	1a	1.0	0.6	1.45	3.9
1,2,3,4-tetrahydro-1-naphthylamine	LS-P	4a	1.0	1.8	1.17	2.8
	NS*	3c	0.5	2.9	1.08	1.9
	RSP***	5f	0.3(5)	1.1	1.05	1.5
	VS	1a	1.0	0.8	1.50	4.5
1,2-methoxyphenylethanamine	LS-P	4g	1.0	1.2	1.25	3.9
	NS	3c	1.0	1.9	1.13	2.3
	VS	3c	1.0	1.1	1.15	2.2

1-benzyl-2,2-diphenylethylamine	LS-P	9b	0.7	4.2	1.07	1.8
	RSP*	5a	1.0	0.5	1.25	3.5
	VS	1a	1.0	1.0	2.19	9.5
2-amino-1-(4-nitrophenyl)-1,3-propanediol	LS-P	4g	1.0	2.2	1.25	4.2
	NS	2a	1.0(45)	2.2	1.26	3.9
	RSP	5e	0.5	0.7	1.15	1.8
	VS*	8a	1.0	10.4	1.13	1.5
2-amino-1,1,3-triphenyl-1-propanol	RSP*	5e	1.0	2.7	1.14	3.0
	NS*	4f	0.5	0.6	1.17	1.5
	VS	1a	1.0	0.2	1.91	4.7
2-amino-1,1-diphenyl-1-propanol	NS	4a	1.0	3.2	1.11	2.0
	VS	6a	1.0	0.8	1.23	2.7
2-amino-1,2-diphenylethanol	LS-P	4a	1.0	1.0	1.23	2.8
	NS	3c	1.0	3.4	1.14	2.5
	VS	3c	0.5	1.3	1.13	2.0
2-amino-1-phenyl-1,3-propanediol	LS-P	4g	1.0	2.3	1.14	2.5

	RSP	5f	1.0	0.9	1.60	6.0
	NS	2a	1.0	1.4	1.27	3.7
2-amino-1-phenylethanol	LS-P	4g	1.0	3.8	1.20	4.0
	RSP*	5e	1.0	3.3	1.08	1.7
2-amino-3-phenyl-1-propanol	LS-P	4a	1.0	2.3	1.13	2.3
	NS***	3c	0.3	2.9	1.05	1.5
	VS	6a	1.0	1.3	1.15	2.0
2-amino-4-methyl-1,1-diphenylpentane	LS-P**	9a	0.5(5)	9.1	1.07	1.5
	NS***	3c	0.3	1.2	1.07	1.7
	VS	1a	2.0	0.4	1.94	4.5
2-chloro-indan-1-ylamine	LS-P	4g	2.0	2.0	1.60	7.2
	VS	6a	0.6	0.8	1.22	2.8
4-chlorobenzylhydramine	LS-P	4g	0.5	2.3	1.08	1.5
4-fluoro- α -methylbenzylamine	LS-P	4g	1.0	2.6	1.12	2.2
	NS**	4a	1.0	7.1	1.11	2.0
4-methoxy- α -methylbenzylamine	LS-P	4g	1.0	2.3	1.11	2.0

	NS**	4a	1.0	6.6	1.07	1.6
	VS	1a	1.0	0.8	1.52	5.6
6-methoxy-1,2,3,4-tetrahydro-1-napthalenylamine	LS-P	4a	1.0	2.0	1.23	4.4
	NS	3c	0.5	3.5	1.07	1.5
	RSP*	5e	1.0	1.1	1.11	2.1
	VS	1a	2.3	0.7	1.70	5.2
<i>cis</i> -1-amino-2-indanol	LS-P	4g	1.0	2.1	1.19	3.1
	NS	3c	1.0	3.8	1.11	2.0
	VS	1a	1.0	0.6	1.28	2.8
N-p-tosyl-1,2-diphenylethylene diamine	LS-P	4g	1.0	0.9	1.15	2.0
	NS	3c	1.0	2.1	1.18	2.6
	VS	8a	1.0	4.4	1.83	3.9
<i>trans</i> -1-amino-2-indanol	LS-P	4a	1.0	1.9	1.28	4.4
	VS	1a	1.0	0.8	1.34	3.7
α -methyl-4-nitrobenzylamine	LS-P	4g	1.0	4.0	1.10	2.0
	NS	3c	1.0	7.1	1.08	1.7

	VS**	3c	0.5	3.1	1.07	1.5
α-methylbenzylamine	LS-P	4g	1.0	2.3	1.15	2.7
	NS*	4a	2.0(45)	4.8	1.13	1.5
	VS	6a	0.5	0.9	1.15	2.0
d) Amino acids & derivatives						
Name ¹	CSP ³	MP ⁴	F(T) ⁵	k ₁ ^{6a}	α ^{6b}	R _s ^{6c}
3,4-dihydroxyphenylalanine	LS-P	4g	1.0	2.7	1.37	3.7
4-chlorophenylalaninol	LS-P	4a	1.0	2.3	1.12	2.3
	NS	4c	1.0	5.6	1.13	2.6
	RSP*	5c	0.5	1.0	1.08	1.5
4-nitrophenylalanine	LS-P	4g	1.0	2.7	1.23	3.2
Homocysteine thiolactone	LS-P	4g	1.0	4.2	1.13	2.2
	NS	3a	1.0	2.9	1.14	2.1
p-chlorophenylalanine	LS-P	4g	1.0	2.3	1.16	2.2
p-fluorophenylalanine	LS-P	4g	1.0	2.2	1.18	2.5
Phenylalanine	LS-P	4g	1.0	2.2	1.20	2.6

Tryptophan	LS-P	4g	1.0	2.0	1.25	3.1
Tryptophanamide	LS-P	4g	1.0	3.2	1.18	2.7
	VS	6a	1.0	1.2	1.22	2.7
Tryptophanol	LS-P	4a	1.0	2.4	1.15	2.9
Tyrosine methyl ester	LS-P **	4g	0.7	2.1	1.08	1.7
	NS	3c	0.3	1.9	1.10	1.7
Tyrosinol	LS-P	4a	1.0	2.4	1.13	2.5
	NS	4a	1.0	6.9	1.14	2.0

¹See section 6.3.3 for all sample information. ²See section 6.3 for classification information. ³All chiral stationary phases (CSP) were 100 x 4.6 mm (i.d.), unless indicated: *150 x 4.6 mm (i.d.), **200 x 4.6 mm (i.d.), ***250 x 4.6 mm (i.d.), ****300 x 4.6 mm (i.d.). See section 6.1 for more information. ⁴See section 6.2 for mobile phase (MP) information. ⁵All flow rates (F) are given in mL/min. All temperature (T) is 25 °C unless otherwise indicated (in °C). ^{6a,b,c} Chromatographic calculations: $k_1 = (t_{R1} - t_0) / (t_0)$; $\alpha = k_2 / k_1$; $R_s = 2(t_{R2} - t_{R1}) / (w_{0.5,1} + w_{0.5,2})$. See Supplemental data for abbreviations and more information.

Table 6.2. Optimized chiral separations of secondary (2°) amines.

a) Pharmaceuticals							
Name ¹	Class ²	CSP ³	MP ⁴	F(T) ⁵	k_1 ^{6a}	α ^{6b}	R_s ^{6c}

Amlodipine	CCB	LS-P	4g	0.7	2.7	1.09	1.9
		NS	3c	1.0	7.7	1.09	1.7
		RSP*	5e	1.0	3.1	1.10	1.5
		VS	4a	1.0	7.6	1.11	2.0
Mexitilane	SCB	LS-P	4g	1.0	7.5	1.08	1.5
		VS**	3c	0.5	1.1	1.10	2.0
Thyroxine	HOR	LS-P	4g	1.0	2.3	1.21	2.8
b) Stimulants							
Name ¹	Class ²	CSP ³	MP ⁴	F(T) ⁵	k ₁ ^{6a}	α ^{6b}	R _s ^{6c}
3,4-methylenedioxyamphetamine (MDA)	CSA I	LS-P***	4g	1.0	3.1	1.06	1.7
		RSP*	5e	0.5	2.2	1.07	1.6
		VS**	7a	0.4	5.1	1.08	1.5
Amphetamine	CSA II	LS-P****	4g	0.3	5.5	1.05	1.5
		NS*****	3c	0.3	2.9	1.05	1.5
		RSP*	5f	0.5(45)	2.4	1.08	1.5
		VS	1a	1.0	1.1	1.18	2.5

Aminorex	CSA I	NS	3c	0.5	4.6	1.06	1.5
		RSP*	5d	1.0	1.7	1.10	2.2
		VS	3c	0.7	2.6	1.10	2.0
Methoxamine	AAA	LS-P**	4e	0.5	3.7	1.06	1.5
		NS	4a	1.0	7.0	1.12	2.2
		RSP	5e	1.0	0.9	1.42	3.6
		VS	4a	0.5	3.2	1.10	1.5
Midodrine	AAA	LS-P*	4g	0.5	7.7	1.07	1.5
		NS	3c	1.0	5.2	1.23	2.9
Norepinephrine (Arterenol)	CAT	LS-P	4g	1.0(45)	3.7	1.13	2.4
Normetanephrine	CAT	LS-P	4a	1.0	3.5	1.14	2.9
		NS	3c	1.0	4.0	1.10	2.0
Norphenylephrine (3-octopamine)	CAT	LS-P	4a	1.0	3.3	1.14	2.8
		VS**	8a	0.5	11.5	1.05	1.5
Octopamine	CAT	LS-P	4a	1.0	3.2	1.13	2.1
		NS	3c	1.0	5.8	1.08	1.8

p-methoxyamphetamine (PMA)	CSA I	LS-P	4g	0.3	2.6	1.05	1.5
		RSP*	5d	0.5(45)	2.2	1.06	1.5
		VS	1a	0.6	1.0	1.17	2.5
p-chloroamphetamine (PCA)	NS	LS-P***	4g	0.3	2.7	1.05	1.5
		RSP*	5d	0.5	2.3	1.06	1.5
Phenylpropanolamine (Norephedrine)	RC I	LS-P	4a	0.8	2.4	1.10	2.0
		NS	4a	0.7	3.6	1.08	1.5
Tranlycypromine	AD	LS-P**	4g	1.0	5.5	1.06	1.5
		NS	3e	1.0(10)	5.0	1.12	2.0
		RSP*	5e	1.0	1.6	1.13	2.8
		VS	6a	0.5(30)	1.5	1.15	2.5
4-hydroxynorephedrine	CAT	LS-P	4a	0.5	2.4	1.09	1.9
		NS	8a	1.0	5.8	1.25	1.5
β-keto-amphetamine (Cathinone)	CSA I	LS-P	8b	1.0	6.0	1.12	2.3
		NS	2b	2.0(45)	1.4	1.44	4.5

		RSP*	5k	0.7	2.2	1.10	2.4
		VS	1a	1.0(15)	1.0	1.22	2.6
c) Reagents							
Name ¹	CSP ³	MP ⁴	F(T) ⁵	k ₁ ^{6a}	α ^{6b}	R _s ^{6c}	
1-(1,1-biphenyl-4-yl) ethanamine	LS-P	4g	1.0	2.4	1.14	2.6	
	NS*	4a	1.0	7.4	1.12	2.5	
	VS	1a	1.0	0.8	1.24	2.6	
1-(1-naphthyl) ethylamine	LS-P	4a	1.0	1.6	1.18	3.3	
	NS	2a	1.0	1.9	1.21	3.2	
	VS	1a	1.0	1.1	1.21	2.8	
1-(2-naphthyl) ethylamine	LS-P	4a	1.0	2.3	1.14	2.9	
1-(4-chlorophenyl) ethylamine	LS-P	4g	1.0	2.9	1.13	2.6	
	VS	3c	0.5	2.1	1.09	1.8	
1-(4-methylphenyl)ethylamine	LS-P	4a	1.0	2.1	1.13	2.3	
	NS*	4a	1.0	5.8	1.08	2.5	
	VS	3c	1.0	1.4	1.15	2.4	

1,1-diphenyl-2-amino-propane	LS-P	4g	1.0	0.8	1.14	2.0
	VS	1a	1.0	0.9	1.30	3.3
1,1-diphenyl-fluoro-2-aminopropane	LS-P**	9b	0.5	5.1	1.06	1.8
	RSP	5a	1.0	1.5	1.14	2.1
	VS	1a	1.0	0.5	1.39	3.2
1,2,2-triphenylethylamine	LS-P	4g	1.0	0.6	1.25	2.8
	NS****	3c	0.3	1.3	1.07	1.5
	VS	1a	1.0	0.6	1.45	3.9
1,2,3,4-tetrahydro-1-naphthylamine	LS-P	4a	1.0	1.8	1.17	2.8
	NS*	3c	0.5	2.9	1.08	1.9
	RSP***	5f	0.3(5)	1.1	1.05	1.5
	VS	1a	1.0	0.8	1.50	4.5
1,2-methoxyphenylethanamine	LS-P	4g	1.0	1.2	1.25	3.9
	NS	3c	1.0	1.9	1.13	2.3
	VS	3c	1.0	1.1	1.15	2.2
1-benzyl-2,2-diphenylethylamine	LS-P	9b	0.7	4.2	1.07	1.8

	RSP*	5a	1.0	0.5	1.25	3.5
	VS	1a	1.0	1.0	2.19	9.5
2-amino-1-(4-nitrophenyl)-1,3-propanediol	LS-P	4g	1.0	2.2	1.25	4.2
	NS	2a	1.0(45)	2.2	1.26	3.9
	RSP	5e	0.5	0.7	1.15	1.8
	VS*	8a	1.0	10.4	1.13	1.5
2-amino-1,1,3-triphenyl-1-propanol	RSP*	5e	1.0	2.7	1.14	3.0
	NS*	4f	0.5	0.6	1.17	1.5
	VS	1a	1.0	0.2	1.91	4.7
2-amino-1,1-diphenyl-1-propanol	NS	4a	1.0	3.2	1.11	2.0
	VS	6a	1.0	0.8	1.23	2.7
2-amino-1,2-diphenylethanol	LS-P	4a	1.0	1.0	1.23	2.8
	NS	3c	1.0	3.4	1.14	2.5
	VS	3c	0.5	1.3	1.13	2.0
2-amino-1-phenyl-1,3-propanediol	LS-P	4g	1.0	2.3	1.14	2.5
	RSP	5f	1.0	0.9	1.60	6.0

	NS	2a	1.0	1.4	1.27	3.7
2-amino-1-phenylethanol	LS-P	4g	1.0	3.8	1.20	4.0
	RSP*	5e	1.0	3.3	1.08	1.7
2-amino-3-phenyl-1-propanol	LS-P	4a	1.0	2.3	1.13	2.3
	NS****	3c	0.3	2.9	1.05	1.5
	VS	6a	1.0	1.3	1.15	2.0
2-amino-4-methyl-1,1-diphenylpentane	LS-P**	9a	0.5(5)	9.1	1.07	1.5
	NS****	3c	0.3	1.2	1.07	1.7
	VS	1a	2.0	0.4	1.94	4.5
2-chloro-indan-1-ylamine	LS-P	4g	2.0	2.0	1.60	7.2
	VS	6a	0.6	0.8	1.22	2.8
4-chlorobenzylhydramine	LS-P	4g	0.5	2.3	1.08	1.5
4-fluoro- α -methylbenzylamine	LS-P	4g	1.0	2.6	1.12	2.2
	NS**	4a	1.0	7.1	1.11	2.0
4-methoxy- α -methylbenzylamine	LS-P	4g	1.0	2.3	1.11	2.0
	NS**	4a	1.0	6.6	1.07	1.6

	VS	1a	1.0	0.8	1.52	5.6
6-methoxy-1,2,3,4-tetrahydro-1-naphthalenylamine	LS-P	4a	1.0	2.0	1.23	4.4
	NS	3c	0.5	3.5	1.07	1.5
	RSP*	5e	1.0	1.1	1.11	2.1
	VS	1a	2.3	0.7	1.70	5.2
<i>cis</i> -1-amino-2-indanol	LS-P	4g	1.0	2.1	1.19	3.1
	NS	3c	1.0	3.8	1.11	2.0
	VS	1a	1.0	0.6	1.28	2.8
N-p-tosyl-1,2-diphenylethylene diamine	LS-P	4g	1.0	0.9	1.15	2.0
	NS	3c	1.0	2.1	1.18	2.6
	VS	8a	1.0	4.4	1.83	3.9
<i>trans</i> -1-amino-2-indanol	LS-P	4a	1.0	1.9	1.28	4.4
	VS	1a	1.0	0.8	1.34	3.7
α -methyl-4-nitrobenzylamine	LS-P	4g	1.0	4.0	1.10	2.0
	NS	3c	1.0	7.1	1.08	1.7
	VS**	3c	0.5	3.1	1.07	1.5

α -methylbenzylamine	LS-P	4g	1.0	2.3	1.15	2.7
	NS*	4a	2.0(45)	4.8	1.13	1.5
	VS	6a	0.5	0.9	1.15	2.0
d) Amino acids & derivatives						
Name ¹	CSP ³	MP ⁴	F(T) ⁵	k_1^{6a}	α^{6b}	R_s^{6c}
3,4-dihydroxyphenylalanine	LS-P	4g	1.0	2.7	1.37	3.7
4-chlorophenylalaninol	LS-P	4a	1.0	2.3	1.12	2.3
	NS	4c	1.0	5.6	1.13	2.6
	RSP*	5c	0.5	1.0	1.08	1.5
4-nitrophenylalanine	LS-P	4g	1.0	2.7	1.23	3.2
Homocysteine thiolactone	LS-P	4g	1.0	4.2	1.13	2.2
	NS	3a	1.0	2.9	1.14	2.1
p-chlorophenylalanine	LS-P	4g	1.0	2.3	1.16	2.2
p-fluorophenylalanine	LS-P	4g	1.0	2.2	1.18	2.5
Phenylalanine	LS-P	4g	1.0	2.2	1.20	2.6
Tryptophan	LS-P	4g	1.0	2.0	1.25	3.1

Tryptophanamide	LS-P	4g	1.0	3.2	1.18	2.7
	VS	6a	1.0	1.2	1.22	2.7
Tryptophanol	LS-P	4a	1.0	2.4	1.15	2.9
Tyrosine methyl ester	LS-P **	4g	0.7	2.1	1.08	1.7
	NS	3c	0.3	1.9	1.10	1.7
Tyrosinol	LS-P	4a	1.0	2.4	1.13	2.5
	NS	4a	1.0	6.9	1.14	2.0

Table 6.3 Optimized chiral separations of tertiary (3°) amines.

a) Pharmaceuticals							
Name ¹	Class ²	CSP ³	MP ⁴	F(T) ⁵	k_1^{6a}	α^{6b}	R_s^{6c}
Atropine	AM	NS	2a	0.5	5.6	1.09	1.7
Brompheniramine	AH	VS	6a	0.7	2.5	1.13	2.0
Bupivacaine	ANE	NS	3c	1.0	1.9	1.21	2.5
		VS	1a	1.0	0.6	1.47	3.7
Carbinoxamine	AH	NS*	4f	0.5	2.2	1.08	1.5
		VS	3c	0.5	3.3	1.10	1.9

Cetirizine	AH	VS**	6a	0.3	1.3	1.08	1.5
Chlophedianol	AH	RSP*	5c	1.0	1.7	1.08	1.5
		VS	6a	0.6	1.6	1.14	2.5
Chlorpheniramine	AH	VS	6a	0.7	2.3	1.12	2.0
Diperodon	ABIO	NS	3c	1.0	5.8	1.13	1.7
		VS	3c	0.5	3.1	1.11	1.5
Disopyramide	SCB	NS***	3c	0.3	1.7	1.07	1.8
		VS	4a	1.0	2.9	1.13	2.1
Homatropine	AM	NS	2b	1.0(45)	2.4	1.19	3.1
		RSP*	5i	1.0	1.6	1.17	2.2
		VS**	9b	0.5	4.6	1.09	1.5
Indapamine	DIU	NS*	6c	0.3	11.0	1.13	1.5
		RSP	5h	0.3(10)	2.6	1.10	1.5
Mepivacaine	ANE	NS	4a	1.0	1.8	1.20	1.8
		VS	6a	0.5(30)	1.4	1.14	2.2
Methoxyverapamil	CCB	NS***	8a	0.5	3.6	1.08	1.5

		VS**	3c	0.5	3.0	1.10	1.5
Naftopidil	AB	NS	3c	0.5	3.2	1.12	1.5
Nicardipine	CCB	NS	3c	0.5	1.7	1.14	1.8
		VS	1a	2.0(45)	0.4	1.51	2.8
Octoclothepin	APC	NS	3c	1.0	7.0	1.13	2.6
		RSP	5a	1.0	2.8	1.35	5.0
		VS*	6d	0.7(45)	0.8	1.17	2.2
Orphenadrine	AH	VS	6a	1.0	1.1	1.23	2.9
Piperoxan	AH	NS	3a	1.5	6.3	1.18	2.3
		VS	3a	0.7	2.3	1.12	2.2
Promethazine	AH	NS	2a	1.0	2.0	1.14	1.6
		VS	1a	2.0	3.0	1.72	7.5
Sulpiride	APC	NS	2b	1.0(45)	2.7	1.30	4.3
Thioridazine	APC	NS	2a	2.0(45)	2.8	1.38	5.0
Tolperisone	AM	NS	3c	0.5	5.2	1.07	1.5
		VS	1a	1.0	0.7	1.33	3.0

Trihexylphenidyl	AM	NS	3c	1.0	3.2	1.13	2.4
		VS	1a	1.0	0.7	1.29	2.7
Trimebutine	AM	NS	3c	0.5	1.5	1.13	1.7
		VS	1a	1.0	0.5	1.36	3.0
Verapamil	CCB	NS***	8a	0.5	4.1	1.09	1.5
		VS**	6a	0.3	1.9	1.08	1.5
b) Stimulants							
Name ¹	Class ²	CSP ³	MP ⁴	F(T) ⁵	k ₁ ^{6a}	α ^{6b}	R _s ^{6c}
Citalopram	AD	NS***	3c	0.3	4.8	1.05	1.6
		VS	3c	0.7	4.2	1.13	2.1
Methadone	CSA II	NS	3c	0.5	1.9	1.11	2.0
		RSP*	5g	0.7(45)	0.9	1.14	2.2
		VS	7b	0.5	2.5	1.12	2.1
Methorphan	CSA II	NS	2b	0.7(45)	3.6	1.09	1.6
		RSP*	5b	1.0	3.7	1.10	1.8
		VS	6b	1.0	1.2	1.27	3.3

Mianserin	AD	NS	3c	1.0	4.5	1.16	2.5
		RSP	5c	1.0	1.6	1.18	2.7
		VS	1a	2.0(45)	1.4	2.13	9.8
Nefopam	ANA	NS	2b	1.0(45)	2.0	1.19	2.6
		RSP	5e	1.0	1.7	1.23	3.5
		VS	1a	0.7(45)	1.5	1.12	2.1
Nicotine	TOB	NS	2b	1.5(45)	0.5	1.60	3.0
N-Methylephedrine	RC I	RSP*	5k	0.7	3.2	1.08	1.7
		VS	3b	1.0	2.7	1.10	1.9
Tetramisole	AP	NS	3c	0.7	3.5	1.12	2.5
Tramadol	CSA IV	VS*	6e	0.3(45)	0.5	1.21	1.5
Trimipramine	AD	VS	1a	1.0	1.0	1.33	3.4
Venlafaxine	AD	NS***	3c	0.3	2.0	1.06	1.6
		VS	3a	1.0	4.7	1.10	2.1
α -pyrrolidinopentiophenone (α -pvp)	CSA I	NS	4a	0.5	1.2	1.15	1.8
		RSP*	6d	0.3(10)	1.8	1.10	1.5

		VS	1a	1.0	0.6	1.44	4.3
c) Reagents							
Name ¹	CSP ³	MP ⁴	F(T) ⁵	k_1^{6a}	α^{6b}	R_s^{6c}	
N,N-dimethyl-1-(1-naphthylethylamine)	NS	3c	1.0	4.7	1.11	2.3	
	VS	8a	1.0	4.2	1.23	2.0	
N,N-dimethyl-1-phenylethylamine	NS	3c	1.0	5.2	1.11	2.2	
α -N,N-dimethylaminophenyl acetonitrile	RSP	5a	0.5	0.9	1.12	1.5	

6.4 Results and Discussion

The following sections will discuss the method development of each CSP from screening to optimization for the chiral separation of amines (*Figure 6.1*).

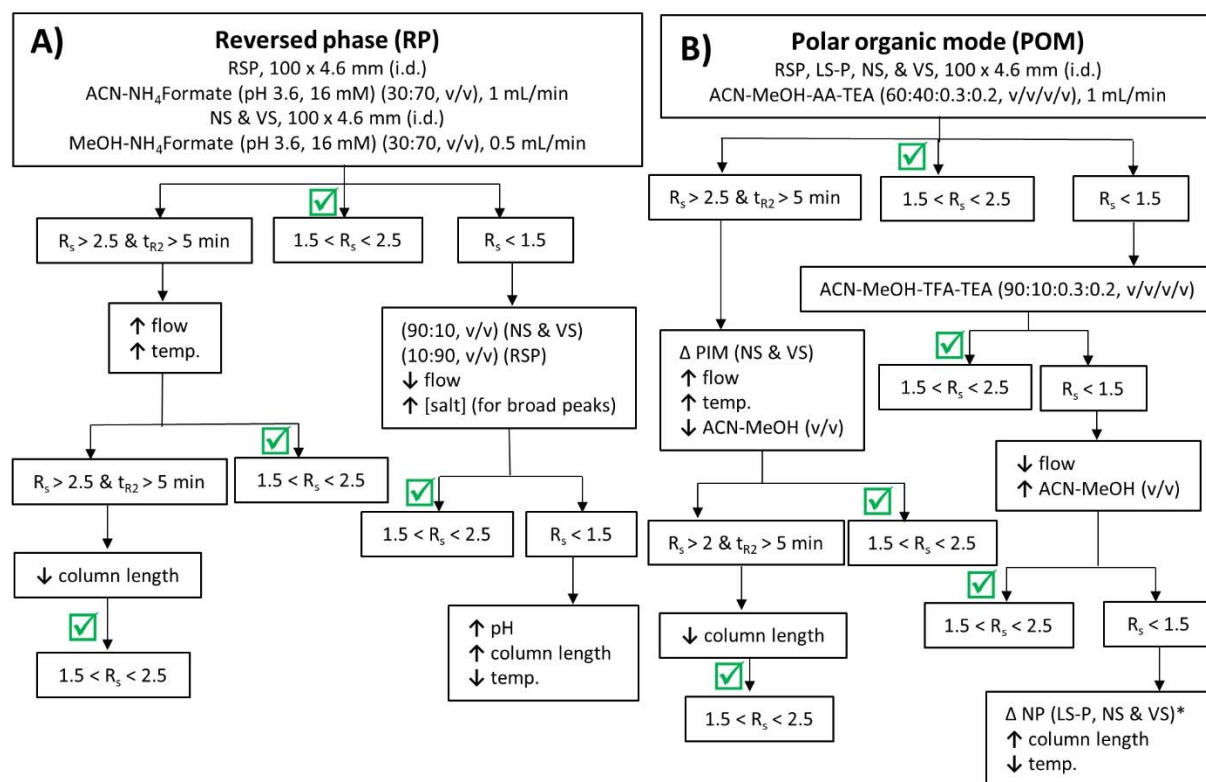


Figure 6.1 Method development of chiral amines. Method development of chiral amines using SPP CSPs: CDShell-RSP (RSP), LarihcShell-P (LS-P), NicoShell (NS), and VancoShell (VS) in (A) reversed phase (RP) and (B) polar organic mode (POM). See Supplemental data for polar ionic mode (PIM) and normal phase (NP) method development and chromatographic parameter abbreviations (R_s , t_{R2}), and section 2.1 for all solvent abbreviations (ACN, MeOH, AA, TEA, NH_4HCO_2). Other abbreviations include temperature (temp.) and Δ , which represents “switch to.” See Figure 6.S1 and section 6.S1 in Supplemental data for more information.

The goals for all separations were to result in a “hit” ($\alpha > 1.05$) from screening and get to baseline separation ($R_s \geq 1.5$) while operating at moderate pressure (<300 bar) and room temperature (25 °C). The optimized results of the 150 tested amines are tabulated in Tables 1-3. The number of baseline separations achieved with each CSP compared to the total possible separations according to the type of amine: 1°, 2°, or 3° is shown in Figure 6.2A. All 150 amines were baseline separated

by at least one CSP and often with multiple CSPs. *Figure 6.2B* illustrates, non-proportionally, the overlap of baseline separations between each CSP, and reports the total number of baseline separations for each CSP in parenthesis.

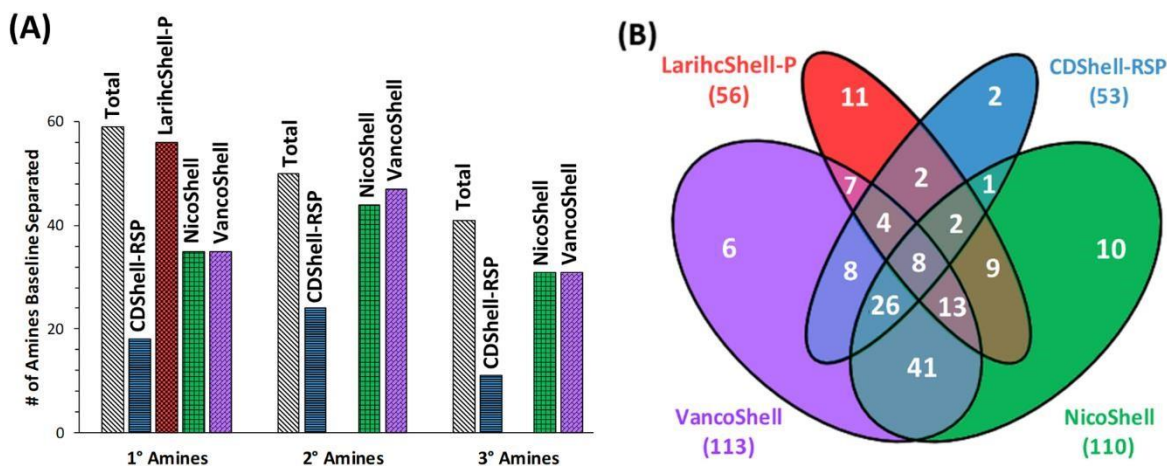


Figure 6.2. Baseline separations results of 150 chiral 1°, 2°, and 3° amines with four superficially porous particle (SPP) chiral stationary phases (CSPs). (A) Number of baseline separations by each CSP compared to the total amines tested. (B) Number of amines baseline separation by each or more than one CSP. See Results and Discussion for further explanation.

The results show that 81% were baseline separated by two or more CSPs, 35% were baseline separated by three or more CSPs, and 5% were baseline separated by all four CSPs. These separations will be addressed according to the principle of complementary separations with the addition of the term, “unique,” which applies to complementary separations where the amine had no separation with any of the other CSPs (*Figure 6.3*).

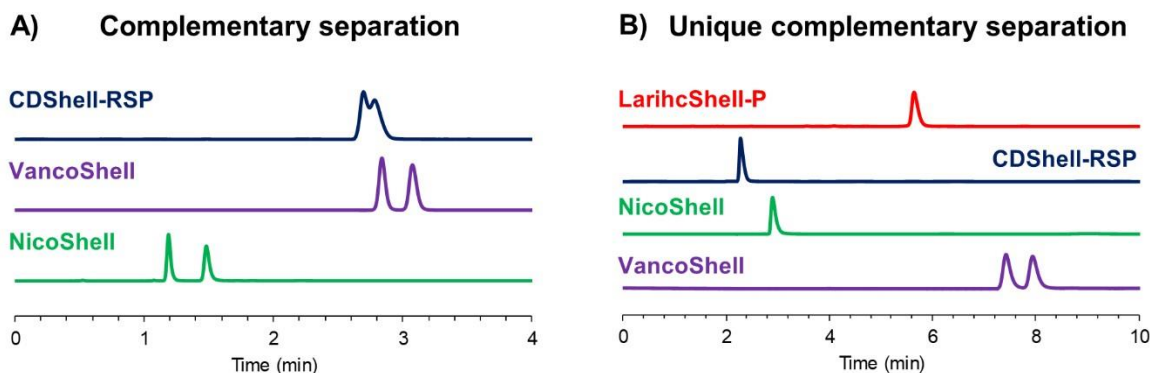


Figure 6.3 The principle of complementary separations. (A, B). The principle of complementary separations: the difference between (A) complementary and (B) unique complementary separations using (A) alprenolol and (B) tramadol. See Tables 1–3 for all chromatographic results. See Section Experimental for all chromatographic parameters and other information.

The numbers represented with just one CSP in Figure 6.2B do not indicate “unique” complementary separations because a different CSP might have had $R_s < 1.5$ for that amine. Also, if the amine was separated by three CSPs, such as RSP, VS, and NS, it was not included in the overlap of two CSPs, like VS and NS (Figure 6.2B).

Overall, LS-P (i.e., the isopropyl cyclofructan-6) was the most powerful CSP for separating 1° amines. LS-P achieved six “unique” complementary separations including phenylalanine, *p*-chlorophenylalanine, *p*-fluorophenylalanine, tryptophan, tryptophanol, and norepinephrine. Also, LS-P performed five other baseline separations that other CSPs could not, which included thyroxine, 1-(2-naphthylethylamine), 3,4-dihydroxyphenylalanine (DOPA), 4-chlorobenzylhydramine, and 4-nitrophenylalanine.

Most stimulants were best separated by RSP (i.e., hydroxypropyl β -cyclodextrin), which is shown in Figure 6.4 with the baseline separation of 18 racemic controlled substances in a single LC-MS

analysis. RSP had one “unique” complementary separation, 3,4-methylenedioxymethamphetamine (MDMA). Also, RSP baseline separated one other amine that was not by other CSPs: α -N,N-dimethylaminophenyl acetonitrile.

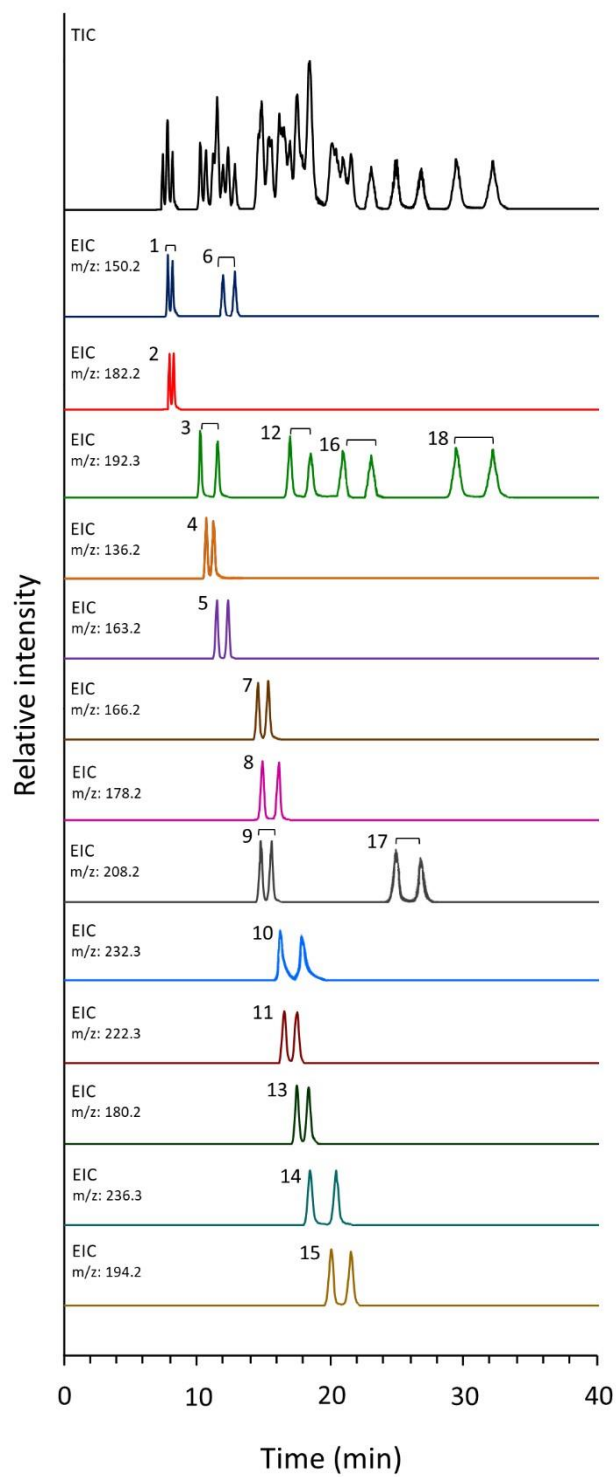


Figure 6.4. Chromatographic enantioseparation of 18 racemic controlled substance stimulant amines using liquid chromatography electrospray-mass spectrometry (LC-ESI-MS). Total ion

chromatogram (TIC) and extracted ion chromatograms (EIC) are shown. Conditions: CDShell-RSP, 150 x 4.6 mm (i.d.), ACN-NH₄HCO₂ (pH 3.6, 16 mM) (10:90), 0.4 mL/min, 25 °C. 1. rac-cathinone, 2. rac-3FMC, 3. rac-pentadrone, 4. rac-amphetamine, 5. rac-aminorex, 6. rac-methamphetamine, 7. rac-PMA, 8. rac-mephedrone, 9. rac-methylone, 10. rac- α -PVP, 11. rac-ethylone, 12. rac-4-MEC, 13. rac-MDA, 14. rac-pentylone, 15. rac-MDMA, 16. rac-3,4-DMMC, 17. rac-MDEA, 18. rac-4-EMC. See sections Experimental and Tables 6.1-3 for other acronyms and information.

NS and VS (i.e., both macrocyclic glycopeptides) dominated the separation of pharmaceuticals and demonstrated the most complementary behavior of any two CSPs. NS had two “unique” complementary separations: atropine and epinephrine, and eight other baseline separations not performed by other CSPs: ephedrine, fenfluramine, naftopidil, nicotine, N,N-dimethyl-1-phenylethylamine, sulpiride, tetramisole, and thioridazine. VS had four “unique” complementary separations including brompheniramine, cetirizine, chlorpheniramine, and tramadol. Also, VS baseline separated two amines, orphenadrine and trimipramine, that other CSPs could not.

6.4.1 Screening and optimization

Screening was performed with all 150 amines with reversed phase (RP) and polar organic mode (POM) (*Figure 6.1*) The POM screening mobile phase comprised of ACN-MeOH-AA-TEA (60:40:0.3:0.2, v/v/v/v).

LS-P utilized POM, and all other CSPs utilized both RP and POM. The RP screening mobile phase for NS and VS was MeOH-NH₄HCO₂ (pH 3.6, 16 mM) (30:70, v/v), while ACN-NH₄HCO₂ (pH 3.6, 16 mM) (30:70, v/v) was used for RSP. These screening solvents offered the best chance for a “hit” based on a thorough investigation of mobile phase additives, which are discussed in the

Supplemental data (*Section 6.S1, Figures 6.S1-S6, Table 6.1*). An optimized separation was targeted at a R_s between 1.5 and 2.5 with an analysis time < 5 min. For “hits,” optimizations were made according to each CSP. LS-P required the least optimization with most optimized separations performed using the screening mobile phase or ACN/MeOH/TFA/TEA (90:10:0.3:0.2, v/v/v/v) (*Table 6.1, Figure 6.1B*). However, if $R_s > 1.5$ was not achieved sometimes a normal phase (NP) solvent, Hep-EtOH/TFA/TEA (60:40:0.3:0.2, v/v/v/v), was used. Since the back pressure was ~60-110 bar using a 100 x 4.6 mm (i.d.) column at 1.0 mL/min with these mobile phases, analysis time was often reduced by increasing the flow rate. RSP had the most separations in the reversed phase mode. If $R_s > 1.5$ was not achieved, the mobile phase was adjusted to ACN-NH₄HCO₂ (pH 3.6, 16 mM) (10:90, v/v) (*Figure 6.1A*). For NS and VS optimization in the reversed phase mode, often MeOH-NH₄HCO₂ (pH 3.6, 16 mM) (90:10, v/v) was used (*Figure 6.1A*). However, most amines were best separated by NS and VS when using the polar organic mode. Frequently, the use of a polar ionic mode (PIM) solvent, MeOH-NH₄HCO₂ (100:1, v/w), was used for the amines that had enantiomeric selectivity in POM (*Section 6.S1.3, Figures 6.S1, 6.S5*). A variety of other optimization factors were investigated to improve R_s , especially for the non-optimal separations ($\alpha < 1.05$), which are not included in *Tables 6.1-3 (Section 6.S1, Figures 6.S1-S6, Table 6.1)*.

6.4.2 Cyclofructan-6-P (LS-P)

The derivatized cyclofructan, LS-P, baseline separated 95% of racemic chiral 1° amines, of which many were reagents used for organic synthesis (*Figures 6.2A, Table 6.1*). Since LS-P had such high selectivities for almost all the racemates, it is best-suited to identify and quantify trace impurities of enantiomeric reagents in a synthetic therapeutic product. For example, rasagiline is used as a therapeutic for Parkinson’s disease, and one of its chemical precursor, 2-chloro-indan-1-ylamine had a R_s of 7.2 with an analysis time under 2 min with LS-P (*Table 6.1c*). This large α

also indicates a facile application for preparatory separations to isolate a single enantiomer in large quantities, especially since most analytes are soluble in these solvents used for LS-P [11]. Also, solvents used with the LS-P column are highly MS compatible compared to other CSPs, like crown ethers, which are commonly used to separate of 1° amines [11]. When a chiral 1° amine also had additional hydrogen bonding functionalities adjacent or connected to the chiral center, R_s increased - which was expected [11,16,29]. Difficult 1° amine separations included amphetamines and sterically hindered 1° amines, like 2-amino-1,1,3-triphenyl-1-propanol, 2-amino-1,1-diphenyl-1-propanol, and aminorex. It should also be noted that most amino acids and derivatives have 1° amine functionalities but have been shown to separate easily using other CSPs not included in this study, like TeicoShell [12,17].

6.4.3 Hydroxypropyl- β -cyclodextrin (RSP)

The RSP β -cyclodextrin CSP baseline separated 35% out of the 150 amines, 30% of the 1° amines, 48% of the 2° amines, and 27% of the 3° amines (*Figure 6.2A*). It was best utilized for the stimulants, which included several controlled substances like amphetamines and cathinones, as well as alkaloids, opioids, and antidepressants (see *Tables 6.1-3*). *Figure 6.4* highlights the use of LC-MS with the baseline separation of 18 racemic controlled substances. Since the RSP primarily was used in the reversed phase mode, these methods had very high MS sensitivity, which enhances its applicability to forensic and toxicology studies. Separations included MDMA, and several synthetic cathinones, especially those that could interact through hydrogen bonding. Analytes that had two hydrogen bonding functionalities, such as pseudoephedrine, had larger R_s compared than those with only one, like methamphetamine, and those with none, like fenfluramine, which enantiomers coeluted, as expected (*Table 6.2b*) [30]. Interestingly, 4-fluoromethcathinone (4-FMC) could not be baseline separated by RSP, but 3-fluoromethcathinone (3FMC) was. However, 4-

FMC and all other stimulants not baseline separated by RSP were separated by a different CSP, which indicates the complementary behavior between all these macrocyclic CSPs.

6.4.4 Macrocyclic glycopeptides (VS & NS)

The native macrocyclic glycopeptide, VS, baseline separated 75% of all the amines: 59% of the 1° amines, 94% of the 2° amines, and 76% of the 3° amines (*Figure 6.2A*). Overall, VS had the best performance, baseline separating more amines than the other tested CSPs. VS separated the most pharmaceutical amines, baseline separating all antihistamines, anesthetics, antidepressants, analgesics, antiarrhythmics, decongestants/bronchodilators, and antianginals. The modified macrocyclic glycopeptide, NS, baseline separated 73% of all the amines, 59% of the 1° amines, 88% of the 2° amines, and 76% of the 3° amines (*Figure 6.2A*). NS has previously been shown to separate nicotine-related compounds, which was further demonstrated in this work [18-19]. Additionally, NS had higher R_s for all β -blockers compared to VS. Carbinoxamine, an antihistamine with a structure similar to chlorpheniramine, was baseline separated using NS, while chlorpheniramine was not. In general, antihistamines were better separated by VS than NS. One example was promethazine, an antihistamine with a phenothiazine structure, which had an extremely high R_s of 7.5 within 3 min using VS (*Table 6.2*). However, another phenothiazine that is used as an antipsychotic, thioridazine, had low R_s using VS, but was baseline separated by NS. Thioridazine is currently under investigation as a treatment for schizophrenia, as is sulpiride and both were only baseline separated by NS. Another class of amines that NS dominantly separated were the catecholamines, except norepinephrine and N-methylephedrine. Since macrocyclic glycopeptides have complex separation mechanisms, it is difficult to predict why certain amines were or weren't separated. Thus, their highly complementary separation behavior contributes greatly to their ease of use and optimization.

6.5 Conclusions

Herein the broadest and most comprehensive separation strategies for chiral amine containing compounds is demonstrated. All 150 chiral amines were easily optimized to a R_s between 1.5 and 2.5, most within 5 min with at least one CSP, and several with more than one CSP. LS-P was shown to be best for 1° amines, while RSP, NS, and VS separated a variety of 1°, 2°, and 3° amines. RSP separated most chiral stimulants, which would provide sensitive forensic drug screening and testing. NS and VS best separated pharmaceuticals and provided the most complementary separations. Further investigation of these CSPs will lead to more information about their separation mechanisms and other novel applications.

6.6 References

1. Food and Drug Administration, New drugs at FDA: CDER's new molecular entities and new therapeutic biological products, <https://www.fda.gov/Drugs/DevelopmentApprovalProcess/DrugInnovation/default.htm>, 2017 (accessed 03 January 2018).
2. A. Calcaterra, I. D'Acquarica, The market of chiral drugs: Chiral switches versus *de novo* enantiomerically pure compounds, *J. Pharm. Biomed. Anal.* 147 (2018) 323-340.
3. J.-T. Liu, R.H. Liu, Enantiomeric composition of abused amine drugs: chromatographic methods of analysis and data interpretation, *J. Biochem. Biophys. Meth.* 54 (2002) 115-146.
4. R.E. Boehm, D.E. Martire, D.W. Armstrong, Theoretical considerations concerning the separation of enantiomeric solutes by liquid chromatography, *Anal. Chem.* 60 (1988) 522-528.
5. Drug Enforcement Administration, Lists of scheduling actions, controlled substances, regulated chemicals, <https://www.deadiversion.usdoj.gov/schedules/orangebook/orangebook.pdf>, 2017 (accessed 03 January 2018).
6. D.A. Spudeit, M.D. Dolzan, Z.S. Breitbach, W.E. Barber, G.A. Micke, D.W. Armstrong, Superficially porous particles vs. fully porous particles for bonded high performance liquid chromatographic chiral stationary phases: Isopropyl cyclofructan 6, *J. Chromatogr. A* 1363 (2014) 89-95.
7. D.C. Patel, Z.S. Breitbach, M.F. Wahab, C.L. Barhate, D.W. Armstrong, Gone in seconds: praxis, performance, and peculiarities of ultrafast chiral liquid chromatography with superficially porous particles, *Anal. Chem.* 87 (2015) 9137-9148.
8. D.C. Patel, M.F. Wahab, D.W. Armstrong, Z.S. Breitbach, Advances in high-throughput and high efficiency chiral liquid chromatographic separations, *J. Chromatogr. A* 1467 (2016) 2-18.
9. C.L. Barhate, L.A. Joyce, A.A. Makarov, K. Zawatzky, F. Bernardoni, W.A. Schafer, D.W. Armstrong, C.J. Welch, E.L. Regalado, Ultrafast chiral separations for high throughput enantiopurity analysis, *Chem. Commun.* 53 (2016) 509-512.

10. D.W. Armstrong, Y. Tang, S. Chen, Y. Zhou, C. Bagwill, J.R. Chen, Macrocyclic antibiotics as a new class of chiral selectors for liquid chromatography, *Anal. Chem.* 66 (1994) 1473-1484.
11. P. Sun, C. Wang, Z.S. Breitbach, Y. Zhang, D.W. Armstrong, Development of new HPLC chiral stationary phases based on native and derivatized cyclofructans, *Anal. Chem.* 81 (2009) 1021510226.
12. X. Zhang, Y. Bao, K. Huang, K. Barnett-Rundlett, D.W. Armstrong, Evaluation of dalbavancin as chiral selector for HPLC and comparison with teicoplanin-based chiral stationary phases, *Chirality*, 22 (2010) 495-513.
13. T.L. Xiao, E. Tesarova, J.L. Anderson, M. Egger, D.W. Armstrong, Evaluation and comparison of a methylated teicoplanin aglycone to teicoplanin aglycone and natural teicoplanin chiral stationary phases, *J. Sep. Sci.* 29 (2006) 429-445.
14. K.H. Ekborg-Ott, J.P. Kullman, X. Wang, K. Gahm, L. He, D.W. Armstrong, Evaluation of the macrocyclic antibiotic avoparcin as a new chiral selector for HPLC, *Chirality* 10 (1998) 627-660.
15. A. Peter, E. Vèkes, D.W. Armstrong, Effects of temperature on retention of chiral compounds on a ristocetin A chiral stationary phase, *J. Chromatogr. A* 958 (2002) 89-107.
16. D.W. Armstrong, R.M. Woods, Z.S. Breitbach, Z.S. Comparison of enantiomeric separations and screening protocols for chiral primary amines by SFC and HPLC, *LC-GC North America* 32 (2014) 742-752.
17. D.W. Armstrong, Y. Liu, K.H. Ekborg-Ott, A covalently bonded teicoplanin chiral stationary phase for HPLC enantioseparations, *Chirality* 7 (1995) 474-497.
18. G. Hellinghausen, J.T. Lee, C.A. Weatherly, D.A. Lopez, D.W. Armstrong, Evaluation of nicotine in tobacco-free-nicotine commercial products, *Drug Test. Anal.* 9 (2017) 944-948.
19. G. Hellinghausen, D. Roy, Y. Wang, J.T. Lee, D.A. Lopez, C.A. Weatherly, D.W. Armstrong, A comprehensive methodology for the chiral separation of 40 tobacco alkaloids and their carcinogenic E/Z-(R,S)-tobacco specific nitrosamine metabolites, *Talanta* 181 (2017) 132-141.
20. C.L. Barhate, D.A. Lopez, A.A. Makarov, X. Bu, W.J. Morris, A. Lekhal, R. Hartman, D.W. Armstrong, E.L. Regalado, Macrocyclic glycopeptide chiral selectors bonded to core-shell particles enables enantiopurity analysis of the entire verubecestat synthetic route, *J. Chromatogr. A* 1539 (2018) 8792.
21. D. Wolrab, P. Frühauf, A. Moulisová, M. Kuchař, C. Gerner, W. Lindner, M. Kohout, Chiral separation of new designer drugs (Cathinones) on chiral ion-exchange type stationary phases, *J. Pharm. Biomed. Anal.* 120 (2016) 306-315.
22. N.L.T. Padivitage, E. Dodbiba, Z.S. Breitbach, D.W. Armstrong, Enantiomeric separations of illicit drugs and controlled substances using cyclofructan-based (LARIHC) and cyclobond I 2000 RSP HPLC chiral stationary phases, *Drug Test. Anal.* 6 (2014) 542-551.
23. D.W. Armstrong, S.M. Han, Y.I. Han, Separation of optical isomers of scopolamine, cocaine, homatropine, and atropine, *Anal. Biochem.* 167 (1987) 261-264.
24. M.D. Dolzan, Y. Shu, J.P. Smuts, H. Petersen, P. Ellegaard, G.A. Micke, D.W. Armstrong, Z.S. Breitbach, Enantiomeric separation of citalopram analogues by HPLC using macrocyclic glycopeptide and cyclodextrin based chiral stationary phases, *J. Liq. Chromatogr. Rel. Technol.* 39 (2016) 154-160.
25. D. Albals, Y.V. Heyden, M.G. Schmid, B. Chankvetadze, D. Mangelings, Chiral separations of cathinone and amphetamine-derivatives: Comparative study between capillary electrochromatography, supercritical fluid chromatography and three liquid chromatographic modes, *J. Pharm. Biomed. Anal.* 121 (2015) 232-243.

26. B. Chankvetadze, L. Chankvetadze, Sh. Sidamonidze, E. Yashima, Y. Okamoto, High performance liquid chromatography enantioseparation of chiral pharmaceuticals using tris(chloromethylphenylcarbamate)s of cellulose, *J. Pharm. Biomed. Anal.* 14 (1996) 1295-1303.
27. S. Chen, Y. Liu, D.W. Armstrong, J.I. Borrell, B. Martinez-Teipel & J.L. Matallana, Enantioresolution of substituted 2-methoxy-6-oxo-1,4,5,6-tetrahydropyridine-3-carbonitriles on macrocyclic antibiotic and cyclodextrin stationary phases, *J. Liq. Chromatogr. Rel. Technol.* 18 (1995) 1495-1507.
28. M.P. Gasper, A. Berthod, U.B. Nair, D.W. Armstrong, Comparison and modeling study of vancomycin, ristocetin A, and teicoplanin for CE enantioseparations, *Anal. Chem.* 68 (1996) 2501-2514.
29. P. Sun, D.W. Armstrong, Effective enantiomeric separations of racemic primary amines by the isopropyl carbamate-cyclofructan6 chiral stationary phase, *J. Chromatogr. A* 1217 (2010) 4904-4918.
30. D.W. Armstrong, W. DeMond, Cyclodextrin bonded phases for the liquid chromatographic separation of optical, geometrical, and structural isomers, *J. Chromatogr. Sci.* 22 (1984) 411-415.

6.7 Supporting Information

6.S1. Method development

Additives and operational parameters have not been widely documented for the SPP CSPs used in this study: CDShell-RSP (RSP), LarihcShell-P (LS-P), NicoShell (NS), and VancoShell (VS). Therefore, the following sections will discuss the mobile phase development for each chromatographic mode utilized by these CSPs: polar ionic mode (PIM), polar organic mode (POM), reversed phase (RP), and normal phase (NP), which is summarized in *Figure 6.S1*. Initial studies were focused on developing a solvent for one or two chromatographic modes that provided a “hit” ($\alpha > 1.05$) for most tested amines while operating at moderate pressure (<300 bar) and room temperature (25 °C). By developing a high-throughput screening method, the amines that were “hit” could easily be brought to baseline resolution ($R_s > 1.5$) during optimization. To evaluate and determine when to utilize each solvent adjustment, the parameters that influence resolution (R_s): efficiency (N), retention factor (k), and selectivity (α), were closely monitored and compared [1]. The dead time, t_0 , was determined by the peak of the refractive index change due to the unretained sample solvent. Retention factors (k) were calculated using $k = (t_R - t_0) / (t_0)$, where t_R is the retention time of the peak and t_0 is the dead time of the column. Selectivity (α) was calculated using $\alpha = k_2 / k_1$, where k_1 and k_2 are retention factors of the first and second peaks, respectively. Resolution (R_s) was calculated using the peak width at half peak height, $R_s = 2(t_{R2} - t_{R1}) / (w_{0.5,1} + w_{0.5,2})$ in which, respectively, where t_{R1} and t_{R2} are retention factors and $w_{0.5,1}$ and $w_{0.5,2}$ are the peak widths at the half peak height of the first and second peaks. The number of plates (N), efficiency, was calculated as $N = 5.54(t_R/w_{0.5})^2$.

Since α has more of an effect on R_s at moderate k and N, α was first targeted to increase R_s . In general, parameters like flow rate, temperature, and the use of longer columns did not significantly

increase α but influenced N and k using longer columns and higher temperatures, but also by additives.

The disadvantage of higher column temperatures was a decrease of α (Figure 6.S2, Table 6.S1). Longer columns also were not the first choice to increase N to obtain baseline R_s because an increased column length caused higher back pressure (>300 bar) so the flow rate was decreased, and longer analysis time was required. Therefore, a variety of mobile phase optimization factors such as an organic modifier, salt concentration, acid-base ratio, and pH were modified to improve R_s before relying on parameters to increase N , like a longer column or lower flow rate (Figure 6.1, 6.S1, 6.S2, 6.S3, 6.S4, 6.S5). Overall, an optimized separation was targeted at a R_s between 1.5 and 2.5 with an analysis time < 5 min.

6.S1.1. Reversed phase (RP)

In RP, the mobile phase consists of a ratio between an organic modifier and buffer. When less organic modifier was present, k increased, and N decreased (Figure 6.S3A, Table 6.S1). The organic modifier was chosen based on the CSP. For example, when the organic modifier was changed from acetonitrile (ACN) to methanol (MeOH) with RSP, methorphan's k greatly increased, but R_s did not (Figure 6.S3B, Table 6.S1). With VS, methorphan's k only slightly increased from ACN to MeOH, but R_s increased significantly

(Figure 6.S3C, Table 6.S1). Thus, ACN was chosen for RSP as the organic modifier and MeOH was chosen for NS and VS. The buffer utilized most was an ammonium formate (NH_4HCO_2) buffer with a pH adjustment to 3.6, mixed with 30% organic modifier: ACN- NH_4HCO_2 (pH 3.6, 16 mM) (30:70, v/v) and MeOH- NH_4HCO_2 (pH 3.6, 16 mM) (30:70, v/v). Several pH values were tested, but the optimal pH was determined to be compound dependent. However, to make the screening

simpler, a lower pH of 3.6 seemed to give the best N , moderate k , and high α (Figure 6.S3D, Table 6.S1). Other ammonium salts like ammonium acetate ($\text{NH}_4\text{CH}_3\text{CO}_2$) and ammonium trifluoroacetate (NH_4TFA) were tested as the buffer, but NH_4HCO_2 was very reproducible and afforded higher mass spectrometry (MS) sensitivity, so it was favored. A 0.1wt% of NH_4HCO_2 was chosen (reported as 16 mM), which provided moderate k and N for most amines. The salt concentration was increased for separations that had broad peak shapes to increase N . The buffer was mixed with the organic modifier and degassed before use. Often, the organic modifier ratio for RSP was decreased to ACN- NH_4HCO_2 (pH 3.6, 16 mM) (10:90, v/v), which decreased N , but often increased α . When comparing k , RSP was very sensitive to the ACN content compared to MeOH for VS and NS. The macrocyclic glycopeptides had the best α at 2 ratios, MeOH- NH_4HCO_2 (pH 3.6, 16 mM) (90:10 or 30:70, v/v). The 90:10 composition was very similar to PIM with the addition of 10% water, which tended to increase N , but many amines lost α with the addition compared to PIM. The 30:70 ratio had high back pressure at just 0.5 mL/min (250 bar), so analysis time tended to be longer with this ratio. When applicable, the 90:10 ratio was used. Occasionally, MeOH was replaced with ethanol (EtOH) when using NS and VS, which generally increased k , and decreased N . NS and VS performed optimal separations for some chiral amines in RP but mainly relied on PIM solvents. RP was not used for LS-P.

Thus, the most significant use of RP was with RSP, which was used for all optimized separations.

6.S1.2. Polar organic mode (POM)

POM mobile phases consist of a mixture of organic solvents, typically ACN-MeOH, with an addition (v/v) of acetic acid (AA) and triethylamine (TEA). Longer retention was observed for amines compared to PIM, due to the decrease in elution strength from the addition of ACN.

Additionally, the back pressure was only ~60 bar using a 100 x 4.6 mm (i.d.) column at 1.0 mL/min so the flow could be greatly increased using a conventional HPLC (<300 bar). For these reasons, a second screening solvent was designed with POM. Past literature recommended a ratio of AA-TEA (0.3:0.2, v/v) and trifluoroacetate (TFA)-TEA (0.3:0.2, v/v) with a ratio of ACN-MeOH that provided adequate retention for LS-P [2]. It was found that a ratio of ACN-MeOH-AA-TEA (60:40:0.3:0.2, v/v/v/v) provided fast analysis (<5 minutes) and large α for most 1°amines using LS-P. The use of TFA-TEA (0.3:0.2, v/v) significantly increased N compared to AA-TEA (0.3/0.2, v/v) with LS-P, but significantly decreased analysis time and reduced R_s when the ratio of ACN-MeOH (60/40, v/v) was used, especially for NS and VS. When the ratio of ACNMeOH was increased, to increase k , NS and VS frequently had decreased R_s (*Figure 6.S4A, Table 6.S1*). However, when the ratio of ACN-MeOH was increased using LS-P, R_s increased (*Figure 6.S4B, Table 6.S1*). An optimal solvent used by LS-P only for higher N and k was ACN-MeOH-TFA-TEA (90:10:0.3:0.2, v/v/v/v) (*Figure 6.S4C, Table 6.S1*). RSP never had higher R_s using POM vs. RP. However, NS and VS frequently did, but the analysis time was often > 5 min. Therefore, PIM optimization was often used, which is described in *section 6.S1.3*.

6.S1.3. Polar ionic mode (PIM)

The macrocyclic glycopeptides are the only CSPs in this study that operate well in PIM, which enhances their ionic interactions with ionizable compounds [3-6]. However, POM screening solvents generally offered higher k values compared to PIM, which was more beneficial for this screening procedure. Thus, PIM was used as an optimization tool for NS and VS. PIM solvents consisted of 100% MeOH and an additive, either an ammonium salt (wt%) like NH_4HCO_2 or NH_4TFA or the addition of acid and base (v/v) such as AA-ammonium hydroxide (NH_4OH) or AA-TEA [5-6]. Initial amounts of 0.1wt% of the ammonium salts were chosen to compare their

results. Higher N values were observed when using NH_4TFA compared to NH_4HCO_2 , but k was slightly lower which reduced R_s (Figure 6.S5A, Table 6.S1). $\text{NH}_4\text{Formate}$ also provided higher MS sensitivity and higher reproducibility than NH_4TFA . When the amount of $\text{NH}_4\text{Formate}$ fluctuated from 0.5wt% to 0.05wt%, less salt increased k and α but decreased N (Figure 6.S5A, Table 6.S1). An equal acid-base amount (v/v) was initially chosen with AA-TEA, and as the ratio of AA-TEA increased, k and N decreased (Figure 6.S5B, Table 6.S1). When substituting TEA with NH_4OH , k and N increased, while α remained similar (Figure 6.S5B, Table 6.S1). Also, NH_4OH was favored because TEA is known to suppress MS ionization [5]. The best PIM solvent seemed to be MeOH- $\text{NH}_4\text{Formate}$ (100:0.1, v/w) due to its simplicity, moderate R_s , and fast analysis (< 5 min) for most amines at 1 mL/min. Typically, the pressure at 1 mL/min with a 100 x 4.6 mm (i.d.) column was observed to be ~100 bar. Thus the flow could be increased, or longer columns used with conventional HPLCs (<300 bar). If analysis time was long and $R_s > 2.5$, k and α could be decreased by increasing the salt concentration, which was especially useful for NS, which primarily used MeOH- $\text{NH}_4\text{Formate}$ (100:0.2, v/w) for PIM optimizations. On the other hand, if more retention was needed, the salt concentration was decreased or the acid-base combination, mostly AA- NH_4OH , was utilized.

6.S1.4. Normal phase (NP)

NP was only used if the amine could not be baseline separated since nonpolar solvents do not benefit the use of MS. NP solvents were comprised of a nonpolar solvent, heptane or hexane, and an organic modifier, EtOH, with the addition of TFA-TEA (0.3:0.2, v/v). When the amount of EtOH was decreased k increased. Also, Hep provided higher k than Hex (Figure 6.S6A, Table 6.S1). Our study began with the use of just Hex and the organic modifier EtOH, with no additives using LS-P. Contrary to crown ethers, LS-P does not need acid-base additives or extreme acidic

conditions for separation [7-8] (*Figure 6.S6A*). However, additives improved α (*Figure 6.S6B*, *Table 6.S1*). Peak fronting was observed for chiral amines when only acid was added, which has been attributed to interactions of the basic amine with the weakly acidic silica support, and no α was observed with only base (*Figure S6B*) [9]. When in combination, the best N and α was observed when using TFA-TEA (0.3:0.2, v/v) (*Figure 6.S6B*, *Table 6.S1*). NP solvents were occasionally used for other CSPs, and these conditions, Hep-EtOH-TFA-TEA (60:40:0.3:0.2, v/v/v/v) or Hex-EtOH-TFA-TEA (70:30:0.3:0.2, v/v/v/v), were found to perform well.

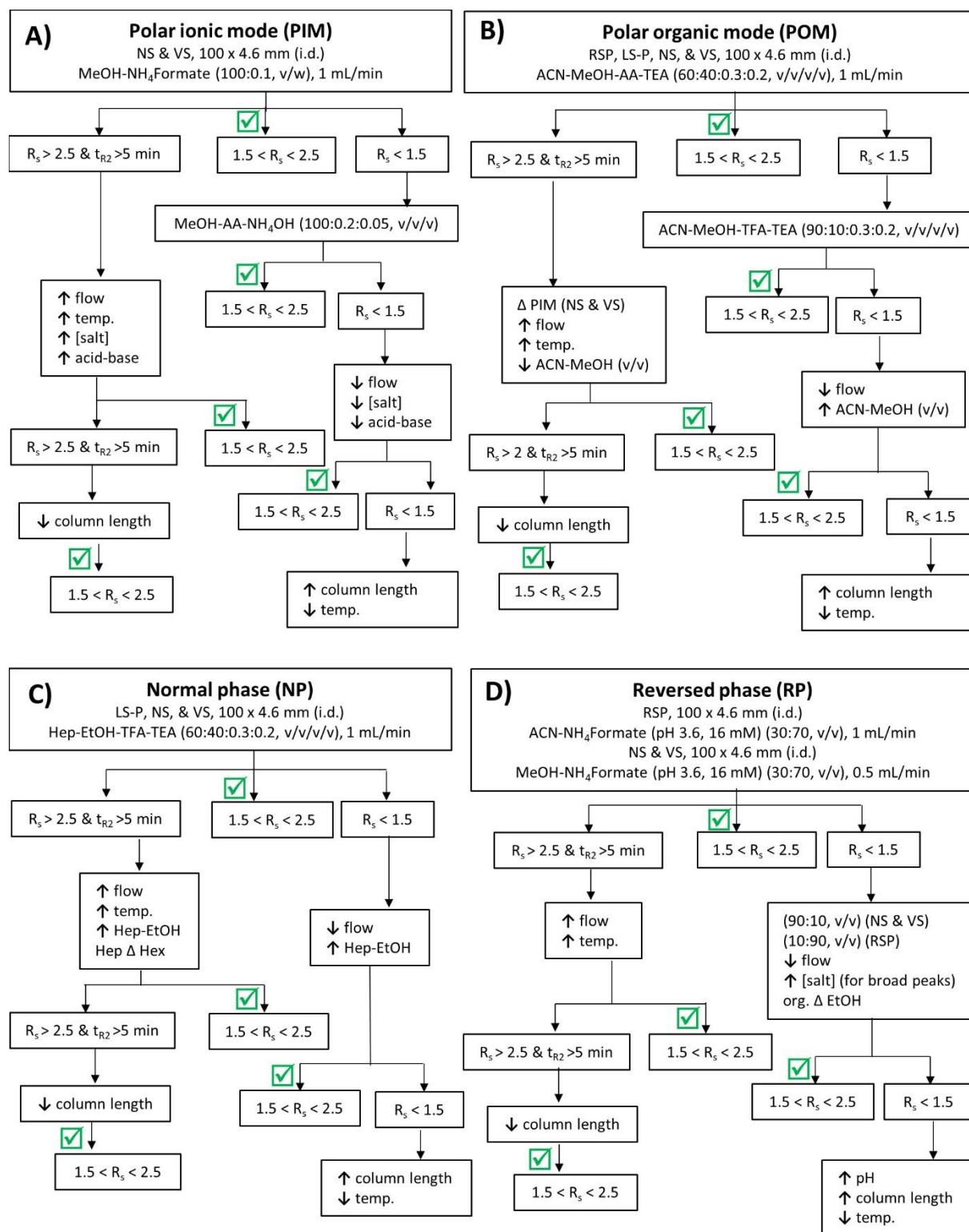


Figure 6.S1(A,B,C,D). Method development of chiral amines using SPP CSPs: CDS_{Shell}-RSP (RSP), Larihc_{Shell}-P (LS-P), Nico_{Shell}

(NS), and VancoShell (VS) in (A) polar ionic mode (PIM), (B) polar organic mode (POM), (C) normal phase, and (D) reversed phase (RP), See section S1 for all solvent abbreviations (ACN, MeOH, AA, TEA, NH₄HCO₂), and section 6.2.4 for all chromatographic parameter abbreviations (R_s, t_{R2}). Other abbreviations include temperature (temp.) and Δ, which represents “switch to.”

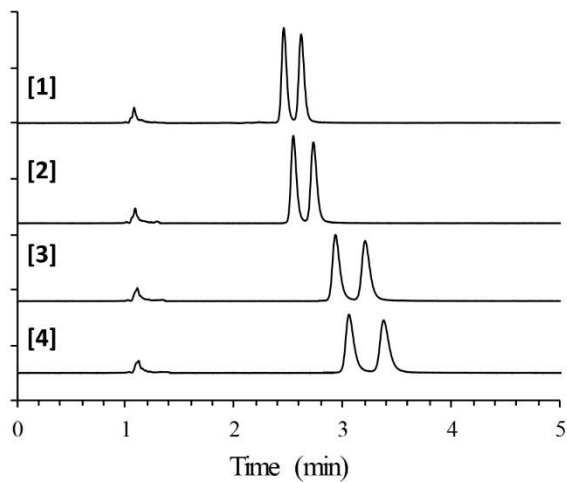


Figure 6.S2 Effect of temperature. All separations of methylone were performed with V, 100 x 4.6 mm (i.d.), at 1.0 mL/min using UV at 220 nm. Mobile phase conditions: MeOH/NH₄HCO₂ (100:0.1, v/w) [1] 30 °C, [2] 25 °C, [3] 15 °C, [4] 10 °C. See section 6.S1 for all abbreviations.

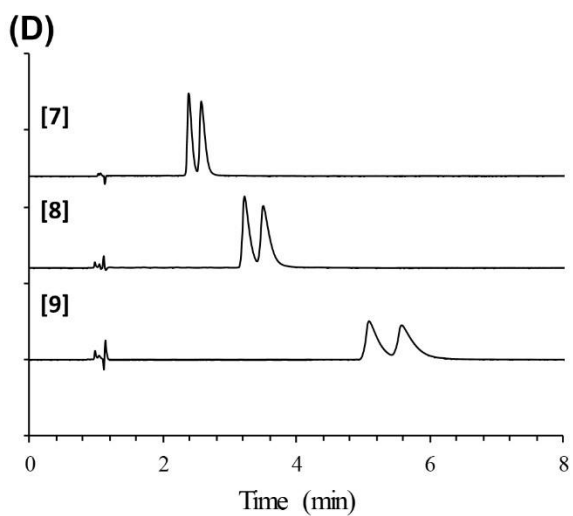
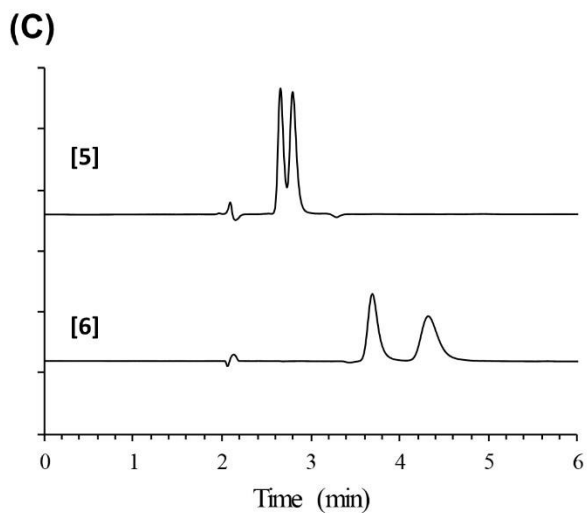
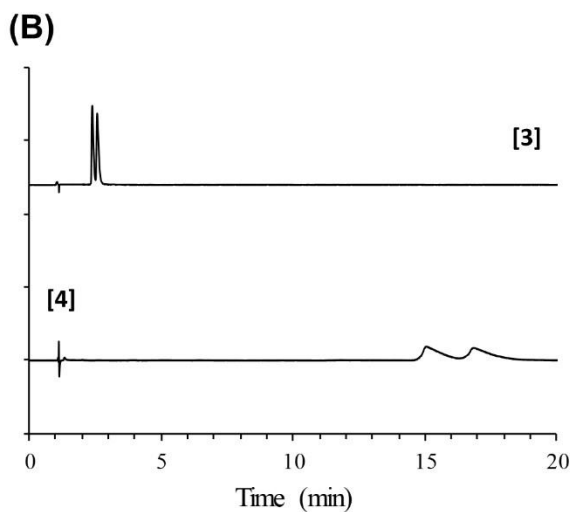
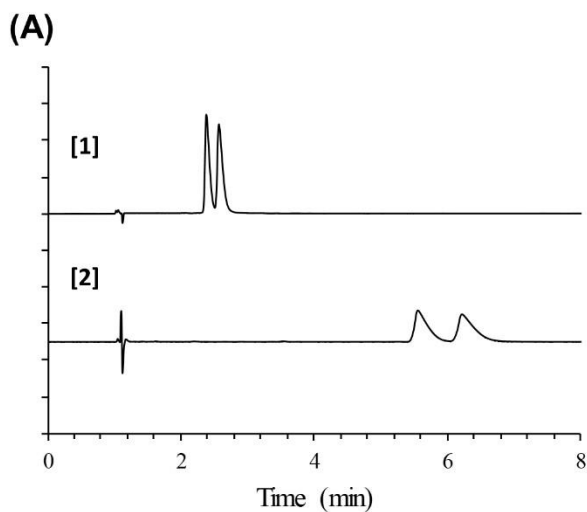


Figure 6.S3(A,B,C,D): Effect of additives in reversed phase All separations were of methorphan with 100 x 4.6 mm (i.d.) columns: (A,B,D) RSP, (C) VS at 1.0 mL/min (except [5,6] at 0.5 mL/min) and 25 °C using UV at 230 nm. Mobile phase conditions: [1,3,5,7] ACN-NH₄HCO₂ (16 mM, pH 3.6) (30:70, v/v), [2] ACN-NH₄HCO₂ (16 mM, pH 3.6) (20:80, v/v), [4,6] MeOH-NH₄HCO₂ (16 mM, pH 3.6) (30:70, v/v), [7] ACN-NH₄HCO₂ (16 mM, pH [5.0]) (30:70, v/v), [8] ACN-NH₄HCO₂ (16 mM, pH [6.2]) (30:70, v/v).

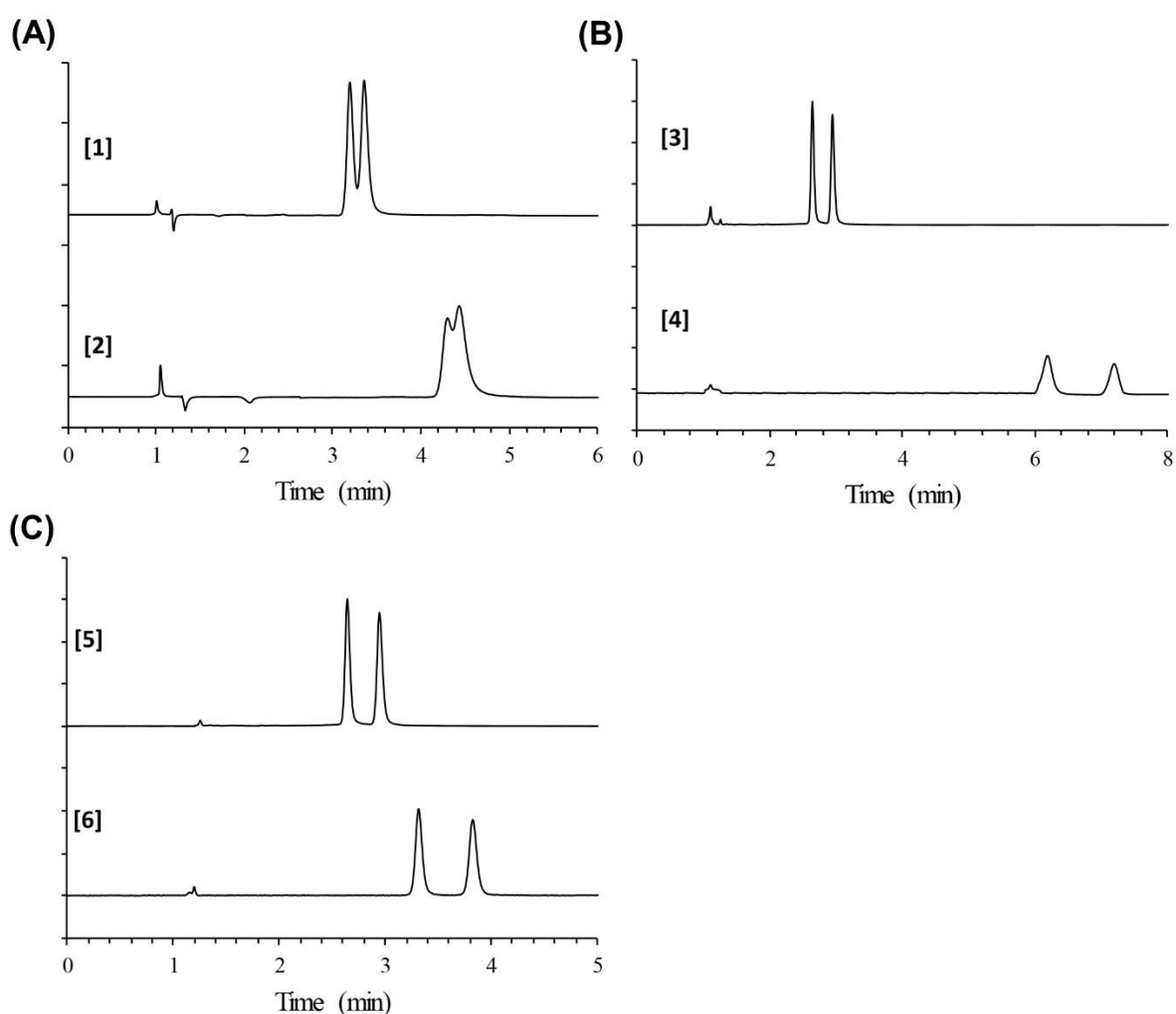


Figure 6.S4(A,B,C): Effect of additives in the polar organic mode. All separations were of 1-(1-naphthylethylamine) with 100 x 4.6 mm (i.d.) columns, (A) VS and (B,C) LS-P, at 1 mL/min and

25 °C using UV at 220 nm. [1,3,5] ACN-MeOH-AA-TEA (60:40:0.3:0.2, v/v/v/v), [2,4] ACN-MeOH-AA-TEA (80:20:0.3:0.2, v/v/v/v), [6] ACN-MeOH-TFA-TEA (90:10:0.3:0.2, v/v/v/v). See section 6.S1 for all abbreviations.

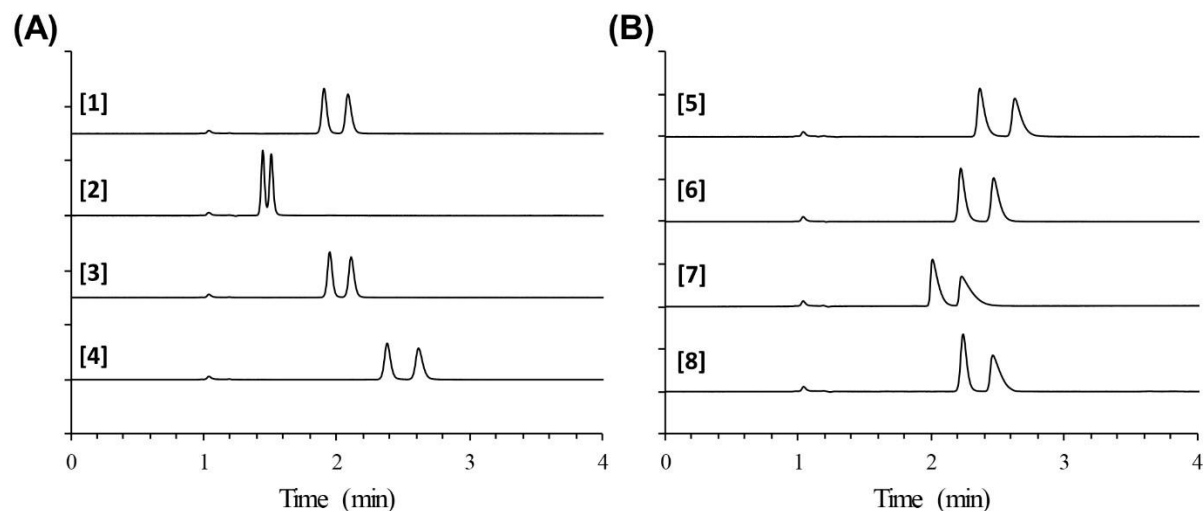


Figure 6.S5(A,B): Effect of additives in the polar ionic mode: (A) salt additives and concentration effect (B) acid and base additive ratios. All separations of amphetamine were performed with V, 100 x 4.6 mm (i.d.), at 1.0 mL/min, and 25 °C using UV at 220 nm. Mobile phase conditions: [1] MeOH-NH₄TFA (100:0.1, v/w), [2] MeOH-NH₄HCO₂ (100:0.5, v/w), [3] MeOH-NH₄HCO₂ (100:0.1, v/w), [4] MeOH-NH₄HCO₂ (100:0.05, v/w), [5] MeOH-AA-TEA (100:0.1:0.1, v/v/v), [6] MeOH-AA-TEA (100:0.1:0.05, v/v/v), [7] MeOH-AA-TEA (100:0.1:0.02, v/v/v), [8] MeOH-AA-NH₄OH (100:0.1:0.02, v/v/v). See section 6.S1 for all abbreviations.

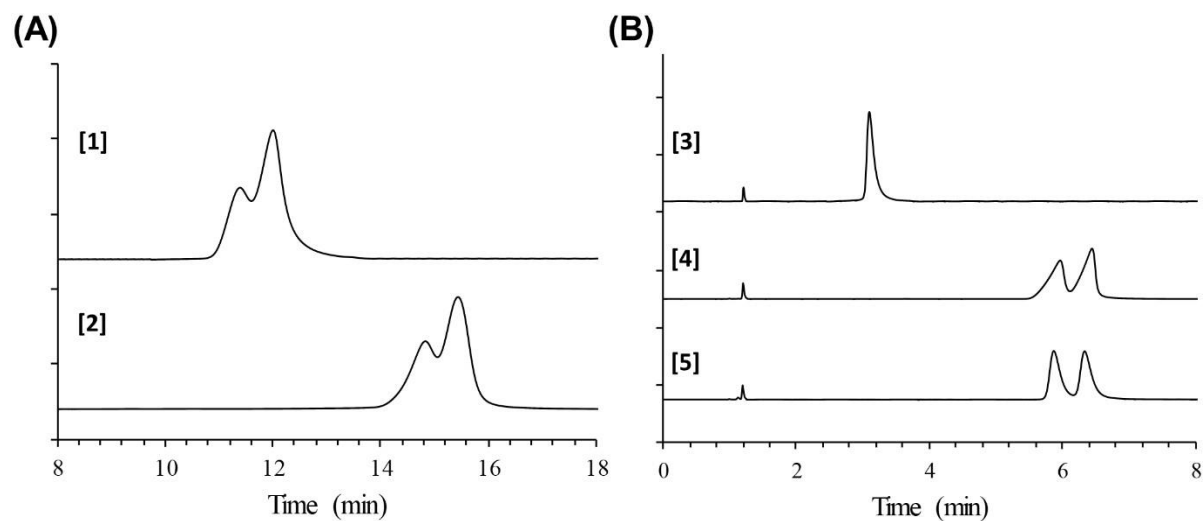


Figure 6.S6(A,B): Effect of additives in normal phase. All separations were of cathinone with LS-P, 100 x 4.6 mm (i.d.), at 1 mL/min, and 25 °C using UV at 254 nm. [1] Hex-EtOH (70:30, v/v), [2] Hep-EtOH (70:30, v/v), [3] Hex-EtOH-TEA (70:30:0.1, v/v/v), [4] HexEtOH-TFA (70:30:0.1, v/v/v), [5] Hex-EtOH-TFA-TEA (70:30:0.3:0.2, v/v/v/v). See section 6.S1 for all abbreviations.

Table 6.S1: Chromatographic data referring to Supplemental figures S2, S3(A,B,C,D), S4(A,B,C), S5(A,B), S6(A,B).

Figure ¹	[#] ²	N (1 st , 2 nd peaks) ^{3a}	k_1 ^{3b}	α ^{3c}	R_s ^{3d}
2	1	12839, 12301	1.5	1.11	1.8
2	2	11512, 11158	1.5	1.12	1.9
2	3	9070, 8710	1.9	1.14	2.1
2	4	7879, 7526	2.1	1.16	2.2
3A	1	6263, 5122	1.4	1.14	1.4
3A	2	4197, 3667	4.6	1.15	1.7
3B	3	7632, 5699	0.4	1.17	1.2
3B	4	2353, 2272	14.1	1.13	1.3
3C	5	8499, 6763	0.3	1.21	1.1
3C	6	4878, 2371	0.8	1.37	2.2
3D	7	6263, 5122	1.4	1.14	1.4

1 Refer to labeled supplemental figure.

2 # indicates the bracketed number labeled in each supplemental figure chromatogram.

3 ^{a,b,c,d} See section 2.4 for calculations, N: efficiency (# plates), k_1 : retention factor of the first peak (min), α : selectivity, R_s : resolution.

3D	8	5033, 3734	2.2	1.12	1.3
3D	9	3955, 3113	4.1	1.12	1.3
4A	7	9401, 8424	2.2	1.07	1.2
4A	8	6508, 4773	3.3	1.04	0.6
4B	9	12839, 12837	1.6	1.18	3.4
4B	10	10168, 10225	5.2	1.19	3.9
4C	1	12839, 12837	1.6	1.18	3.4
4C	2	15559, 15190	2.3	1.22	4.0
5A	1	12994, 11723	0.9	1.18	2.1
5A	2	14954, 14007	0.5	1.14	1.3
5A	3	12172, 11469	1.0	1.17	2.4
5A	4	11732, 10688	1.4	1.17	2.5
5B	5	10399, 8542	1.4	1.19	2.4
5B	6	9963, 7615	1.2	1.20	2.5
5B	7	6412, 3257	1.0	1.21	1.7
5B	8	11329, 5413	1.2	1.20	2.0
6A	1	2269,2443	10.2	1.06	0.7

6A	2	3298, 3011	13.8	1.06	0.7
6B	3	4208	2.1	1.00	0
6B	4	3070, 4891	5.0	1.10	1.2
6B	5	8693, 8364	5.8	1.12	1.5

6.S5 References:

1. P. Sandra, Resolution–definition and nomenclature, *J. High. Resolut. Chromatogr.* 12 (1989) 82-86.
2. D.W. Armstrong, R.M. Woods, Z.S. Breitbach, Z.S. Comparison of enantiomeric separations and screening protocols for chiral primary amines by SFC and HPLC, *LC-GC North America* 32 (2014) 742-752.
3. U.B. Nair, S.S.C. Chang, D.W. Armstrong, Y.Y. Rawjee, D.S. Eggleston, J.V. McArdle, Elucidation of vancomycin's enantioselective binding site using its copper complex, *Chirality* 8 (1996) 590-595.
4. A. Berthod, Chiral recognition mechanisms with macrocyclic glycopeptide selectors, *Chirality* 21 (2009) 167-175.
5. CHIROBIOTIC™ Handbook, 5th ed.; Advanced Separation Technologies, Inc., NJ, 2004, https://www.sigmaaldrich.com/content/dam/sigma-aldrich/docs/Sigma/General_Information/chirobiotic_handbook.pdf (accessed 03 January 2018).
6. T.E. Beesley, J.T. Lee, Method development strategy and applications update for CHIROBIOTIC chiral stationary phases, *J. Liq. Chromatogr. Rel. Technol.* 32 (2009) 1733-1767.
7. Y.-C. Na, N.L.T. Padivitage, M.K. Dissanayake, D.W. Armstrong, Binding characteristics of native cyclofructan 6 and its derivatives with metal ions, *Supramol. Chem.* 26 (2014) 705-713.
8. W.H. Pirkle, J.M. Finn, J.L. Schreiner, B.C. Harper, A widely useful chiral stationary phase for the high-performance liquid chromatography separation of enantiomer, *J. Am. Chem. Soc.* 103 (1981) 3964-3966.
9. P. Sun, C. Wang, Z.S. Breitbach, Y. Zhang, D.W. Armstrong, Development of new HPLC chiral stationary phases based on native and derivatized cyclofructans, *Anal. Chem.* 81 (2009) 1021510226.

Chapter 7

A comprehensive methodology for the chiral separation of 40 tobacco alkaloids and their carcinogenic E/Z-(R,S)-tobacco-specific nitrosamine metabolites

7.1 Abstract

The predominant enantiomer of nicotine found in nature is (S)-nicotine and its pharmacology has been widely established. However, pharmacologic information concerning individual enantiomers of nicotine-related compounds is limited. Recently, a modified macrocyclic glycopeptide chiral selector was found to be highly stereoselective for most tobacco alkaloids and metabolites. This study examines the semisynthetic and native known macrocyclic glycopeptides for chiral recognition, separation, and characterization of the largest group of nicotine-related compounds ever reported (tobacco alkaloids, nicotine metabolites and derivatives, and tobacco-specific nitrosamines). The enantioseparation of nicotine is accomplished in less than 20 seconds for example. All liquid chromatography separations are mass spectrometry compatible for the tobacco alkaloids, as well as their metabolites. Ring-closed, cyclized structures were identified and separated from their ring-open, straight chain equilibrium structures. Also, E/Z-tobacco-specific nitrosamines and their enantiomers were directly separated. E/Z isomers also are known to have different physical and chemical properties and biological activity. This study provides optimal separation conditions for the analysis of nicotine-related isomers, which in the past have been reported to be ineffectively separated which can result in inaccurate results. The methodology of this study could be applied to cancer studies, and lead to more information about the role of these isomers in other diseases and as treatment for diseases.

7.2 Introduction

Tobacco smoke has been reported to contain at least 60 carcinogens and several have been directly related to cancer [1]. Tobacco and its derived products constitute a leading preventable cause of death in the United States (US) [2]. The Food and Drug Administration (FDA) regulates all commercial tobacco products via the Family Smoking Prevention and Tobacco Control Act and the extension, the Deeming Rule [3-4]. Recently, the FDA also announced a comprehensive plan for lowering the nicotine (NIC) content in cigarettes to make them less or non-addictive [5]. To facilitate dependence, the reduced amount has been estimated to be 0.05 mg NIC compared to the current range of 0.5-1.5 mg NIC yield in one cigarette [1,6]. One challenge might be that smokers turn to other tobacco products for the higher NIC content compared to reduced NIC content cigarettes, such as smokeless tobacco products, which are connected to oral and esophageal cancers [7]. Smokeless tobacco products, like moist snuff, have been determined to contain tobacco-specific nitrosamines (TSNAs), which have been shown to be responsible for oral cavity cancer from smokeless tobacco [7]. The most prevalent and toxic TSNAs have been reported as *N*'-nitrosonornicotine (NNN) and 4-(methylnitrosamino)-1-(3-pyridyl)-1-butanone (NNK) [1].

The other main TSNAs, *N*'-nitrosoanatabine (NAT) and *N*'-nitrosoanabasine (NAB), haven't shown as potent carcinogenicity in laboratory animals [7-8]. In one study, 12 rats were treated with racemic NNN and 96 oral cavity tumors and 153 esophageal tumors were observed [8]. Also, the (S)-NNN enantiomer was determined to be more tumorigenic than (R)-NNN indicating that the stereochemistry of this compound is highly important [8].

In 2017, the FDA proposed, "The mean level of *N*'-nitrosonornicotine in any batch of finished smokeless tobacco product not exceed 1 microgram per gram ($\mu\text{g/g}$) of tobacco (on a dry weight basis) at any time through the product's labelled expiration date as determined by specified product testing." [9]. Current commercial US smokeless tobacco products contain NNN levels ranging

from 1 to 10 $\mu\text{g/g}$ dry weight [10]. NNN is formed by the nitrosation of NIC and nornicotine (NNIC), which is a tobacco alkaloid native to tobacco, as well as a nicotine metabolite [7]. The level of NNIC is dependent on the leaf senescence and curing process [7,11]. Tobacco strains with less (S)-NNIC have been reported to contain less (S)-NNN [11]. Therefore, genetic engineering efforts have been focused on reducing the inherent amount of NNIC [11]. Also, NNN can be formed endogenously, which was shown when NNN was found in saliva after using NIC replacement therapies [12]. Furthermore, NNN metabolizes to another TSNA, *N*'-nitrosornicotine-1-*N*-oxide (NNNO), which has been shown to be less carcinogenic than NNN in F344 rats and Syrian golden hamsters [13].

The other major carcinogen found in unburnt tobacco and tobacco smoke is NNK, an achiral TSNA, which is formed from NIC during the curing and processing of tobacco [7]. NNK was found to be the only potent lung carcinogen that formed tumors in rats, mice, and hamsters [14]. Metabolites of NNK and other TSNAs are known to bind to DNA once activated, forming adducts that can cause oncogene activation leading to tumor development if they persist [7]. Long-term exposure to these mutation events can lead to cancer and death [7]. NNK is known to metabolize mainly to 4-(methylnitrosamino)-1-(3pyridyl)-1-butanol, NNAL, and its glucuronides [15]. Since NNK and NNAL are only found in tobacco and not from any other source, they can be used as highly specific biomarkers of carcinogen exposure, especially second-hand smoke exposure [16]. Also, the ratio of NNAL-glucuronide to NNAL has been used as a biomarker of susceptibility to lung cancer [16].

NNAL has been reported to have similar toxicity as NNK, with a higher tumorigenicity of the R-NNAL enantiomer than (S)-NNAL, due to preferential metabolic activation [17]. NNK, NNAL, and NNN were reported to form E/Z isomers [18-20]. The relative level of E isomers was higher

than Z isomers [18-20]. Some previous reports have shown the separation of a few TSNAs, but most do not report the separation of both their enantiomers and E/Z isomers [20-23]. Thus, some researchers have expressed confusion because the tops of their TSNA chromatographic peaks show splitting [24]. However, TSNAs are known to interconvert between E/Z isomers [18-20]. Chiral capillary electrophoresis has been used to separate E/Z-NNK and (R,S)-(E/Z)-NNAL [20]. Also, achiral nitrosamines, other than TSNAs, have been separated by LC into their E/Z isomers. For example, fish toxicants like 6',7'-acetylenic nitrosamines were efficiently resolved with an achiral LC method [25]. Using a similar LC method, but with the addition of chiral derivatizing agents, the indirect separation of (R)-(E/Z) and (S)-(E/Z)-TSNA isomers were performed [18-19]. The approach described in this work provides a direct and efficient separation of both E/Z isomers and their enantiomers as well as indicating if isomeric interconversions occur under "ordinary" conditions. In jaundice phototherapy, toxic, unconjugated bilirubin is isomerized to several E/Z configurations [26]. This isomerization makes bilirubin become more soluble in plasma so it can be excreted by the liver [26]. Therefore, E/Z isomers have different physical and biological properties and should be further studied with TSNAs.

TSNAs are nitrosated metabolites of chiral tobacco alkaloids, which have similar structures as NIC [7]. NIC is predominantly found as the (S)-(-) enantiomer in tobacco plants [27]. The percent (R)-(+)-NIC in tobacco, and medicinal products derived from tobacco was reported to be in the 0.1 to 1.2% range [27]. The pharmacology of (R)-(+)-NIC has not been an area of great concern, most likely because human exposure and intake of (R)-(+)-NIC is minimal. However, the individual enantiomers have been examined for their use as therapies for neurodegenerative diseases. These studies have reported that NIC enantiomers have different pharmacological effects, such as oxidative stress, weight loss, and binding mechanisms [28-30]. (R)-NIC has been reported as

eighty times less cytotoxic than (S)-NIC, when considering their metabolites [30]. A recent study determined new smoking products (e-liquids), which have synthetic NIC (tobacco-free nicotine, TFN), contained 50% of (R)-(+)-NIC [31]. Since new products contain higher (R)-NIC levels than in tobacco-derived products, it was suggested that the pharmacology of (R)-NIC should be more extensively studied [31]. The binding affinity of (R)-NIC to nicotine acetylcholine receptors was estimated to be 10 times lower than (S)-NIC, which might result with a less stimulating dopaminergic response [30]. New TFN products with higher (R)-NIC might be analogous to commercial products with less addictive NIC levels.

While (S)-NIC is the main alkaloid in tobacco products, minor chiral alkaloids also are present including NNIC, anatabine (AT), and anabasine (AB) [32]. The R-enantiomers of minor tobacco alkaloids have been reported to be present at higher relative levels than (R)-(+)-NIC [32]. Most biomarker strategies utilize tobacco alkaloids or their metabolites, such as the major chiral metabolite, cotinine (COT). COT is used to measure NIC uptake, due to its long half-life, such as in smoking cessation trials and tobacco exposure tests [33]. However, tobacco alkaloids are useful to differentiate the use of tobacco while using NIC replacement therapies [34]. Also, chiral alkaloids have been reported to be useful as therapies for neurodegenerative diseases by mimicking NIC's neuropharmacological and neuroprotective effects [30,35]. Enantiomers are well known to have different pharmacological effects, e.g. (R)-AB was reported to be more toxic and cause more birth defects than (S)-AB [36]. So, if these alkaloids were developed into medicinal products, the FDA would require, in their words, "the pharmacology and toxicology of the enantiomer should be characterized for the principal effects and any other pharmacological effect, with respect to potency, specificity, maximum effect, etc." [37]. However, most analytical methods do not have the capability to analyze the individual enantiomers of these alkaloids and metabolites, so new

more effective methods are needed. To quantitate and perform biological studies, it would be useful if such “chiral methods” were compatible with mass spectrometry (MS).

Some separation approaches for chiral nicotine-related compounds, more importantly the carcinogenic compounds, have been reported, but most have disadvantages that limit the analysis. Most analyses are similar to those of achiral nitrosamine analysis and do not have the capability of separating enantiomers, such as a study which determined the amount of TSNAs in replacement liquids for electronic cigarettes [38]. One chiral approach reported the separation of NIC and several alkaloids using a packed liquid chromatography (LC) microcolumn with a β -cyclodextrin mobile phase but required three hours [39].

Other previous approaches mainly utilized chiral gas chromatography (GC) or chiral derivatization LC [18,23,32]. GC isn't best suited for the biological analysis of these compounds due to the thermal liability of the sample. Chiral derivatization LC methods increase cost and analysis times and rely on the purity of the chiral derivatization agent. The best approach for chiral separations of nicotine-related compounds is using LC chiral stationary phases (CSPs). Enantioseparations of three tobacco alkaloids using LC CSPs have been reported, but they used normal phase solvents, which are not compatible with MS [36,40].

These alkaloids might be possible targets for neurodegenerative therapies, but these methods won't be compatible for biological analysis [30].

Recently, a fast, high efficiency, mass spectrometry compatible, chiral LC approach was developed to analyze NIC in TFN commercial e-liquids [31]. Herein we examine this approach for applicability for the sensitive identification and enantiomeric quantification of most nicotine-related compounds and metabolites in commercial tobacco products and biological samples. Focus

is paid to the LC separation of carcinogenic compounds, like NNN or NNK, and other complex isomeric mixtures that have not been reported to separate previously. This study examines the effectiveness of new and known macrocyclic glycopeptide chiral selectors in resolving the most comprehensive set of chiral nicotine-related compounds yet investigated, including minor tobacco alkaloids, metabolites, synthetic related compounds, and E/Z-TSNAs [31,41-44]. Further, only LC-MS compatible formats were considered.

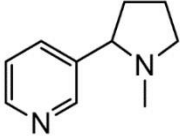
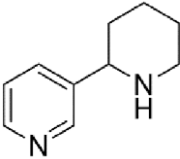
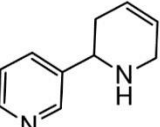
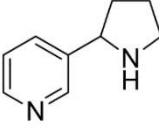
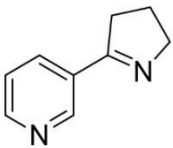
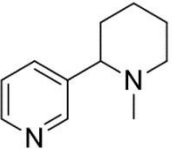
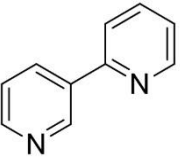
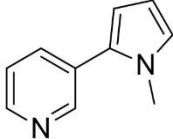
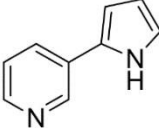
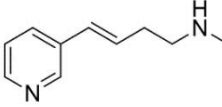
7.3 Materials and methods

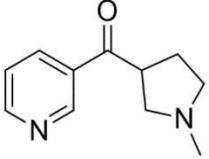
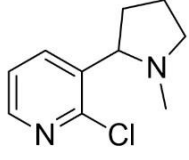
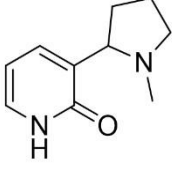
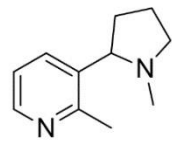
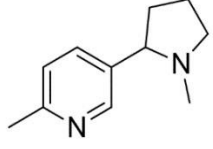
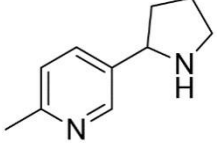
Native vancomycin (VancoShell, V, 100 x 4.6 mm inner diameter (i.d.)) and teicoplanin (TeicoShell, T, 100 x 4.6 mm i.d.), hydroxypropyl- β -cyclodextrin (CDShell-RSP, 100 x 4.6 mm i.d.), quinine (Q-Shell, 100 x 4.6 mm i.d.) and modified macrocyclic glycopeptide (NicoShell, N, 100 x 4.6 mm i.d.) CSPs were bonded to superficially porous particles (SPP), and obtained from AZYP, LLC. (Arlington, TX, USA).

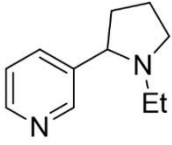
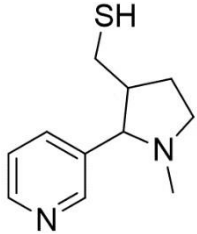
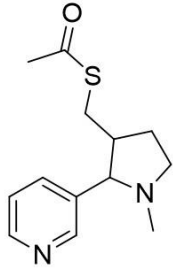
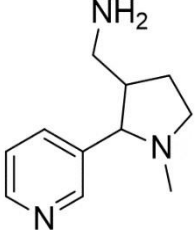
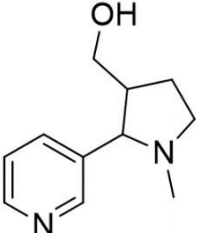
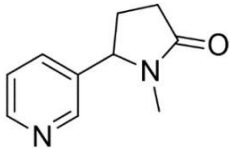
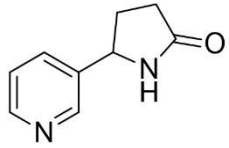
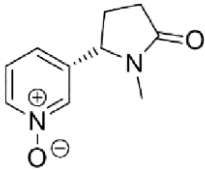
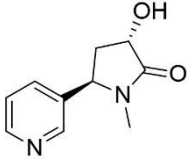
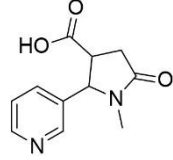
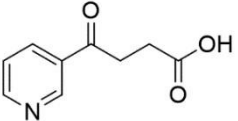
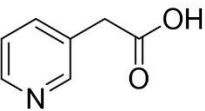
An Eclipse XDB-C18 (C18), 5 μ m, 150 x 4.6 mm i.d. column was obtained from Agilent Technologies (Palo Alto, CA, USA). A broad set of nicotine-related compounds were selected (see *Table 5.1* for structures drawn as manufacturer label and acronyms, * denotes chiral compounds) and all chiral compounds were obtained as racemic analytical standards from Toronto Research Chemicals (Toronto, Canada) except cotinine-N-oxide (CNO) and *trans*-3'-hydroxycotinine (T3HC). Also, individual enantiomers of AT, AB, NIC, NNIC, COT, NNN, NAT, and NAB were obtained. An achiral compound, metanicotine (MET) was obtained as an E isomer. TSNAs were obtained as racemates, but these compounds are also known to exist as a mix of E/Z isomers and were not labelled accordingly. The standards were diluted with methanol to concentrations of 1 mg/mL and stored 24 hours before analysis.

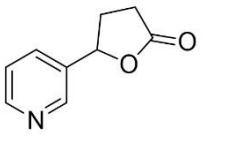
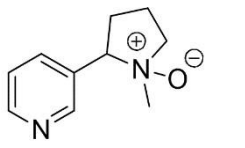
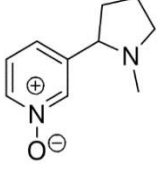
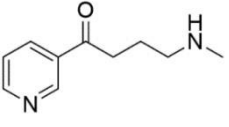
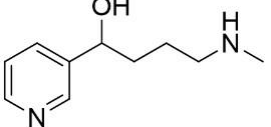
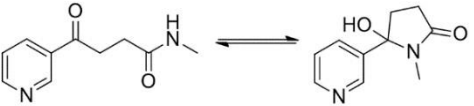
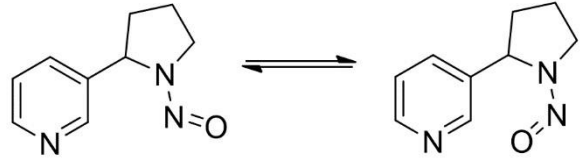
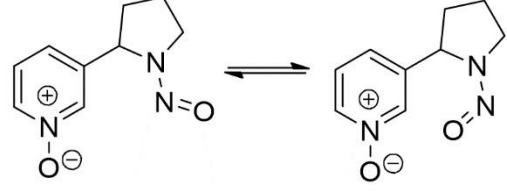
Table 7.1. Structures of nicotine-related compounds (all chiral compounds denoted by *).

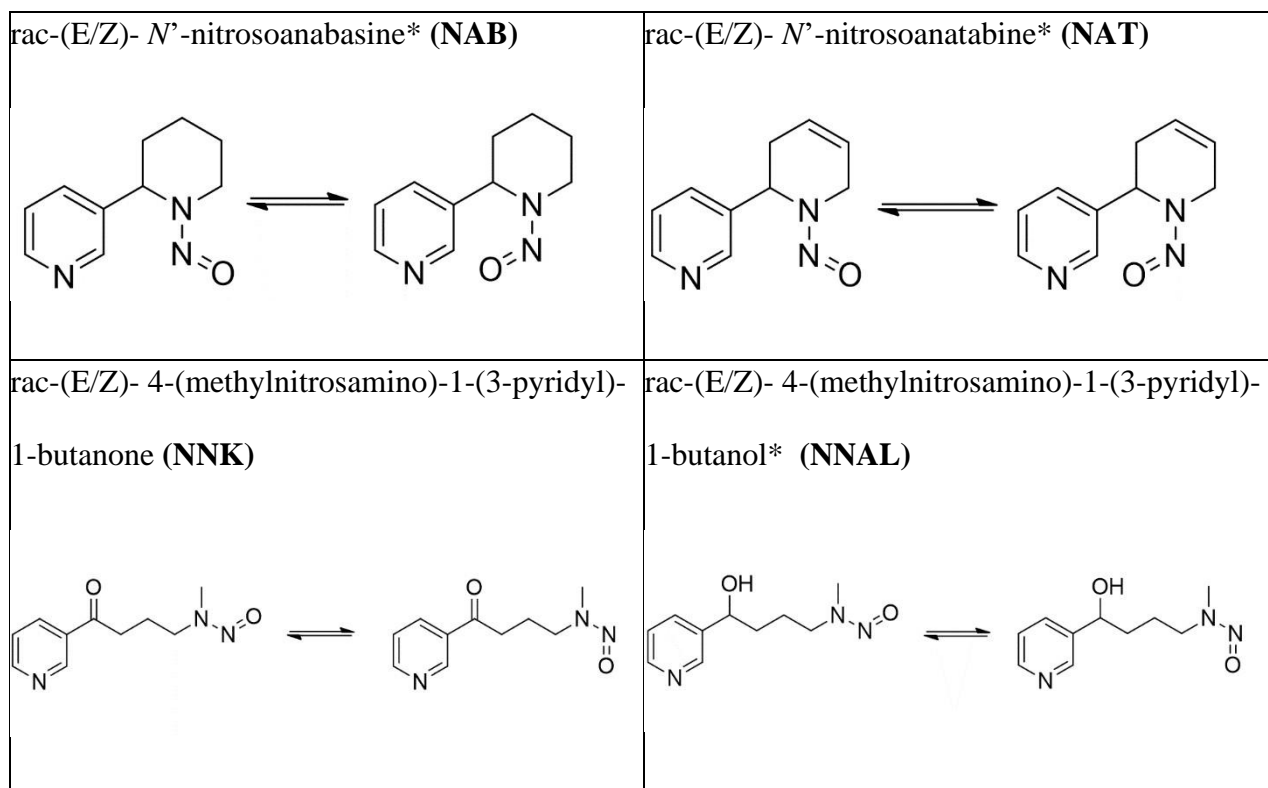
a) Tobacco alkaloids

<p>Nicotine* (NIC)</p> 	<p>Anabasine* (AB)</p> 	<p>Anatabine* (AT)</p> 	<p>Nornicotine* (NNIC)</p> 	<p>Myosmine (MYS)</p> 
<p>Nmethylanabasine* (MAB)</p> 	<p>2,3'-bipyridyl (BPY)</p> 	<p>β-nicotyryne (β-NT)</p> 	<p>β-nornicotyryne (β-NNT)</p> 	<p>Metanicotine (E) (MET)</p> 
<p>b) Synthetic derivatives</p>				

<p>1-methyl-3nicotinoylpyrrolidine(2CN) * (1M3NP)</p> 	<p>2-chloronicotine* (2CN)</p> 	<p>2-hydroxynicotine* (2HN)</p> 	<p>2-methylnicotine* (2MN)</p> 	<p>6-methylnicotine* (6MN)</p> 
<p>6-methylnornicotine* (6MNN)</p> 	<p>rac-(2S,3S & 2R,3R)-trans-3'thiomethyl nicotine* (T3TMN)</p>	<p>rac-(2S,3S & 2R,3R)-trans-3'acetylthiomethylnicotine* (T3ATMN)</p>	<p>rac-(2S,3R & 2R,3S)-trans-3'aminomethyl nicotine* (T3AMN)</p>	<p>rac-(2S,3S & 2R,3R)-trans-3'hydroxymethyl nicotine* (T3HMN)</p>

<p>N-ethyl-nornicotine*</p> <p>(NENN)</p> 				
<p>c) Metabolites</p>				
<p>Cotinine*</p> <p>(COT)</p> 	<p>Norcotinine*</p> <p>(NCOT)</p> 	<p>(5S)-Cotinine-Noxide</p> <p>(CNO)</p> 	<p><i>trans</i>-(3S,5R)-3'-hydroxy-cotinine</p> <p>(T3HC)</p> 	<p><i>rac-trans</i>-(2S,3R & 2R,3S)-cotinine carboxylic acid*</p> <p>(4TCCA)</p> 
<p>γ-oxo-3-pyridinebutyric acid</p> <p>(OPBA)</p> 	<p>5-(3-pyridyl)tetrahydro-2furanone*</p> <p>(5THF)</p>	<p>3-pyridylacetic acid</p> <p>(LAC)</p> 	<p><i>rac</i>-Nicotine-1'-N-oxide* (S,S & R,R)</p> <p>(NNO)</p>	<p>Nicotine-1-oxide*</p> <p>(NO)</p>

				
4-(methylamino)-1-(3-pyridyl)-1-butanone (NAN)	rac -4-(methylamino)-1-(3-pyridyl)-1-butanol* (NAL)	N-methyl-4-(3-pyridyl)-1-butanol (OPBN) to 5'-hydroxycotinine* (5HCOT)		
				
d) (E/Z)-Tobacco-specific nitrosamines				
		rac-(E/Z)-N'-nitrosornicotine-1-N-oxide* (NNNO)		
rac-(E/Z)-N'-nitrosornicotine* (NNN)				



High performance LC grade methanol (MeOH) was obtained from Sigma-Aldrich (St. Louis, MO, USA) as well as acetonitrile (ACN), acetic acid (HOAc), ethanol (EtOH), triethylamine (TEA), ammonium hydroxide (NH₄OH), ammonium formate (NH₄Formate), and ammonium trifluoroacetate (NH₄TFA).

Water was purified by a Milli-Q water purification system (Millipore, Billerica, MA, USA).

A 1260 high performance LC instrument (Agilent Technologies, Palo Alto, CA, USA) was used in this study. It consisted of a 1200 diode array detector, autosampler, column oven, and quaternary pump. Also, a Shimadzu triple quadrupole LC-MS instrument, LCMS-8040, (Shimadzu, Tokyo, Japan) was used. All MS was operated in positive ion mode with an electron spray ionization source. The parameters were set as follows: nebulizer gas flow, 3 L/min; drying gas flow, 15 L/min; desolvation line temperature, 250 °C; heat block temperature, 400 °C. All separations were

carried out at room temperature, unless otherwise noted, using an isocratic method. All analytes were screened, then optimized using a variety of mobile phases in the polar ionic mode (PIM), polar organic mode (POM), and reversed phase (RP) with all stationary phases. The mobile phases were degassed by ultrasonication under vacuum for 5 minutes. The UV wavelengths 220 and 263 nm were utilized for detection. Chiral separations were optimized (as shown in *Table 7.2*) with the following mobile phases: PIM1: 100/0.1wt%: MeOH/NH₄TFA; PIM2: 100/0.025wt%: MeOH/NH₄Formate; PIM3: 100/0.5wt%: MeOH/NH₄Formate; PIM4: 100/0.2wt%: MeOH/NH₄Formate; PIM5: 100/0.2/0.05: MeOH/HOAc/NH₄OH; POM1: 60/40/0.3/0.2: ACN/MeOH/HOAc/NH₄OH; POM2: 50/50/0.3/0.2: ACN/MeOH/HOAc/NH₄OH; POM3: 100: MeOH; RP1: 90/10: MeOH/16 mM NH₄Formate pH 3.6; RP2: 90/10: EtOH/16 mM NH₄Formate pH 3.6; RP3: 30/70: MeOH/16 mM NH₄Formate pH 3.6; RP4: 30/70: ACN/16 mM NH₄Formate pH 3.6; RP5: 10/90: ACN/16 mM NH₄Formate pH 3.6.

The dead time, t_0 , was determined by the peak of the refractive index change due to the unretained sample solvent. Retention factors (k) were calculated using $k = (t_R - t_0) / (t_0)$, where t_R is the retention time of the first peak. Selectivity (α) was calculated using $\alpha = k_2 / k_1$, where k_1 and k_2 are retention factors of the first and second peaks, respectively. Resolution (R_s) was calculated using the peak width at half peak height, $R_s = 2(t_{R2} - t_{R1}) / (w_{0.5,1} + w_{0.5,2})$. Each sample was analyzed in triplicate. The relative standard deviation (%RSD) was determined to be within $\pm 1.0\%$ for the resolution of all analytes. Peak area calculations were determined by peak deconvolution according to a previous report [45]. The relative standard deviation (%RSD) was determined to be within $\pm 3.0\%$ for the area ratios reported.

7.4 Results

The enantioseparation of NIC can be obtained in 18 seconds with a $R_s = 2.6$ (*Figure 7.1*).

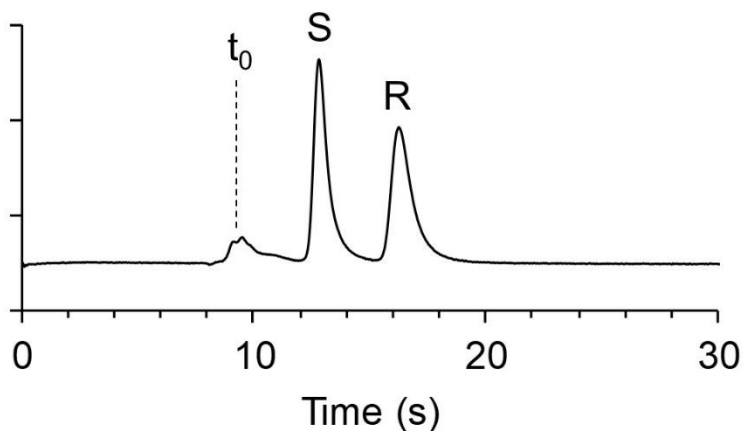


Figure 7.1. Ultra-fast LC enantioseparation of nicotine (NIC) using NicoShell, 50 x 4.6 mm (i.d.), PIM4 at 4 mL/min. S: S-NIC; R: R-NIC; t_0 : impurities at dead time. See Materials and methods for other acronyms and calculations ($k_1 = 0.7$, $\alpha = 1.64$, $R_s = 2.6$).

Table 7.1 provides the structures and names of 40 nicotine-related compounds analyzed in this study. The optimized, baseline separation conditions for all chiral nicotine-related compounds using macrocyclic glycopeptides are given in Table 7.2.

Table 7.2. Optimized enantiomeric separations of nicotine-related compounds using macrocyclic glycopeptides.

Class ^{1a}	Name ^{1b}	CSP ²	MP ³	T ⁴	F ⁵	k_1^{6a}	α^{6b}	R_s^{6c}
Tobacco alkaloids	NIC	N	PIM4	45	1.5	0.5	1.60	3.0
	AB	V	POM1	45	1.0	3.2	1.21	2.6
		N	PIM4	45	1.0	3.0	1.16	2.8
	AT	V	RP1	25	1.0	2.0	1.18	2.9

		N	PIM3	45	1.0	1.1	1.45	5.2
	NNIC	V	PIM2	45	0.7	4.1	1.10	1.5
		N	PIM3	45	1.0	2.7	1.14	2.3
	MAB	V	PIM4	25	0.5	1.3	1.38	3.2
		N	PIM5	25	1.0	1.9	1.24	2.5
Synthetic derivatives	1M3NP	N	PIM3	45	1.0	1.7	1.17	2.6
	2CN	V**	RP2	25	0.5	3.4	1.08	1.5
		N	PIM5	45	1.0	0.6	1.55	5.4
	2HN	N	PIM3	30	1.0	2.0	1.30	3.5
	2MN	V	RP1	30	0.7	2.3	1.11	1.7
		N	PIM4	45	1.5	1.1	1.17	2.2
	6MN	V**	PIM5	25	0.3	2.3	1.09	1.5
		N	PIM4	45	1.5	0.6	1.42	3.1
	6MNN	V	PIM1	25	1.0	2.3	1.20	2.7
		N	PIM4	45	2.0	3.7	1.26	3.6
	NENN	V	PIM5	25	1.0	2.3	1.19	2.5
		N	PIM4	45	2.0	0.5	1.76	4.6

	T3ATMN	V**	PIM2	25	0.5	1.3	1.06	1.5	
		N	RP1	45	1.0	0.8	1.58	5.7	
	T3AMN	V	RP1	45	0.5	5.0	1.15	1.5	
		N	PIM4	45	0.5	4	1.21	1.5	
	T3HMN	V	RP2	25	0.5	3.9	1.14	1.9	
		N	PIM4	25	1.0	0.5	1.42	2.7	
	T3TMN	V	RP2	25	0.5	2.7	1.15	1.7	
		N	PIM4	25	1.0	0.4	1.72	3.5	
	Nicotine metabolites	COT	T**	POM3	25	0.5	0.7	1.12	1.5
		NCOT	T	POM3	25	1.0	0.9	2.64	9.3
		4TCCA	T*	RP3	45	0.5	0.9	1.18	2.0
		5THF	T	POM3	25	0.3	0.7	1.15	1.5
NNO		N	POM2	25	0.7	1.4	1.21	2.2	
NO		V	RP1	45	0.5	1.4	1.12	1.6	
		N	PIM3	45	1.0	0.4	2.18	3.0	
NAL		N	PIM4	25	0.5	5.9	1.09	1.8	
5HCOT	V	POM1	25	1.0	0.4	1.58	3.5		

^{1a,b} See *Table 7.1* and Materials and methods. ²Refer to Materials and methods for information concerning chiral stationary phases (CSP). * denotes 150 x 4.6 mm (i.d.), ** denotes 2 columns coupled, 200 x 4.6 mm (i.d.). ³Refer to Materials and methods for information concerning mobile phase conditions. ⁴T: column temperature (° C) ⁵F: flow rate (mL/min) ^{6a,b,c} Chromatographic parameters calculated according to Materials and methods.

NicoShell separated 19 compounds, VancoShell separated 15 compounds, and TeicoShell separated 4 compounds. Racemic AT, AB, and NNIC had higher resolution with NicoShell compared to VancoShell, but were baseline separated with VancoShell. NIC could not be baseline separated with VancoShell and TeicoShell. Addition of methyl groups to either adjacent carbons of the pyridine nitrogen, 2-methylnicotine (2MN) and 6-methylnicotine (6MN), increased resolution with VancoShell in comparison to NicoShell. 2MN and 6MN, in comparison to NIC, decreased selectivity with NicoShell, but increased selectivity with VancoShell. Addition of chlorine groups to NIC, 2-chloronicotine (2CN), increased resolution using NicoShell and VancoShell. Addition of oxygen functionalities to the pyridinium nitrogen, nicotine-1-oxide (NO), compared to NIC, increased selectivity with NicoShell and VancoShell. However, oxygen functionalities added to the pyrrolidinium group, nicotine-1'-oxide (NNO), resulted in less than a baseline separation with VancoShell. Also, NNO had decreased selectivity and longer retention than NIC and NO with NicoShell. Addition of alkyl groups to AB or NNIC, N-methylanabasine (MAB) or N-ethyl-nornicotine (NENN), had different effects depending on the CSP. In comparison to AB, MAB had increased resolution using NicoShell, but similar resolution with VancoShell. When comparing to NNIC, NENN had increased resolution for both NicoShell and VancoShell. Synthetic *rac-trans* nicotine-related compounds were also compared, which differed by peripheral functional groups. All *rac-trans* enantiomers were baseline separated by NicoShell and VancoShell. COT, norcotinine (NCOT), 4-*trans*-cotinine-carboxylic acid (4TCCA), and 5-(3-

pyridyl)-tetrahydro-2-furanone (5THF) were only baseline separated by TeicoShell, while 1-methyl-3-nicotinoylpyrrolidine (1M3NP), 2hydroxynicotine (2HN), 4-(methylamino)-1-(3-pyridyl)-1-butanol (NAL), NIC, and NNO were only baseline separated by NicoShell.

The only macrocyclic glycopeptide that separated 5'-hydroxycotinine, 5HCOT, was VancoShell, but 5HCOT was also separated by CDShell-RSP, which is shown in *Figure 7.2A*.

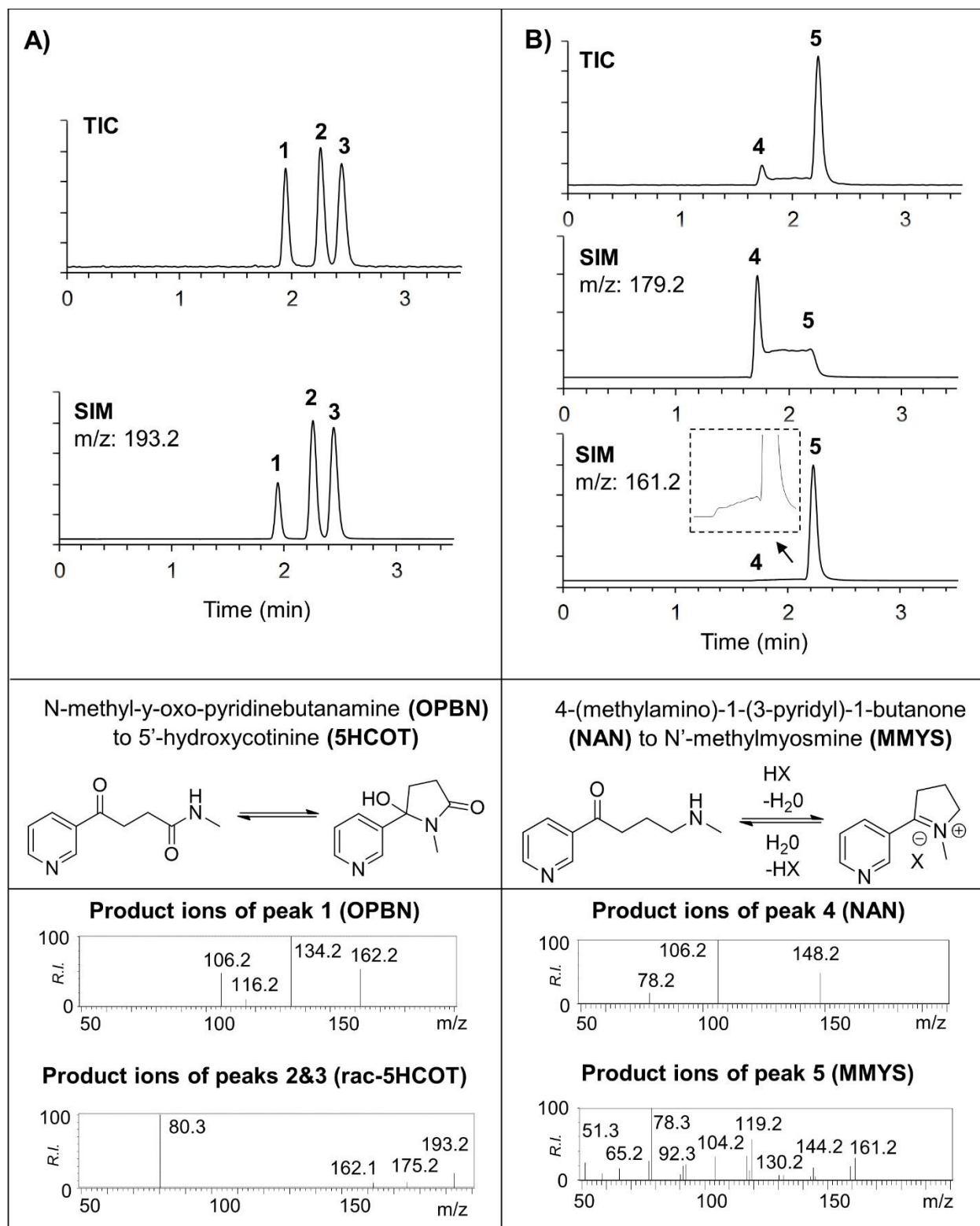


Figure 7.2. Separation of ring-closed and ring-open equilibrating tobacco alkaloids. (A) OPBN

(peak 1) to 5HCOT (peaks 2,3) (TIC scan from 110 to 220 m/z and product ion scan from 50 – 200 m/z) (**B**) NAN (peak 4) to MMYS (peak 5) (TIC scan from 150 – 220 m/z and product ion scan from 50 - 200 m/z) Conditions: CDShell-RSP, 100 x 4.6 mm (i.d.), RP5, 1.0 mL/min, 25 °C.

R.I.: Relative intensity, TIC: total ion chromatogram, SIM: selective ion monitoring. See

Materials and methods for other acronyms and information.

Figure 7.2A also depicts a third component in the total ion chromatogram and selective ion monitoring chromatogram, which was identified as *N*-methyl- γ -oxo-pyridinebutanamine, OPBN, based on the manufacturer label and mass spectra obtained. The manufacturer label marks 5HCOT and OPBN as equilibrating structures with the same mass, forming ring-open and ring-closed structures. The product ion scans for the two compounds were similar for peaks 2 and 3, but different for peak 1. Peaks 2 and 3 were identified as the chiral compound, 5HCOT, and peak 1 was identified as OPBN. The ratio of racemic HCOT to OPBN was 85:15 at 263 nm. 4-(methylamino)-1-(3-pyridyl)-1-butanone (NAN) was analyzed using CDShell-RSP, but wasn't expected to result in multiple peaks because it isn't chiral (Figure 7.2B). There were two chromatographic peaks (peaks 4 and 5) at a ratio of 90:10 at 263 nm, and a raised baseline between the two peaks. A raised baseline between two related peaks indicates that there is an interconversion on the chromatographic time scale (see Discussion). The additional peak was identified as *N*'-methylmyosmine (MMYS) based on the mass spectra obtained. The product ion scans had different fragmentation patterns for each peak. The raised baseline was present in the selective ion monitoring of each peak. Figure 7.3 shows the separation of 10 tobacco alkaloids and 7 nicotine metabolites.

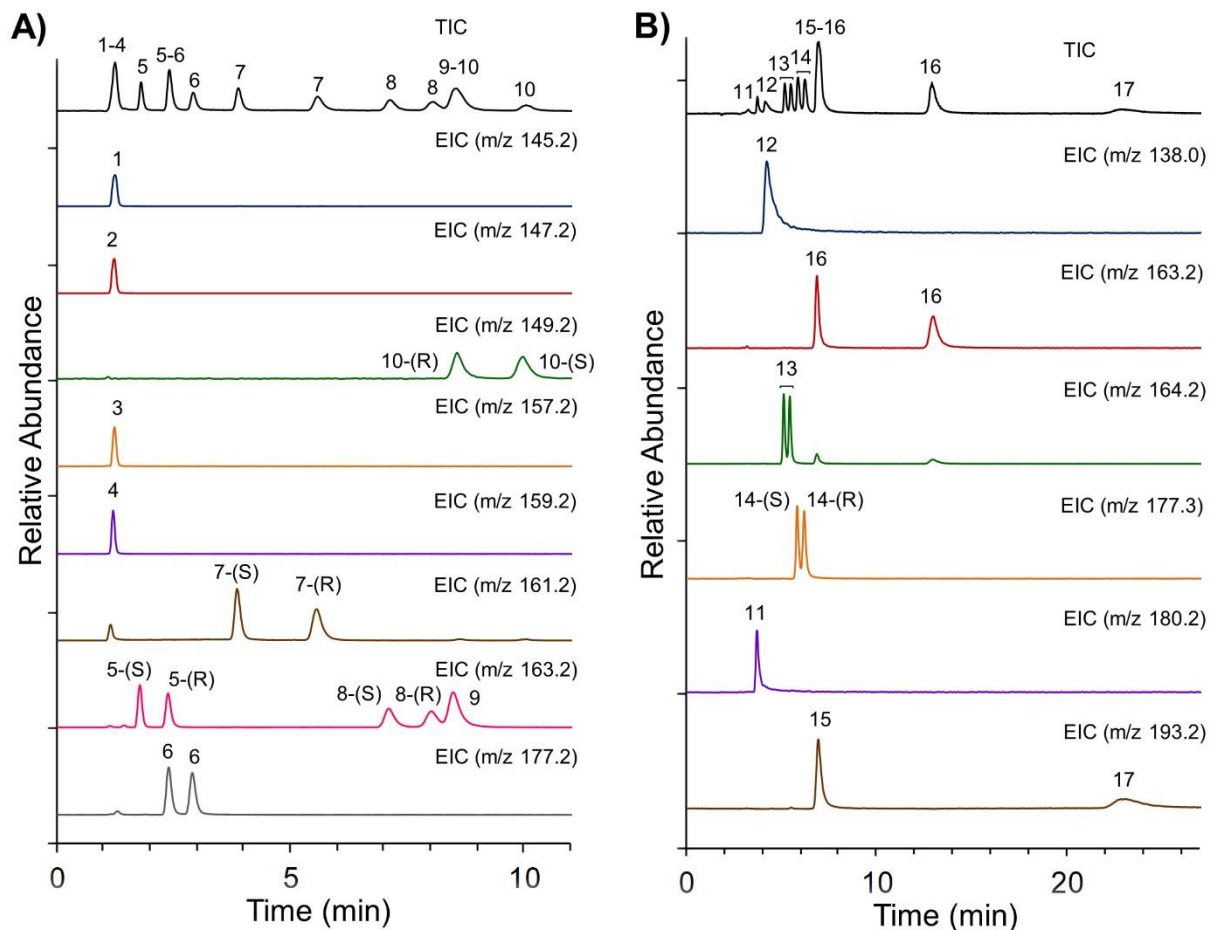


Figure 7.3. Chromatographic separation and detection of 10 tobacco alkaloids (A) and 7 nicotine metabolites (B). Total ion chromatograms (TIC) and extracted ion chromatograms (EIC) are shown. (A) Conditions: NicoShell, 100 x 4.6 mm (i.d.), PIM4, 1 mL/min. Tobacco alkaloids: 1. β -NNT, 2. MYS, 3. BPY, 4. β -NT, 5. (S,R)-NIC, 6. MANB, 7. (S,R)-ANT, 8. (S,R)-ANB, 9. MET, 10. (R,S)-NNIC. (B) Conditions: TeicoShell, 150 x 4.6 mm (i.d.), POM3, 0.5 mL/min. Nicotine metabolites: 11. OPBA, 12. LAC, 13. rac-5THF, 14. (S,R)-COT, 15. T3HC, 16. rac-NCOT, 17. (S)-CNO.

NicoShell enantioseparated 5 chiral tobacco alkaloids in 10 minutes (*Figure 7.3A*). Also, 3 enantioseparations of chiral nicotine metabolites were obtained with TeicoShell in 14 minutes (*Figure 7.3B*). For identification, the appropriate m/z value was selected, and the ion chromatogram of interest extracted. The components that had the same m/z were identified by spiking the sample with a standard.

The separation of NNAL is shown in *Figure 7.4A* and resulted in two pairs of chromatographic peaks that had similar areas.

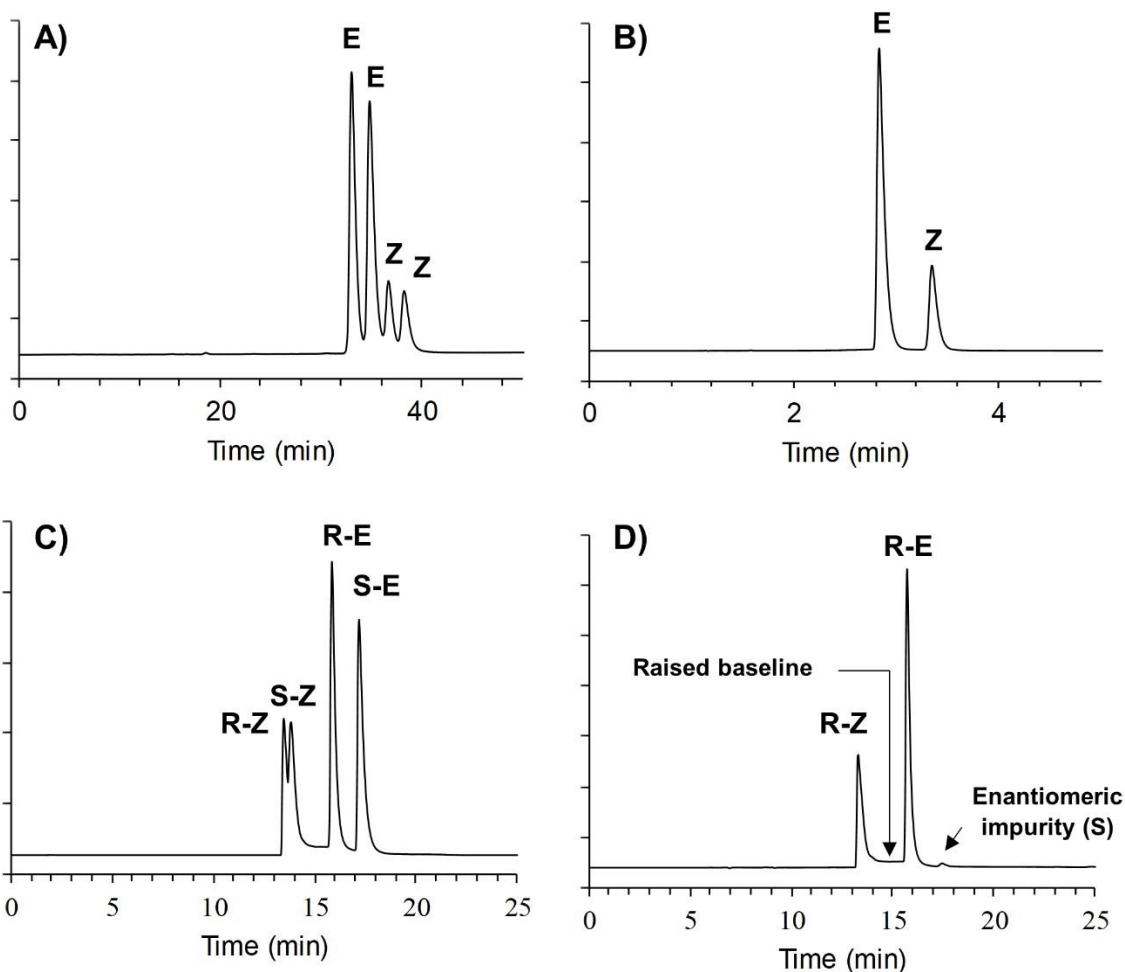


Figure 7.4. The direct separation of tobacco-specific nitrosamines. R = R-NNN, S = S-NNN, E = E isomer, Z = Z isomer based on previous reports (see Discussion), see Materials and methods and Table 7.1 for other acronyms used. (A) rac-NNAL, TeicoShell, 100 x 4.6 mm (i.d.), RP3, 0.3 mL/min, 25 °C. (B) NNK, CDShell-RSP, 100 x 4.6 mm (i.d.), RP4, 1.0 mL/min, 25 °C. (C) rac-NNN, Q-Shell, 250 x 4.6 mm (i.d.), RP3, 0.3 mL/min, 25 °C. (D) R-NNN, Q-Shell, 250 x 4.6 mm (i.d.), RP3, 0.3 mL/min, 25 °C.

The ratio of each pair was 75:25 at 263 nm. The separation of NNK is shown in *Figure 7.4B*, with two chromatographic peaks at a ratio of 75:25 at 263 nm. *Figure 7.4C* shows 4 distinct peaks from the separation of racemic NNN with the Q-Shell column. When pure enantiomers were injected, (R)-NNN in *Figure 7.4D*, each enantiomer showed two peaks at a ratio of 65:35 at 263 nm with a raised baseline between them (*Figure 7.4C and 7.4D*). Single enantiomers were spiked into the original sample to identify each enantiomeric peak. An enantiomeric impurity was observed in the (R)-NNN sample and identified as (S)-NNN (*Figure 7.4D*). The elution order of NNN and NNIC enantiomers were different than the other tobacco alkaloids and metabolites (*Figure 7.3A, 7.3B, and 7.4D*). Additionally, a reversal of elution for AB was observed when switching between PIM and POM solvents (*Figure 7.S1A and 7.S1B*). Racemic NAB was separated into 2 peaks of equal area, while (S)-NAB was separated into 2 peaks at a ratio of 80:20 at 263 nm (*Figure 7.S2A and 7.S2B*). NAT was separated into 2 peaks that each had a peak shoulder at a ratio of 80:20 at 263 nm (*Figure 7.S2C*). NNNO was separated into 4 peaks with similar ratios at 263 nm with a raised baseline using NicoShell coupled to TeicoShell (*Figure 7.S2D*). The separation of each TSNA resulted with similar MS fragmentation patterns for each respective peak.

7.5 Discussion

The chiral selectors examined in this study were shown to have both broader and higher selectivity for tobacco alkaloids and their metabolites than other approaches (*Table 7.2*) [27,39-40]. Higher selectivities and efficiencies allows the use of shorter columns and higher flow rates, which produces faster analysis times, and often sharper peaks, and better detection (*Figure 1*) [32,39-40]. In turn, this can be useful in high throughput screening, and studying biotransformations and the biokinetics and dynamics of low levels of tobacco alkaloid metabolites [46]. For such studies, it is essential for the stereoselective separation methods to be compatible with ESI-MS detection as were all methods herein (*Table 7.2*). Separations that didn't work well for one macrocyclic glycopeptide separated with a different related one, which is known as complementary behaviour (*Table 7.2*). The "principle of complementary separations" states that a partial separation with one chiral selector can be brought to baseline with one of the other related selectors [47]. Complementary separations were seen with NIC and several derivatives (2HN, 1M3NP, NNO), which had poor resolution using VancoShell, but worked well with NicoShell. Also, TeicoShell baseline separated the metabolites that VancoShell and NicoShell didn't. Usually within a class of structures several functionalities differ, which might enhance the separation using one macrocyclic glycopeptide, but inhibit another. It is unclear why some compounds had poor resolution using NicoShell and VancoShell due to the complex interaction mechanisms of macrocyclic glycopeptides. However, complementary separations offer an effective solution for difficult separations, which has been exploited for high-throughput screening [46]. This significant characteristic provides a high likelihood of baseline separating any structure within a certain class, as in the case of the tobacco alkaloids and their metabolites (*Figure 7.3A and 7.3B*). Utilizing multiple chiral selectors and chromatographic solvents also gave rise to a reversal of elution order.

So, this method could also be applied to situations that require a certain elution profile of enantiomers, such as in determining enantiomeric purity or in preparative separations.

Additional chromatographic peaks were observed in the separation of some tobacco alkaloids (*Figure 7.2 and 7.4*). *Figure 7.2* shows the separation of 5HCOT, which has been reported as the chiral cyclized, ring-closed form of the straight-chain structure, OPBN [33,48-49]. 5HCOT was previously reported to be quickly and favourably formed in water, which agrees with our results [49]. Some chromatographic separations have been challenging as indicated in previous reports [50]. The separation approach of this study provides two methods (*Table 7.2 and Figure 7.2A*). A raised baseline was not observed, but in the separation of NAN a raised baseline was seen between the NAN chromatographic peak and the additional peak, MMYS, indicating interconversions on the chromatographic time scale (*Figure 7.2B*). NAN was previously reported to equilibrate with MMYS by a dehydration/hydration reaction, but little was found in the literature about their roles in metabolism [33,48-49,51]. NAN and MMYS might have faster interconversion rates than the other ring-closed and straight-chain equilibrating structures, in *Figure 7.2A*, due to the observed raised baseline at ordinary conditions. The reproducibility of a separation was highly dependent on the time between sample preparation and analysis. It was observed that differences in this time and temperature would change the ratio between the chromatographic peaks. Also, if another solvent was used to dissolve the analyte for analysis, the equilibration time was much different. Furthermore, other equilibrating structures have been reported to exist between these structures [48]. Detection and separation of these components has not been reported in the literature, but with this procedure, it is now possible.

A single enantiomer of NNN was separated into 2 chromatographic peaks at ratio of 70/30, which agrees with a previous report of NNN's E and Z isomeric ratio in tobacco and were labelled

accordingly (*Figure 7.4D*) [19]. E/Z isomers in TSNA_s have not been extensively studied. Reports of some have been performed, such as NNN, NNK, and NNAL, concluding there is generally a higher concentration of the E isomer than the Z isomer [18-20]. Our results indicate that this also is true for NAB and NAT (*Figure 7.4B*, and *S2*). Upon further inspection, a raised baseline was observed between the peaks. This indicates the diastereomeric interconversion of E and Z isomers on the chromatographic time scale (*Figure 4D*). In general, decreasing the temperature of the column lowered the baseline between the converting peaks. On the other hand, higher column temperatures increased the rate of conversion, such that no peak separation was observed. Perhaps, this explains why previous reports that use GC at high temperatures didn't observe E/Z isomers during TSNA analysis [23]. The interconversion rate between E/Z isomers was different because some TSNA_s had distinct raised baselines, like NNN, while others like NNK didn't (*Figure 7.4B and 7.4D*). However, a raised baseline was observed at higher temperatures for NNK, so it does interconvert, but slowly at ordinary conditions. Previous reports of some pharmacokinetics of racemic TSNA_s have been investigated, such as their half-lives. An observed trend was that a short half-life correlated to the carcinogenicity of the TSNA, so more potent TSNA_s were eliminated faster [52]. However, the half-lives and interconversion rates of single enantiomers have not been reported, which may be different, especially since they contain equilibrating isomers. This equilibration was observed to be stable under room temperature conditions as shown in previous literature, but due to the raised chromatographic baseline, there is difficulty in isolating pure E or Z isomer [18-19]. Since E/Z isomers were observed for all TSNA_s, further investigation of the enantiomers and their respective isomers as well as other TSNA metabolites, such as their half-lives, might be useful to determine their stereoselective roles and routes in metabolism.

Since the FDA has issued the mandatory regulation of NNN levels in smokeless tobacco products, manufacturers will have to quantify the amount of NNN in their finished products [9]. This may lead to confusion, as some manufacturers might use achiral LC methods, which might broaden or split their chromatographic peaks [24]. Since these splits are most likely E/Z isomers of the TSNAs, it is important that they be included in the quantification required by the FDA. However, E/Z isomers are known to have different physical and biological properties, so studies might be needed to evaluate whether these E/Z isomers contribute differently to cancer and other diseases [26]. The methodology of this study can be applied, as the results of this study clearly demonstrate a comprehensive approach for the analysis and enantioseparation of these nicotine-related compounds. Further investigation is ongoing, but with the methods presented in this study, more pharmacological information concerning individual enantiomers and other isomers of nicotine-related compounds can effectively and quickly be obtained. These studies would lead to a more complete knowledge about tobacco alkaloids and their metabolites and their roles or therapeutic use for cancer and other diseases.

7.6 References

1. S.S. Hecht, Tobacco carcinogens, their biomarkers, and tobacco-induced cancer, *J. Nat. Rev. Cancer* 3 (2003) 733-744.
2. U.S. Department of Health and Human Services, The health consequences of smoking—50 years of progress: A report of the Surgeon General. Atlanta, GA: U.S. Department of Health and Human Services, Centers for Disease Control and Prevention, National Center for Chronic Disease Prevention and Health Promotion, Office on Smoking and Health, 2014.
3. Food and Drug Administration. Family smoking prevention and tobacco control and federal retirement reform. Public law 111–31—June 22, 2009.
4. Food and Drug Administration, Deeming tobacco products to be subject to the federal food, drug and cosmetic act, as amended by the family smoking prevention and tobacco control act; regulations on the sale and distribution of tobacco products and required warning statements for tobacco products, *Fed. Regist.* 79 (2016) 28973.
5. Food and Drug Administration, Protecting American families: comprehensive approach to nicotine and tobacco. <https://www.fda.gov/NewsEvents/Speeches/ucm569024.htm>, 2017 (accessed August 17, 2017).

6. D.K. Hatsukami, M. Kotlyar, L.A. Hertsgaard, Y. Zhang, S.G. Carmella, J.A. Jensen, S.S. Allen, P.G. Shields, S.E. Murphy, I. Stepanov, S.S. Hecht., Reduced nicotine content cigarettes: effects on toxicant exposure, dependence and cessation, *Addiction* 105 (2010) 343-355.
7. D. Hoffmann, S.S. Hecht, Nicotine-derived *N*-nitrosamines and tobacco related cancer: current status and future directions, *Cancer Research* 45 (1985) 935-944.
8. S. Balvo, S. James-Yi, C.S. Johnson, M.G. O'Sullivan, I. Stepanov, M. Wang, D. Bandyopadhyay, F. Kassie, S. Carmella, P. Upadhyaya, S.S. Hecht, (S)-*N'*-nitrosornicotine, a constituent of smokeless tobacco, is a powerful oral cavity carcinogen in rats, *Carcinogenesis* 34 (2013) 2178-2183.
9. Food and Drug Administration, Tobacco product standard for *N'*-nitrosornicotine level in finished smokeless tobacco products, *Fed. Regist. Proposed Rules* 82 (2017) 8004-8053.
10. S.S. Hecht, I. Stepanov, D.K. Hatsukami, Major tobacco companies have technology to reduce carcinogen levels but do not apply it to popular smokeless tobacco products, *Tob. Control* 6 (2011) 443.
11. R.S. Lewis, A.M. Jack, J.W. Morris, V.J.M. Robert, L.B. Gavilano, B. Siminszky, L.P. Bush, A.J. Hayes, R.E. Dewey, RNA interference (RNAi)-induced suppression of nicotine demethylase activity reduces levels of a key carcinogen in cured tobacco leaves, *Plant Biotech. J.* 6 (2008) 346-354.
12. A. Knezevich, J. Muzic, D.K. Hatsukami, S.S. Hecht, I. Stepanov, Nornicotine nitrosation in saliva and its relation to endogenous synthesis of *N'*-nitrosornicotine in humans, *Nicotine Tob. Res.* 15 (2013) 591-595.
13. S.S. Hecht, R. Young, Y. Maeura, Comparative carcinogenicity in F344 rats and Syrian golden hamsters of *N'*-nitrosornicotine and *N'*-nitrosornicotine-1-*N*-oxide, *Cancer Lett.* 20 (1983) 333-340.
14. S.S. Hecht, Biochemistry, biology, and carcinogenicity of tobacco-specific N-nitrosamines, *Chem. Res. Toxicol.* 11 (1998) 559-603.
15. S.G. Carmella, S. Akerkar, S.S. Hecht, Metabolites of the tobacco-specific nitrosamine 4(methylnitrosamino)-1-(3-pyridyl)-1-butanone in smokers' urine, *Cancer Res.* 53 (1993) 721-724.
16. S.S. Hecht, Human urinary carcinogen metabolites: biomarkers for investigating tobacco and cancer, *Carcinogenesis* 23 (2002) 907-922
17. P. Upadhyaya, P.M.J. Kenney, J.B. Hochalter, M. Wang, S.S. Hecht, Tumorigenicity and metabolism of 4-(methylnitrosamino)-1-(3-pyridyl)-1-butanol enantiomers and metabolites in the A/J mouse, *Carcinogenesis* 20 (1999) 157-1582.
18. S.S. Hecht, T.E. Spratt, N. Trushin, Absolute configuration of 4-(methylnitrosamino)-1-(3-pyridyl)-1butanol formed metabolically from 4-(methylnitrosamino)-1-(3-pyridyl)-1-butanone, *Carcinogenesis* 18 (1997) 1851-1854.
19. S.S. Hecht, C.B. Chen, M. Dong, R.M. Ornaf, D. Hoffman, T.C. Tso, Chemical studies on tobacco smoke L1: studies on non-volatile nitrosamines in tobacco, *Beitrag zur Tabakforschung* 9 (1977) 1-6.
20. Y. Yang, C. Yu, M. Zhou, N. Pang, N. Li, H. Nie, J. Liao, Y. Bai, H. Liu, Metabolic study of 4(methylnitrosamino)-1-(3-pyridyl)-1-butanone to the enantiomers of 4-(methylnitrosamino)-1-(3-pyridyl)-1-butanol in vitro in human bronchial epithelial cells using chiral capillary electrophoresis, *J. Chromatogr. A* 1218 (2011) 6505-6510.
21. S.G. Carmella, S.S. Hecht, High-performance liquid chromatographic analysis of metabolites of the nicotine-derived nitrosamines, *N'*-nitrosornicotine and 4-(methylnitrosamino)-1-(3-pyridyl)-1butanone, *Anal. Biochem.* 145 (1985) 239-244.

22. J. Yang, S.G. Carmella, S.S. Hecht, Analysis of N'-nitrosornicotine enantiomers in human urine by chiral stationary phase liquid chromatography-nanoelectrospray ionization-high resolution tandem mass spectrometry, *J. Chromatogr. B* 1044-1055 (2017) 127-131.
23. S.G. Carmella, E.J. McIntee, M. Chen, S.S. Hecht, Enantiomeric composition of N'-nitrosornicotine and N'-nitrosoanatabine in tobacco, *Carcinogenesis* 21 (2000) 839-843.
24. J. Jiang, L. Li, M. Wang, J. Xia, W. Wang, X. Xie, Theoretical explanation of the peak splitting of tobacco-specific N-nitrosamines in HPLC, *Bull. Korean Chem. Soc.* 33 (2012) 1722-1728.
25. S.L. Abidi, Chromatographic investigations of the configurational and geometrical isomerism of allylic N-terpenyl-N-hydroxyethylnitrosamines, *J. Chromatogr. A* 288 (1984) 277-292.
26. D.A. Lightner, T.A. Wooldridge, A.F. McDonagh, Configurational isomerization of bilirubin and the mechanism of jaundice phototherapy, *Biochem. Biophys. Res. Commun.* 86 (1979) 235-43.
27. D.W. Armstrong, X. Wang, N. Ercal, Enantiomeric composition of nicotine in smokeless tobacco, medicinal products, and commercial reagents, *Chirality* 10 (1998) 587-591.
28. M.D. Aceto, B.R. Martin, I.M. Uwaydah, E.L. May, L.S. Harris, C. Izzola-Conde, W.L. Dewey, T.J. Bradshaw, W.C. Vincek, Optically pure (+)-nicotine from (+/-)-nicotine and biological comparisons with (-)-nicotine, *J. Med. Chem.* 22 (1979) 174-177.
29. D. Yildiz, N. Ercal, D.W. Armstrong, Nicotine enantiomers and oxidative stress, *J. Toxicol.* 130 (1998) 155-165.
30. D. Pogocki, T. Ruman, M. Danilczuk, M. Danilczuk, M. Celuch, E. Walajtys-Rode, Application of nicotine enantiomers, derivatives and analogues in therapy of neurodegenerative disorders, *Eur. J. Pharmacol.* 563 (2007) 18-39.
31. G. Hellinghausen, J.T. Lee, C.A. Weatherly, D.A. Lopez, D.W. Armstrong, Evaluation of nicotine in tobacco-free-nicotine commercial products, *Drug Test. Analysis* 9 (2017) 944-948.
32. D.W. Armstrong, X. Wang, J.T. Lee, Y.S. Liu, Enantiomeric composition of nornicotine, anatabine, and anabasine in tobacco, *Chirality* 11 (1999) 82-84.
33. J. Hukkanen, P. Jacob, N.L. Benowitz, Metabolism and disposition kinetics of nicotine, *Pharm. Reviews* 57 (2005) 79-115.
34. P. Jacob III, L. Yu, A.T. Shulgin, N.L. Benowitz, Minor tobacco alkaloids as biomarkers for tobacco use: comparison of users of cigarettes, smokeless tobacco, cigars, and pipes, *Am. J. Public Health* 89 (1999) 731-736.
35. L.P. Dwoskin, L. Teng, S.T. Buxton, A. Ravard, N. Deo, P.A. Crooks, Minor alkaloids of tobacco release [³H] dopamine from superfused rat striatal slices, *Euro. J. Pharm.* 276 (1995) 195-199.
36. S.T. Lee, K. Wildeboer, K.E. Panter, W.R. Kern, D.R. Gardner, R.J. Molyneux, C.W. Chang, F. Soti, J.A. Pfister, Relative toxicities and neuromuscular nicotinic receptor agonistic potencies of anabasine enantiomers and anabaseine, *Neurotoxicol. And Teratol.* 28 (2006) 220-228.
37. Food and Drug Administration, FDA's policy statement for the development of new stereoisomeric drugs, *Chirality* 4 (1992) 338-340.
38. H.-J. Kim, H.-S. Shin, Determination of tobacco-specific nitrosamines in replacement liquids of electronic cigarettes by liquid chromatography-tandem mass spectrometry, *J. Chromatogr. A* 1291 (2013) 4855.
39. D.W. Armstrong, L.A. Spino, S.M. Han, J.I. Seeman, H.V. Secor, Enantiomeric resolution of racemic nicotine and nicotine analogues by microcolumn liquid chromatography with β -cyclodextrin inclusion complexes, *J. Chromatogr. A* 411 (1987) 490.

40. Y. Tang, W.L. Zielinski, H.M. Bigott, Separation of nicotine and nornicotine enantiomers via normal phase HPLC on derivatized cellulose chiral stationary phases, *Chirality* 10 (1998) 364.
41. D.W. Armstrong, Y. Tang, S. Chen, Y. Zhou, C. Bagwill, J.R. Chen, Macrocyclic antibiotics as a new class of chiral selectors for liquid chromatography, *Anal. Chem.* 66 (1994) 1473-1484.
42. D.W. Armstrong, Y. Liu, K.H. Ekborgott, A covalently bonded teicoplanin chiral stationary phase for HPLC enantioseparations, *Chirality*, 7 (1995) 474-497.
43. K.H. Ekborg-Ott, J.P. Kullman, X. Wang, K. Gahm, L. He, D.W. Armstrong, Evaluation of the macrocyclic antibiotic avoparcin as a new chiral selector for HPLC, *Chirality* 10 (1998) 627-660.
44. A. Peter, E. Vekes, D.W. Armstrong, Effect of temperature on retention of chiral compounds on a ristocetin A chiral stationary phase, *J. Chromatogr. A*, 958, (2002) 89-107.
45. A. Feurcova, M. Vancova, J. Mydlova, J. Lehotay, J. Krupcik, D.W. Armstrong, Interconversion of oxazepam enantiomers during HPLC separation. Determination of thermodynamic parameters, *J. Liq. Chromatogr. Relat. Technol.* 29 (2006) 2889-2900.
46. C.L. Barhate, L.A. Joyce, A.A. Makarov, K. Zawatzky, F. Bernardoni, W.A. Schafer, D.W. Armstrong, C.J. Welch, E.L. Regalado, Ultrafast chiral separations for high throughput enantiopurity analysis, *Chem. Commun.* 53 (2016) 509-512.
47. M.P. Gasper, A. Berthod, U.B. Nair, D.W. Armstrong, Comparison and modeling study of vancomycin, ristocetin A, and teicoplanin for CE enantioseparations, *Anal. Chem.* 68 (1996) 2501-2514.
48. Neurath, G.B. Aspects of the oxidative metabolism of nicotine, *Clin. Investig.* 72 (1994) 190-195.
49. T.L. Nguyen, E. Dagne, L. Gruenke, H. Bhargava, N. Castagnoli Jr., The tautomeric structures of 5hydroxycotinine, a secondary mammalian metabolite of nicotine, *J. Org. Chem.* 46 (1981) 758-760.
50. G.B. Neurath, M. Dunger, D. Orth, Detection and determination of tautomers of 5'-hydroxynicotine and 2-hydroxynicotine in smoker's urine, *Med. Sci. Res.* 20 (1992) 853-858
51. P.G. Haines, A. Eisner, Identification of pseudo-oxynicotine and its conversion to Nmethylmyosmine, *J. Am. Chem. Soc.* 72 (1950) 1719-1721.
52. J.D. Adams, E.J. LaVoie, D. Hoffman, On the pharmacokinetics of tobacco-specific N-nitrosamines in Fischer rats, *Carcinogenesis* 6 (1985) 509-511.

Chapter 8

Summary and Future Outlook

This dissertation demonstrates different techniques which can be adopted to increase efficiencies in analytical scale chromatographic separations. Chapter 2 discusses the advantages of using superficially porous particles instead of fully porous particles for enantiomeric separations using SFC. Chapter 3 discusses the effect of water as a mobile phase additive in SFC on different stationary phase chemistries and demonstrates significant gains in efficiency with polar stationary phases. This chapter also highlights the use of water to tune peak shapes under overload conditions. Chapter 4 focuses on replacement of toxic methanol with nontoxic and environmentally friendly azeotropic ethanol. The replacement results in lower environmental impact along with lower cost. It also produced increased chromatographic efficiency and decreased retention times Chapter 5 investigates the effect of incorporating water in the SFC mobile phase for different stationary phases used for achiral separations in SFC and introduces a cyclofructan-6 based stationary phase for SFC separations. Chapter 7 and 8 discuss novel methodologies incorporating advantages offered by superficially porous particles. With a constant increase in demand for high throughput separations, strategies for enhancing efficiency have become essential and future research will also focus on such novel strategies. With growing concerns about the environmental impact of humans, it has become highly necessary to come up with research methodologies with minimal impact. Using azeotropic ethanol as the primary organic modifier in SFC will require coming up with new methodologies and stationary phases in future. More research on particle morphologies that will result in a gain in efficiency need to be conducted. Manufacturers of instruments should develop instruments with higher pressure tolerances so that even smaller particles can be used for chromatography.

Appendix A

List of Co-authors and Citations

Chapter 2. Daipayan Roy and Daniel W. Armstrong, *Journal of Chromatography A*, **1605** (2019), 360339

Chapter 3. Daipayan Roy, M. Farooq Wahab, Terry A. Berger, and Daniel W. Armstrong, *Analytical Chemistry*, **91** (2019), 14672-14680.

Chapter 4. Daipayan Roy, M. Farooq Wahab, Mohsen Talebi, and Daniel W. Armstrong, *Green Chemistry*, **22** (2020), 1249-1257.

Chapter 5. Liudmyla Khvalbota, Daipayan Roy, M. Farooq Wahab, Sepideh Khaki Firooz, Andrea Machyňáková, Ivan Špánik, Daniel W. Armstrong, *Analytica Chimica Acta*, **1120** (2020), 75-84

Chapter 6. Garrett Hellinghausen, Daipayan Roy, Jauh T. Lee, Yadi Wang, Choyce A. Weatherly, Diego A. Lopez, Kate A. Nguyen, John D. Armstrong, Daniel W. Armstrong, *Journal of Pharmaceutical and Biomedical Analysis*, **155** (2018), 70-81.

Chapter 7. Garrett Hellinghausen, Daipayan Roy, Yadi Wang, Jauh T. Lee, Diego A. Lopez, Choyce A. Weatherly, Daniel W. Armstrong, *Talanta*, **181** (2018), 132-141.

Biographical Information

Daipayan Roy was born in Kolkata, India and obtained his bachelor's in science (BSc) degree from University of Calcutta in 2013. He went on to get a master's in science degree (MSc) from Savitribai Phule Pune University in 2015. His master's thesis work was conducted in Council of Scientific and Industrial Research- National Chemical Laboratory (CSIR-NCL) in Pune with focus on digestive ripening of gold nanoparticles. He joined University of Texas at Arlington in fall 2015 and joined Dr. Daniel W. Armstrong's research group in January 2017. His research work mainly revolves around chromatography including high performance liquid chromatography and supercritical fluid chromatography. He has presented his work at various conferences and has published ten papers during his stay at the University of Texas at Arlington.